
UNIVERSITY OF
BIRMINGHAM

# STUDIES ON THE LUBRICATION OF ROLLER COMPACTION FORMULATIONS

By

**Jason Dawes**

A thesis submitted to The University of Birmingham for the degree of

**DOCTOR OF ENGINEERING**

School of Chemical Engineering
College of Engineering & Physical Sciences
The University of Birmingham
September 2013

## Abstract

The tablet is the preferred route of delivery for pharmaceutical products due to its relative ease of manufacture and high patient compliance. However, complex tablet formulations can present a number of process challenges, necessitating careful design of both the formulation and the process. This thesis sets out to investigate some of the issues involved with the lubrication of roller compaction formulations in order to gain a greater understanding of the role of lubricants during roller compaction – an area of research which has received relatively little attention.

Roller compaction of unlubricated and lubricated pharmaceutical formulations was carried out using an auger fed, instrumented roller compactor. Magnesium stearate had a profound impact on powder feeding: a significant increase (approximately 80-90%) in ribbon mass throughput and a consequential increase in roll gap, compared to an unlubricated formulation were observed. Adhesion of the formulation to the roll surface was not observed when a sufficient amount of magnesium stearate was added to the formulation. Pressure applied across the width of the roll was more uniform for the lubricated formulations, and the nip angle increased from 14.7° to 18.9° due to enhanced densification in the feed chamber immediately before the counter-rotating rollers. However uncontrolled shear induced mixing that occurs during powder feeding through the hopper and auger feeder assembly may have an unpredictable impact on the lubricity of the formulation, particularly when scaling up the roller compaction process.

A novel use of external lubrication has been applied in which magnesium stearate was metered directly on the roll surface during roller compaction. A scalable parameter: travelling

roll distance per shot ($D_{pS}$), has been defined which ensures that an equal amount of magnesium stearate is applied to the roll surface per rotation at any roll speed and roll dimension. The minimum amount of external magnesium stearate required to prevent roll adhesion depends on the relative adhesiveness of the formulation. Whilst some amount of magnesium stearate is transferred from the rollers to the surface of the ribbon, it was a significant reduction from the common 0.5-1.0% w/w added intra-granularly to less than 0.01% w/w required extra-granularly.

The impact of a novel co-processed range of excipients (LubriTose™) and sodium stearyl fumarate (Alubra™) on the roller compaction process was investigated. The roller compaction of a placebo formulation was equivalent to that observed using magnesium stearate as a lubricant. Granules roller compacted from the LubriTose™ excipients had a capacity to retain their lubricating properties post roller compaction. The ejection forces of tablets compacted from the roller compacted granule containing either magnesium stearate or Alubra™ (intra-granular only) compared to the ejection force of tablets from the initial lubricated powder increased by 100% and 300% respectively after compaction of only 10 tablets. However, when using the LubriTose™ excipient the ejection forces of the tablets from the granule were actually lower than the tablets from initial powder.

A statistical analysis on data generated by Bristol-Myers Squibb demonstrated the potential use of drug product surrogacy. Response variables measured during the manufacture of two drug products deemed to have similar material properties (specific surface area and particle size) were found to be statistically similar, whilst a third drug product with very different material properties was found to have statistically different measured responses.

## List of Publications

Sections of the work contained in this thesis have already been published in the following form;

[1] Dawes, J., Allenspach, C., Gamble, J. F., Greenwood, R., Robbins, P., and Tobyn, M., Application of external lubrication during the roller compaction of adhesive pharmaceutical formulations. Pharmaceutical Development and Technology, 2013; 18(1):246-256.

[2] Dawes, J., Gamble, J. F., Greenwood, R., Robbins, P., and Tobyn, M., An investigation into the impact of magnesium stearate on powder feeding during roller compaction. Drug Development and Industrial Pharmacy, 2012; 38(1):111-122.

## List of Conferences Attended

The work contained in this thesis has been presented at the following conferences;

[1] PharmSci the Science of Medicine, The Academy of Pharmaceutical Sciences, Heriot Watt University, 2nd September – 4th September 2013 (poster presentation)

[2] PARTEC – International Congress on Particle Technology, Nuremberg, Germany, 23-25th April 2013 (oral presentation)

[3] Powder Fouling – measuring predicting and understanding reliability in powder handling, ICHEME, University of Birmingham, 27th November 2012 (oral presentation)

[4] AAPS Annual Meeting and Exposition, Chicago, US, 14-18th October (poster presentation)

[5] 11th UK Particle Technology Forum – formulation with particles, Loughborough University, 4-5th April 2012 (poster presentation)

[6] Powder Flow – controlling regulating and modifying powder flow, Formulation Science and Technology, London, 6th December 2011 (poster presentation)

[7] PharmSci the Science of Medicine, The Academy of Pharmaceutical Sciences, Nottingham University, 31st August – 2nd September 2011 (oral presentation)

**Dedicated to my Parents**

**Richard and Tracy Dawes**

## Acknowledgements

I thank - first and foremost - my wife, Claire, and my daughter, Jessica, for their endless encouragement, love, support and understanding during the numerous challenging periods of completing this degree. I simply would not have been able to achieve this without them. I would also like to express my heartfelt thanks and love to my Parents and my Father-in-law and Mother-in-law for their encouragement, support and understanding.

I would like to express my deepest gratitude and appreciation to all my supervisors: Dr Richard Greenwood, Mr John Gamble, Dr Phil Robbins and Dr Mike Tobyn for their supervision, invaluable guidance and support through the EngD, without which this thesis would not have been possible.

I would also like to thank my colleagues at Bristol-Myers Squibb for their guidance and friendship; in particular I would like to thank Dr Ana Ferriea for her helpful discussions on DoE and multivariate data analysis for chapter 7 and Mr Martin Vernon for never being short of questions or interest

Finally, I would like to acknowledge the financial support from Bristol-Myers Squibb and the Engineering and Physical Sciences Research Council.

# Table of Contents

## List of Figures

## List of Tables

# CHAPTER 1

# INTRODUCTION

# CHAPTER 1

# INTRODUCTION

## 1.1 Tablet manufacturing and roller compaction overview

The tablet is the predominant solid oral dosage form, in terms of the range of medicines that are available in this form and the volume of sales from them. Patient preference and relative speed of manufacture are the basis of the success of this dosage form. However, solid dosage form manufacturing is often a complex task with numerous challenges involving both the process and the formulation. A breakdown of some of the issues involved is showed schematically in Figure 1-1.

Although a proportion of tablets are made by the "direct compression" route a majority of dosage forms go through an intermediate granulation step. Granulation is a particle size enlargement technique by which a raw powder blend with initially small particle size and poor flow properties is agglomerated to produce granules with a larger particle size distribution. There are two widely used approaches to granulation: wet granulation and dry granulation. In wet granulation a liquid binder is mixed within a formulation using a high shear blender; particle agglomeration occurs due to the existence of capillary forces and liquid bridges. The subsequent granules are then dried to remove excess water and if needed milled to achieve a desired size distribution. Dry granulation uses the application of pressure to

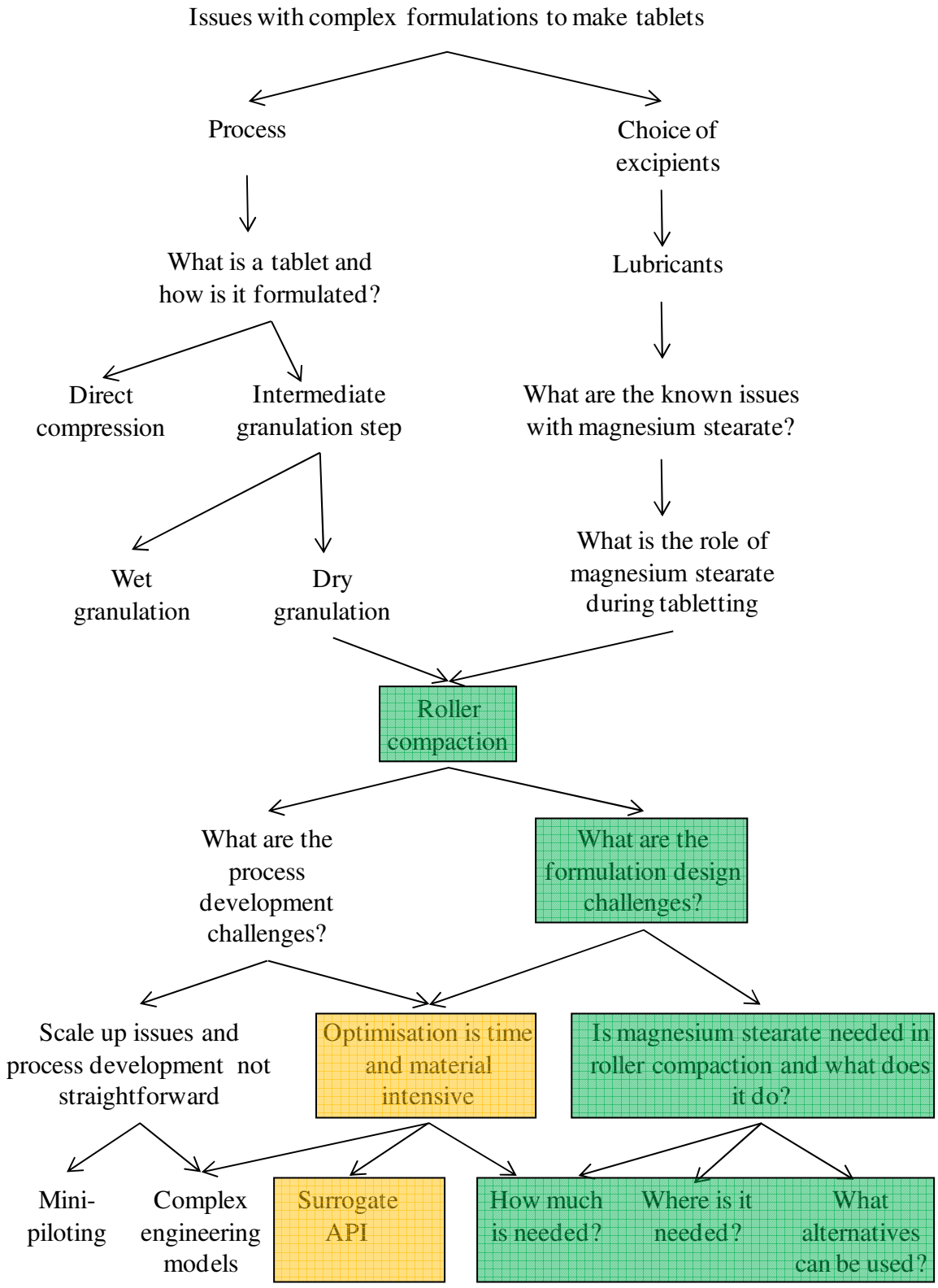


**Figure 1-1 – Breakdown diagram showing the context of tabletting issues and the research questions of direct relevance to this work (Green boxes indicate the primary strand of tabletting issues and research questions investigated in the thesis, orange boxes indicate secondary tabletting issues and research questions).**

create a ribbon compact which is subsequently milled to produce granules with an increase in particle size.

Roller compaction is an intermediate processing step, used in the dry granulation process route, in which a powdered formulation is compacted between two counter rotating rolls to produce a ribbon compact. The roller compacted ribbon is subsequently milled to produce granules of a desired particle size range. The main advantage of roller compaction over wet granulation is the absence of water and thereby does not require the use of a drying stage. This affords both a reduction in processing time and provides a more suitable processing route for active pharmaceutical ingredients (APIs) that are moisture or heat labile. The increase in particle size of the roller compacted granule compared to the raw powder elicits several advantages: improves powder flow properties, reduces bulk volume aiding in tablet die dosage filling, improves content uniformity, helps prevent active ingredients from segregating, minimizes storage and enhances transport, reduces potential environmental and safety hazards such as reducing the incidence of dust generation. However, one disadvantage is that the process can be less accommodating to slight changes in the properties of the input materials. As well as this sensitivity, roller compaction of formulations has also been seen to reduce the tabletability of the subsequent granules [Inghelbrecht and Remon, 1998b].

The process itself, whilst conceptually simple, is not fully understood and scale-up and manufacturing strategies are typically based on empirical processes and operator experience. It has not been the subject of intensive academic study, despite its increasing adoption by the pharmaceutical industry, where it is the preferred granulation route in a significant number of pharmaceutical companies [Miller, 1997, Miller and Sheskey, 2003].

In addition to the API a roller compaction formulation would usually contain a number of inert pharmaceutical grade excipients such as diluents and fillers (both plastically

deforming and brittle fracture materials), flow aids, disintegrants and lubricants. A typical dry granulation process route involves first blending the excipients (not including lubricants) with the API to produce a homogenous mixture [Ragnarsson *et al.*, 1979].

One excipient that is almost always added to the blend prior to roller compaction granulation is a material, which when used in the final blend of the tabletting process, acts as a lubricant. Magnesium stearate is well known for the adverse effects it imparts on the quality of the tablet product, such as decreased tensile strength [He *et al.*, 2007, Herting and Kleinebudde, 2008] and increased dissolution times [Kikuta and Kitamori, 1994, Yamamura *et al.*, 2009]. Furthermore, since magnesium stearate is obtained from natural sources (although animal sourced magnesium stearate is sometimes perceived as being more "effective", the pharmaceutical industry tends to use vegetable sourced material), its properties can be quite variable from one batch to the next and from vendor to vendor [Barra and Somma, 1996].

To minimise these deleterious effects the lubricant is generally added separately from the other excipients in the preblend. This lubrication blending stage is a critical process step, which needs to be carefully controlled to prevent over-lubrication. The strategy often used is to limit the amount of shear induced mixing and thereby limiting the formation of a lubricant film on the surfaces of the APIs/excipients within the formulation. Over blending the lubricated formulation at this stage can cause undesired quality issues.

After the lubrication blending stage the formulation is introduced into the hopper of the roller compactor where it is transported to the counter rotating rollers by the action of a screw feeder. Pressure is applied to the powder bed between the rollers and a ribbon compact is formed. Following roller compaction, the ribbon compact is broken up in a rotary mill and

the granules collected. Both the action of the screw feeder and the residence time within the rotary mill are possible locations where further uncontrolled shear induced mixing of the lubricated material may occur, and hence could have an unpredictable impact on the lubricity of the formulation, although this effect has previously not been studied.

The roller compacted, and milled, granule is usually further lubricated, to prevent adhesion to tablet dies and limit the friction between the die wall and tablet surface during tablet ejection. Again a similar strategy as discussed previously is used to limit the degree of shear induced mixing. The granule is then compacted into a tablet product, and it is at this stage that the uniquely beneficial properties of magnesium stearate are manifested. The final product is usually subjected to a coating process before being packaged and shipped.

## 1.2 Business case

As showed schematically in Figure 1-1, there are a number of challenges involved in the tablet manufacturing process. One such issue is the addition of magnesium stearate into the formulation as a lubricant. It would be of both interest and benefit to Bristol-Myers Squibb to be able to gain a greater understanding of the impact of magnesium stearate on the roller compaction process, and hence if possible move to alternative engineering solutions or formulation strategies to alleviate the well known issues of magnesium stearate on the final quality attributes of the tablet product.

In addition to the potential to streamline manufacturing processes, Bristol-Myers Squibb is also required by the industry regulatory bodies to develop greater formulation and process understating. Under the Quality by Design (QbD) paradigm, it is of vital importance to identify all critical process parameters (CPP) and any excipients which have the ability to influence the critical to quality attributes (CQAs) of the finished product [Wang *et al.*, 2010].

This means that any possible sources of variability must be investigated and if needed mitigation strategies should be identified. In terms of solid dosage forms (tablets) the CQAs are typically considered to be tensile strength, disintegration time, dissolution time and API stability. Pharmaceutical lubricants are well known to affect all of these parameters and furthermore they are a potential source of variability, since they are highly sensitive to mixing and they can have significantly different properties from vendor to vendor. Since the role of lubricants during roller compaction is not explicitly known, it is of interest to elucidate their effect on the roller compaction of pharmaceutical formulations and hence determine the actual need for their inclusion within the formulation.

## 1.3 Project aims

From its point of addition during the manufacturing process to its final use by the patient, a pharmaceutical solid dosage form contains the lubricant. During this time the magnesium stearate provides one essential role and that is during the tablet ejection phase the duration of which is in the order of milliseconds. Post tablet ejection the inclusion of the magnesium stearate within the tablet product elicits a number of undesirable product quality attributes. Furthermore, variability in the vendor supplied magnesium stearate can also lead to inconsistent manufacturing performance and may in some cases lead to product failure. Despite this, due to the increasing demands placed on the speed of the tablet manufacturing process, the role that magnesium stearate fulfils within those few milliseconds during the tabletting process is vital to the successful manufacture of solid dosage forms.

However, the role and necessity of lubricants during the initial phase of roller compaction is not quite as well defined. Compared to the tabletting process, roller compaction occurs on a much slower time scale where the compaction event takes place over the order of hundreds of milliseconds rather than units of milliseconds. Due to the continuous

nature of compaction during roller compaction the demands on powder performance such as rapid tablet die filling are not as essential. Furthermore, although easy removal of the roller compacted ribbon from the roll surface post compaction is desirable, as an intermediate product which is subsequently broken up in a mill the aesthetic finish of the ribbon will not impact the quality in the same way as the aesthetic finish of the tablet product. Beyond the need to prevent adhesion to the roll surface, the inclusion of magnesium stearate within the formulation prior to roller compaction is neither well understood nor well characterised. As such this thesis attempts to understand the role of lubricants during roller compaction and thus either provides a rationale for its inclusion in roller compaction formulations or present alternative methods by which its mechanistic action can be replicated.

The broad project aims are summarized schematically in Figure 1-2, more specifically the aims of this project were:

- To develop a greater understanding of the role of magnesium stearate within pharmaceutical formulations during roller compaction, and hence through scientific understanding replicate the beneficial effects that magnesium stearate may provide.
- To investigate in the first instance the application of external lubrication during the roller compaction process.
- To investigate the use of other lubricants and alternative formulation strategies as a substitute for magnesium stearate.

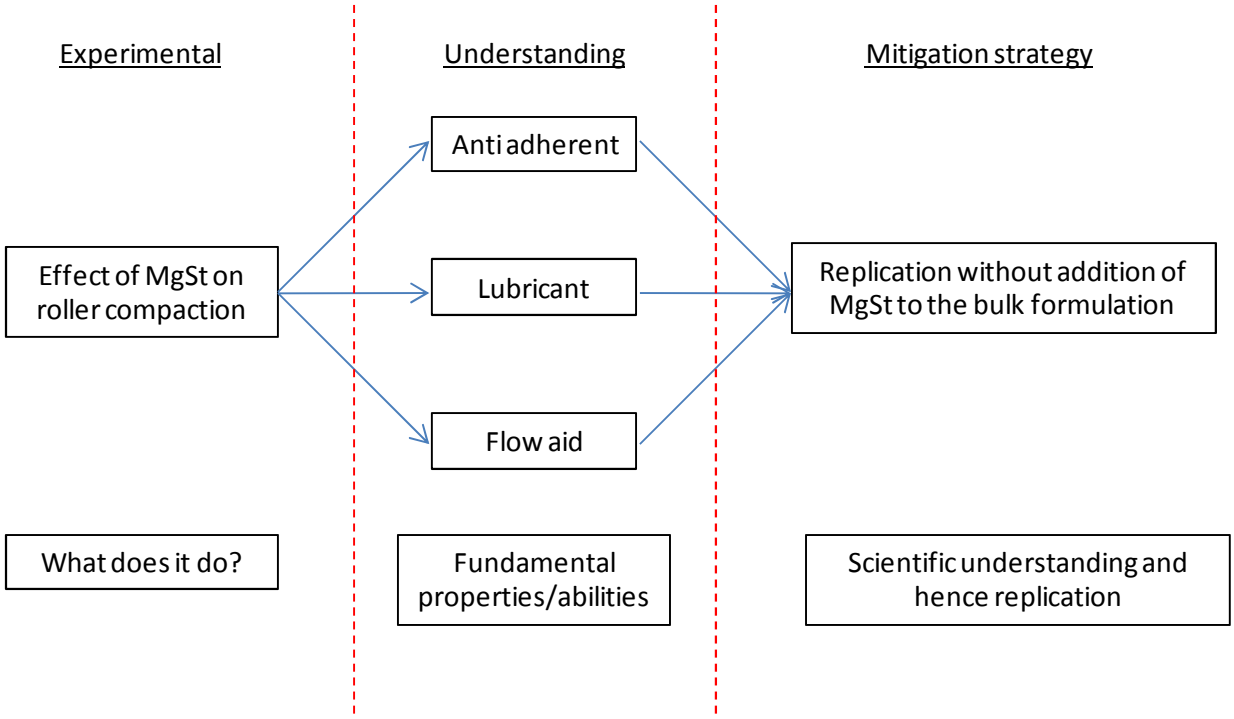


**Figure 1-2 – Schematic overview of the aims of the project (MgSt – magnesium stearate).**

In addition to the studies on the lubrication of roller compaction formulations, this thesis includes the statistical analysis of a data set generated by Bristol-Myers-Squibb. An initiative currently under investigation is the use of surrogate APIs. The basic premise behind the initiative is to investigate the applicability of a surrogate API as a method to gain insight into the manufacturability of newly developed drug products. The business need for such a technique is that newly developed drug products may be both in short supply/high demand and costly to produce. This makes extensive manufacturability studies requiring large amounts of drug product unfeasible. There is, however, a potential opportunity to use the large inventory of stock drug products that are no longer in development. If any drug product contained within the inventory is sufficiently similar in its material properties to the new drug product then it can be used as a surrogate. Manufacturability of the new drug can then be investigated using the surrogate inventory drug product. The aim of the surrogate API data analysis is therefore;

- To use a range of statistical techniques to test the surrogate API hypothesis.

- Compare the response data of two APIs deemed to have similar material properties and the response data of two APIs deemed to have dissimilar properties.

## 1.4 Overview of the thesis contents

The content of the thesis is set out as follows; In Chapter 2 the literature pertinent to the mechanism of both lubrication and roller compaction is reviewed. The chapter follows the format and expands on the information presented in Figure 1-1.

Details of all the materials and methods used throughout the study can be found in Chapter 3. A description of each method along with an explanation of the basic principles required to understand each analytical technique used is included. Where appropriate, to enable the reader to gain a greater understanding of the techniques used, suitable literature is referenced.

Chapter 4 is the first experimental chapter and seeks to understand the role of magnesium stearate during roller compaction. Roller compaction performance of a typical placebo formulation, both with and without magnesium stearate, is investigated using a full analysis of the properties of the feed powder, roller compacted ribbons and granule properties. Particular attention is focused on the impact of magnesium stearate on the formulation during the feeding and compaction process during roller compaction. A greater depth of understanding was permissible through the use of instrumented roll technology that allowed the collection of large amounts of information regarding the densification of material with the pre-nip area and compaction zone.

A potential technique which could be used to prevent powder adhesion during roller compaction is introduced in Chapter 5. The technique is used to directly apply magnesium

stearate to the surface of the rolls as a method to replicate the anti-adhesive properties that are inherent from including magnesium stearate within the formulation. A number of drug products from the Bristol-Myers Squibb portfolio which differ in their particle size and morphology have been used as model adhesive drug formulations to investigate the practical use of external lubrication.

Chapter 6 investigates the use of potential alternative lubricants and formulation strategies to replicate the lubrication properties of magnesium stearate. A relatively new co-processed excipient known commercially as LubriTose™ has been compared to sodium stearyl fumarate and glyceryl monostearate. The roller compaction performance of placebo formulations using the alternative lubricants and formulation strategies is compared to the results obtained in Chapter 4. The study then expands further by manufacturing tablets via the dry granulation process route to investigate the impact of inter-granular lubrication on both the tabletting process and the tablet properties in the absence of extra-granular lubrication.

Chapter 7 identifies a different strand of tabletting issues from Figure 1-1, and considers the statistical analysis of surrogate API use. As noted in sections 1.2 and 1.3, the ability to use a surrogate, particularly for new product dosage form development has significant industrial and business benefits.

Finally the general conclusions and recommendations for further work are presented in Chapter 8. For clarity and convenience a definition of symbols is provided within the text when they are first introduced.

# CHAPTER 2

# LITERATURE REVIEW

# CHAPTER 2

# LITERATURE REVIEW

## 2.1 Overview

An overview of the basic strategy used to manufacture tablets was provided in section 1.1. The purpose of this chapter is to expand on the tabletting issues and research questions presented in Figure 1-1. The chapter is set out as follows; the first section discusses the problems associated with the use of magnesium stearate during tabletting, a detailed review of the lubricating mechanism of magnesium stearate is provided as well as the reasons for its inclusion in a formulation prior to the tablet compaction process.

A detailed background on roller compaction theory is provided in the second section. In this section the common challenges encountered during formulation and process development are highlighted.

The third section concentrates on the primary strand presented in Figure 1-1, the current knowledge of the impact of magnesium stearate on roller compaction is reviewed and opportunities to answer the question posed are discussed. A review of a technique used to apply external lubrication during tabletting is given as well as a review of potential alternative

lubricants and formulation strategies that could be used to mitigate the known effects of magnesium stearate.

The final section follows the secondary strand presented in Figure 1-1. A review of the literature on the common approaches to formulation and process optimisation is provided. It is in this section that the background information and concept behind the surrogate API initiative is explained in greater detail.

## 2.2 Use of lubricants in pharmaceutical formulations

Lubricants are often considered as an essential excipient during pharmaceutical processes; their actions can be broadly split into three categories [Miller and York, 1988, Moody *et al.*, 1981, Shah and Mlodozeniec, 1977, Wang *et al.*, 2010]:

1. Glidants – promote flow.
2. Anti-adherents – prevent powder adhesion.
3. Lubricants – minimize die wall friction facilitating tablet ejection and scrape-off.

The following attributes are associated with good lubricants [Wang *et al.*, 2010]:

1. Low shear stress.
2. Relatively high melting point.
3. Large specific surface area/small particle size.
4. Amphiphilic activity.
5. Film forming tendency.

In addition Miller and York described the ideal properties of pharmaceutical lubricants, suggesting that the ideal lubricant should [Miller and York, 1988]:

1. Be effective in small quantities.

2. Have no adverse effect on the formulation.
3. Be inert and cosmetically acceptable with respect to the other ingredients.

Unfortunately no such lubricant exists. The aim of the following section is to gain a greater understanding of the mechanism of lubrication and understand why they do what they do and why they exhibit well known deleterious effects on the properties of tablets; specific attention will be paid to magnesium stearate.

### 2.2.1 Mechanism of lubrication

The primary function of lubricants in pharmaceutical formulations is to act as a friction reducing agent and as an anti-adhesive; as such it is important to first understand the concept of friction and adhesion.

#### 2.2.1.1 Frictional theory

Friction is the resistive force that arises when two solid objects, which are initially in contact, are displaced relative to each other and parallel to the plane of contact. The frictional force to be overcome is proportional to the area of contact, as given in Equation 2-1. However, the area of contact is a difficult parameter to measure since particles are seldom atomically smooth. Instead the surface topography is composed of asperities. When two particles come into contact the real area of contact is determined by the deformation of these asperities under the load.

$$F = S \times A \qquad \textbf{Equation 2-1}$$

where F is the frictional force, S is the shear strength of the junction and A is the surface area in contact.

A coefficient of friction (μ) is defined as the ratio between the shear strength of the junction (S) and the yield strength of the softer material (W) as given in Equation 2-2:

$$\mu = \frac{S}{W} \qquad \textbf{Equation 2-2}$$

It is therefore the role of the lubricant to reduce the strength of the shear junction formed between two particles and hence lower the frictional force required to separate the particles.

In fluid lubrication two contacting particles will be completely separated from each other by the fluid lubricant and hence the frictional force required to displace the particles relative to one another will depend solely on the viscosity of the fluid lubricant. However, in powder lubrication the contacting surfaces are not fully separated and hence the frictional force will depend both on the properties of the lubricant and of the underlying excipient surfaces. This type of lubrication is known as boundary lubrication, and in this case the friction force is given by Equation 2-3 [Moody *et al.*, 1981]:

$$F = \alpha A \times S_s + (1 - \alpha) A \times S_l \qquad \textbf{Equation 2-3}$$

where α is the fraction of contact between excipients over which the shear junction is formed and the subscripts s and l denote the shear strength of the surface and the lubricant respectively.

The mechanism for boundary lubrication is demonstrated schematically in Figure 2-1, in boundary lubrication the underlying surfaces of particles are still in contact. The frictional force between the underlying surfaces is higher than between the lubricant particles. The aim of boundary lubrication, therefore, is to minimise the actual contact area between two particles by forming a complete layer of lubricant over the surface. From Equation 2-3, it can

be inferred that the frictional force is minimised when the fractional contact area between excipients surfaces is minimised.

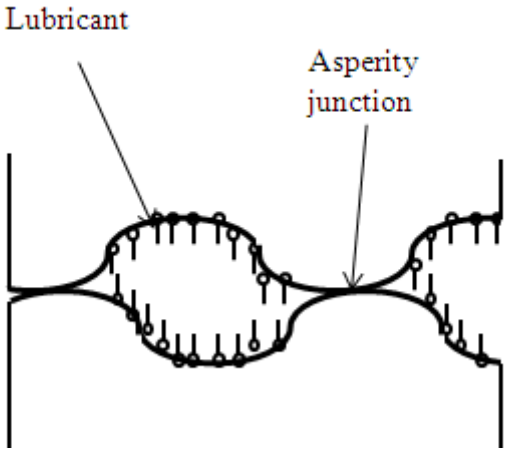


**Figure 2-1 – Schematic representation of the boundary lubrication.**

#### 2.2.1.2 Frictional theory applied to powder failure

If a force is applied to a block granular material, for small values of applied force there will be a small amount of elastic deformation. However, once the force reaches a critical value the material will divide into two blocks which are able to slide past one other. An assumption is made that when a powder fails it does so as two rigid blocks separated by a narrow plastic zone. The so called plastics zone is considered to be of negligible width and hence is often referred to as the yield, slip, or failure plane [Nedderman, 1992]. Shear stresses acting on the slip plane are independent on the extent or rate of deformation; however, it is dependent on the normal stress acting on the plane as shown in Equation 2-4:

$$\tau = f(\sigma) \qquad \textbf{Equation 2-4}$$

where τ is the applied shear stress and σ is the applied normal stress.

There exist a number of materials for which this relationship is linear, such materials are known as ideal Coulomb materials, and the Coulomb yield criterion takes the form shown in Equation 2-5:

$$\tau = \mu\sigma + c$$ **Equation 2-5**

where c is constant related to the critical stress above.

Equation 2-5 is an expression for the shear strength of the material; the two parameters of interest are the cohesion between the particles and the frictional resistance between the particles. In terms of powder failure it is more desirable for the powder block to exhibit low levels of shear strength. Therefore to improve flow of powders the added lubricants should reduce both the cohesion and internal friction.

#### 2.2.1.3 Adhesion theory

The most widely accepted adhesion model is that proposed by Johnson, Kendall and Roberts widely known as the JKR theory, [Johnson *et al.*, 1971, Wang *et al.*, 2010]. Based on the JKR theory the radius of the contact area (a) is given by Equation 2-6. Due to the adhesion that occurs between particles in contact with each other, or in contact with a surface, separation cannot take place until a critical pull-off force ($F_s$) is reached, as given in Equation 2-7.

$$a = \left(\frac{R}{K}\left[F + 3\pi R\Delta\gamma + \sqrt{6\pi R\Delta\gamma F + (3\pi R\Delta\gamma)^2}\right]\right)^{1/3}$$ **Equation 2-6**

$$F_s = \frac{3}{2}\pi R\Delta\gamma$$ **Equation 2-7**

Where R is the equivalent radius of two spheres in contact given by Equation 2-8, K is the equivalent elastic constant of the two spheres given by Equation 2-9, $\Delta\gamma$ is the work of adhesion given by Equation 2-10 and F is the external force.

$$R = R_1R_2/(R_1 + R_2)$$ **Equation 2-8**

$$\mathrm{K} = \frac{4}{3}\left(\frac{1-\upsilon_1{}^2}{\mathrm{E}_1} + \frac{1-\upsilon_2{}^2}{\mathrm{E}_2}\right)^{-1}$$ **Equation 2-9**

$$\Delta\gamma = \gamma_1 + \gamma_2 - \gamma_{12}$$ **Equation 2-10**

where, υ is the Poisson's ratio, E is the elastic modulus, $\gamma$ is the surface energy and $\gamma_{12}$ is the interfacial surface energy. The subscripts 1 and 2 refer to sphere 1 and 2 respectively.

Lee, suggests that the adhesion force ($F_{ad}$) can be considered as the summation of the Van der Waals ($F_{van}$), capillary ($F_{cp}$) electrostatic ($F_{el}$) and chemical bonding ($F_{cb}$) forces, as given in Equation 2-11 [Lee, 2004]:

$$F_{ad} = F_{van} + F_{cp} + F_{el} + F_{cb}$$ **Equation 2-11**

In addition to Equation 2-11, the geometric properties of the particle will also affect the real area of contact and hence the adhesive force. Further complicating the issue of adhesion is that the surface roughness of particles reduces during compaction and hence the apparent adhesive forces increase during compaction due to increasing contact area.

Therefore, in terms of reducing adhesive forces, a lubricant must be able to reduce the intrinsic adhesive interactions and reduce the contact areas between particles and equipment surfaces.

### 2.2.2 Properties of magnesium stearate

Magnesium stearate is by far the most commonly used lubricant in the pharmaceutical industry since it exhibits most attributes associated with good lubricants. The polar head of the magnesium stearate molecule, as shown in Figure 2-2, adheres at the periphery of the particle/equipment surface whilst its hydrocarbon chain protrudes perpendicular to the surface [Miller and York, 1988].

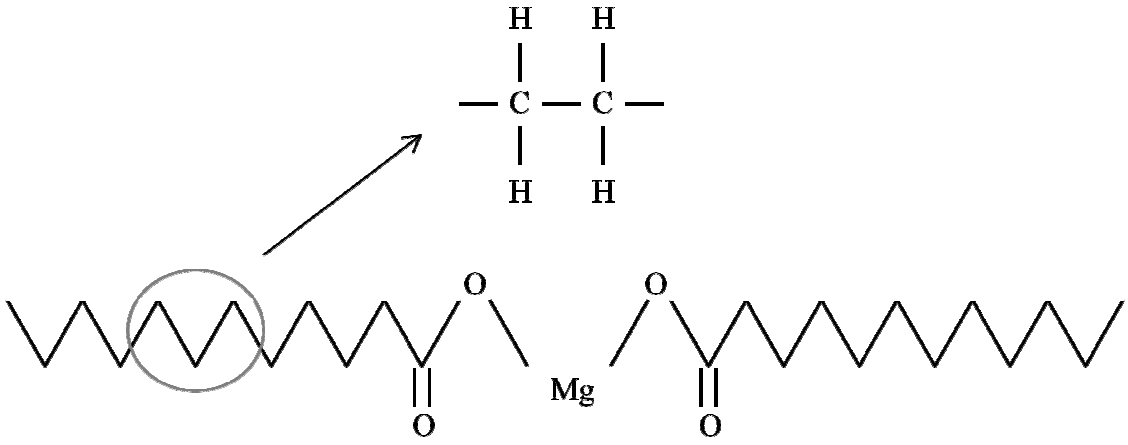


**Figure 2-2 – schematic representation of a molecule of magnesium stearate.**

Magnesium stearate is considered to be a variable product. It can be sourced from either bovine or vegetable sources, but since the increase in serious and life threatening bovine diseases; such as bovine spongiform encephalopathy (BSE), manufacturers and pharmaceutical companies have switched to vegetable sources [Hamad *et al.*, 2008]. However, changes in magnesium stearate source can produce unpredictable and undesirable affects on both the lubrication efficacy during processing and on the quality attributes of the final product [Barra and Somma, 1996, Rao *et al.*, 2005].

Magnesium stearate is manufactured by either the reaction of a stearic acid with a magnesium compound or the reaction of magnesium chloride with a sodium or ammonium stearate [Bracconi *et al.*, 2003]. Of the variables involved during the manufacture of magnesium stearate the most important are considered to be the medium pH and the drying phase. The medium pH has been observed to impact the particle morphology where an alkaline pH leads to a more amorphous and irregular shape of particles, whilst an acidic pH produces more plate-like structures [Ertel and Carstensen, 1988, Miller and York, 1985a, Miller and York, 1985b]. The drying and cooling phase of the precipitate also affects the crystal structure. Furthermore, commercial magnesium stearate is not a pure chemical entity and contains a portion of magnesium palmitate as well as other stearic acids. As such a

complete understanding of the properties of magnesium stearate and its effect on frictional performance as well as its affect on the quality attributes of the final product requires an understanding of the solid state properties of magnesium stearate.

A number of researchers have investigated the variability of the solid state (molecular, particle and bulk level) properties of magnesium stearate; fewer have attempted to link these properties to the actual lubrication performance of magnesium stearate. There are a number of contradictions and differences of opinion in the literature. However, there is some agreement that particle size and crystal habit are amongst the most influential of the parameters.

#### 2.2.2.1 Particle size

The primary particle size of magnesium stearate is often difficult to measure due to the cohesive nature of magnesium stearate, meaning that it often exists as agglomerates. However, the particle size of magnesium stearate is often regarded as one of the most important parameters and determines both lubricating performance and effect on quality attributes of the final tablet product. Attempts to disperse the agglomerated magnesium stearate into its primary particle size vary from researcher to researcher. Some examples include; ultrasonification in water with stirring at 75 rpm [Rao *et al.*, 2005]; dispersion in water with the aid of the surfactant Tween 20 [Barra and Somma, 1996]; dispersion in isotonic saline containing 0.004% sodium lauryl sulphate with sonification [Billany and Richards, 1982]; dispersion in isopropanol with the aid of the surfactant Tween 20 [Phadke and Eichorst, 1991]; other researchers simply state that particle size was measured without indicating the dispersion method used [Patel *et al.*, 2007].

A number of researchers have concluded that smaller particle size implies improved lubrication performance. For example Barra and Somma investigated the lubrication potential

of 13 lots of magnesium stearate; they concluded that of the lots investigated those with a smaller particle size elicited an improvement in lubricating performance [Barra and Somma, 1996]. Furthermore it was observed that on milling the lubricating potential of the larger particle size magnesium stearate was significantly improved. In contradiction to this work Rao *et al.*, concluded that magnesium stearate with a small primary particle size does not explicitly imply an improvement in lubrication performance since smaller particles may have an increased tendency to agglomerate [Rao *et al.*, 2005]. Deagglomeration of magnesium stearate would require increased shearing force and may explain to some degree why the effect of magnesium stearate on scale up (where shear forces will be larger than at the laboratory/pilot scale) is not always straightforward to predict. Agglomeration potential was investigated using zeta potential [Hamad *et al.*, 2008]; it was concluded that magnesium stearate with a high absolute zeta potential showed less tendency to agglomerate.

The theory underlying the improved lubrication performance of magnesium stearate with decreased particle size is based on surface area coverage. Magnesium stearate with a smaller particle size will more effectively coat the surface of host excipients creating a more complete film and thus diminishing the contact points between excipients thus reducing the overall friction given in Equation 2-3. Conversely, magnesium stearate with a larger particle size will not create a complete film coating on the host excipients as such the strong excipient-excipient bonds are formed. Experimental evidence of this was reported by Barra and Somma; it was observed from SEM images of the failure plane of tablets that tablet fracture occurs at the contact points between the particles when magnesium stearate with a small particle size was used, whereas tablet fracture occurred within the particles when magnesium stearate with a large particle size was used [Barra and Somma, 1996].

#### 2.2.2.2 Crystal habit

The crystal habit of magnesium stearate has been measured by a number of researchers using a diverse range of techniques. It is reasonably well agreed that the crystal habit of magnesium stearate is an important attribute which in part determines the lubricating performance of magnesium stearate. Despite its hydrophobic nature magnesium stearate can exist in a number of different hydrated forms; anhydrous, monohydrous, dihydrous, and, trihydrous forms have all been identified. Commercial magnesium stearate is often an unspecified mixture of hydrates. The hydrate form influences the angle of inclination of the hydrocarbon chain relative to the plane of the magnesium atom head groups [Ertel and Carstensen, 1988] and this in turn affects the long d-spacing. Water associated with the crystal lattice has been measured using the differential scanning calorimetry (DSC) and thermogravimetric analysis (TGA) [Ertel and Carstensen, 1988, Rao *et al.*, 2005], whilst other researchers have used X-ray diffraction [Barra and Somma, 1996, Bracconi *et al.*, 2003, Ertel and Carstensen, 1988, Miller and York, 1985b, Rao *et al.*, 2005, Swaminathan and Kildsig, 2001, Wada and Matsubara, 1994].

The lubrication performance of magnesium stearate is in part dependent upon the interaction of the crystal lattice since it is this interaction which determines the shearing properties of the magnesium stearate. It has been suggested that the association of water into the long lattice of the crystal decreases the shearing force required to cleave the magnesium stearate [Wada and Matsubara, 1994]. Furthermore the anhydrous form of magnesium stearate is associated with a more irregular structure [Ertel and Carstensen, 1988] which imparts less lubricating performance, whilst the dihydrate form of magnesium stearate is associated with a highly crystalline structure [Barra and Somma, 1996].

An interesting property of the hydrate forms is that the dihydrate form of magnesium stearate is not an intermediate product between the anhydrous and trihydrate forms. It has been observed that hydration of the anhydrous form (at 70% RH) immediately forms a trihydrate and that subsequent dehydration converts the trihydrate form immediately back to the monohydrate form [Swaminathan and Kildsig, 2001]. In addition the uptake of moisture elicits a change in crystal form; it was observed using x-ray diffraction that amorphous magnesium stearate becomes more crystalline by taking water into the crystal lattice [Swaminathan and Kildsig, 2001].

#### 2.2.2.3 Lubricant distribution on the surfaces and within the blend

Due to its lamella structure magnesium stearate is often envisaged as a 'deck of cards', with a remarkably low resistance to shear stress, hence the mechanism of magnesium stearate mixing is usually referred to as the stack of cards theory [Shah and Mlodozeniec, 1977]. Solid lubricants such as magnesium stearate are considered to be adsorbed to the surface of particles and during prolonged mixing the magnesium stearate 'spreads' over the surface of the particles due to delamination and deaggregation of the primary magnesium stearate particles. This type of uniform surface coverage is similar to a Langmuir-type adsorption. The Langmuir equation is given in Equation 2-12, a plot of p/q vs. p which yields a straight line confirms for many systems the correctness of Langmuir's theory of monomolecular adsorption.

$$\frac{p}{q} = \frac{1}{K_1} + \frac{K_2 p}{K_1} \qquad \textbf{Equation 2-12}$$

where p is the equilibrium pressure of the gas, q is the quantity of gas adsorbed per unit surface or unit mass of solid and $K_1$ and $K_2$ are constants.

The validity of a Langmuir-type adsorption of magnesium stearate onto the surface of host particles was investigated by Hussain *et al.* using SEM and energy-dispersive x-ray to obtain a semi-quantitative measure for magnesium stearate coverage on the surface of host sodium chloride particles [Hussain, 1988]. It was observed that a plot of mixing time/surface coverage (p/q) vs. mixing time (p) yielded a straight line. It was concluded from this data that magnesium stearate is at least initially adsorbed as a monolayer onto the surface of a host sodium chloride particle. Following further mixing it was observed that the magnesium stearate was non-uniformly distributed across the host particle surface and was concentrated at gross crystal defects and ridges, suggesting that the lubricant film formed was both molecular and particulate in nature. It should be noted that based on Equation 2-12; p/q vs. p would not pass through the origin at time t=0 minutes, as such it is likely that at low mixing times the mixing time/surface coverage would deviate from the Langmuir theory straight line.

Based on a literature survey Roblot-Treupel concluded that there are three possibilities for the distribution of magnesium stearate on the surfaces of excipient particles that researchers tend to favour [Roblot-Treupel and Puisieux, 1986]:

1. Formation of a monomolecular film – the inter-particulate surfaces are separated only by a few molecules of stearate, friction depends on the lubricant and the underlying surfaces.
2. Formation of a uniform continuous layer of the mono-particulate type – inter-particulate surfaces are separated by a relatively thick layer of magnesium stearate and friction depends only on the lubricant.
3. Progressive filling of the cavities – impact of magnesium stearate associated with the equalisation of the surfaces and hence diminished contact points.

The ability to spread over the surface of the host particles and the low resistance to shear stress inherent of magnesium stearate complies with the fundamental properties required for a good boundary lubricant as demonstrated by Equation 2-3 on page 16.

It is the spreading of magnesium stearate over the excipient and API surfaces which results in the deleterious effects on the tablet product. As such, the typical strategy employed during lubrication of pharmaceutical formulations is to blend the formulation to homogeneity prior to addition of the lubricant. Subsequently, upon the addition of the lubricant, a formulation is mixed for a small number of revolutions such that the lubricant is non-homogeneously distributed in order to maximise the beneficial attributes afforded by the presence of magnesium stearate within the formulation whilst attempting to minimise the adverse effects. As suggested by Kushner and Moore two zones can be identified during the mixing of a lubricant [Kushner IV and Moore, 2010]:

(1) A highly sensitive domain at the beginning where the extent of lubrication and product quality attributes can change significantly due to a small change in processing conditions.

(2) A domain where extent of lubrication and product quality attributes is affected only by a significant change in processing conditions.

Manufacturing of pharmaceutical formulations is typically conducted within the highly sensitive zone and as such additional mixing during downstream processes, which is often overlooked, could potentially have an impact on the overall product quality.

#### 2.2.2.4 Ideal lubricant properties

The ideal solid state properties for magnesium stearate were concluded to be [Rao *et al.*, 2005]:

| | |
|---|---|
| Bulk Level | Absence of agglomerates. |
| Particle Level | Reduced particle size. |
| | Increased specific surface area. |
| | Plate-like crystal habit. |
| Molecular Level | Dihydrate. |
| | Increased d-spacing. |
| | Water present in two thermodynamic states. |

### 2.2.3 Known issues of magnesium stearate on the tablet properties

The effect of magnesium stearate on tablet properties is well documented in the literature, and it is well known both from the theoretical discussion above and in practice that magnesium stearate can elicit deleterious properties on the critical to quality attributes of the final tablet product. Two of the most important tablet properties are tablet hardness and disintegration/dissolution time. The experimental literature investigating the effect of magnesium stearate on tablet properties is discussed in the subsequent sections.

#### 2.2.3.1 Tablet hardness

Tablet hardness is a critical to quality tablet property; the compressed tablet must have sufficient strength to be able to withstand subsequent handling processes, such as tablet coating, packaging, transportation and any handling conditions imposed on the tablet from the end user.

It is well known that magnesium stearate, in sufficient quantity, causes a deleterious effect on the tablet strength. Furthermore the extent of this reduction is in some way related to the properties of the magnesium stearate powder and the degree of shear induced mixing during processing. However, the properties of the formulation to be lubricated will also determine the relative sensitivity to magnesium stearate. For example, Almaya and Aburub investigated the effect of magnesium stearate on the initial particle size and the deformation

characteristics of a formulation in which three typical pharmaceutical excipients were investigated: microcrystalline cellulose, starch and dicalcium phosphate. It was observed that the tablet strength of unlubricated microcrystalline cellulose was not dependent upon the initial particle size, however, after lubricating with magnesium stearate the tablet tensile strength of microcrystalline cellulose with the smaller initial particle size was less affected than that of the larger particle size. With starch, a plastic material it was found that the smaller initial particle size produced tablets with greater tensile strength both with and without magnesium stearate [Almaya and Aburub, 2008]. In stark contrast the tablet tensile strength of dicalcium phosphate, which is a brittle material, was observed to be independent of particle size regardless of magnesium stearate content. A number of researchers have also observed that the tensile strength of tablets compacted using plastically deforming materials is more sensitive to magnesium stearate than tablets compacted from materials which exhibit brittle fracture [Almaya and Aburub, 2008, Zuurman *et al.*, 1994, Zuurman *et al.*, 1999].

Zuurman *et al* investigated the effect of magnesium stearate on the porosity expansion of various pharmaceutical excipients. The relaxation of a tablet is a balance between the stored elastic energy (driving force for expansion) and the particle bonding formed during compaction (counteracting force). Microcrystalline cellulose was observed to undergo increased porosity expansion after tabletting compared to the brittle material γ-sorbitol. The increase in porosity was hypothesised to be due to the interaction between the particles. The interaction between two excipient particles in contact (A-A) will be significantly stronger than the interaction between a lubricant particle and an excipient particle (A-B) and the interaction of two lubricant particles (B-B). In the case of an excipient with plastic deformation characteristics well mixed with magnesium stearate the A-B and B-B interactions will dominate both before and after compaction; however, for a brittle material whilst the A-B and

B-B interactions will dominate before compaction, upon compaction the particle will fracture generating clean surfaces which will allow the A-A interactions to dominate [Zuurman *et al.*, 1999].

As well as deformation characteristics the apparent sensitivity of tablet strength to magnesium stearate will depend on the specific surface area of the formulation ingredients. Van Veen *et al.* investigated the effect of magnesium stearate on the tablet strength of microcrystalline cellulose, silicified microcrystalline cellulose and a physical mixture of silicon dioxide and microcrystalline cellulose. It was observed that the physical mixture of silicon dioxide and microcrystalline cellulose produce tablets of superior tablet tensile strength (at equivalent magnesium stearate addition levels), and this was attributed to the high surface area of the silicon dioxide 'mopping' up the magnesium stearate particles [Van Veen *et al.*, 2005].

#### 2.2.3.2 Powder hydrophobicity and tablet disintegration/dissolution time

The deleterious effect of magnesium stearate on the dissolution profiles of tablets is well known and is often explained by the magnesium stearate developing a hydrophobic film coating around the host excipient/API particles which inhibits ingress of water into the tablet. Llusa *et al.* used the Washburn method to investigate the effect of magnesium stearate on the rate at which fluid permeates through a powder mixture of lactose and microcrystalline cellulose. It was observed that the both increased amount of magnesium stearate and the increased strain applied during mixing have a deleterious effect on the water permeability of the powder; however, the shear rate was observed to have a less significant effect [Llusa *et al.*, 2010].

Dissolution of the tablet product is of the upmost importance since this is one of two potential rate limiting steps to drug adsorption. Magnesium stearate is well known for its hydrophobic properties and hence its impact of reducing wettability of a tablet formulation. Such reduced tablet wettability can lead to water 'sitting' on the surface of the tablet rather than penetrating into the tablet and this in turn can lead to an increase in the drug dissolution time of tablet products. A number of researchers have investigated the affect of magnesium stearate on drug dissolution and they are summarised in Table 2-1

**Table 2-1 – Effect of magnesium stearate on the dissolution profile of some selected APIs from the literature**

| Drug Product | magnesium stearate (% w/w) | Dissolution media | Effect on dissolution | Reference |
|---|---|---|---|---|
| Acetaminophen | 0.1 – 3.0 % | Phosphate buffer (pH 6.8) | Significant rate reduction at levels > 0.1 % w/w | [Uchimoto *et al.*, 2011] |
| Ibuprofen | 0.0 – 5.0 % | Phosphate buffer (pH 6.8) | Rate unaffected at 1.0 %, but reduced at 5 % | [Rashid *et al.*, 2010] |
| Ranitidine Hydrochloride | 0.8 – 1.1 % | Artificial gastric juice (pH 1.2) | Rate reduction at higher level | [Uzunović and Vranić, 2007] |
| Ketorolac Tromethamine | 2.25 % | - | Dissolution time increase with mixing time | [Chowhan and Chi, 1986] |
| Hydrochlorothiazide | 1.0 % | Hydrochloric acid | Increased dissolution time of capsules at end of run compared to beginning | [Desai *et al.*, 1993] |
| Aztreonam | 1.0 % | Hydrochloric acid | As above but to a lesser degree | [Desai *et al.*, 1993] |

There is a widespread agreement that inclusion of magnesium stearate affects the dissolution rate of tablet products. However, the magnitude of the effect depends on the solubility of the drug product. Hydrophilic APIs are less affected by the presence of magnesium stearate than hydrophobic APIs.

The affect of mixing time on the API dissolution rate can be observed during capsule filling, where tablets from the start of the run dissolve faster than those from the end of the run, attributed to over lubrication in the feed frame [Desai *et al.*, 1993].

The increase in dissolution time as a result of adding magnesium stearate to the tablet formulation has led to research into magnesium stearate as an excipient for extended release formulations. Typical extended release dosage forms require expensive excipients to create a slow release matrix. The use of magnesium stearate has been observed to prolong the dissolution rate of extended release drugs [Dürig and Fassihi, 1997, Fukui *et al.*, 2001]. However, in other cases the drug dissolution is limited by the polymer matrix rather than the effect of magnesium stearate on water uptake [Sheskey *et al.*, 1995].

### 2.2.4 Role of magnesium stearate during tablet manufacturing

#### 2.2.4.1 Effect on the formulation properties

Powder flow properties are of the upmost importance in pharmaceutical manufacturing processes. For tabletting, reproducible and reliable die filling is a necessity to achieve constant tablet weight and hence content uniformity. A number of techniques have been used extensively to study the flow properties of pharmaceutical powders; such as, gravitational displacement rheometer (GDR) [Faqih *et al.*, 2007b, Mehrotra *et al.*, 2007, Pingali *et al.*, 2009, Vasilenko *et al.*, 2011], shear cell [Liu *et al.*, 2008, Podczeck and Miah, 1996, Shah *et al.*, 2008], powder rheometers (FT4, texture analyser) [Freeman, 2007, Freeman *et al.*, 2009, Léonard and Abatzoglou, 2010, Navaneethan *et al.*, 2005, Shah *et al.*, 2008, Zhou *et al.*, 2010b], angle of repose [Shah *et al.*, 2008, Zhou *et al.*, 2010a] and bulk and tapped density ratios [Liu *et al.*, 2008, Shah *et al.*, 2008].

GDR has been used to investigate the effect of magnesium stearate on the avalanching behaviour of pharmaceutical formulations. In the GDR technique, powder is loaded into a cylindrical drum and rotated on a load cell, as the powder rotates avalanches occur which results in a change in the centre of mass inside the rotating drum. The size of the avalanche, and hence the magnitude of the shift in centre of mass, is related to the cohesivity of the material. Magnesium stearate was observed to improve the flow of initially cohesive materials such as regular lactose and microcrystalline cellulose (Avicel 101 grade). However it was observed to have limited effect on initially relatively free flowing material such as flast-flo lactose; furthermore the biggest improvement in flow properties was as a result of the initial addition of 0.25% w/w magnesium stearate to the formulation; further increases in magnesium stearate level elicited only minor improvements in flow [Faqih *et al.*, 2007b].

Materials which showed poor flow properties were observed to develop larger avalanches and thus the powder bed underwent a greater degree of dilation. The difference in avalanche size was attributed to the density of cohesive bonds. In the case of a free flowing material the interaction between the powder particles is weak and they are easily disrupted. However, in a cohesive material the interactions are considerably stronger and hence the powder bed must expand further to reduce the density of these interactions before the powder can flow in the form of an avalanche [Pingali *et al.*, 2009]. Inclusion of magnesium stearate in the formulation reduces the strength of the interaction forces and hence limits the bed expansion required before avalanching occurs. Interestingly it was observed using GDR that the improvement in flow properties was greatest when both magnesium stearate and colloidal silica were added to the formulation; however, when added alone the colloidal silica elicited a greater improvement in flow than magnesium stearate.

A powder rheometer, FT4, has been used to measure the flowability of pharmaceutical formulations. During testing a blade is twisted helically through a bed of powder, the forces acting on the blade are continuously recorded and the total work done to move the blade through the powder bed is reported [Freeman, 2007, Freeman *et al.*, 2009]. The cohesivity of the material is related to the amount of work required to move the blade through the powder bed where a higher amount of work required is indicative of a more cohesive material. Navaneethan *et al.*, investigated the use of powder rheometry to determine the effect of lubrication on the flow properties of granules prepared from a number of cohesive APIs. It was observed that the addition of lubricants resulted in a significant reduction in the work done to move the paddle through the powder bed. Furthermore the biggest reduction was observed at the initial introduction of magnesium stearate to the formulation, and further increases in magnesium stearate concentration had little effect on reducing the work done [Navaneethan *et al.*, 2005].

Shear cells have also been used to investigate the effect of magnesium stearate on flow properties of lubricants. Translational shear cells were first developed by Jenike [Jenike and Shield, 1959]; the original design was limited by the finite amount of shear which could be applied to the powder bed [Carr and Walker, 1968]. A revised shear cell design uses a rotating shear head which allows the application of very high shear permitting steady state failure to be achieved. Two types of rotational shear cells are available; annular (such as the schulze shear cell [Bindhumadhavan *et al.*, 2005, Mansa *et al.*, 2008] or Brookfield shear cell [Saw *et al.*, 2013]) and a full area rotational shear cell (such as FT4 [Freeman *et al.*, 2009] and Peschl shear cell [Schmitt and Feise, 2004]). A number of researchers have reported that addition of magnesium stearate elicits an improvement in the flow of properties of powder formulations [Podczeck and Miah, 1996, Vasilenko *et al.*, 2011, Zhou *et al.*, 2010a, Zhou *et al.*, 2010b].

However, Léonard and Abatzoglou cautioned against the use of such techniques since if the operator does not remain vigilant the powder can fail as a monolithic block against the equipment surfaces rather than within the powder itself. They showed that modification of the bottom platform to increase friction can help prevent powder failing as a monolithic block [Léonard and Abatzoglou, 2010]. Occurrence of slip at the instrument wall/powder surface interface is more likely following the addition of magnesium stearate (or any other lubricant) into the powder sample.

Angle of repose is a measurement of the angle that a heap of powder poured through a funnel forms with a surface. The more cohesive a material the more stable the heap will become and hence the larger the angle formed. It has been observed [Zhou *et al.*, 2010a] that traditional mixing of magnesium stearate with lactose monohydrate elicited no change in angle of repose (compared to the untreated lactose). However, after mechanofusion (an energy intensive process whereby host materials are dry coated with guest particles via high shear mixing and impact collisions) with magnesium stearate the angle of repose was significantly reduced indicating an improvement in flow. Interestingly, the addition of colloidal silica had a significant effect on the angle of repose even after traditional low shear mixing.

Vromans and Lerk investigated the effect of magnesium stearate on the densification properties of directly compressible formulations. It was observed that whilst in some cases the effect of magnesium stearate was to reduce the compactibility of the formulation, in others the effect was to increase the compactibility [Vromans and Lerk, 1988]. This increase in compactibility was attributed to the increased densification kinetics elicited by the incorporation of magnesium stearate. However, this observation was dependent upon the material's sensitivity to magnesium stearate; materials like amylase and anhydrous lactose

were affected by magnesium stearate even though an increase in densification was observed. Liu *et al.* observed that addition of magnesium stearate to pure ibuprofen powder elicited an improvement in the Hausner ratio and an increase in the initial poured bulk density [Liu *et al.*, 2008]. Furthermore, Mehrotra *et al.*, also observed the effect of magnesium stearate on the densification properties of a mixture of microcrystalline cellulose and lactose; again the amount of shear applied during mixing had a much more significant impact than the rate of shear [Mehrotra *et al.*, 2007].

#### 2.2.4.2 Effect on the process

Friction between the die surface and tablet surface during the ejection of tablet compacts from the tablet press is a major issue during tablet manufacture. The force required to overcome this friction, often referred to as the ejection force, can have an undesirable effect on the quality of the tablet product, such as capping and lamination. A number of researchers have investigated the effect of magnesium stearate on the tabletting process, and it is widely reported that reduction of the ejection force of tablets during tablet ejection results in fewer processing issues [Korachkin *et al.*, 2008, Léonard and Abatzoglou, 2011, Rashid *et al.*, 2010, Takeuchi *et al.*, 2005]. Some researchers have investigated the effect of magnesium stearate on other tablet compaction properties such as the transmission of forces through the powder bed and maximum and residual die wall force [Takeuchi *et al.*, 2005]. It was observed that the addition of magnesium stearate increases the maximum die wall force whilst reducing the residual die wall force, demonstrating improvement in compaction properties.

## 2.3 Roller compaction

### 2.3.1 Roller compaction theory

Roller compaction is a dry granulation method in which a powder blend is compacted between two counter rotating rolls forming a ribbon compact, which is subsequently milled into granules of a desired size range. Unlike wet granulation, roller compaction does not require the use of a liquid binder and thus it is suitable for actives that are sensitive to moisture. Additionally since there is no need for a drying stage, it is also more suitable for actives that are sensitive to heat [Kleinebudde, 2004], whilst frictional affects will generate heat during roller compaction, the heating is less prolonged.

A typical roller compactor consists of a powder feed system, either gravity fed or force fed, which can be mounted horizontally, vertically or at an incline. The purpose of the feeding system is to transfer powder blend from the hopper to the rolls. An additional function of the screw feeder is the removal of air and pre-densification of the powder blend; this can be assisted by the use of vacuum de-aeration.

Due to the resistance to volume decrease during compression, the powder forces the rolls to move apart. Roll separation is opposed by the application of a hydraulic force on the rollers. The steady-state roll gap (at a fixed roll speed) for a particular formulation is therefore an equilibrium between the amount of powder being fed to the rolls, *i.e.* feed auger rotational speed, and the hydraulic force applied to the rolls.

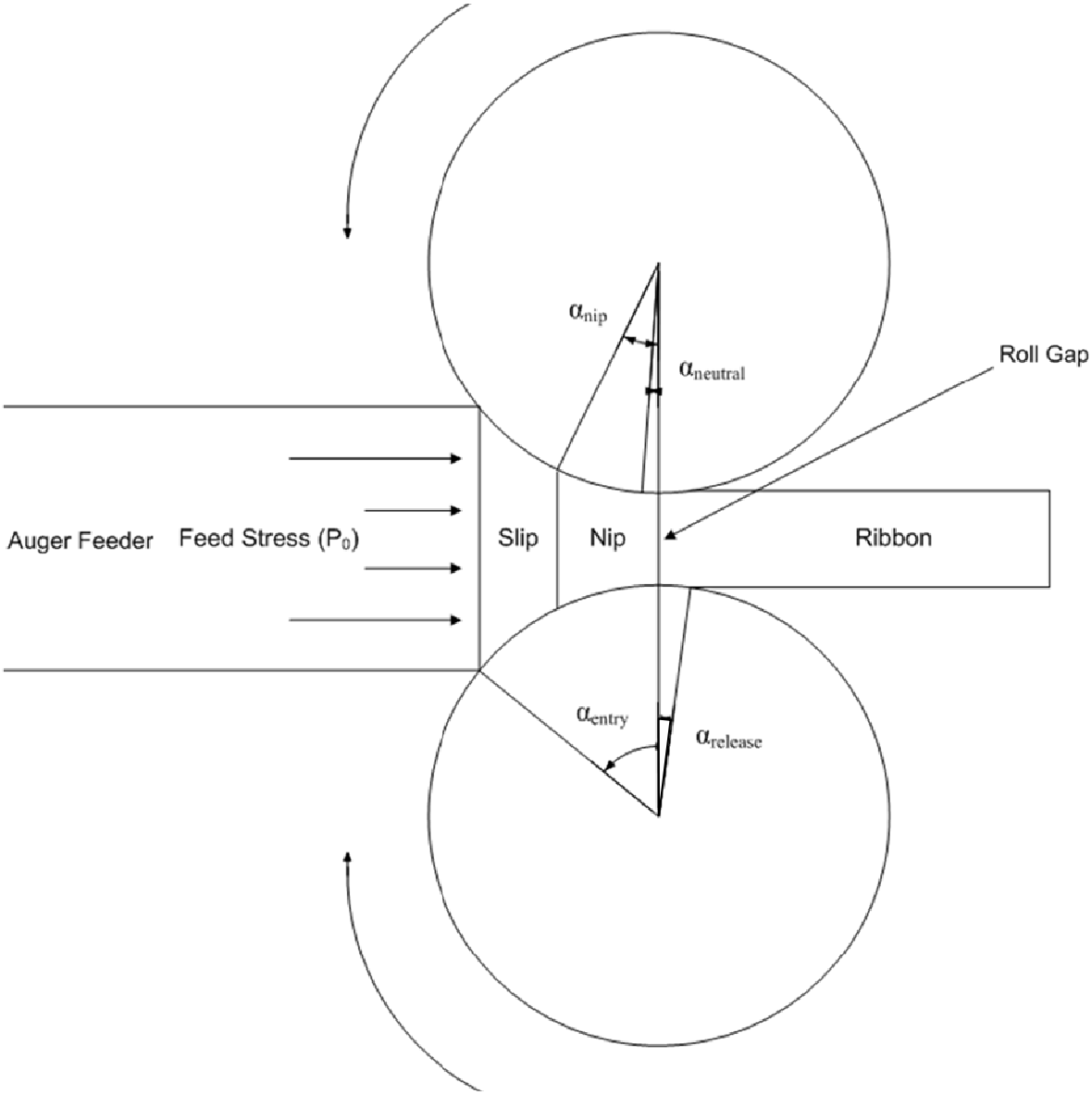


**Figure 2-3 - Schematic representation of the various regions of a roll compactor ($\alpha_{neutral}$ is the neutral angle, $\alpha_{nip}$ is the nip angle, $\alpha_{entry}$ is the entry angle and $\alpha_{release}$ is the release angle).**

The compaction event during roller compaction is usually split into three distinct zones [Bindhumadhavan *et al.*, 2005, Johanson, 1965]:

(i) The slip region, where the rolls move faster than the powder and hence relative slip occurs; in this zone the pressure is relatively low and hence densification of the powder blend is due to particle rearrangement.

(ii) The nip region, where the powder is 'gripped' at the roll surface and drawn in between the rolls; as the powder is forced into a smaller volume the pressure greatly increases causing particle deformation and/or fracture; a compact is formed as particle bonding occurs.

(iii) The release region, where the ribbon slips on the roll surface causing it to accelerate as it is released from the rolls [Schönert and Sander, 2002]; the pressure rapidly reduces and porosity expansion occurs due to elastic recovery.

Maximum compression during roll compaction occurs prior to the minimum roll gap and is usually referred to as the neutral angle. The nip angle (α), defined with reference to the minimum gap is the transition between the slip region and the nip region and is the point at which compaction begins [Patel *et al.*, 2010]. Figure 2-3 shows a schematic representation of the roll compaction process, denoting the various regions and angles.

Successful operation and control of the roller compaction process can only be achieved through sufficient knowledge of both the properties of the input material and how the roller compaction settings affect the properties of the roller compacted ribbons and subsequent granule, and thereby the tablet properties. The following sections review the roller compaction literature and discuss the effect of both the input material properties and the roller compaction settings on the quality of the granules and subsequent tablets.

#### 2.3.1.1 Control physics of roller compaction

The operation of the roller compactor is controlled using the parameters outlined above; the interplay of these parameters is shown schematically in Figure 2-4. Successful roller compaction requires two conditions to be satisfied: (1) the rollers are not starved of input material, and (2) the rate of roller compacted ribbon throughput does not choke or flood the mill. The rate of powder feed transported to the roll surface is controlled primarily by the

rotational speed of the feed auger. For a constant roll pressure, roll speed and input material increasing the auger speed will increase the throughput of roller compacted ribbon. Since the width of the roll surface is fixed by the geometry of the roller compactor and the length of ribbon per unit time is determined by the roll speed (as outlined in section 3.2.1.3) the only way ribbon throughput can be increased in this scenario, is through an increase in ribbon thickness. An increase in ribbon thickness is accompanied by an increased in roll gap.

The maximum pressure applied to the ribbon and hence the maximum densification achieved during roller compaction is primarily determined by the hydraulic roll pressure acting on the slave roll. Therefore, for a fixed roll speed, auger speed and input material increasing the hydraulic roll pressure will increase the density of the roller compacted ribbon. Again the width of the roll surface is fixed by geometry and the length of ribbon per unit time is determined by the roll speed. Furthermore at a fixed auger speed the mass of ribbon manufactured per unit time is constant. Therefore in order to increase the density of the roller compacted ribbon the thickness of the ribbon (and hence it volume) must reduce. The reduction of ribbon thickness is accompanied by a reduction in the roll gap.

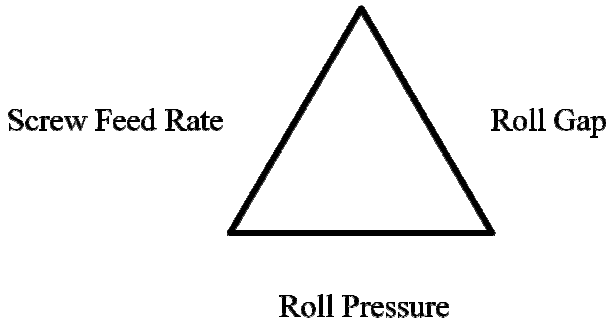


**Figure 2-4 – Interplay of roll pressure, screw feed rate and roll gap during roller compaction.**

### 2.3.2 Roller compaction formulation challenges

The appropriate selection of formulation excipients is critical for successful manufacture of a pharmaceutical solid dosage form, and the same is just as critical when

roller compacting a formulation. There is a plethora of materials which have been investigated in the literature, some of which are discussed in the following sections.

#### 2.3.2.1 Traditional excipients

The effect of the initial particle size of microcrystalline cellulose was investigated by Herting and Kleinebudde. They observed that a decrease in particle size of the starting material had a negative effect on the flow properties of the blend material; however, it increased the tensile strength of the roller compacted ribbon and increased the median particle size of the subsequent granules [Herting and Kleinebudde, 2007]. The tensile strength of the tablets compacted from granules using microcrystalline cellulose with a smaller particle size was higher than the corresponding batches using the larger particle size. The observation of reduced tabletability of granules following roller compaction is a common observation in the literature and is often attributed to work hardening during plastic deformation [Malkowska and Khan, 1983]; the sole use of microcrystalline cellulose was observed to produce granules with favourable properties, however, they exhibited poor recompressibility [Inghelbrecht and Remon, 1998b].

Herting and Kleinebudde provide an argument to support the work hardening phenomenon often considered to be the cause of reduced tabletability due to roller compaction. They observed that yield pressure of roller compacted granules obtained from Heckel plots increased with increasing roll pressure, indicating an increased resistance to plastic deformation. Furthermore, even though the same sized granules were used during tabletting studies granules, compressed from microcrystalline cellulose with a smaller initial particle size distribution exhibited higher tensile strength [Herting and Kleinebudde, 2008]. However, the contribution of work hardening on the tabletability of roller compacted granules is contested by Sun and Himmelspach; in a study on the loss of tabletability of

microcrystalline cellulose they investigated the effect of multiple compaction runs on the tensile strength of subsequent tablets; it was observed that whilst increasing compaction runs elicited an increase in granule size, the tensile strength of tablets compacted from the same sieve cut of granules was not affected by the number of compaction runs [Sun and Himmelspach, 2006].

Interestingly, not all materials exhibit the same reduction in tablet tensile strength following roller compaction; Wu and Sun investigated the effect of size enlargement of brittle granules composed of either spray dried lactose, mannitol or anhydrous calcium phosphate dibasic on tablet properties. From the three sieve cuts tested it was observed that the tensile strength of the lactose tablets was hardly affected by granule size; whereas the tensile strength of the mannitol and anhydrous dibasic calcium phosphate tablets were slightly affected by granule size (where smaller granules produced tablets with higher tensile strength) [Wu and Sun, 2007]. This observation was in stark contrast with the very significant differences in tensile strength of microcrystalline cellulose tablets compacted from different granule sizes. Riepma *et al.* investigated the re-tabletability of two different types of crystalline lactose. It was observed that the tensile strength of tablets was dependent on the initial properties of the lactose and the size of the milled granules rather than the strength or porosity of the slugs [Riepma *et al.*, 1993]. A number of lactose types, with differing flow properties and particle size, were investigated by Inghelbrecht and Remon. Unlike in direct compression, lactose with exceptional flow properties was found to be counterproductive and actually caused problems during roller compaction. Lactose with initially smaller particle size was found to produce the highest quality granule [Inghelbrecht and Paul Remon, 1998].

Bacher *et al.* made a number of observations in a series of papers investigating the effect of roller compaction of different grades of calcium carbonate and sorbitol on tablet

properties [Bacher *et al.*, 2007, Bacher *et al.*, 2008a, Bacher *et al.*, 2008b]. It was demonstrated that in some cases the choice of formulation excipients can have as much impact as changing the roller compaction settings. From the three grades of calcium carbonate and sorbitol investigated it was observed that both morphological properties and particle size had an impact on the recompactability. Furthermore the fine portion of the roller compacted granule was found to be important in controlling the tablet weight and hence drug content uniformity. It was argued [Bacher *et al.*, 2008b] using sorbitol with a smaller particle size improves the drug homogeneity and decreases the demixing potential of the granule. A comparison between the granule properties of calcium carbonate and sorbitol prepared by both roller compaction and wet granulation was investigated. The flow properties of the roller compacted granule were found to depend on the starting material. Furthermore the granules from wet granulation had increased compaction and compression properties. The tensile strengths of the both types of tablets were affected by the size of sorbitol in the initial pre-granulation powder blend [Bacher *et al.*, 2008a].

Bozic *et al.* investigated the use of roller compaction to produce tablets containing a high (75% w/w) drug load of macrolide antibiotic with microcrystalline cellulose. As a brittle material the amount of macrolide antibiotic in the formulation dominated the compression characteristics of the blend and as such the tabletability of the granule was equivalent to that of the original powder. Furthermore, the capping tendency of tablets compressed from the granule was reduced compared to the raw powder, attributed to the partial amorphisation of the originally crystalline drug product [Bozic *et al.*, 2008].

Moore *et al.* investigated the use of sodium lauryl sulphate on the tablet hardness and dissolution profile of poorly soluble drug substances. The effect of sodium lauryl sulphate on the tablet tensile strength was found to depend on the point of addition. Adding sodium lauryl

sulphate at the initial blending stage reduced the tablet strength, whilst addition of sodium lauryl sulphate at the extra-granular (post roller compaction) lubrication stage had no effect on the tablet tensile strength. Dissolution rate was increased by the inclusion of sodium lauryl sulphate. However, the improvement was independent of the point of addition [Moore *et al.*, 2010].

The use of starch as a roller compaction excipient was investigated by Chang *et al.* Due to its poor compressibility properties it was found that increasing starch content in the formulation elicited a reduction in solid fraction and ribbon tensile strength, which in turn led to a reduction the particle size of the subsequent granule [Chang *et al.*, 2008].

#### 2.3.2.2 Controlled release formulations

The use of roller compaction as a technique for the preparation of controlled release tablet formulations has been investigated by a number of authors.

Skinner *et al.* investigated the effect of hydroxypropylcellulose as a binder during roller compaction. It was observed that appropriate levels of binder could impart good compaction characteristics into the granulation. However, increasing the level of binder in the formulation increased the dissolution time of drug product due to its gelling properties [Skinner *et al.*, 1999].

Hariharan *et al.* used a design of experiments (DoE) to help aid formulation selection for the production of controlled released tablets containing a highly water soluble drug. Hydroxypropylene methylcellulose was used as a matrix gelling agent. Drug release was prolonged to the highest degree at high levels of hydroxypropylene methylcellulose and compritol. However, replacing the microcrystalline cellulose in the formulation with

hydroxypropylene methylcellulose and compritol produced tablets with inferior tensile strength [Hariharan *et al.*, 2004].

#### 2.3.2.3 Controlled water addition as a process aid

A number of researchers have investigated the addition of water to formulations prior to roller compaction. Wu *et al.* investigated the effect of moisture content on the nip angle and pressure profile during roller compaction. It was observed that at below 10% w/w water levels the addition of water had little effect on the properties of the powder and resultant roller compaction process. However, above 10% w/w there was a sudden decrease in the flow properties in the blend and a corresponding increase in maximum pressure during roller compaction. Furthermore the ribbon was observed to split indicating poor ribbon properties [Wu *et al.*, 2010].

Inghelbrecht and Remon investigated the addition of water to formulations prior to roller compaction as a method to reduce the dust produced. Addition of water at a level of 8-10% w/w reduced the production of fines; however, it also prolonged the drug dissolution rate [Inghelbrecht and Remon, 1998a].

For hygroscopic materials, such as microcrystalline cellulose, the adsorption of a layer of water at the particle surface can reduce the effect of inter-particulate interactions and as such have a similar response to magnesium stearate in terms of reducing the inter-particulate friction. However, the use of controlled addition of water during roller compaction is counter-intuitive particularly for drug products which are sensitive to moisture.

### 2.3.3 Roller compaction process development challenges

The degree of complexity in controlling and optimising roller compaction is increased by adding the range of parameters used to control the process. Roller compaction is often

described as being multivariate in nature [Mansa *et al.*, 2008]. This is due to the number of operator parameters used to control the process; auger rotation speed, roll speed, hydraulic roll pressure, roll surface type, roll gap and mill settings.

#### 2.3.3.1 Feeding system

Generally roller compactors will involve one of two methods of feeding powder to the roll surface: (1) gravity; or, (2) screw feeder. Due to the high demands on roller compaction mass throughput it is much more common to use mechanical screw fed feeders which can both increase mass throughput and aid in the transmission of powders with poor flow properties. The screw feeder provides two main functions: (1) delivers powder from the storage hopper to the rollers, and (2) pre-densifies the material and removes air prior to compaction.

The screw feeder, however, is not without issues; Guigon and Simon observed that the rotation of the auger feeder has a local effect on the velocity of the powder causing the powder to accelerate forward and stop as the leading edge of the last flight of the screw rotates. This periodic feeding of powder into the roller resulted in heterogeneity in the rolling direction of the roller compacted ribbon [Guigon and Simon, 2003]. Conversely, to the work of Guigon and Simon, Lecompte *et al.* did not observed the periodic effect on pressure profiles induced by the screw feeder [Lecompte *et al.*, 2005]. The roll press design used by Lecompte *et al.* differed to that of Guigon and Simon because the end of the screw feeder was located further away from the rollers which allowed more time for powder to rearrange across the width of the roll. The effect was observed, however, if the roller compactor was underfed, suggesting that the roll gap also has an effect on the heterogeneity of pressure applied across the roll width.

The importance of optimising the auger feeder to roll speed ratio was investigated by Hervieu and Dehont. They showed that the influence of the auger speed to roll speed ratio on the product quality can be more important than typical adjustments of the hydraulic roll pressure. Three feeding regimes can be identified: (1) sub-feeding (roll speed too high, screw speed too low), (2) Over-feeding (roll speed too low, screw speed too high) and (3) "good compaction rate" [Hervieu and Dehont, 1994]. The affect of auger speed and roll speed on the roller compaction of lactose and microcrystalline cellulose was the subject of an investigation by Falzone *et al.* It was observed that different factors were important for the two excipients suggesting that there is no "one size fits all" statistical model which can be derived to determine roller compaction performance [Falzone *et al.*, 1992].

#### 2.3.3.2 Compaction zone

A number of authors have investigated the effect of hydraulic roll pressure during roller compaction. The common observation is that the aim of increasing particle size and hence flowability of the roller compacted granule is contradictory to retaining re-compactability. For instance, the effect of roller compaction on the tabletability of ibuprofen was investigated by Patel *et al.* It was observed that increasing the compaction pressure during roller compaction resulted in larger granules which had a higher yield pressure; furthermore, a higher compaction pressure at the tablet compaction stage was required to produce the same degree of densification [Patel *et al.*, 2008]. An investigation by Weyenberg *et al.* reported similar findings. It was observed that for granule size and flow an increase in hydraulic roll pressure was advantageous. However, the tablet tensile strength was adversely affected by high hydraulic roll pressure during roller compaction [Weyenberg *et al.*, 2005]. Furthermore, even at low compaction force, the flowability of roller compacted granules containing calcium carbonate was improved over the raw material [Freitag and Kleinebudde,

2003]. As such it is often recommended during roller compaction to aim for the lowest possible compaction pressure to achieve the desired granule flow rate and thus retain the compactability of the subsequent granules.

Rambali *et al.* investigated the effect of roller compaction settings on tablet strength, dissolution and bioadhesive characteristics of a buccal bio-adhesive tablet. As observed previously, it was found that granule size was increased by compaction force. However, increasing compaction force during roller compaction adversely affected tablet tensile strength. Interestingly, it was also observed that granule size had no effect on the tablet weight relative standard deviation and as such they recommended the use of lower compaction pressure during roller compaction. Furthermore, the bioadhesive characteristics were improved in tablets compacted from smaller granules, attributed to the increase in surface area available for wetting after tablet disintegration. However, the conclusions from this study were contradictory: in contrast to tablet hardness, the drug dissolution rate increased with an increase in roller compaction pressure, again indicating that the desired output properties of the tablets are achieved by different means [Rambali *et al.*, 2001].

The effect of roller compaction on the pore size of subsequent tablets was investigated by Freitag *et al.* It was observed that increasing the compaction force during roll compaction increased the microhardness of the roller compacted ribbons and reduced the fines content of the subsequent granules. The reduced fines content elicited an increase in pore volume of the compacted tablets and hence lowers tensile strength [Freitag *et al.*, 2004]. The higher pore volume in the tablets compacted from granules which experience a higher amount of pressure during roller compaction may help explain the differences in dissolution observed by Rambali *et al.* The ingress of water into the tablet is limited by the tortousity of the pore structure; tablets with a larger pore volume will allow water ingress at a faster rate.

#### 2.3.3.3 Roll surface and type

Roller compactors have been manufactured with numerous types of roll surfaces such as smooth, knurled, serrated and pockets. Daugherity and Chu investigated the effect of roll surface on roller compaction. It was observed that using rolls with a greater serration volume increased the roller compacted ribbon thickness (for equivalent roller compactor settings); furthermore the increase in roll gap was accompanied by an increase in nip angle, demonstrating the effect of friction at the roll surface [Daugherity and Chu, 2007]. The effect of friction at the cheek plate surface can be reduced by the use of concavo-convex rollers [Parrott, 1981]

## 2.4 The role of magnesium stearate during roller compaction

A wealth of literature can be found on the effect of magnesium stearate on powder properties and the tablet compaction process. However, the literature involving a systematic study of the impact of magnesium stearate on roller compaction is limited to only a handful of researchers. Furthermore in the granule tabletability studies discussed above, [Herting and Kleinebudde, 2007, Herting and Kleinebudde, 2008, Inghelbrecht and Remon, 1998b, Sun and Himmelspach, 2006], tablet compacts were made from sieve cuts of the roller compacted granules. The authors did not compensate for the impact of magnesium stearate on the full size range of the roller compacted granules. Tablet strength is well known to decrease due to the development of a hydrophobic film on the surface of powders/granules. For a fixed amount of magnesium stearate the extent of this film coverage will depend on the surface area of the granules. Since granules with a larger particle size will have less specific surface area one may assume that a more complete film is developed on these particles. Granules with a more extensive lubricant coating will likely exhibit lower tensile strength. The lubrication effect may explain the apparent lack of sensitivity of brittle granules. Upon recompaction the

brittle granules will undergo extensive fragmentation generating fresh surfaces free of magnesium stearate. He *et al.* investigated the work hardening effect of roller compacted granules with both unlubricated and lubricated powders and granules. Conversely to the previous papers in the absence of intra- and inter-granular magnesium stearate no reduction in tablet tensile strength was observed. However, following addition of magnesium stearate there was a significant loss in tabletability of the roller compacted granule [He *et al.*, 2007]. The authors concluded that the common practice of adding the lubricant to the initial raw powder is the most likely cause for loss of tabletability.

Most of the literature investigating the impact of magnesium stearate during roller compaction is limited to studying the effects on the properties of the roller compacted ribbon and re-compressibility of the subsequent granules rather than the actual powder feeding process (e.g. [He *et al.*, 2007, Hein *et al.*, 2008, Herting and Kleinebudde, 2007, Herting and Kleinebudde, 2008, Sun and Himmelspach, 2006]). However, a handful of researchers have attempted to elucidate how magnesium stearate affects powder flow into a gravity fed roller compactor. It has been observed that without the addition of a lubricant the flow of microcrystalline cellulose (MCC) into a gravity fed roll compactor was slower at the equipment surface than at the centre, leading to ribbon compacts with loosely compacted edges. However, with the addition of magnesium stearate the flow of MCC into the roll compactor was more homogenous leading to ribbons with less variation in density across the ribbon width [Miguelez-Moran *et al.*, 2008]. In a further study X-ray tomography was used to characterise the density distribution of roller compacted ribbons which confirmed the effects of magnesium stearate on density distributions across the ribbon width [Miguelez-Moran *et al.*, 2009]. The limitation of these studies is that they were conducted on a custom built

gravity fed roller compactor; as such the influence of magnesium stearate on the screw feeding of powder during roller compaction is not considered.

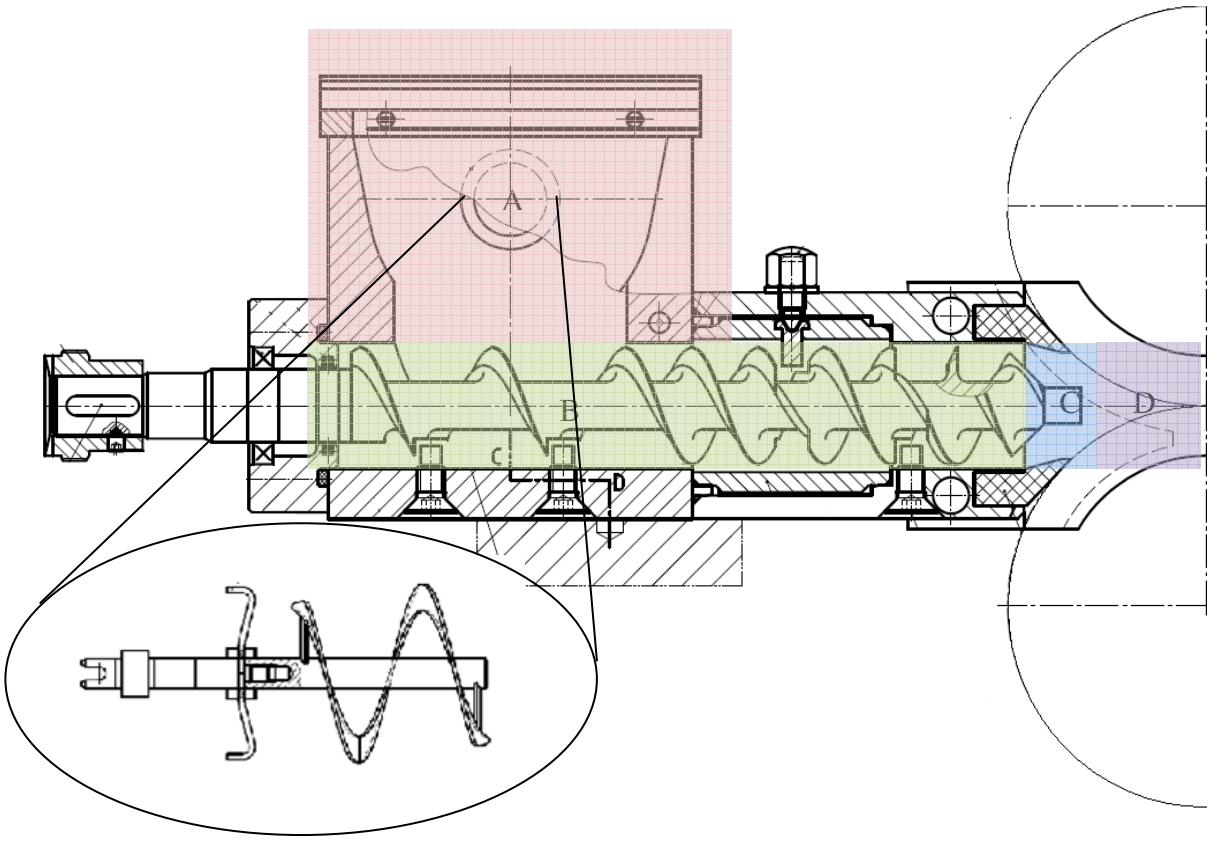


**Figure 2-5 – Schematic overview of the Alexanderwerk WP 120, the feeding system is split into the following regions; (A) hopper and hopper stirrer, (B) feed auger, (C) cheek plates and pre-nip chamber, (D) roll surface and nip region. The hopper stirrer is shown in the insert. Figure reproduced with permission from Alexanderwerk [Alexanderwerk AG].**

Figure 2-5 depicts the feeding system of the Alexanderwerk WP 120. The powder formulation is introduced into the feed hopper, which incorporates a hopper stirrer located at the bottom of the hopper which is used to prevent powder bridge formation and to ensure a consistent flow of powder into the feed auger chamber (A). Powder is transported forward by the action of the feed auger chamber (B) to the nip region (C) where it is drawn in between the rolls (D) and compressed into a ribbon compact. The inclusion of the hopper stirrer will

create a region of localised mixing which could theoretically impact the lubricity of a formulation.

Akseli *et al.* evaluated the use of ultrasonics as a technique to measure the effect of lubrication on density distributions of ribbons manufactured using the Fitzpatrick roller compactor (a vertically screw fed roller compactor). The location of lubricant in the system was varied from no lubrication, lubrication at the equipment surfaces and lubrication in the bulk formulation. Consistent with the observation by Miguelez-Moran *et al.*, a higher compact density was recorded at the centre of the ribbon than the edges in the unlubricated condition. The density differential was reduced both by the use of lubricated equipment surfaces and by the addition of lubrication to bulk blend [Akseli *et al.*, 2011]. The increase in density homogeneity across the width of the ribbon was attributed to the reduction in friction at the interface between the powder and equipment surfaces.

The reduction in friction that is evident from the addition of lubricants may not always be advantageous during roll compaction as friction between the powder and the roll surface is necessary to enable powder to be drawn into the rolls. One could suggest that, due to its friction lowering properties, the addition of magnesium stearate prior to roller compaction is liable to increase slip at the roll surface. As a consequence, the nip angle would be expected to reduce, resulting in an undesirable decrease in both dwell time and maximum pressure between the rolls [Miguelez-Moran *et al.*, 2008]. On the contrary, the reduction in friction at the cheek plate surface can be advantageous as seen from previous studies [Miguelez-Moran *et al.*, 2009, Miguelez-Moran *et al.*, 2008] given that flow is less impeded at the wall surface, resulting in a more homogenous density distribution along the width of the ribbon. Synonymous to tablet press surfaces, roll surfaces exhibit powder sticking in the absence of magnesium stearate [Kleinebudde, 2004]; however, due to the non-homogenous distribution

of magnesium stearate throughout a powder blend, variability in the final blend could become a problem. Additionally, further mixing during downstream processing could further increase the lubricity of the formulation. Whilst in theory the presence of magnesium stearate could be beneficial during roll compaction, there are a number of potential adverse effects, such as reducing the nip angle and hence the dwell times as well as limiting powder draw through the rollers.

Clearly, the addition of magnesium stearate can have numerous adverse effects on both the roller compacted ribbon and tablet properties. This thesis attempts to address the gap in the knowledge space by systematically investigating the impact of magnesium stearate on powder feeding during roller compaction. Further elucidation of the affect of magnesium stearate on the compaction zone will be studied via the use of instrumented rollers.

### 2.4.1 How much is needed?

Removal of magnesium stearate from the formulation would provide numerous advantages for solid dosage forms, particularly for delivery systems that are required to dissolve rapidly such as effervescent and / or orally disintegrating tablets and APIs that are poorly soluble or produce weak compacts, such as tablets with high drug loading. Additionally, large dispersible tablets, which require high amounts of lubricants due to their size, suffer the undesirable effect of forming a magnesium stearate film on top of the water in which they are dispersed.

The literature discussed in section 2.2.4.1, would suggest that there is a limiting amount of magnesium stearate which should be added to the formulation, beyond this limiting amount there are no further benefits. A more in depth understanding of the minimum amount

of magnesium stearate required in the formulation during roller compaction could potentially aid formulation design.

### 2.4.2 Importance of the local presence of magnesium stearate

When considering the mechanism by which magnesium stearate reduces frictional forces and adhesive forces during tabletting one must consider that any magnesium stearate located within the bulk of the tablet is effectively superfluous, i.e. only magnesium stearate located at the interface between the tablet and the equipment surfaces provides a functional role. As such, the ability to apply a film of magnesium stearate directly to the equipment surfaces should provide sufficient anti-adhesion, even in the absence of magnesium stearate from the blend, to prevent powder adhesion. Several researchers have investigated the use of such a technique to apply lubrication directly to the equipment surfaces during tabletting [Gruber *et al.*, 1991, Jahn and Steffens, 2005, Papp *et al.*, 2010, Yamamura *et al.*, 2009]. Gruber *et al.* introduced a method to apply magnesium stearate directly to tablet punch surfaces; they found that, compared to the conventional method of adding magnesium stearate extra-granularly, tablets compressed using externally applied magnesium stearate were harder, faster dissolving and had less tendency towards capping [Gruber *et al.*, 1991]. The external lubrication system was developed further by Jahn and Steffens. Their equipment differed slightly from that used by Gruber *et al*., as the coating system was operated in a continuous spray mode instead of a pulsing mechanism, the main advantage being that it is better suited to use with higher throughput tablet presses and is easier to implement since the spray does not need to be timed with the tablet press. They investigated the effect of lubrication spray rate on the ejection force of a number of different pharmaceutical excipients. Ejection force is a real-time measurement of the degree of lubrication and high ejection forces can result in stress to the tablets and in some cases can lead to tablets shattering upon ejection. They found

that the ejection force was reduced by increasing the lubricant spray rate; however, there was a minimum attainable ejection force, unique to each material, beyond which any further increase in spray rate caused no further decrease in ejection force, suggesting that for each material an optimum level of lubrication exists [Jahn and Steffens, 2005]. Overall, the amount of lubricant per tablet was found to be significantly less using external lubrication; however, the total consumption of magnesium stearate was higher due to the continuous nature of the operation, with the majority of the material sprayed being removed via vacuum extraction. Yamamura *et al*. also demonstrated that a significant decrease in the lubrication concentration of the final dosage form was possible, whilst successfully preventing the formulation from adhering to the tooling surfaces when using external lubrication. It was also found that the crushing strength was higher at the minimum level needed to prevent sticking. Surprisingly despite this increase in crushing strength the dissolution time was still shorter for tablets that had been lubricated externally [Yamamura *et al.*, 2009]. Papp *et al.* also reported the benefits of using external lubrication when manufacturing orally disintegrating tablets which are required to dissolve rapidly [Papp *et al.*, 2010].

Whilst external lubrication has been applied extensively during tabletting, to date there has been no published investigation into the use of externally applied lubrication for a roller compaction process.

### 2.4.3 What are the alternatives to magnesium stearate

In the literature there are three strategies that are generally used to mitigate the effect of magnesium stearate; (i) replacement lubricants [Aoshima *et al.*, 2005, Shah *et al.*, 1986, Uchimoto *et al.*, 2010]; (ii) use of novel co-processed excipients which demonstrate reduced sensitivity to the effects of magnesium stearate [Arida and Al-Tabakha, 2008, Rashid *et al.*, 2011]; and, (iii) addition of compendial excipients to the formulation which have exhibited a

negating affect to the deleterious effects of magnesium stearate [Jonat *et al.*, 2004, Meyer and Zimmermann, 2004, Ong *et al.*, 1993, Rowe, 1988, Wang and Chowhan, 1990].

#### 2.4.3.1 Alternative lubricants

As discussed previously, one of the properties attributed to the effect of magnesium stearate on tablet dissolution is its inherent hydrophobicity. As such, some of the potential alternative lubricants under investigation include hydrophilic lubricants such as sodium stearyl fumarate [Shah *et al.*, 1986], glycerin fatty esters (triglycerin behenate) [Uchimoto *et al.*, 2010] and sucrose fatty acid ester [Aoshima *et al.*, 2005]. It has been observed that glycerin fatty acids can provide similar lubricating efficacy as magnesium stearate at similar levels of addition. Moreover they have been have observed to decrease tablet ejection forces to a greater degree, attributed to its longer carbon chain (22 carbons compared to 18 carbons for magnesium stearate) [Uchimoto *et al.*, 2010]. Furthermore the addition of glyceryl behenate to the formulation was observed to have less of an impact on the disintegration time of placebo tablets containing lactose monohydrate, corn starch and hydroxypropylcellulose. Sodium stearyl fumarate has also been observed to have lubricating properties equivalent to magnesium stearate, whilst due to its hydrophilic nature has less of an effect on the dissolution rate of s*alicylic acid* [Shah *et al.*, 1986]. However, not all hydrophilic lubricants show a similar effect on the dissolution rate; it has been observed that sucrose fatty acid esters had a similar effect to magnesium stearate on the dissolution rate of *acetylsalicylic acid*. Furthermore a significantly higher amount of sucrose fatty acid was required to instigate equivalent lubricating properties to magnesium stearate [Aoshima *et al.*, 2005].

A number of other molecules have been investigated for their lubricating properties [Miller and York, 1988, Wang *et al.*, 2010];

- Stearates other than magnesium (such as; calcium, sodium and zinc)
- Fatty acids, hydrocarbons and fatty acids
- Fatty acid esters
- Alkyl sulphate
- Inorganic materials

#### 2.4.3.2 Novel co-processed excipients

Another strategy is the design of excipients which are less sensitive to the effect of magnesium stearate. A number of excipients have been developed which involve co-processing two or more traditional excipients together to produce a pharmaceutical product which has improved performance in comparison to a physical mixture of the two excipients. The typical strategy in this case is the co-processing of a plastically deforming material with a brittle fracture material such as Cellactose® which is a material co-processed with cellulose (25%) and lactose monohydrate (75 %). Cellactose® is considered to consist of a cellulose core coated with a layer of lactose. As such upon compaction the hydrophobic layer that is formed on the surface of the excipient after mixing with magnesium stearate is broken as the lactose fractures leaving the lubricant free surfaces of the cellulose [Arida and Al-Tabakha, 2008]. As such the co-processed Cellactose® shows a lower degree of lubricant sensitivity than that of a physical mixture of the two excipients.

Starch has also been of interest in the line of co-processed excipients; with starch being co-processed with magnesium silicate. In a tablet matrix starch exhibits a wicking action increasing the water permeability of the tablet. However, mixing of magnesium stearate with pure starch has been shown to impede the ingress of water into the starch molecule. Conversely, when co-processed with magnesium silicate the permeability of starch

was unaffected by the presence of magnesium stearate; furthermore it was observed that both the tensile strength of tablets and the dissolution rate of paracetamol was unaffected by magnesium stearate [Rashid *et al.*, 2011].

An investigation of a novel range of excipients (LubriTose™) is discussed in Chapter 6. The LubriTose™ range of excipients involves the co-processing of compendial excipients (microcrystalline cellulose, lactose anhydrous, spray dried lactose or mannitol) with glyceryl monostearate. The manufacturer's claim is that the co-processed material is less sensitive to the mixing sensitivity often exhibited by magnesium stearate whilst at the same time having less of an effect on the tablet tensile strength and dissolution properties of the final tablet product.

#### 2.4.3.3 Formulation additives

Another strategy to mitigate the effects of magnesium stearate on the quality attributes of the final tablet product is to use colloidal additives such as silica or sodium lauryl sulphate. It has been observed that co-mixing of these materials prevents the increase in disintegration and dissolution time often elicited as a result of mixing magnesium stearate into the formulation [Lerk and Bolhuis, 1977, Lerk *et al.*, 1977, Ong *et al.*, 1993, Wang and Chowhan, 1990].

It has been proposed that the mechanism involved is due to the attractive force between magnesium stearate and colloidal silica being greater than the attractive force between either magnesium stearate and the other excipient particles and colloidal silica and the other excipient particles [Ong *et al.*, 1993, Rowe, 1988, Wang and Chowhan, 1990]. Due to the attractive force between the colloidal silica and magnesium stearate the magnesium stearate becomes 'enrobed' by the colloidal silica and hence less magnesium stearate is

available to coat the other excipient and drug particles. However, the disadvantage of this effect is that the magnesium stearate imparts less of a lubricating effect on the tablet formulation [Ragnarsson *et al.*, 1979].

## 2.5 Roller compaction process development and optimisation

Optimisation of the roller compaction process is difficult and is often achieved by the trail-and-error and operator experience. Developing manufacturing processes in this way is both time consuming and costly. The following section discusses the techniques that have been used to improve process development.

### 2.5.1 Instrumented roll technology

The use of rollers with integrated pressure transducers has allowed for a greater amount of information to be elucidated from the compaction zone during roller compaction. The periodicity of the screw feeder and its effect on the pressure applied during roller compaction was investigated by Simon and Guigon. Consistent with their visual observations [Guigon and Simon, 2003] the pressure measured by two sensors on each side of the roll width showed that the pressure profile follows the periodicity of the screw feeder. This was attributed to the local velocity of the powder moving out of the screw feeder [Simon and Guigon, 2003]. The use of the roll pressure sensors allows the measurement of the actual force applied to the ribbon during roller compaction and of the measurement of the nip angle [Bindhumadhavan *et al.*, 2005, Schönert and Sander, 2002]. Furthermore, the instrumented roll provides an important role in developing mathematical models for roller compaction and the use of roller compaction simulators.

### 2.5.2 Techniques used to monitor roller compaction processes

A number of off-line techniques are used as standard to measure the quality of roller compacted ribbons and subsequent granules. They are discussed in detail in the materials and methods chapter; this section discusses the use of non-compendial techniques used to monitor the quality of roller compacted ribbons during manufacture. A number of researchers have investigated the use of novel techniques to measure the ribbon quality; these include near-infrared spectroscopy, acoustic emissions and thermal effusivity.

#### 2.5.2.1 Near-infrared spectroscopy

Lim *et al.* investigated the use of near infrared chemical imaging to measure the density homogeneity of roller compacted ribbons. The technique is based on the principle that the density of the compact affects the absorbance of the diffuse reflectance. Measuring the density distribution along the ribbon length and width showed that the roller compacted ribbon had a higher density in the centre and exhibited a sinusoidal density pattern, induced by the rotation of the auger feeder, along the length [Lim *et al.*, 2011]. The use of in-line near-infrared monitoring of the roller compacted ribbons was investigated by Feng *et al.* the technique showed a high degree of sensitivity in detecting subtle periodic variations in ribbon density. The source of these variations was correlated with the roll speed; further investigation of the motion of the roll indicated that the rolling motion of the slave roller demonstrated significant eccentricity [Feng *et al.*, 2008]. However, the applicability of in-line near-infrared is limited by the fact that roller compaction is inherently a dusty operation and as such the dusty environment interferes with the near-infrared sensor. The use of near-infrared spectroscopy to monitor ribbon quality was investigated by Gupta *et al.*; the breaking force of roller compacted ribbons was observed to correlate with the near-infrared measurement,

furthermore, since the particle size distribution of the roller compacted granules was correlated with the ribbon breaking force a correlation was also observed between the near-infrared measurement and particle size [Gupta *et al.*, 2004].

Further to the investigations discussed in section 2.3.2.3, regarding the use of the controlled addition of water to roller compaction blends, Gupta *et al.* used near-infrared spectroscopy to monitor the effect of moisture content on roller compaction. The tensile strength of roller compacted ribbons was found to be a function of both roll pressure during compaction and water content. As such multivariate data analysis using principal component analysis was required to develop a robust model for monitoring ribbon tensile strength of roller compacted ribbons using near-infrared [Gupta *et al.*, 2005a].

The application of near-infrared was also used to investigate content uniformity of roller compacted blends containing acetaminophen [Gupta *et al.*, 2005b]. The concentration of acetaminophen was tracked by changes in the intensity in the 1640 to 1670 nm wave range. The limitation of using near-infrared spectroscopy as an online tool during roller compaction is that the signal is influenced by the dust generated.

#### 2.5.2.2 Acoustic techniques

The use of acoustic relaxation emission as a method to monitor the roller compaction of microcrystalline cellulose and maize starch was investigated by Salonen *et al.* It was observed that the intensity of the acoustic relaxation emission increased with increasing compaction force, and this was attributed to differences in the Young's modulus of the roller compacted ribbon. Furthermore the intensity of the signal was related to the material under compression [Salonen *et al.*, 1997].

The propagation of acoustic waves through a ribbon compact depends on the mechanical properties (*i.e.* Young's modulus, mass density, Poisson's ratio). The time of flight of an acoustic wave through ribbon compacts was investigated by Akseli *et al.* The time of flight was observed to decrease with increased ribbon density due to stronger interparticulate bonding enhancing the pressure wave. Furthermore, the technique was able to detect the density homogeneity across the ribbon width [Akseli *et al.*, 2011].

#### 2.5.2.3 Thermal effusivity techniques

Ghorab *et al.* observed that there was a correlation between the thermal effusivity and the compaction pressure applied during roller compaction and the square root of solid fraction for ribbons of microcrystalline cellulose and anhydrous lactose. Furthermore there was a correlation between the thermal effusivity and tensile strength of microcrystalline cellulose. However, due to extensive fragmentation exhibited by lactose, an increase in compaction pressure resulted in an increase in solid fraction, but not in tensile strength; this was also observed with the thermal effusivity result [Ghorab *et al.*, 2007]. The use of thermal effusivity was limited to offline analysis due to the need for a static 30 second measurement time. Furthermore, it was only possible to make measurements on intact ribbon samples with a smooth surface.

### 2.5.3 Mini-piloting and engineering design

Mini-piloting techniques take advantage of both;

(i) Mathematical models that are either derived from first principles and continuum mechanics (such as the Johanson model or the slab method) or executed in computational software packages (such as discrete elemental method (DEM) or finite elemental method (FEM)); or,

(ii) Experimental techniques which seek to develop either mechanistic understanding through compaction replication (compaction simulation) or stochastic relationships through the implementation of a carefully developed design of experiments (DoE).

Whilst the use of roller compaction models is not considered in this thesis, a brief summary of the techniques is introduced in Table 2-2 and a more detailed review of the Johanson model is provided in Section 2.5.3.1 and 2.5.3.2.

**Table 2-2 – Overview of roller compaction models**

| Model | Brief Description | References |
|---|---|---|
| Johanson model | A continuum based one dimensional model used to calculate the pressure distribution between the rolls. Requires experimental values of angle of wall friction, effective angle of friction and the compressibility of the material. The nip angle occurs at the point where the pressure gradients are equal. Model uses the Jenike-Shield yield function in the slip region and the pressure-density relation in the non-slip region. Limited by the overly simplified material laws and plane-strain assumption of powder movement through rollers. | [Balicki and Michrafy, 2003, Bindhumadhavan *et al.*, 2005, Dec *et al.*, 2003, Johanson, 1965, Sommer and Hauser, 2003] |
| Slab method | Uses a static analysis model and assumes plane-strain condition. Deformation zone is split into trapezoidal slabs and a force balance is done on each slab. Nip angle is not calculated in the slab method and as such must be assumed or calculated using the Johanson model. | [Balicki and Michrafy, 2003, Dec *et al.*, 2003, Peter *et al.*, 2010] |
| Finite element method (FEM) | Unlike other models FEM models can be both two-dimensional and three-dimensional. Furthermore, the more complex material laws are used to model the powder in the slip and non-slip | [Dec *et al.*, 2003, Muliadi *et al.*, 2012] |

| | | |
|---|---|---|
| | regions and velocity distributions through the thickness of the ribbon can be captured (i.e. plane-strain assumption not required). However, computing the model is computationally expensive and symmetry across the roll gap centre is assumed. | |
| Compaction simulator | Experimental material sparing technique were a tablet press is used to determine optimum compaction conditions (maximum pressure between rollers, ribbon porosity) to produce granules with favourable tabletting properties. Simulated 'ribbon' compacts can be milled and compacted into tablets. Can be used for roller compaction feasibility studies. The compaction simulator does not adequately capture the ribbon variability often associated with inconsistent powder feeding through a screw feeder. | [Gereg and Cappola, 2002, Hein *et al.*, 2008, Zinchuk *et al.*, 2004] |

#### 2.5.3.1 Mathematical modelling techniques

Mathematical modelling techniques are based on developing mathematical models to predict the ribbon properties given input parameters which engineers could use in the aid of design. On a basic level the problem to be solved for roller compaction can be described by the following differential equation as given by [Sommer and Hauser, 2003]:

$$\frac{1}{\sigma}\frac{d\sigma}{d\theta} = -f(\theta, \xi, \eta) \qquad \textbf{Equation 2-13}$$

Equation 2-13 relates the pressure between the rolls to some function of $\theta$ - rolling angle, $\xi$ - machine variables (roller geometry, gap) and $\eta$ - material parameters (bulk density, compressibility and flow); the solution must satisfy certain boundary conditions. Johanson has the accolade of being the first person to solve this differential equation by using two simple

material yield laws - Jenike-Shield and tablet material law. However, there is an argument that these laws are too simple and more complex models have since been developed such as the slab method [Balicki and Michrafy, 2003, Peter *et al.*, 2010] and FEM [Dec *et al.*, 2003, Michrafy *et al.*, 2011a, Michrafy *et al.*, 2011b, Muliadi *et al.*, 2012] which uses a modified Drucker-Prager Cap (DPC) model.

#### 2.5.3.2 Johanson model

The classical roller compaction model developed by Johanson in the 1960's, it is still widely applied today due to its ease of use. It is a continuum based one-dimensional model which can be used to calculate the pressure distribution between the rolls. A number of assumptions regarding the powder are made, namely that it is:

- Isotropic, frictional and cohesive
- Compressible
- Powder undergoes continuous shear deformation
- The nip region can be modelled as a plain-strain condition
- Coulomb friction law is valid
- Obeys the effective yield function proposed by Jenike and Shield

Johanson suggested that during roller compaction the powder exhibits two distinct regions of behaviour:

(1) Slip region – in the slip region the powder is said to be moving towards the minimum gap at a slower velocity than the rollers as such it experiences relative slip. In this region the pressure acting on the powder is small and the material law governing the powder behaviour is the effective yield function proposed by Jenike-Shield as shown in Equation 2-14 and Figure 2-6:

$$\sin(\delta) = \frac{\sigma_1 - \sigma_2}{\sigma_1 + \sigma_2} \qquad \textbf{Equation 2-14}$$

where $\sigma_1$ is the major principle stress and $\sigma_2$ is the minor principle stress (measuring using a shear cell as described in Section 3.2.2.3.

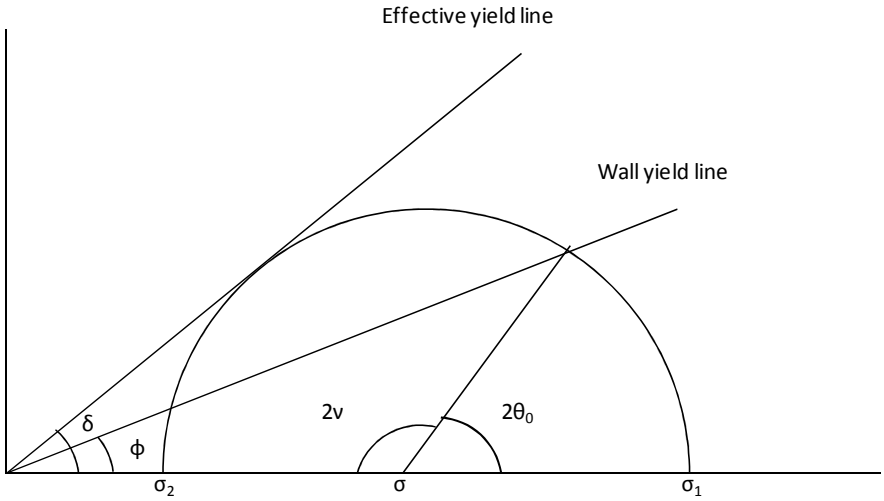


**Figure 2-6 - Mohr Circle.**

Using the effective yield function proposed by Jenike-Shield and the Mohr circle shown in Figure 2-6, the angle of wall friction (Φ), effective angle of internal friction (δ) and the acute angle (υ) can be calculated:

$$\nu = \frac{\pi - \sin^{-1}\left(\frac{\sin \Phi}{\sin \delta}\right) - \Phi}{2} \qquad \textbf{Equation 2-15}$$

(2) Non-slip region – Johanson hypothesised that there is a transition from the region of slip to a region of non-slip, which occurs at some rolling angle referred to as the angle of nip ($\alpha_{nip}$). At this point the powder moves at the same velocity as the rollers and is drawn in towards the minimum gap. Pressure rapidly increases and a coherent ribbon compact is made. In the nip region it is assumed that there is no slip between the powder and the roll surface as such, as shown in Figure 2-7, the volume of powder, $V_\alpha$, first entering the nip region enclosed within an arc segment ΔL moving towards the nip angle must be compressed into any volume $V_\theta$ at any given rolling angle within the same arc segment ΔL. For the process to operate under steady state conditions the mass of powder enclosed in $V_\alpha$ must be the same as the mass

of powder enclosed in $V_\theta$. The volume of powder is therefore related to the density by Equation 2-16:

$$\frac{\rho_\alpha}{\rho_\theta} = \frac{V_\alpha}{V_\theta} \quad \textbf{Equation 2-16}$$

where $\rho_\alpha$and $\rho_\theta$ is the density of the powder at the nip angle and at some rolling angle θ respectively and $V_\alpha$and $V_\theta$ are the volume of powder at the nip angle and at some rolling angle θ respectively.

Application of Equation 2-16 for roller compaction requires the assumption that roller compaction can be modelled under plane-strain condition. That is; two differential slices between the rollers as shown in Figure 2-7, have the same arc length, roll width and contain the same mass of powder. Therefore the density of the material within each slice depends only on the distance between the two roll surfaces.

Johanson proposed a pressure density law as shown in Equation 2-17 which relates the pressure between the rollers to the density of the compact and a compressibility factor k which is derived from uni-axial compaction experiments:

$$\frac{\sigma_\alpha}{\sigma_\theta} = \left(\frac{\rho_\alpha}{\rho_\theta}\right)^k \quad \textbf{Equation 2-17}$$

where $\sigma_\alpha$ and $\sigma_\theta$ are the pressure between the rollers at the nip angle and at any given rolling angle θ respectively

The distance between the two roll surfaces (S) at any rolling angle ($\theta$) can be calculated using Equation 2-18:

$$S_\theta = D(1 - \cos\theta) + S_{min} \quad \textbf{Equation 2-18}$$

Given that the lower limit to which Equation 2-18 applies is at the nip angle Equation 2-17 and Equation 2-18 can be combined to relate the pressure at a given rolling angle to the pressure at the nip and volume of a slice at the nip angle and the volume of a slice at some rolling angle:

$$\sigma_\theta = \sigma_\alpha \left[\frac{(1 + S/D - \cos\alpha)\cos\alpha}{(1 + S/D - \cos\theta)\cos\theta}\right]^k \qquad \textbf{Equation 2-19}$$

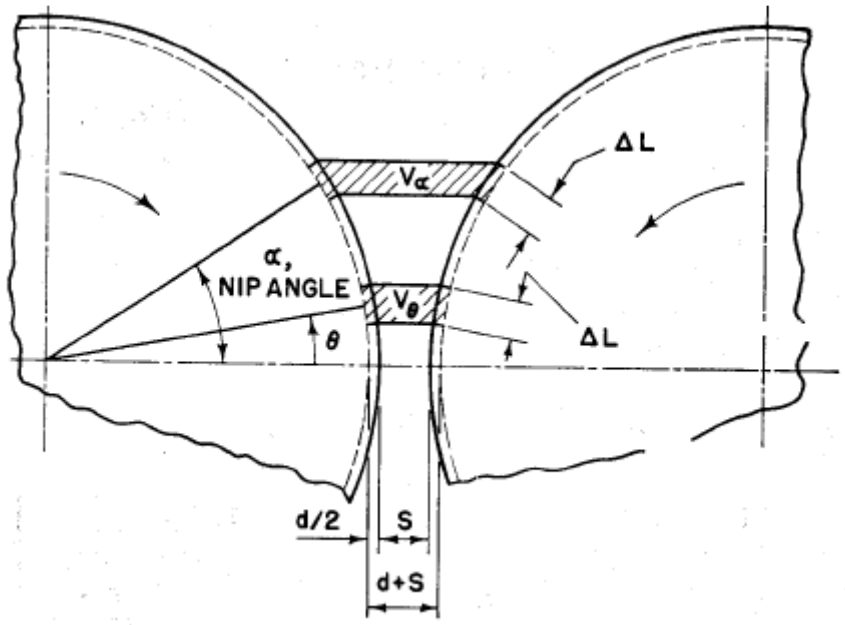


**Figure 2-7 – Density of differential slices between the rollers.**

The parameters that can be measured experimentally that are required as inputs for the Johanson model include the angle of wall friction, effective angle of internal friction and the compressibility of the material [Johanson, 1965].

One final parameter is required in order to solve the Johanson model, this is the nip angle. Johanson hypothesises, perhaps without justification [Sommer and Hauser, 2003], that the pressure gradients between the slip region and the non-slip region must be equal. The pressure gradients for the slip and non-slip regions are given in Equation 2-20 and Equation

2-22 respectively, the nip angle can be calculated from the intercept of these two equations as shown in Figure 2-8.

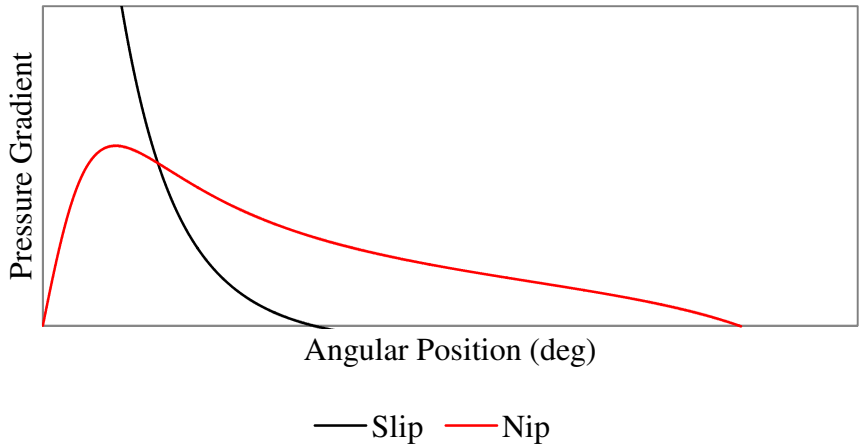


**Figure 2-8 – Calculating the nip angle**

To calculate the pressure gradient within the slip region a hyperbolic system of partial differential equations was obtained by combining the equation of the effective yield locus (Equation 2-15) with the equations of equilibrium. By combining the chosen top boundary at $\theta = \frac{\pi}{2} - v$, and the friction condition along the roll surface in the slip region, the pressure gradient can be determined by the acute angle and the yield criterion as follows:

$$\frac{d\sigma}{dx} = \frac{4\sigma\left({}^{\pi}/_{2} - \theta - v\right)\tan\delta}{\frac{D}{2}[1 + S/D - \cos\theta][\cot(A - \mu) - \cot(A + \mu)]} \qquad \textbf{Equation 2-20}$$

Where:

$$A = \frac{\theta + v + {}^{\pi}/_{2}}{2} \qquad \textbf{Equation 2-21}$$

The pressure gradient in the nip angle can be obtained by differentiating Equation 2-19:

$$\frac{d\sigma}{dx} = \frac{k\sigma_\theta\left(2\cos\theta - 1 - {}^{S}/_{D}\right)\tan\theta}{\frac{D}{2}\left[d/D + \left(1 + {}^{S}/_{D} - \cos\theta\right)\cos\theta\right]} \qquad \textbf{Equation 2-22}$$

Whilst the Johanson model has proved valuable in the development of process understanding for roller compaction it does have some limitations due to it overly simplistic material laws. For instance one of the model inputs for the Johanson model is the effective angle of internal friction. However, it is known that this parameter is not constant and changes with increasing normal force. Furthermore, the Johanson model does not take into account roll speed effects which will have an influence on the roll gap and roll pressure and hence on the final compact properties.

### 2.5.4 Surrogate API

R&D commonly has in inventory a large amount of material from projects that have been terminated or placed on hold. As such another possibility to overcome the challenges facing the R&D environment in the pharmaceutical industry is by using a surrogate material in the initial formulation development work, while sparing the stock of the new product being developed for confirmatory runs once the formulation has been optimized.

The surrogate material will be a lot of material from a different compound (for which there is a large amount in inventory) with physical properties that are very similar to the drug substance being developed. The underlying hypothesis of a surrogate material is that materials with similar properties will exhibit similar performance during processing.

To test the feasibility of using a surrogate material in drug product development a database containing the specific surface area and particle size measured from 256 lots from 36 compounds was analysed with the purpose of identifying pairs of lots with similar properties that could be surrogate candidates for each other. The pair selected for the proof-of-concept

study was subject to the same processing conditions (same formulation using 10% drug load, roller-compaction and tabletting settings) to assess if there was a difference in the performance of the two lots selected. A further study involved comparing the performance of a dissimilar material, to the two materials chosen for surrogacy, to clarify the importance of having similar properties. The details of this work can be found in Chapter 7.

## 2.6 Conclusion

An extensive review of the literature has been conducted; whilst the addition of magnesium stearate prior to tablet compaction is essential for the successful manufacture of pharmaceutical dosage forms, it imparts deleterious properties to the quality attributes of the final tablet product. Both tablet tensile strength and dissolution rate are adversely affected. On the contrary, addition of magnesium stearate reduces inter-particulate friction and improves the flow of powdered formulations. Furthermore, without adequate magnesium stearate in the formulation one experiences adhesion to the punch surfaces and high ejection forces, both of which are detrimental to product.

Granules produced during roller compaction often have inferior tabletability properties to that of the initial powder blend. A number of authors attribute this observation to either particle size enlargement, work hardening or a combination of the two. There is also some evidence that the loss of tabletability may be as a result of lubricating the initial roller compaction feedstock. As with tabletting, the use of magnesium stearate during roller compaction provides a number of useful functions. For instance, adhesion to the roll surface can be prevented, whilst at the same time density distribution observed across the ribbon width, which is attributed to the impact of friction at the equipment surfaces, can be reduced.

Due to the fact that the use of lubricants, such as magnesium stearate, during roller compaction and subsequent tabletting has the potential to impart undesirable properties into the final product it is of great interest to systematically investigate the impact of magnesium stearate on the roller compaction and hence justify a rationale for its inclusion. Furthermore a novel use of external lubrication during roller compaction, the use of which is not included in the literature, will be investigated in the first instance.

The current environment in the pharmaceutical industry is placing an increasing pressure on the R&D divisions of all major pharmaceutical companies to decrease drug delivery timelines to keep a healthy pipeline of drug products. One of the main challenges to accelerate formulation development is that typically the amount of API available during the early stages of development is limited or that it is costly to make. Despite this, due to the complex material behaviour observed with powder feeding and compaction during roller compaction, process design is usually accomplished using a trial and error approach which can be time consuming, expensive and may not lead to the optimal solution. This in turn has necessitated the development of a number of material sparing techniques known as mini-piloting techniques. A potential extension on these mini-piloting techniques is the application of surrogate APIs.

# CHAPTER 3

# METHODOLOGY AND MATERIALS CHARACTERISATION

# CHAPTER 3

# METHODOLOGY AND MATERIALS CHARACTERISATION

## 3.1 Materials

### 3.1.1 Excipients

The pharmaceutical excipients used during this study were microcrystalline cellulose (Avicel PH102) (FMC, Ireland), lactose anhydrous and lactose monohydrate (Kerry Bioscience, USA), croscarmellose sodium (FMC, Ireland), magnesium stearate (Mallinckrodt Inc., USA), sodium stearyl fumerate (Alubra®, FMC Biopolymer, Philadelphia, USA), colloidal silicon dioxide, micronized silicon dioxide (Evonik Industries, Germany) and Talc (Sigma-Aldrich Corp., USA). A specialised coprocessed material LubriTose™ MCC and LubriTose™ AN were kindly supplied by Kerry Sheffield BioScience, (Almere, The Netherlands).

### 3.1.2 Active pharmaceutical ingredients (APIs)

The following APIs were investigated in Chapter 5; *Ibipinabant, Pravastatin,* BMS-663068, BMS-791325 and BMS-754807 (Bristol-Myers Squibb, New Jersey, USA). In Chapter 6 the following API was used; Atenolol (Surfachem, UK).

### 3.1.3 Other ingredients

A dilute suspension of magnesium stearate was prepared using propan-2-ol *(*GPR Rectapur, VWR, France*)* as the spray medium for the external lubrication process. The samples for the inductively coupled plasma optical emission spectroscopy technique were microwave digested using concentrated nitric acid (grade - super purity acid, ROMIL, Cambridge, UK).

## 3.2 Materials characterisation

### 3.2.1 Density characterisation

#### 3.2.1.1 True density

The true density of the powder blends was determined using helium pycnometry (AccuPyc II 1340, Micromeritics Instrument Co., Norcross, GA, USA). A schematic representation of the helium pycnometer is provided in Figure 3-1. Briefly, the technique involves sealing the material inside a sample chamber of known volume $V_c$ and injecting helium gas to fill the available void space creating a pressure inside the sample chamber, $P_1$. The helium gas is then purged into an expansion chamber of known volume $V_x$ and the reduced pressure, $P_2$, inside the chamber is measured. The volume of the sample, $V_s$, can then be calculating using the principle of the ideal gas law as shown in Equation 3-1:

$$V_s = V_c - \frac{P_2 V_x}{(P_2 - P_1)} \qquad \textbf{Equation 3-1}$$

The mass of material (M) added to the sample chamber is measured prior to analysis and thus the true density of the material can be calculated using Equation 3-2.

$$\rho_{true} = \frac{M}{V_s} \qquad \textbf{Equation 3-2}$$

Since water can act as an impurity during testing, sample preparation requires that the samples are dried at 50°C for at least 12 hours prior to analysis. Day of use calibration of the AccuPyc was performed using two standard stainless steel balls of known mass and volume (Micromeritics Instrument Co., Norcross, GA, USA).

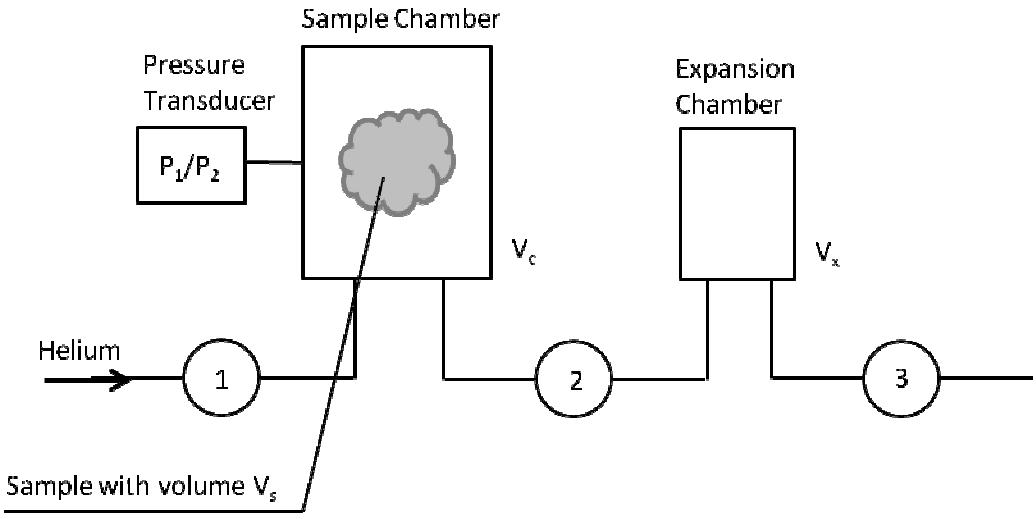


**Figure 3-1 – Schematic diagram for measuring true density using the Accupyc**

### 3.2.1.2 Bulk and tapped density

Bulk and tapped density were measured using a graduated cylinder. A powdered sample of known mass is poured into the graduated cylinder and the fill height, $h_b$, is recorded. The bulk density is then calculated using Equation 3-3.

$$\rho_{bulk} = \frac{M}{\left(\frac{\pi D^2}{4}\right) \times h_b} \qquad \textbf{Equation 3-3}$$

The kinetics of volume reduction due to tapping is measured by tapping the graduated cylinder 25, 50, 100, 250 and 500 times, and measuring the tapped fill height, $h_t$, at each number of taps using a VanKel tapping machine (VanKel, Varian Inc. North Carolina, USA). The tapped density is then calculated using Equation 3-4.

$$\rho_{tap} = \frac{M}{\left(\frac{\pi D^2}{4}\right) \times h_t} \qquad \textbf{Equation 3-4}$$

From the bulk and tapped density two parameters can be derived known as the Carr's Index (Equation 3-5) and the Hausner ratio (Equation 3-6):

$$CI(\%) = \frac{\rho_{tap} - \rho_{bulk}}{\rho_{tap}} \times 100 \qquad \textbf{Equation 3-5}$$

$$H = \frac{\rho_{tap}}{\rho_{bulk}} \qquad \textbf{Equation 3-6}$$

The Carr's Index (CI) and the Hasuner ratio (H) give a simple method to assess powder flow, Table 3-1 gives a description of powder flow based on the Carr's Index value. A material with a Hausner ratio above 1.5 is said to be more cohesive and less free flowing.

**Table 3-1 – Flow descriptors based on the Carr's Index**

| CI (%) | Flow Description |
|---|---|
| 5-15 | Free-flowing to excellent flow (granules) |
| 12-16 | Free-flowing to good flow (powders) |
| 18-21 | Fair to passable powdered granule flow |
| 23-28 | Easy fluidisable powders (poor flow) |
| 28-35 | Cohesive powders (poor flow) |
| 35-38 | Cohesive powders (very poor flow) |
| >40 | Cohesive powders (very very poor flow) |

### 3.2.1.3 In-gap ribbon porosity

A method to calculate In-Gap ribbon porosity, $\varepsilon_{ribbon(in\text{-}gap)}$ (%), has been described previously [Gamble *et al.*, 2010]. Briefly; the volume of ribbon (in-die), $V_{ribbon}$ ($cm^3$), produced in one minute is theoretically determined using Equation 3-7:

$$V_{\text{ribbon}} = (\pi . D_r . w_r . v_r . S . t) + nV_k \qquad \textbf{Equation 3-7}$$

where; $D_r$ is the roll diameter (cm); $w_r$ is the width of the rolls (cm), $v_r$ is the roll speed (rpm), $S$ is the roll gap (cm), $t$ is the production time (minutes) and $nV_k$ ($cm^3$) is a correction factor to account for the volume of material within the knurling of the roll surface where $n$ is the number of knurled rollers being used.

In-gap ribbon density, $\rho_{ribbon(in\text{-}gap)}$ (g/cm$^3$), is then calculated using Equation 3-8:

$$\rho_{\text{ribbon(in-gap)}} = \frac{M_{\text{ribbon}}}{V_{\text{ribbon}}} \quad \textbf{Equation 3-8}$$

Ribbon true density, $\rho_{true}$, was measured using helium pycnometry, therefore, the in-gap ribbon porosity, $\varepsilon_{ribbon}$, can be calculated using Equation 3-9:

$$\varepsilon_{\text{ribbon(in-gap)}} = \left(1 - \frac{\rho_{\text{ribbon(in-gap)}}}{\rho_{\text{true}}}\right) \times 100\% \quad \textbf{Equation 3-9}$$

#### 3.2.1.4 In-die tablet porosity

The in-die tablet porosity is calculated from the dimensions of the tablet press and the mass of the tablet, $M_{tablet}$. The volume of the tablet in-die, $V_{\text{tablet(in-die)}}$, is calculated from the punch dimensions, $D_p$, and the distance between the upper and lower punch, $h_{min}$ as shown in Equation 3-10:

$$V_{\text{tablet(in-die)}} = \frac{\pi {D_p}^2}{4} \times h_{min} \quad \textbf{Equation 3-10}$$

The in-die tablet porosity can then be calculated by substituting the tablet mass and volume into Equation 3-8 and Equation 3-9.

#### 3.2.1.5 Porosity after relaxation

Ribbon porosity after relaxation was determined using the Geopyc (Micromeritics Instrument Co., Norcross, GA, USA). The Geopyc consists of a graduated cylindrical sample chamber and a plunger as shown in Figure 3-2. A free flowing dry medium (Dryflo, Micromeritics Instrument Co., Norcross, GA, USA) is filled to a height of 3.2 mm in the sample chamber and the plunger is then used to seal the chamber. The sample chamber and plunger are loaded onto the Geopyc and a blank run is performed using a consolidation force

of 51 N (for a sample chamber diameter of 25.4 mm), whereby the plunger is forced into the chamber compressing the dryflo, until a force of 51 N is reached. The Geopyc monitors the horizontal displacement, $l_1$, and converts this into the volume of dryflo, $V_{dryflo}$, as shown in Equation 3-11:

$$V_{dryflo} = l_1 \times CF \quad \textbf{Equation 3-11}$$

where $CF$ $cm^3/mm$ is the conversion factor to convert linear displacement to volume (0.5153 $cm^3/mm$ for a sample chamber with diameter 25.4 mm)

Ribbon samples are prepared by cutting the collected ribbons into smaller sections with approximate dimensions: 32 mm x 11 mm x ribbon thickness. Two sections of ribbon are added to the sample chamber and a second run on the Geopyc with the same consolidation force is performed. The volume is calculated again using Equation 3-12:

$$V_{dryflo+sample} = l_2 \times CF \quad \textbf{Equation 3-12}$$

where $V_{dryflow+sample}$ is the combined volume of the sample and dryflo and $l_2$is the linear displacement accounting for the volume of the sample and the dryflo.

The volume of the sample $V_{sample}$ is then calculated using Equation 3-13:

$$V_{sample} = V_{dryflo+sample} - V_{dryflo} \quad \textbf{Equation 3-13}$$

The mass of the ribbon sample, which is determined using an analytical balance, is recorded in the Geopyc along with the true density data (measured using Accupyc 1340) and thus the porosity can be calculated using Equation 3-14:

$$\varepsilon_{sample} = \left(1 - \frac{\left(\frac{M_{sample}}{V_{sample}}\right)}{\rho_{true}}\right) \qquad \textbf{Equation 3-14}$$

where $\varepsilon_{sample}$ is the ribbon sample porosity (%) and $M_{sample}$ is the sample mass (g)

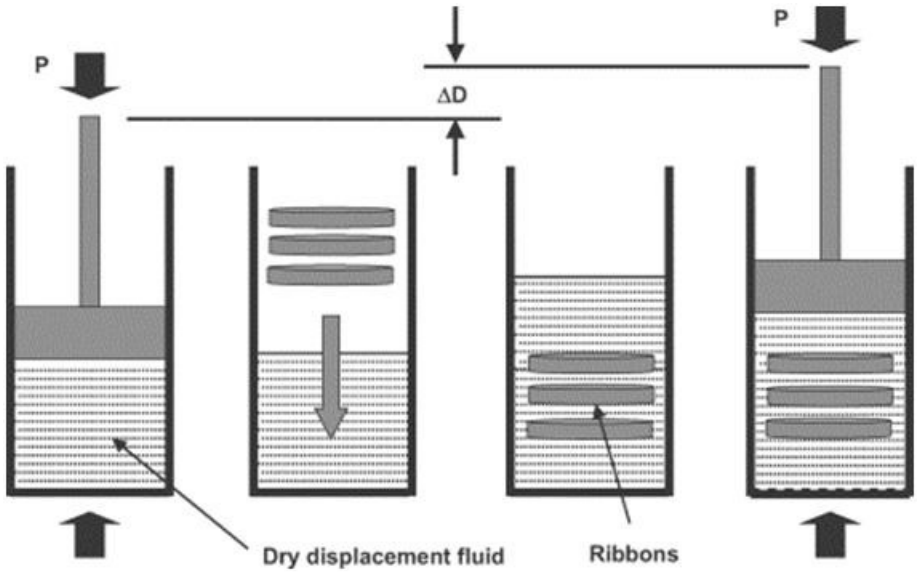


**Figure 3-2 - Schematic diagram for measuring ribbon porosity using the Geopyc 1340 [Zinchuk *et al.*, 2004]**

### 3.2.2 Flow properties

#### 3.2.2.1 Erweka

Granule flowability was determined using the Erweka powder flow tester GTB model (Erweka, Heusenstamm, Germany). Approximately 50 g of material is poured into a 200 ml hopper with an outlet orifice of 11.3 mm. A stirrer is located within the hopper and the stirring speed is set to 2. The time taken for the sample to discharge from the hopper to the collecting vessel is recorded.

#### 3.2.2.2 Powder rheometry

The FT 4 powder rheometer [Freeman, 2001, Freeman, 2007] is a multifunctional device that it is capable of measuring dynamic flowability, consolidation and shear properties of a given powder. A major advantage of the FT 4 is the inclusion of a conditioning cycle, as

shown in Figure 3-3, which, theoretically, provides a reproducible packing arrangement. The difficulty faced in measuring rheological properties of particulate solids is that they are very dependent on the presence, or absence, of air [Freeman, 2007]. Unlike with elastic solids and viscous liquids, when a force is applied to a powder bed consolidation occurs, i.e. particles rearrange into a closer packing arrangement. Upon removal of the force the powder bed will not return to its original state, and as such the bulk density is dependent not only on the current consolidation but also the consolidation history.

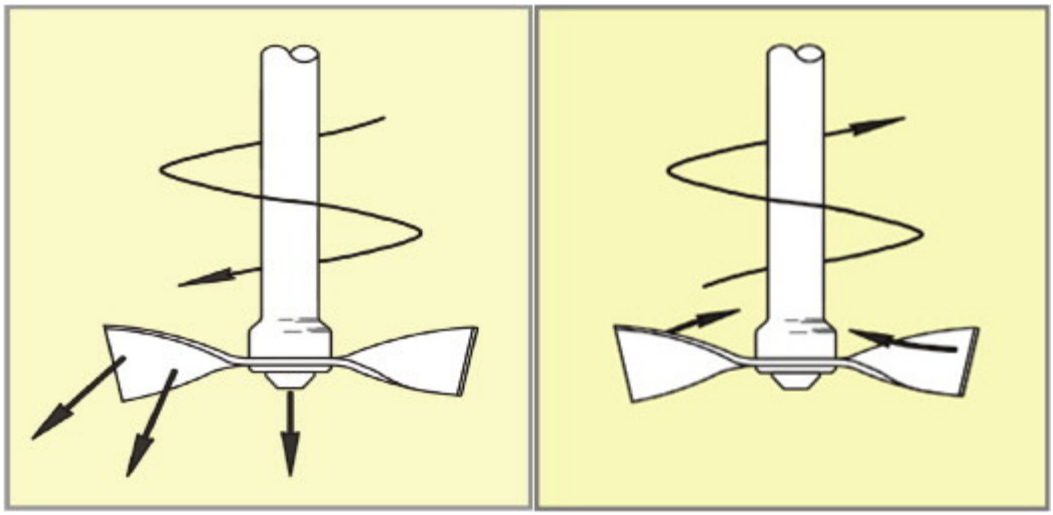

**Figure 3-3 – Conditioning cycle of the FT4, downward motion creates a bulldozing action along the entire length of the blade, upward motion causes shear with minimal consolidation [Freeman, 2007]**

Dynamic flowability testing is conducted by filling a 50 mm bore borosilicate glass cylinder with a powder and moving a 48 mm diameter twisted blade rotationally and axially through the powder. As per the recommendation of the manufacturers a conditioning cycle was performed before each test cycle. The test cycle then follows and the blade moves along a downward helical path (-10° at a blade tip speed of 100 mm/sec) in the opposite direction to the conditioning cycle such that compaction is imposed and the powder is forced to flow around the blade [Freeman, 2004]. The equipment is capable of continuously monitoring the forces acting on the blade and hence the work done in moving the powder can be derived. The work done during this conditioned state is known as the basic flowability index (BFE) and is

defined as the energy required to complete a standard test upon a conditioned state [Freeman, 2004].

The BFE is used as a baseline to calculate several indices which can be used to characterise how a powder will behave;

$$Compaction\ Index = \frac{Energy\ required\ for\ a\ consolidated\ sample}{BFE} \quad \textbf{Equation 3-15}$$

The powder is either tapped or compressed under a known force. This is particularly useful when trying to predict how a powder will behave during storage; it typically ranges from 2-6, but can be from unity to >40.

$$Aeration\ ratio = \frac{BFE}{Energy\ required\ for\ an\ aerated\ sample} \quad \textbf{Equation 3-16}$$

Addition of air reduces the bed packing density and hence the number of contact points between particles, and as a consequence powders will generally flow much more easily. Some powders will become fluidised, in which case, the powder will readily flow; whilst this can be advantageous it can, in some situations, be undesirable. The aeration ratio is a measure of the propensity of the powder to become aerated or fluidised values can vary widely from 1.5 to more than 1000

$$Flow\ rate\ index = \frac{Flowability\ energy\ at\ low\ flow\ rate}{Flowability\ energy\ at\ high\ flow\ rate} \quad \textbf{Equation 3-17}$$

When the blade rotates faster it generally causes more air to be entrained and hence powders tend to flow more easily at higher tip speeds. An ideal powder would have a flow index of around 1; however, most powders, especially cohesive powders, can be as high as 3-4. In addition to the conditions given above, other factors such as attrition and segregation will affect the repeatability of the so called BFE for a given powder.

### 3.2.2.3 Schulze shear cell

A ring shear cell was used to measure the flowability of powders under different pre-consolidation stresses. The bulk sample is loaded into the bottom ring of the shear cell and the top ring is placed on top. The bottom of the shear cell and the underside of the lid are rough to prevent the powder from slipping at the equipment surface. The lid is fixed in position via a crossbeam as shown in Figure 3-4. During operation, a normal force is applied to the lid via the central axis causing pre-consolidation of the sample. The bottom ring is then rotated relative to the lid causing shear deformation of the bulk solid. As the bulk solid shears a prevailing shear force will cause incipient failure, the magnitude of which is directly proportional to the moment force acting on the tie rods $F_1$ and $F_2$. The basic principle behind the shear cell is that this shear force is equivalent to the frictional force on the powder.

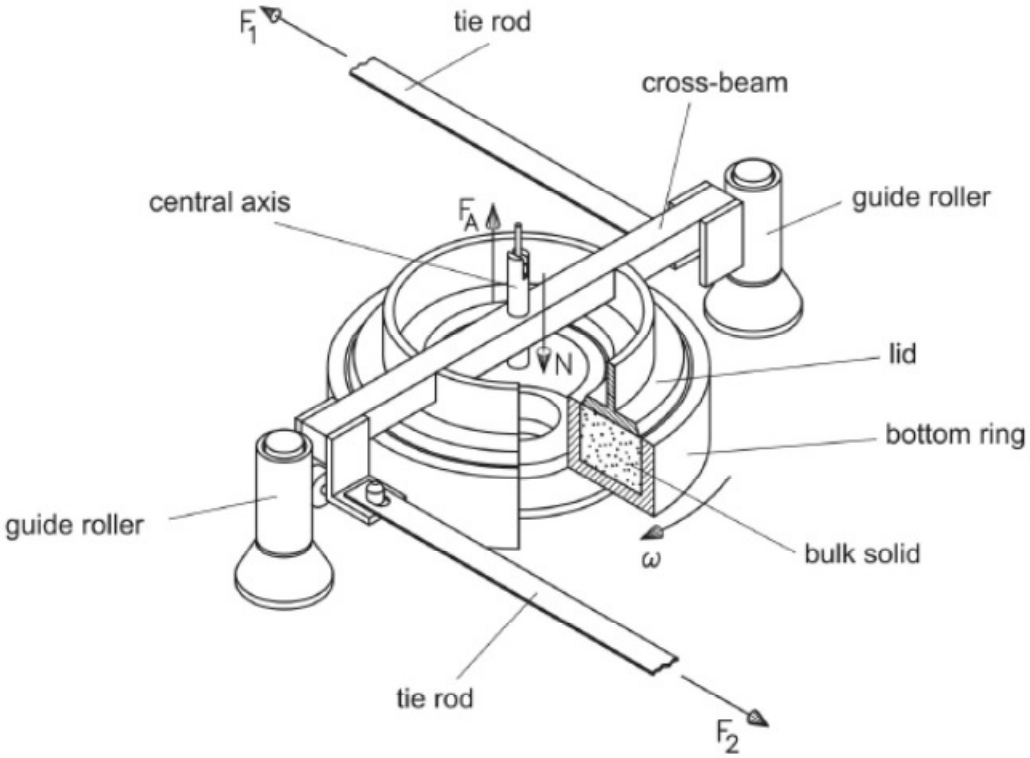


**Figure 3-4 – Schematic illustration of a ring shear tester [Schulze]**

At the start of the test the sample is consolidated under a normal stress $\sigma_{pre}$, and the bottom of the shear cell is rotated, generating an increasing shear force. Initially the increase

in shear force with respect to time is linear indicating that elastic flow is occurring; however, once the force becomes sufficiently large plastic deformation occurs causing the powder to flow and the slope of the increase begins to flatten. Once the shear stress remains constant at a value $\tau_{pre}$, the sample is said to be experiencing steady state flow and is critically consolidated with respect to the normal stress $\sigma_{pre}$. After the pre-shear stage the normal force and shear force acting on the sample is reduced to zero. The second stage of the test involves lowering the normal stress to a value $\sigma_{sh1} < \sigma_{pre}$ and then rotating the shear cell causing the shear force to increase again. Since the sample is now overconsolidated the sample will dilate before incipient flow can occur; this is identified by a reduction in the shear stress. The shear stress in which the sample experiences incipient flow $\tau_{sh1}$ is recorded against $\sigma_{sh1}$ on a shear stress diagram. The sample is then consolidated back to pre-shear stress $\sigma_{pre}$ and presheared again to steady state. After the shear force is returned to zero, a second normal stress is applied $\sigma_{sh2} < \sigma_{sh1} < \sigma_{pre}$ and another point on the shear diagram is plotted. This process is completed for several points to construct a yield locus as shown in Figure 3-5. An important note about the yield locus constructed in this way is that it is only valid for the given pre-shear normal stress $\sigma_{pre}$; different yield loci will be obtained at different pre shear normal stresses.

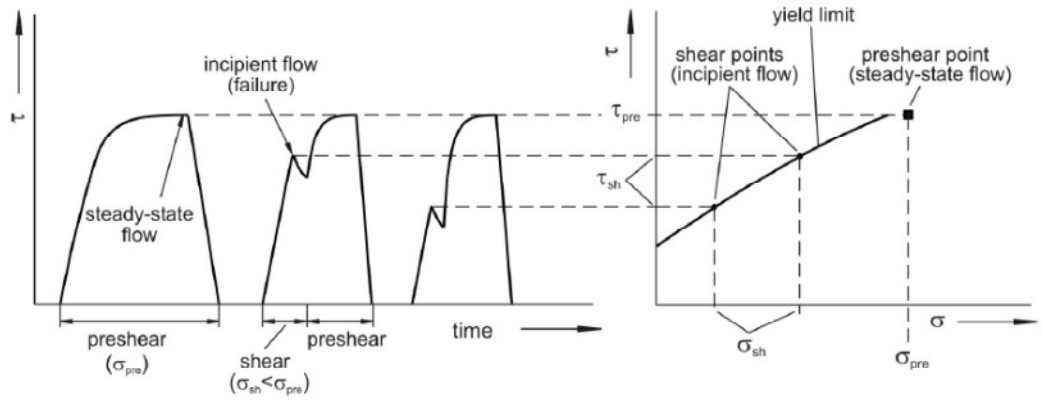


**Figure 3-5 – Determination of the yield stress line for a given preshear point (σpre, τpre) [Schulze]**

An estimate of the flow function can be obtained by constructing Mohr circles tangential to the yield locus. Mohr circles represent the normal stress and shear stress acting on the powder bed in a two dimensional space; they are calculated as follows:

A vertical stress $\sigma_V$ acting on a confined bulk solid will result in a horizontal stress $\sigma_H$ due to stress transmission as shown in Figure 3-6 (a). If we assume that the sides of the confining walls are frictionless then no shear stress will be experienced. However if the force is instead applied to an angular slice, θ, of the bulk solid resolution of stress acting at that angle reveals that both a normal stress and shear stress is acting on the bulk solid as shown in Figure 3-7. Resolution of the stresses allows the normal stress and shear stress experienced on an angular slice at all angles to be calculated using the Equation 3-18 and Equation 3-19[Nedderman, 1992] :

$$\sigma = p + Rcos(2\theta + 2\lambda) \quad \textbf{Equation 3-18}$$

$$\tau = Rsin(2\theta + 2\lambda) \quad \textbf{Equation 3-19}$$

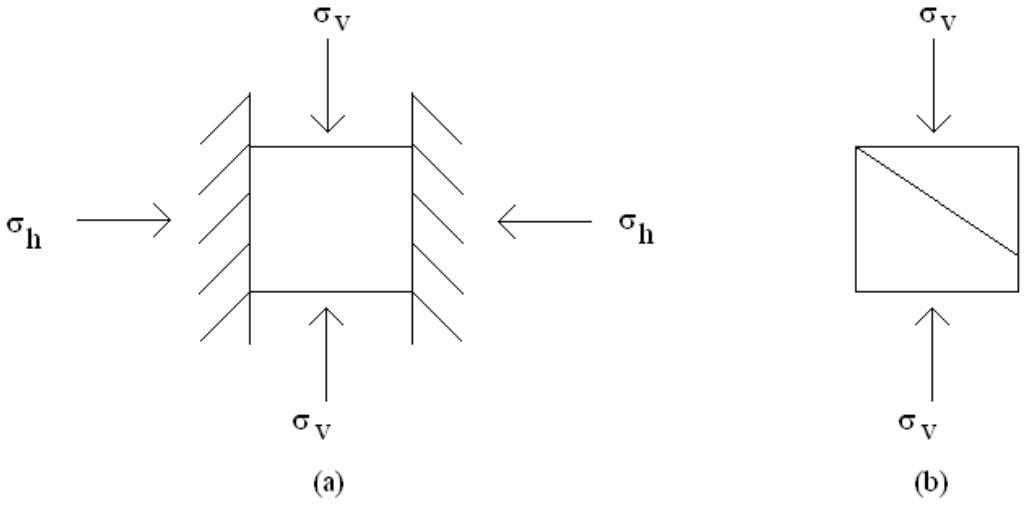


**Figure 3-6 Vertical and horizontal forces acting on (a) confined bulk solid; and, (b) unconfined bulk solid**

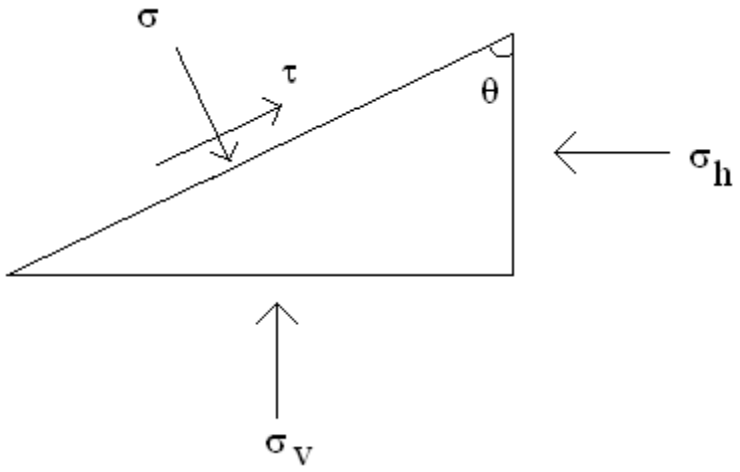


**Figure 3-7 – stress and forces acting on a wedge shaped element**

A plot of the normal and shear stresses on a shear stress diagram results in a circle, referred to as a Mohr stress circle. The centre of the Mohr stress circle is always located on the σ axis, i.e. τ=0. The vertical stress is known as the major stress principle stress and is located at ($\sigma_1$, 0), whilst the horizontal stress is known as the minor principle stress and is located at ($\sigma_3$, 0). If the vertical stress is reduce to zero and the confining walls removed, reapplication of the vertical stress will cause the powder bock to fail, i.e. divide as two rigid blocks at some angle α to the horizontal. The stress required to break the block is referred to as the unconfined yield strength $\sigma_c$. Since in this condition there is no horizontal force the Mohr stress circle passes through the origin. Failure of the bulk solid in this way is analogous to the initiation of flow.

An example of shear cell results is shown in Figure 3-8, the larger Mohr circle which models the confined yield strength passes through the preshear point ($\sigma_{pre}$, $\tau_{pre}$) and is tangential to the yield locus. As such the major principal stress ($\sigma_1$, 0) and minor principal stress ($\sigma_3$, 0) can be defined. The smaller Mohr circle, Figure 3-8, defining the unconfined yield strength is also tangential to the yield locus; however the minor principal stress is 0 and

the major principal stress is at the point ($\sigma_c$, 0). The flow function can then be calculated as the ratio of $\sigma_1$ to the unconfined yield strength $\sigma_c$ as given in Equation 3-20.

$$ff = \frac{\sigma_1}{\sigma_c}$$ **Equation 3-20**

From the yield locus plotted on the shear stress diagram the so called angle of friction can be calculated. The constitutive equation relating normal stress to shear stress is given in Equation 3-21:

$$\tau = \mu\sigma + c$$ **Equation 3-21**

where μ is the slope of the yield locus (known as the coefficient of friction) and c is the intercept of the yield locus with the τ axis.

The angle of friction is then simply calculated using Equation 3-22:

$$\varphi = \tan^{-1}\mu$$ **Equation 3-22**

However, strictly speaking the yield locus is rarely completely linear and as such the angle of friction calculated in this way is done so using a linearized yield locus and thus is referred to as the linear angle of friction $\varphi_{lin}$. The linearized yield locus line is tangential to both Mohr circles. A second angle of friction is defined as the effective angle of friction, which is the slope of an effective yield locus which passes through the origin and is tangential to the largest Mohr circle.

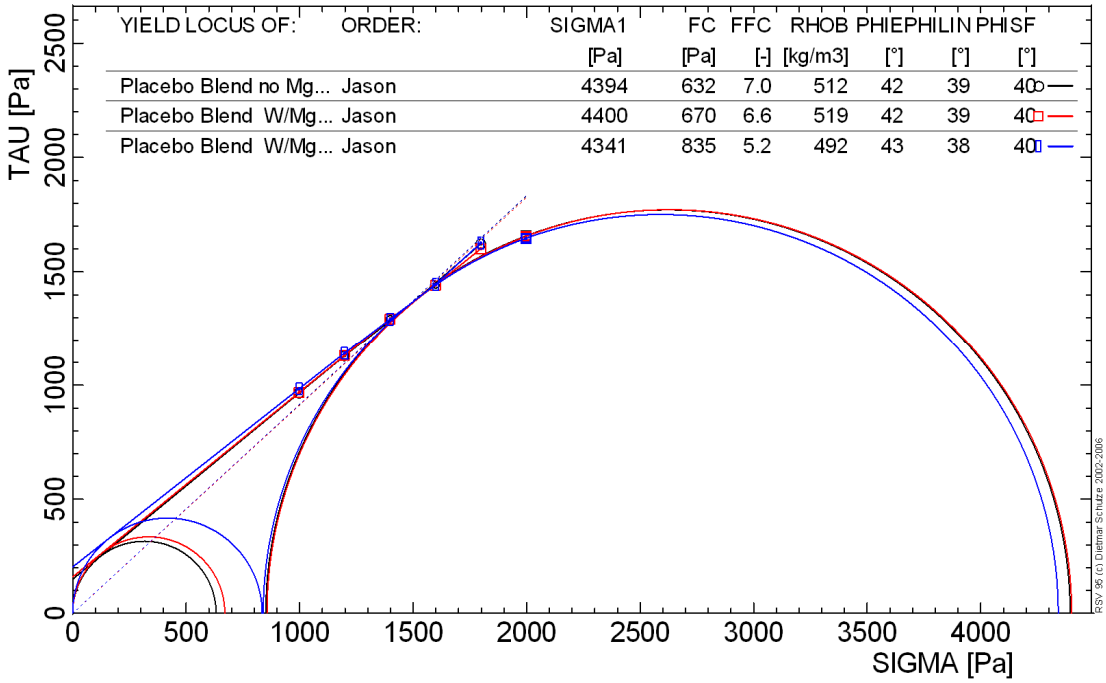


**Figure 3-8 Stress diagram and corresponding Mohr circles**

Wall friction is measured in a similar way to internal friction; however, the bottom shear cell ring has a smooth surface and thus slip at the wall surface occurs as opposed to slip in the bulk sample. A shear stress diagram is plotted at different consolidation stresses, the angle of the slope to the σ axis is known as the angle of wall friction.

### 3.2.3 Mechanical strength testing

#### 3.2.3.1 Ribbon tensile strength

Ribbon tensile strength was measured using the three-point bend method on a texture analyser (Stable Micro systems, Surrey, UK), as described previously [Zinchuk *et al.*, 2004] and shown in Figure 3-9. Ribbon samples, cut to approximate dimensions 32 mm x 11 mm x ribbon thickness, were placed on two supporting beams separated by a distance of 20 mm. A force was then applied to the mid-point of the top face of the sample until fracture occurred. The tensile strength of the ribbon sample is then calculated using Equation 3-23 [Zinchuk *et al.*, 2004]:

$$\sigma_T = \frac{3}{2}\frac{F \times s}{W \times t^2}$$ **Equation 3-23**

where $\sigma_T$ is the ribbon tensile strength (MPa), F is the breaking force (N), s is the distance between the two support beams (mm), W is the ribbon sample width (mm) and t is the ribbon sample thickness (mm)

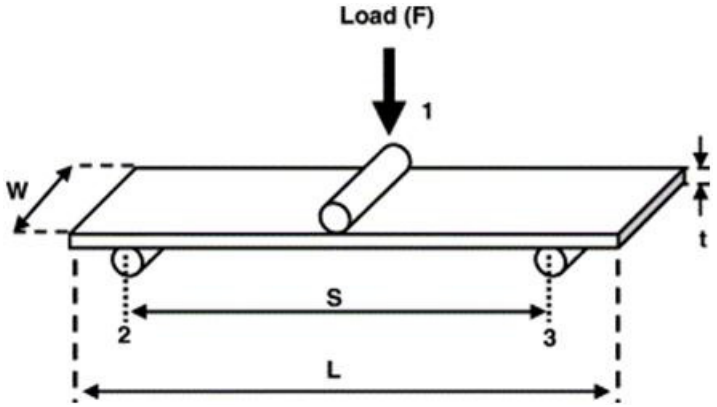


**Figure 3-9 - Three-point bend test for ribbon tensile strength [Zinchuk *et al.*, 2004]**

A three-point beam bending clamp was used for fracture strength determinations and load was applied at a rate of 0.5mm/s using a 5 kg load cell (Stable Micro systems, Surrey, UK).

#### 3.2.3.2 Tablet tensile strength

Diametrical crushing strength of tablets was determined using a tablet hardness tester (Pharmatron, Dr Schleuniger, Switzerland) which is capable of providing a constant strain rate to cause fracture to a tablet undergoing a compressive stress. The tensile strength of tablets can be calculated from the diametrical crushing strength using Equation 3-24 [He *et al.*, 2007]:

$$\sigma_d = \frac{2F_d}{\pi D t}$$ **Equation 3-24**

where $\sigma_d$ is the tensile strength (MPa), $F_d$ is the load required to cause fracture (crushing strength) (N), D is the tablet diameter (mm) and t is the tablet thickness (mm).

### 3.2.4 Granule size distribution

#### 3.2.4.1 QicPic

Granule size distribution was determined using a QicPic dynamic imaged based particle sizing system (Sympatec GmbH, System- Partikel-Technik, Clausthel-Zellerfeld, Germany). Samples were riffled (Retsch, Haan, Germany) to an aliquot size of approximately 1-3 g prior to analysis to ensure they were representative of the bulk. The measuring range was set to 5-3410 µm, and the dispersion method was by gravimetric means using a drop height of 50 cm. Silhouette images were taken at a rate of 400 frames per second. The calculated particle size is based on the equivalent spherical diameter.

### 3.2.5 Tablet performance

#### 3.2.5.1 Dissolution

Dissolution analysis was performed on a VanKel VK 7010 (Varian, Inc, US) using the USP 2 paddles method. Spectra absorbance was measured using an Agilent technology spectrophotometer (Agilent Technologies, Wokingham, UK); samples were automatically withdrawn from the dissolution vessel medium at 5 minute intervals and spectra were taken using a 1 cm flow cell. Atenolol had a characteristic spectral absorbance peak at 272 nm. 900 ml of reverse osmosis (RO) water at a temperature of 37 ℃ was used as the dissolution medium.

Standards were prepared using pure Atenolol dissolved in 250 ml of RO water. The concentration of the standards was based on the drug loading of the tablets calculated using Equation 3-25 and shown in Table 3-2:

**Table 3-2 – Mass of Atenolol required to make desired standard concentration (250 ml of RO water)**

| Atenolol Drug Loading (%) | Standard Concentration (mg/ml) | Mass of Atenolol (mg) |
|---|---|---|
| 10 | 0.044 | 11.11 |
| 20 | 0.089 | 22.22 |
| 40 | 0.178 | 44.44 |

$$\frac{xm_t}{V_{dis}} = \frac{m_{Atenolol}}{V_{standard}} \quad \textbf{Equation 3-25}$$

where x is the drug loading (% w/w Atenolol), $m_t$ is the tablet mass (0.4 mg), $V_{dis}$ is the volume of dissolution medium (0.9 L), $V_{standard}$ is the volume of RO water used for the standard (250 ml) and $m_{Atenolol}$ is the mass of pure Atenolol required to make the standard at the require concentration

### 3.2.5.2 Beer-Lambert law

The absorbance is linearly related to the concentration of Atenolol dissolved in the dissolution media by Beer-Lambert Law [Atkins and de Paula, 2006] shown in Equation 3-26:

$$A = \varepsilon bc \quad \textbf{Equation 3-26}$$

where A is absorbance (-), ε is the molar absorbtivity ($L.mol^{-1}.cm^{-1}$), b is path length of the sample (cm) and c is the concentration of the compound (Atenolol) in solution (mol/L)

The applicability of the linear relationship between absorbance and concentration of Atenolol is demonstrated in Figure 3-10, which shows the absorbance of the three dissolution standards given in Table 3-2. Using this linear relationship the concentration of Atenolol dissolved in the dissolution media at each time point can be calculated using Equation 3-27:

$$\frac{A_{sample} \times \left(\frac{m_{Atenolol}}{V_{standard}}\right)}{A_{standard} \times \left(\frac{xm_t}{V_{dis}}\right)} = \%\ Dissolved \quad \textbf{Equation 3-27}$$

where $A_{sample}$ and $A_{standard}$ are the absorbance of the sample dissolution media and the standard respectively.

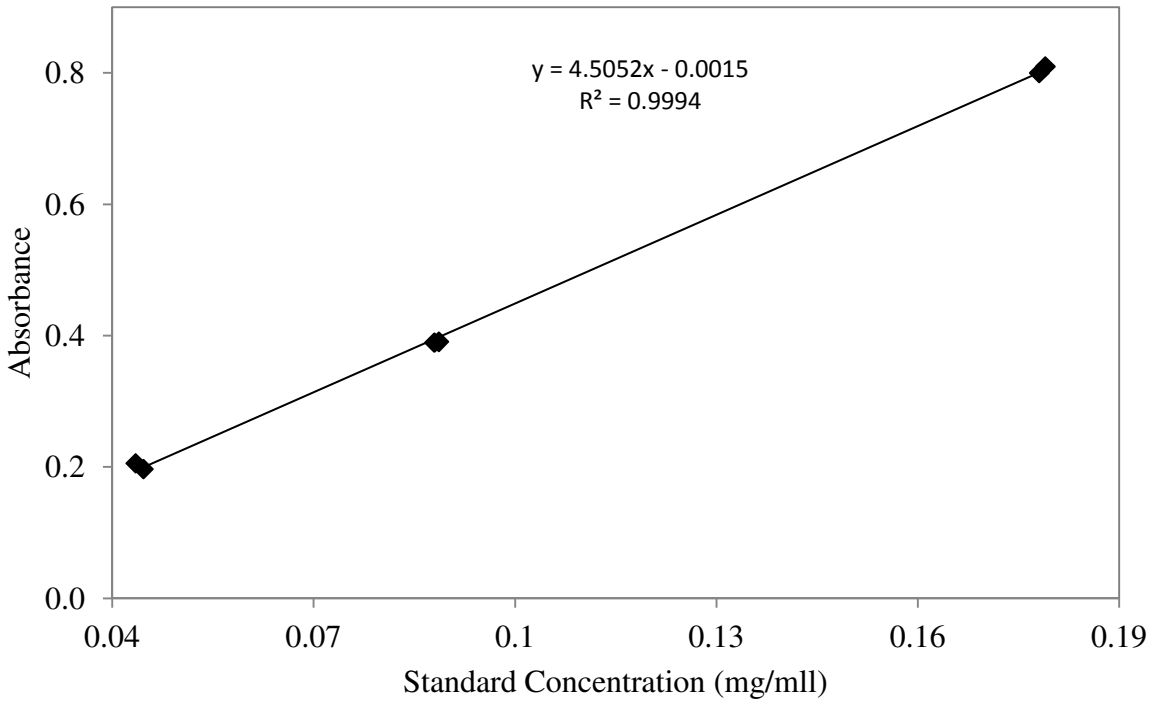


**Figure 3-10 – linear relationship between measured absorbance (at wavelength 272 nm) and the actual standard concentration (mg/ml) (Data shown is for individual data points)**

### 3.2.6 Spectroscopic techniques

#### 3.2.6.1 Near-Infrared imaging

Near infrared (NIR) chemical imaging data was collected using a Sapphire® NIR chemical imaging system and processed using ISys® software (Malvern, Worcestershire, UK). Calibration scanning was conducted prior to data collection by first performing a background scan using a highly reflective white ceramic surface, followed by a dark scan using a mirrored surface. Spectra were taken between 1400 and 2400 nm with a 10 nm step size, and 16 co-adds. Analysis of the data was performed using a partial least squares (PLS) model based on 4 principal components.

#### 3.2.6.2 Near-Infrared spectroscopy

Diffuse reflection spectra were taken directly from the surface of the pre-lubricated roller surface described in Chapter 4. NIR spectra were measured on an FT-NIR spectrometer (Thermo Antaris, Madison, WI, USA). Diffuse reflection spectra using the integrating sphere were recorded from 1100-2300 nm using 64 scans at 8 $cm^{-1}$ resolution.

#### 3.2.6.3 Inductively coupled plasma – optical emission spectroscopy

Inductively coupled plasma – optical emission spectroscopy (ICP-OES, Varian VISTA, Santa Clara, CA, USA) was used to determine the magnesium stearate content of the roller compacted granule manufactured using the external lubrication system. It was carried out by Mrs Gina Green (Intertek Pharmaceuticals Service, Manchester, UK). A set of standards were created using a formulation containing a ratio of 3:2 microcrystalline cellulose (Avicel PH 102) to lactose anhydrous with a magnesium stearate content of 0, 0.01, 0.025, 0.05 or 0.1 % w/w. The samples were prepared by mixing all of the ingredients in a high shear blender (Mixer Granulator P 1 – 6, Diosna, Osnabrück, Germany) with a 1 litre blending vessel, an impeller speed of 458 rpm and a chopper speed of 1503 rpm for 5 minutes. Two replicate blends were prepared for each of the concentrations with a total batch size of 215 g used in order to achieve a targeted blend vessel fill volume of 50 %. For ICP-OES sample preparation, a 0.25 g aliquot of each standard was mixed with 8 ml of concentrated nitric acid and microwave digested (Mars 5, CEM, Buckingham, UK). Matrix matched standards were prepared at the concentrations 0, 0.01, 0.05, 0.1 and 0.5 ppm magnesium by diluting pure 1000 ppm magnesium (Romil Pure Chemistry, Cambridge, UK) with deionised water. The content of magnesium was determined by analysing the intensity of 4 magnesium wavelengths (279.6 nm, 279.8 nm, 280.3 nm, and 285.2 nm); the results were averaged from the intensity at each of these wavelengths. In all cases the correlation coefficient was > 0.99

and recovery of all check standards was acceptable (within 70-130 %). The magnesium stearate content in the blend/standards was calculated from the magnesium content using Equation 3-28:

$$\%\, w/w_{MgSt} = \frac{X_{ppm}}{Df \times \frac{Mw_{Mg}}{Mw_{MgSt}}} \qquad \textbf{Equation 3-28}$$

Where $X_{ppm}$ is the measured magnesium in parts per million, Df is the dilution factor Df= $\frac{M_{sample}}{V}$ (where $M_{sample}$ is the mass of sample and v is the volume of liquid used), $Mw_{Mg}$ and $Mw_{MgSt}$ are the molecular weights of magnesium and magnesium stearate respectively (24.31 and 591.24 g/mol).

The content of the magnesium stearate in the roller compacted ribbon was determined using the same sample preparation/analysis method as for the standard calibration run. The compacted ribbons were first milled using the Alexanderwerk integrated mill using a primary sieve screen 2.5 mm, a secondary sieve screen 1.0 mm and a rotary mill speed of 60 rpm. The bag was rotated by hand to prevent sampling bias from the top layer of granules. The results are shown in Chapter 5.

## 3.3 Manufacturing process

### 3.3.1 Dispensing

Materials were dispensed as received using either a Mettler Toledo SR32001 DeltaRange Balance (Mettler Toledo, Painesville, USA) if the mass was greater than 100 g or a Sartorius BP 3100 S (Data Weighing Systems, Inc., Elk Grove, USA) if the mass was less than 100 g. All materials were screened prior to blending using 1000 µm sieve screen except magnesium stearate, sodium stearyl fumerate and colloidal/micronized silicon dioxide which were screened using a 500 µm sieve screen.

### 3.3.2 Formulation

The composition of the formulations used is given in Table 3-3. The magnesium stearate used in this study was acquired from Mallinckrodt; studies have shown that magnesium stearate (vegetal) acquired from Mallinckrodt is probably a dihydrate or a mixture of hydrates' [Swaminathan and Kildsig, 2001]. Croscarmellose sodium was added to the formulations to represent a model disintegrant and was fixed at a representative concentration of 5 % w/w [Guest, 2009]. Microcrystalline cellulose (grade Avicel 102) and lactose anhydrous were used as model binders and kept at a constant ratio of 3:2. As such the total mass of croscarmellose sodium was the same in all formulations (5 % w/w), whilst the mass of microcrystalline cellulose and lactose anhydrous was reduced (maintaining the same ratio) to keep a total batch size of 2500 g following addition of magnesium stearate. The details of any deviation from this platform formulation are given in the individual experimental chapters.

**Table 3-3– Quantities of excipients used for each formulation on weight basis (%w/w)**

| Excipient | Un-lubricated | Lubricated |
|---|---|---|
| Microcrystalline cellulose | 57.00 % | 56.70 % |
| Lactose Anhydrous | 38.00 % | 37.80 % |
| Croscarmellose sodium | 5.00 % | 5.00 % |
| Magnesium stearate | - | 0.50 % |
| Total | 2500.00 g | 2500.00 g |

### 3.3.3 Blending

The generic blending operation was performed using a tumble blender (GEA Process Engineering Inc, Copenhagen, Denmark) with either a 5 or 10 litre intermediate bulk container (IBC) (to achieve a 40-60% blender fill). A two step blending strategy was used by which all excipients (added in the following order; microcrystalline cellulose, anhydrous lactose, croscarmellose sodium) except magnesium stearate were initially blended for 10 minutes at 15 rpm (150 revolutions), after which the magnesium stearate was added and the

formulation was blended for a further 7 minutes at 15 rpm (105 revolutions). Formulations not containing magnesium stearate were blended for the first 10 minutes only.

### 3.3.4 Roller compaction

#### 3.3.4.1 Roller compactor parameters

Roller compaction was performed using an Alexanderwerk WP120 roller compactor (Alexanderwerk, Remscheid, Germany), which has a horizontal force fed screw feeder and vertically aligned rollers. The user controllable parameters include: roll surface design (smooth and knurled surfaces were utilised in this study), feed auger rotation speed (18.7 – 81.3 rpm), roll speed (3.4 – 14.8 rpm), hydraulic roll pressure (18 – 230 bar), upper and lower mill screen size and the rotational speed of the rotary mill (24.7 – 107.3 rpm). The actual roller compactor settings used for each section of work are given in section 3.3.4.2, whilst the milling conditions were not used as a variable parameter throughout this project and were fixed at the following settings: primary milling screen = 2.5 mm, secondary milling screen = 1.0 mm and a rotary mill speed of 60 rpm. Other optional parameters include vacuum de-aeration (designed to help remove void air from highly voluminous formulations) and roll gap control. Roll gap control is via a PID feedback control system in which a desired roll gap can be set. In roll gap control mode roll speed and hydraulic roll pressure are maintained at the operator set point, whilst the screw speed is automatically adjusted until the desired roll gap is achieved. Deviation from the set roll gap will be corrected for automatically by adjustment of the screw speed; for example, if the actual roll gap is less than the set point then the screw speed will increase and vice versa. A physical model explaining the interplay between roller compaction parameters and roll gap was described in detail in section 2.3.1.1. Vacuum de-aeration and roll gap control were not utilised during this study.

### 3.3.4.2 Ribbon manufacturing strategy

**Table 3-4 - Roller compaction parameter settings for un-lubricated and lubricated placebo formulations**

| Screw Speed (rpm) | Roll Gap (mm) | Hydraulic Pressure (bar) | Roll Speed (rpm) |
|---|---|---|---|
| 25 | 2.2 | 45 | 3.4 |
| 30 | 2.2 | 60 | 3.4 |
| 32 | 2.2 | 80 | 3.4 |
| 34 | 2.2 | 110 | 3.4 |
| 45 | 2.2 | 200 | 3.4 |

The experimental strategy presented in chapter 4 was designed to obtain ribbons of varying porosity by altering the processing conditions. This was achieved by determining the minimum hydraulic pressure required to manually maintain a roll gap of 2.2 mm (without the aid of roll gap control) at a range of auger feeder rotational speeds for an un-lubricated placebo formulation; the parameters are shown in Table 3-4. These process conditions (auger rotation speed, roll speed and hydraulic pressure) were then repeated for a lubricated placebo formulation. In order to monitor batch-to-batch variability, each condition was repeated 6 times. For each condition the roller compactor was considered to be operating under steady state conditions once the roll gap remained constant for at least one minute. Three types of roll configuration were tested for both the un-lubricated and lubricated conditions, that is – knurled upper/knurled lower roll, knurled lower/smooth upper roll and smooth upper/smooth lower roll. Ribbons were collected for one minute and the mass, $M_{ribbon}$ (g), was measured using an analytical balance (Sartorious AG, Goettingen, Germany). In order to nullify the effect of mill retention time, the milling section was dismantled and thus ribbon was collected instead of granule.

**Table 3-5 – Experimental design to include roll speed as a factor for external lubrication trials**

| Factor | Low | Medium | High |
|---|---|---|---|
| Screw speed (rpm) | 30 | 50 | 70 |
| Roll speed (rpm) | 4 | 7 | 10 |
| Pressure (bar) | 50 | 75 | 100 |

The initial test of the AccuSpray external lubrication system, detailed in chapter 5, was to investigate the impact of externally applied magnesium stearate on the roller compaction behaviour of a placebo formulation compared to that of an un-lubricated and internally lubricated (0.5 % w/w magnesium stearate) placebo formulation under normal operating conditions. As such, the roller compactor conditions were the same as those used in chapter 4 (Table 3-4). The impact of external lubrication on roll surface was also investigated using three types of roll configuration, that is – knurled upper/knurled lower roll, knurled lower/smooth upper roll and smooth upper/smooth lower roll. To determine the effect of roll speed on the ability of the AccuSpray external lubrication system to prevent formulations from sticking to the roll surface during roller compaction the operating parameters were extended to include varying roll speeds in an experimental design given in Table 3-5. Roller compaction of the formulations containing drug product was performed using one roller compactor setting only due to the limited availability of materials the roller compactor settings used were screw speed = 50 rpm, roll speed = 7 rpm and hydraulic roll pressure = 75 bar. The purpose of these tests was to provide evidence that adhesion of adhesive formulations, typical of pharmaceutical formulations, to the rolls could be prevented without the presence of magnesium stearate within the formulation.

For the study involving LubriTose, detailed in chapter 6, the roller compactor settings were not used as a variable and were fixed at the following conditions; screw speed = 30 rpm, roll speed = 3.4 rpm and hydraulic roll pressure = 60 bar.

#### 3.3.4.3 Instrumented roll technology

##### 3.3.4.3.1 Pressure profile

The Alexanderwerk roller compactor used at Bristol-Myers Squibb, Moreton, has an instrumented lower roll which is capable of simultaneously measuring the pressure applied to the ribbon compact between the rollers and the angular displacement of the rollers. A typical pressure profile is given in Figure 3-11(a). In the figure the pressure profiles (green, purple and blue lines) represent the pressure profile from each of the three transducers. The average of the three pressure profiles (red line) is also shown. The black line which cuts through the graph is the angular position of the transducer; this only gives the relative position of the transducer compared to its initial starting position, i.e. the rolling angle is set at zero when the instrument is turned on regardless of its starting position. The limitation of this design is that the angular position which relates to the minimum gap is not known. As a consequence one must assume that the minimum gap coincides with the angular position of the maximum pressure recorded in the pressure profile. The functionality of the instrumented roller could be improved if the angular position referred to an absolute position which would allow the minimum gap to be known exactly. This would allow direct and accurate measurement of the nip angle, i.e. the angular position at which pressure is first applied relative to the absolute position of the minimum gap. The value for pressure is displayed on the right y-axis whilst the value for angular displacement is displayed on the left y-axis. The location of the three pressure transducers across the width of the roll is shown in Figure 3-11(b); these pressure transducers simultaneously measure the pressure profile applied at the centre and edges of the

roll. Greater detail regarding the instrument roller can be found within the following references [Nesarikar *et al.*, 2012a, Nesarikar *et al.*, 2012b]

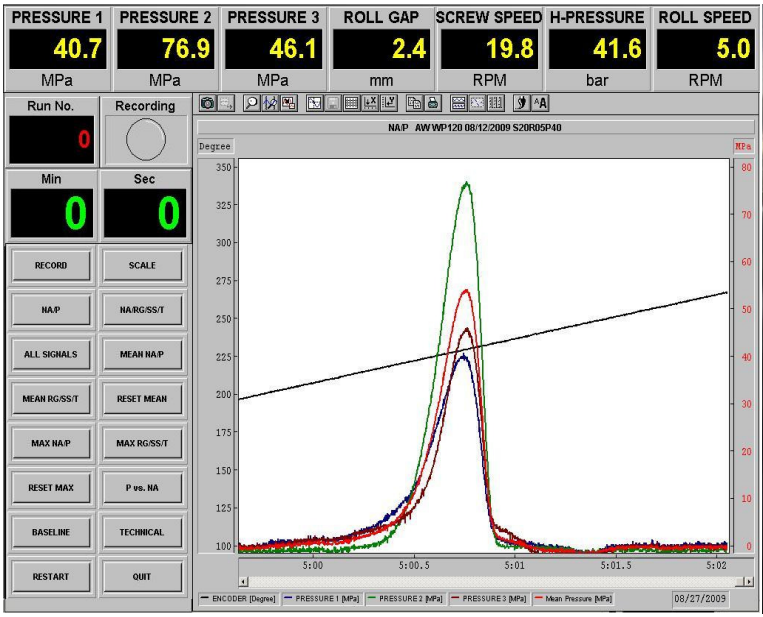


**Figure 3-11 (left) Typical pressure profile within the nip region during roller compaction; (right) location of the three pressure transducers across the width of the ribbon**

#### 3.3.4.3.2 Calculating nip angle

The nip angle is measured using the method described previously by Bindhumadavan *et al.* [Bindhumadhavan *et al.*, 2005], which involves fitting a line to the linear region of the pressure increase and pressure decrease regions of the pressure profile (Pressure vs. Angle). The difference between the x-axis intercept of the two lines is defined as the nip angle.

#### 3.3.4.3.3 Calculating the in-gap ribbon density at a given roll angle

The distance between the two roll surfaces, ($S_\theta$) at any given roll angle ($\theta$) and the corresponding horizontal distance away from the minimum roll separation ($X_\theta$), as shown in Figure 3-12, are calculated using Equation 3-29 and Equation 3-30 respectively:

$$S_\theta = S_{min} + D(1 - \cos\theta) \qquad \textbf{Equation 3-29}$$

$$X_\theta = \frac{D}{2}\sin\theta \qquad \textbf{Equation 3-30}$$

where $S_{min}$ is the minimum roll separation (mm) and D is the roll diameter (mm).

Splitting the nip region into trapezoids of infinitesimal thickness the in-gap powder density and porosity can be calculated using the same approach outlined in section 3.2.1.3 and using Equation 3-7 to Equation 3-9. In this way the densification kinetics of the ribbon compact as it transitions through the nip region can calculated.

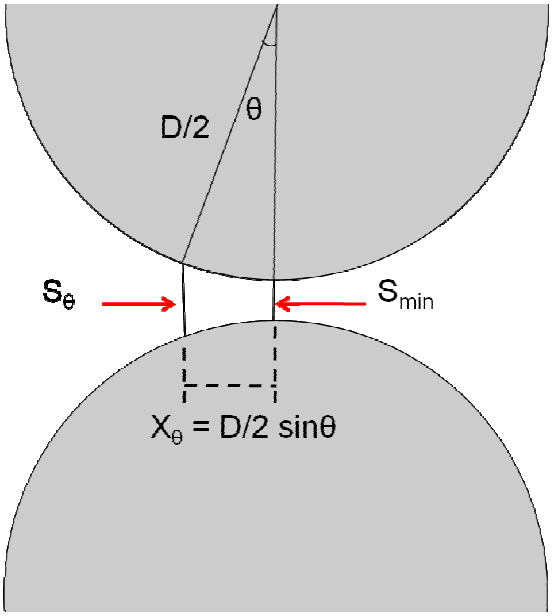


**Figure 3-12 Schematic diagram of the distance between the two roll surfaces and the horizontal distance away from the minimum roll gap at any given roll angle**

#### 3.3.4.3.4 Pressure distribution efficiency

The pressure distribution efficiency ratio is calculated as the difference between the pressures recorded at the edges of the roll surface compared to the pressure recorded by the pressure transducer located at the centre, as shown in Equation 3-31. The pressure distribution efficiency ratio is used as relative number through which the roller compaction lubricating efficacy of the various lubricants can be compared.

$$\frac{(P_1 + P_3)/2}{P_2}$$ **Equation 3-31**

#### 3.3.4.4 External lubrication

The AccuSpray™ system was originally developed to provide a method of applying a thin film of magnesium stearate directly to the punch tips and die surfaces of a rotary tablet press. The exact metering of the substance is controlled by a patented high-speed piezoelectric valve allowing for consistent spray rates. The upper spray nozzle aims at the upper punch tip whilst the lower spray nozzle is located at the next tablet station and aims inside the tablet die (see Figure 3-13 for clarity). The system is controlled to time the magnesium stearate spray with the rotation of the tablet press, such that every punch/tablet die is spray coated at the exact time it passes the spray nozzle. The equipment was modified to retro fit the Alexanderwerk roller compactor, such that the upper spray nozzle was aimed at the upper roll and the lower spray nozzle was aimed at the lower roll. The position of the nozzle relative to the roll surface was limited by the geometry of the roller compactor.

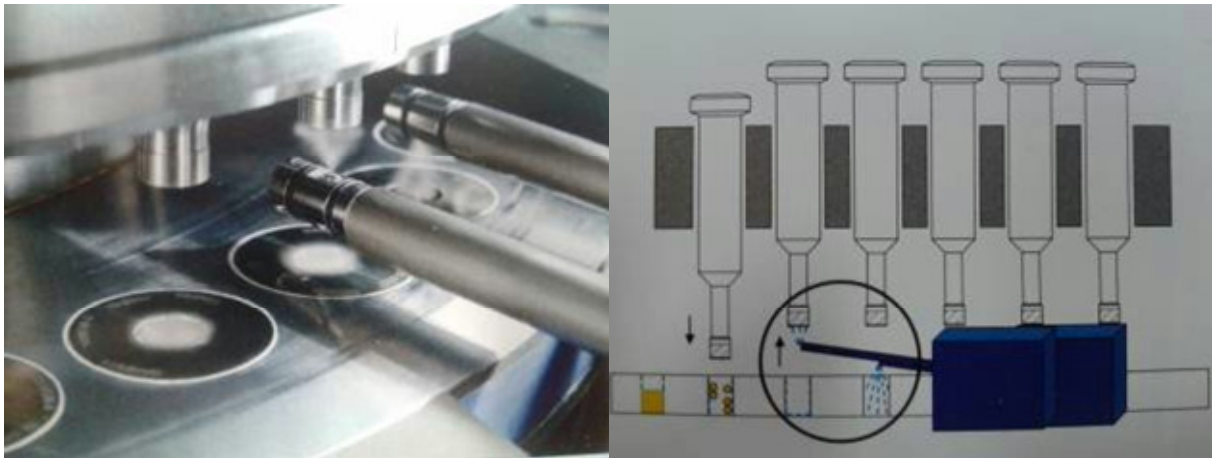

**Figure 3-13 – (left) Position of AccuSpray nozzles on a rotary press, (right) Schematic diagram of the relative position of the upper and lower AccuSpray nozzles**

The set-up of the AccuSpray system with the roller compactor can be seen in Figure 3-14; there are two identical spray guns (see Figure 3-15) allowing the top and bottom roller to be coated simultaneously. The user controlled parameters of the AccuSpray include shot frequency (Hz), magnesium stearate valve opening time (ms), compressed air pressure (bar), compressed air valve opening time (ms) and concentration of the magnesium stearate/IPA

solution (% w/w). The spray rate of the AccuSpray™ was controlled by an analogue signal generator, operated using a square signal wave, to provide an intermittent pulsing spray rate. The initial test setup was designed to calculate the spray rate of the AccuSpray™ as a function of the user generated analogue frequency. The number of shots per minute as a function of frequency was measured as shown in Figure 3-16. An empirical relationship ($R^2$ = 0.998), which converts user generated frequency to spray rate ($S_{pm}$) is given in Equation 3-32:

$$y = 30.0x \quad \textbf{Equation 3-32}$$

where x is the user generated analogue frequency (Hz) and y is the spray rate ($min^{-1}$)

The spray rate alone is not a scalable parameter since a constant spray rate would provide different amounts of roll surface coverage at different scales (*e.g.* roll circumference) and at different roll speeds. A travelling roll distance, shown schematically in Figure 3-17 is therefore defined as the arc length of the roll surface which is formed between the angle displacement θ between two shots of the AccuSpray™ external lubrication system, as given in Equation 3-33:

$$D_{ps} = \frac{\theta}{360} \times (\pi D) \quad \textbf{Equation 3-33}$$

where $D_{ps}$ is the arc length, or roll distance travelled per shot (cm), θ is the angular displacement of the roll between shots and D is the roll diameter.

The angular displacement between shots is a function of the rotational velocity of the rolls and the spray rate of the AccuSpray™ as given in Equation 3-34:

$$\theta = 360 \times \frac{v_r}{S_{pm}} \quad \textbf{Equation 3-34}$$

where $v_r$ is the rotational speed of the rollers (rpm).

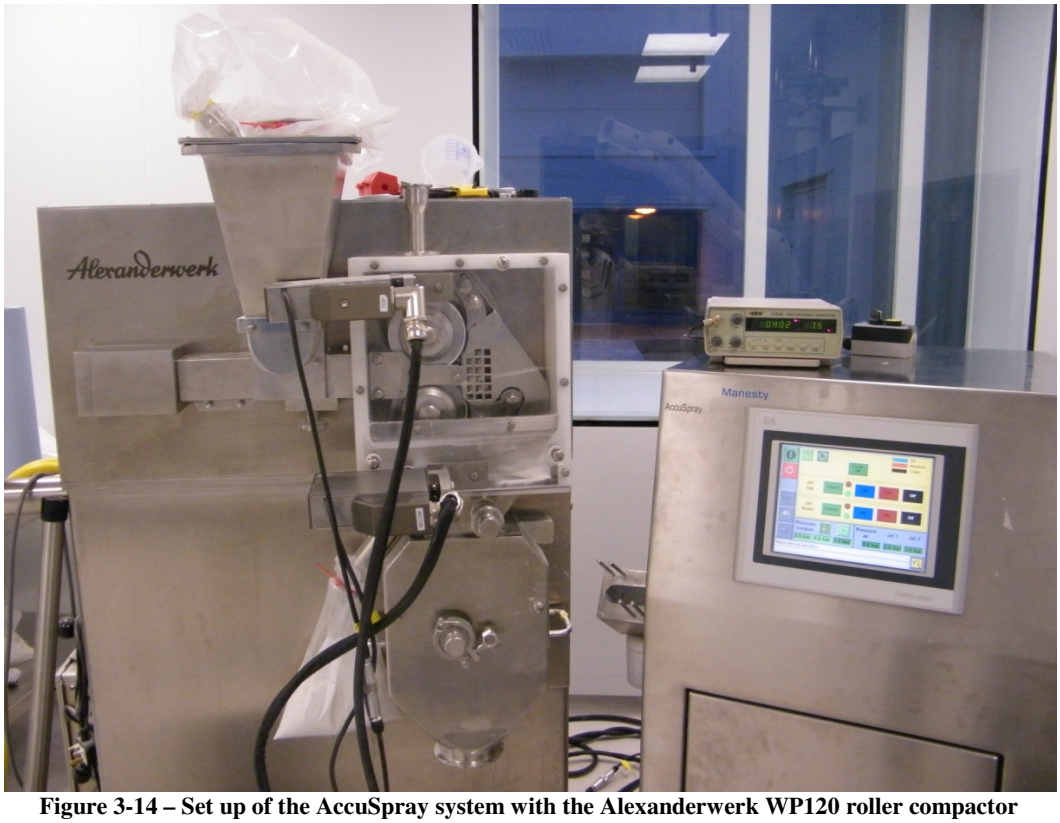


**Figure 3-14 – Set up of the AccuSpray system with the Alexanderwerk WP120 roller compactor**

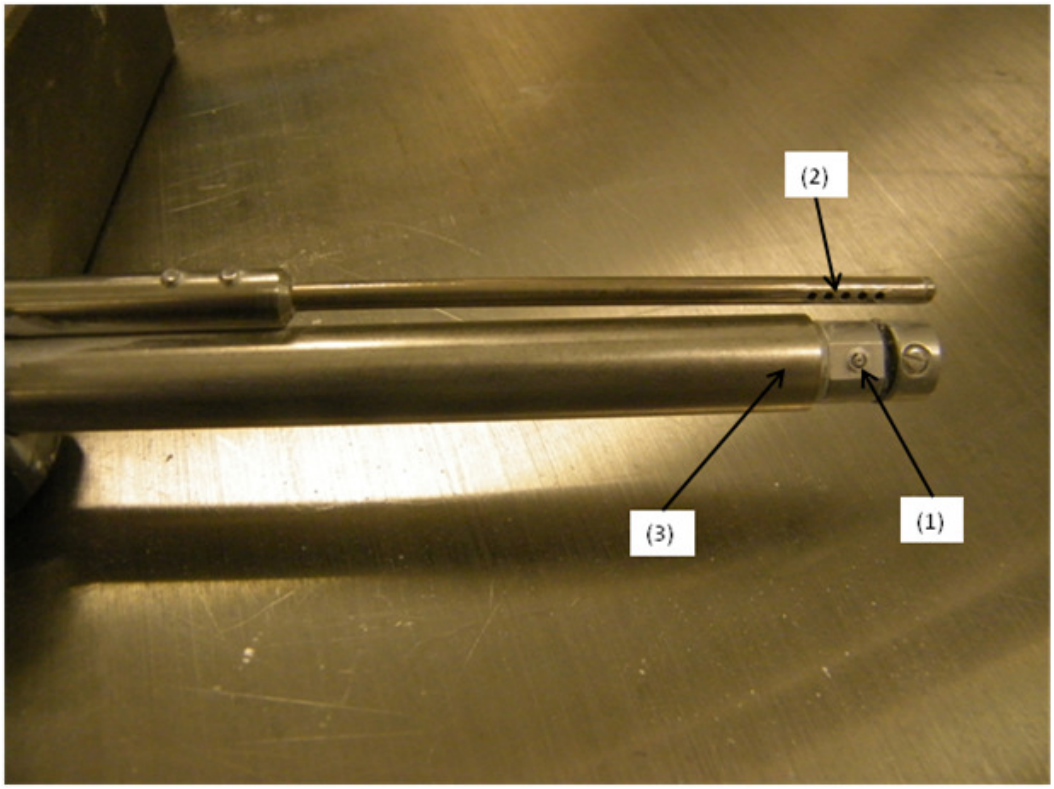


**Figure 3-15 - Close up image of the spray gun equipment showing (1) nozzle for magnesium stearate/IPA suspension ejection, (2) nozzle for compression air jet and (3) protective sleeve which closes when not in operation to protect the nozzle from dust.**

The distance per shot is therefore calculated using Equation 3-35:

$$D_{ps} = \frac{v_r}{S_{pm}} \times (\pi D) \qquad \textbf{Equation 3-35}$$

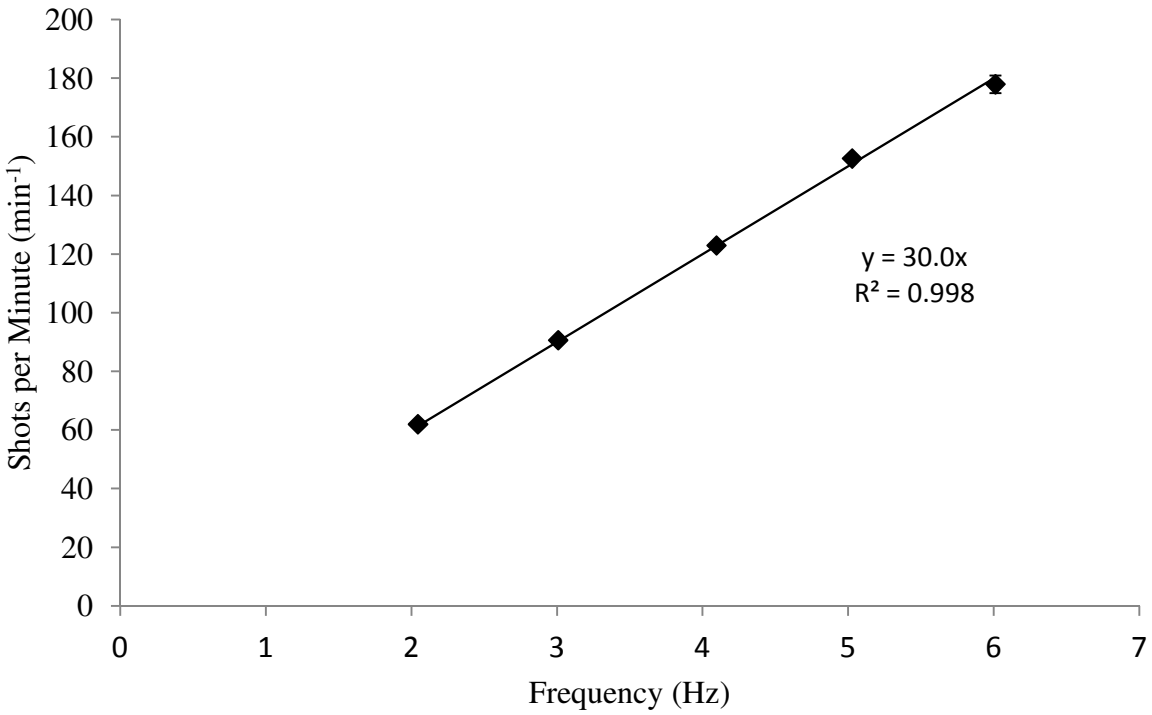


**Figure 3-16 - Plot of the number of shots per minute for a given frequency on the signal generator, frequency can be converted to shots per minute using the y = mx equation from the graph**

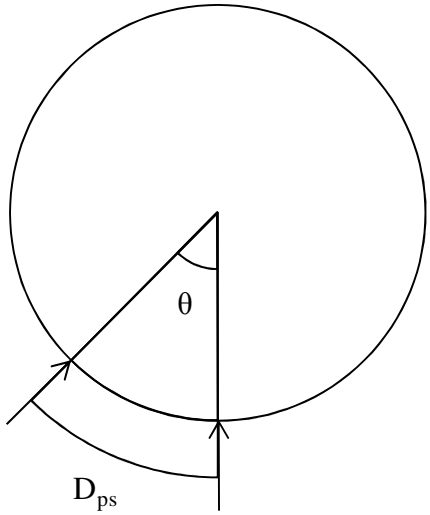


**Figure 3-17 – Schematic representation of the arc length (roll distance travelled) between two shots from the AccuSpray**

An appropriate air pressure must be utilised, in conjunction with probe distance from the surface to be sprayed, to obtain a suitable spray angle such that the optimal area of roll surface coverage is achieved, where a lower air pressure and/or an increased probe distance gives wider surface area coverage on the roll surface. The valve opening time determines the duration of the spray; the spray rate should be sufficient to allow adequate magnesium stearate to be applied to the roll surface, but not so excessive that the solvent does not flash off before reaching the roll surface. Initial studies showed that an air pressure of 2 bar gave sufficient spread of the spray to cover the entire width of the roll surface, and a valve opening time of 1 ms was sufficient to both prevent sticking under the conditions studied, and avoid build up of solvent at the roll surface.

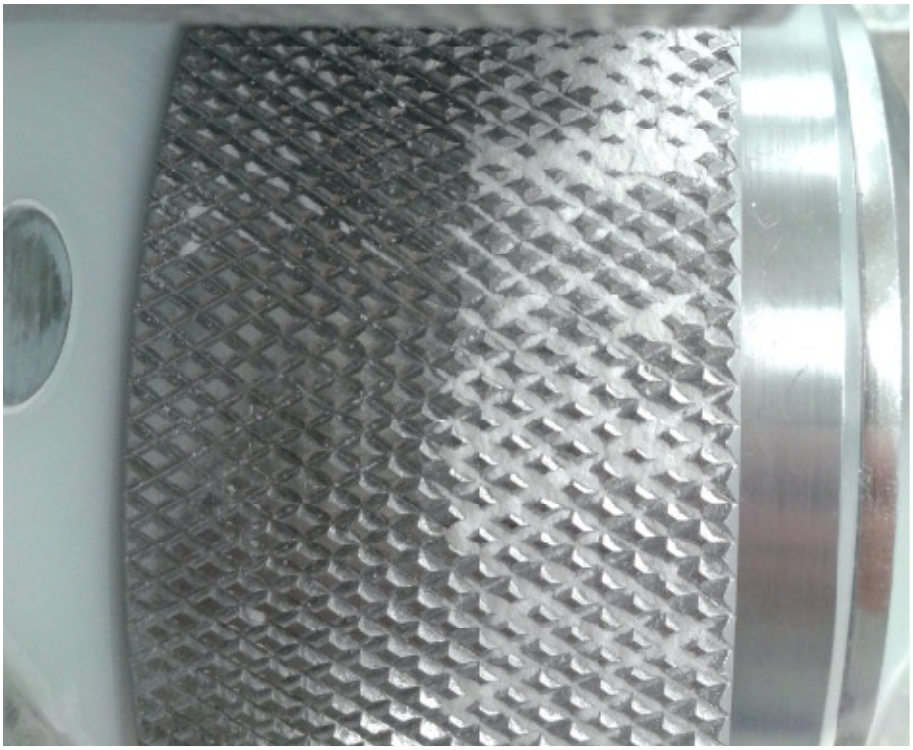

**Figure 3-18 – image showing the importance of roll surface coating of the external lubrication process, in this case the outlet of the spray nozzle is concentrated on the left side of the roll surface, as can be observed the left half of the roll surface is free of adhered ribbon. On the right side of the roll surface no external magnesium stearate was applied and it can be observed that powder has adhered to the roll surface.**

The variables investigated in chapter 5 were the spray frequency, defined as the travelling roll distance per shot, whereby the shot frequency increases with roll speed such that the travelling roll distance per shot stays constant, and the concentration of the magnesium stearate/IPA suspension (8 and 6 % w/w). Initial studies revealed that a suspension concentration of 10 % w/w and above resulted in blockage of the spray system, and that 4 % w/w was insufficient to prevent the formulation from sticking to the roll surface (using the fixed valve opening and air pressure settings). The positioning of the spray nozzle relative to the roll surface was found to be a key parameter for controlling the coating of external magnesium stearate across the width of the roll surface. An example of incorrect roll surface coverage and its influence on adhesion is provided in Figure 3-18.

### 3.3.5 Tabletting

Tablets were compacted using a Stylcam 100R rotary tablet press simulator (Medel'Pharm, Neyron, France) in direct cam operating mode, with flat faced circular punches with a diameter of 11.28 mm producing standard cylindrical tablets. The Stylcam 100R is equipped with a load cell and displacement gauge allowing acquisition of pressure profiles and punch displacement with use of the Analis software. 400 mg of formulation was hand filled into the tablet die and compacted into a tablet with a desired solid fraction of 0.85. The tablet thickness required to give a tablet of 0.85 solid fraction was calculated using Equation 3-36 - Equation 3-38.

$$V_{Tablet} = \frac{\pi D_{(die)}^{\ 2}}{4} \times t \qquad \textbf{Equation 3-36}$$

where $V_{Tablet}$ is the volume of the tablet ($cm^3$), $D_{Die}$ is the diameter of the tablet die (cm), and t is the thickness of the tablet (cm).

$$\rho_{Tablet} = \frac{M}{V_{Tablet}} = SF \times \rho_{True}$$ **Equation 3-37**

where $\rho_{Tablet}$ is the density of the tablet (g/cm$^3$), M is the tablet mass (g), SF is the solid fraction (-) and $\rho_{true}$ is the true density of the formulation (g/cm$^3$).

Since the diameter of the tablet die and the tablet mass is constant for each tablet (*i.e.* 11.28 mm and 400 mg respectively) Equation 3-36 and Equation 3-37 can be combined to find the tablet thickness necessary to achieve a target solid fraction of 0.85:

$$t = \frac{M}{\left(\frac{\pi D_{(die)}^{\ 2}}{4}\right) \times SF \times \rho_{True}}$$ **Equation 3-38**

# CHAPTER 4

# STUDIES ON THE LUBRICATION OF ROLLER COMPACTION FORMULATIONS

# CHAPTER 4

# STUDIES ON THE LUBRICATION OF ROLLER COMPACTION FORMULATIONS

## 4.1 Introduction

It was discussed in section 1.1 that despite its widespread adoption within the pharmaceutical industry, roller compaction remains a relatively under researched technique. A number of gaps in the knowledge space regarding roller compaction formulation issues were identified in Figure 1-1. This chapter is the first in a series of investigations into the impact of lubrication on the roller compaction process. The role of lubricants during roller compaction was questioned in section 2.4; following on from that discussion this chapter attempts to investigate the role of magnesium stearate during roll compaction of a BMS platform placebo formulation and includes a systematic evaluation of the roller compaction behaviour of both un-lubricated and lubricated placebo formulations. Particular attention will also be focused towards assessing the potential for further magnesium stearate mixing within the feeding system. This chapter is focused on the roller compaction process as a whole and as such investigates the effect of magnesium stearate on the powder pre-blend, the roller compaction process and the characterisation of the roller compacted ribbons and the subsequent granules.

## 4.2 Results and discussion

The following section contains the experimental results for the lubrication of roller compaction placebo formulations. The order of the results section is set out to methodically investigate the process of roller compaction. As such the first part of the results section characterises the effect of lubrication on the properties of the powder blend. The second part investigates the effect of lubrication on the roller compaction process, and is divided into the following sections (i) the feeding system as a whole, (ii) powder discharge through hopper outlet, (iii) powder transmission through the feed auger, (iii) the effect of lubrication on the pressure profile in the nip region; and, (iv) the effect of the roll surface. The final part of the results section investigates the effect of lubrication on the properties of the compacted ribbons and subsequent granules.

### 4.2.1 Materials characterisation

#### 4.2.1.1 Density

The measured true density of the un-lubricated and lubricated (0.5% w/w) formulations was found to be 1.59 and 1.58 g/cm$^3$ respectively. A summary of the bulk/tapped density and the calculated flow indices (Carr's index and Hausner ratio) for the un-lubricated and lubricated (0.5% w/w) formulations is given in Figure 4-1. It was observed that the addition of 0.5% w/w magnesium stearate caused a significant (ANOVA) increase in both bulk and tapped density, the measured bulk and tapped density for the un-lubricated formulation was 0.43 and 0.59 g/cm$^3$ respectively, whilst the bulk and tapped density for the lubricated formulation was 0.45 and 0.63 g/cm$^3$. The Carr's index and Hausner ratio are used as an indirect method of assessing powder flow. No statistically significant differences were observed between the unlubricated and lubricated formulations.

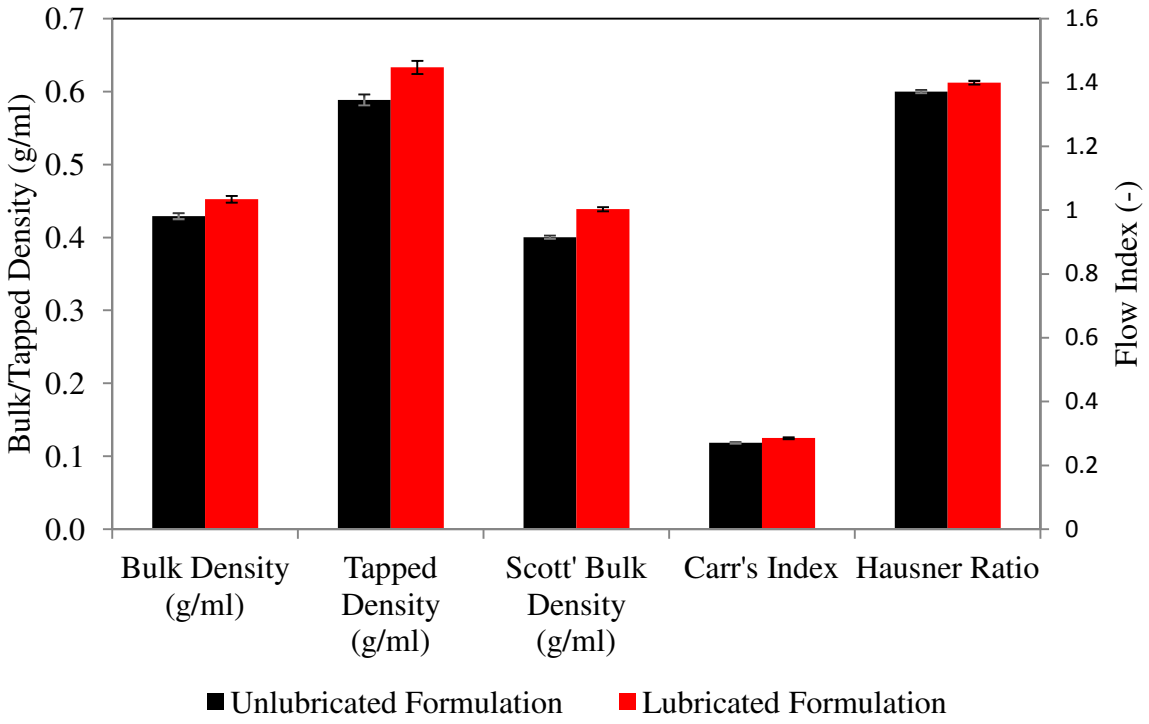


**Figure 4-1 – Bulk/tapped density and the calculated flow indexes for the un-lubricated and lubricated (0.5% w/w) formulations. Error bars show standard deviation n=6.**

#### 4.2.1.2 Erweka flow rate

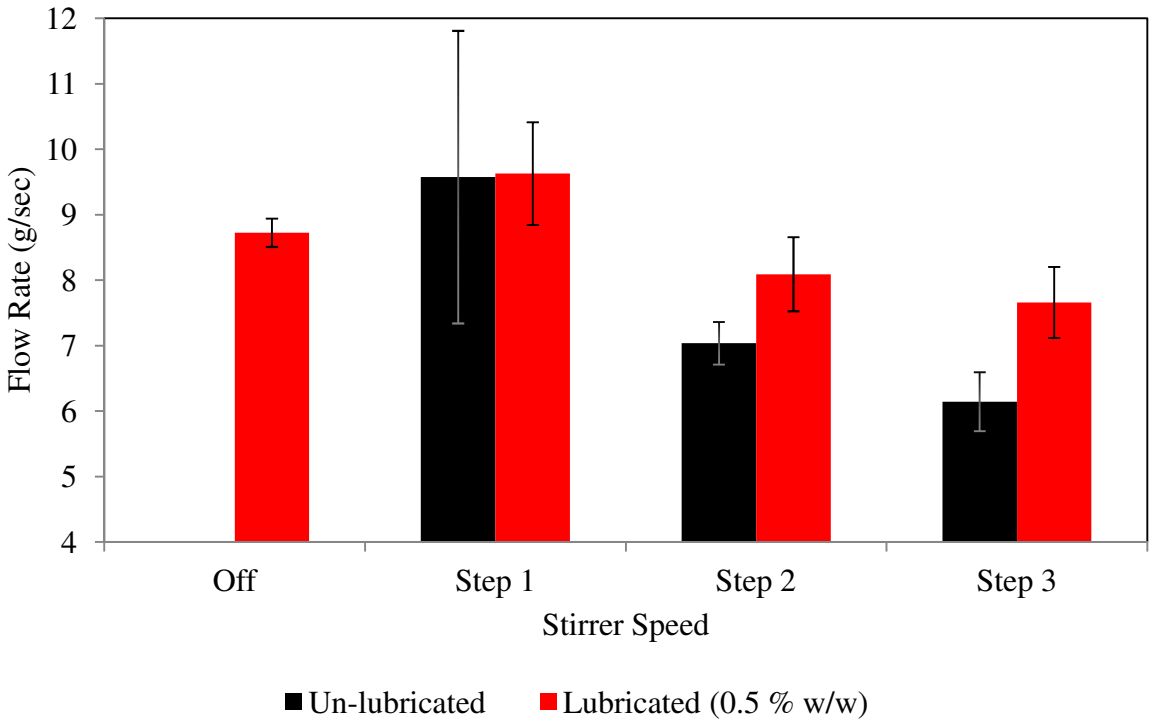


**Figure 4-2 – Flow rate of un-lubricated and lubricated (0.5 % w/w magnesium stearate) powders through a 15 mm orifice using the Erweka flow rate measuring device. Error bars show standard deviation n=3.**

The powder flow rate through a 15 mm orifice is shown in Figure 4-2. Four conditions were investigated, one without the influence of the hopper stirrer and three conditions using varied hopper stirrer rotational speeds. It was observed that the un-lubricated formulation was unable to flow through the Erweka without the influence of the hopper stirrer. The addition of 0.5% w/w magnesium stearate leads to a significant increase in powder flow rate at stirrer step speed 2 and 3.

#### 4.2.1.3 Powder rheometry

The flow parameters of the unlubricated and lubricated formulations measured using the FT4 are shown in Figure 4-3 and Figure 4-4. The basic flow energy (BFE) is a measure of the amount of energy required to move a blade helically through a bed of powder. Initially (test 1 and 2) the BFE for both unlubricated and lubricated formulations is similar; however on repeated test cycles the BFE for the lubricated formulation is observed to reduce (stability index = 0.6) whilst the BFE for the unlubricated powder increases slightly (stability index = 1.2). It is hypothesised that this is due to the magnesium stearate coating the vessel walls and the blade surface. As such, the BFE for the lubricated formulation is less of a reflection on the actual powder flow characteristics and is more of an indication of the flow of material against the vessel wall. That is the FT4 demonstrates the effect of the lubrication at the equipment surfaces. The gap in the data between test 7 and test 8 represents the change from stability test to variable flow rate test. During the stability test (1-7) the blade rotates through the powder bed with a tip speed of 100 mm/s each time. The first test point for the variable flow rate test (test 8) is conducted at a tip speed of 100 mm/s, the tip speed is then sequentially reduced (70, 50, and 10 mm/s) for the remaining three tests. The increase in required energy for the unlubricated formulation indicates that it is more sensitive to flow rate than the lubricated formulation. As the tip speed reduces less air is entrained in the powder bed and hence

powder flow is more restricted; a powder which is sensitive to flow rate is indicative of a more cohesive powder.

The specific energy (SE) is the energy required to rotate the blade in the opposite direction such that the paddle 'lifts' the powder in the vessel. It can be used as an indicator for the cohesion of materials. The SE is significantly lower for the lubricated formulation than the unlubricated formulation.

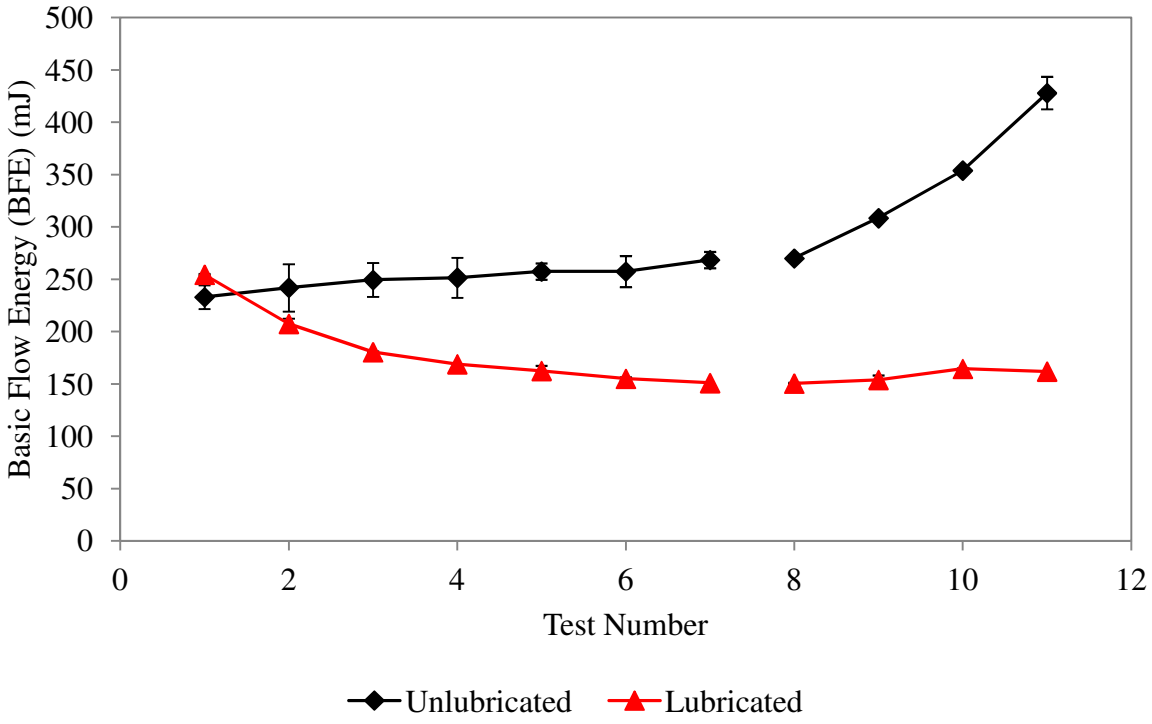


**Figure 4-3 – Stability (test number 1-7) and variable flow rate (test number 8-11) for unlubricated and lubricated placebo formulation. Error bars show standard deviation.**

In contradiction to the data presented above the conditioned bulk density – that is the bulk density of the material contained within the sample vessel following a conditioning cycle – is similar in both the unlubricated and lubricated formulations. The conditioned bulk density measured using the FT4 is a semi automated process, as such reduces the potential operator error that is associated with the technique used to measure the tapped density and Scott's bulk density. Furthermore, the FT4 conditioning cycle is reported to give a more reproducible and

homogenous powder packing arrangement eliminating the potential influence of handling history of the powder [Freeman, 2001, Freeman, 2007].

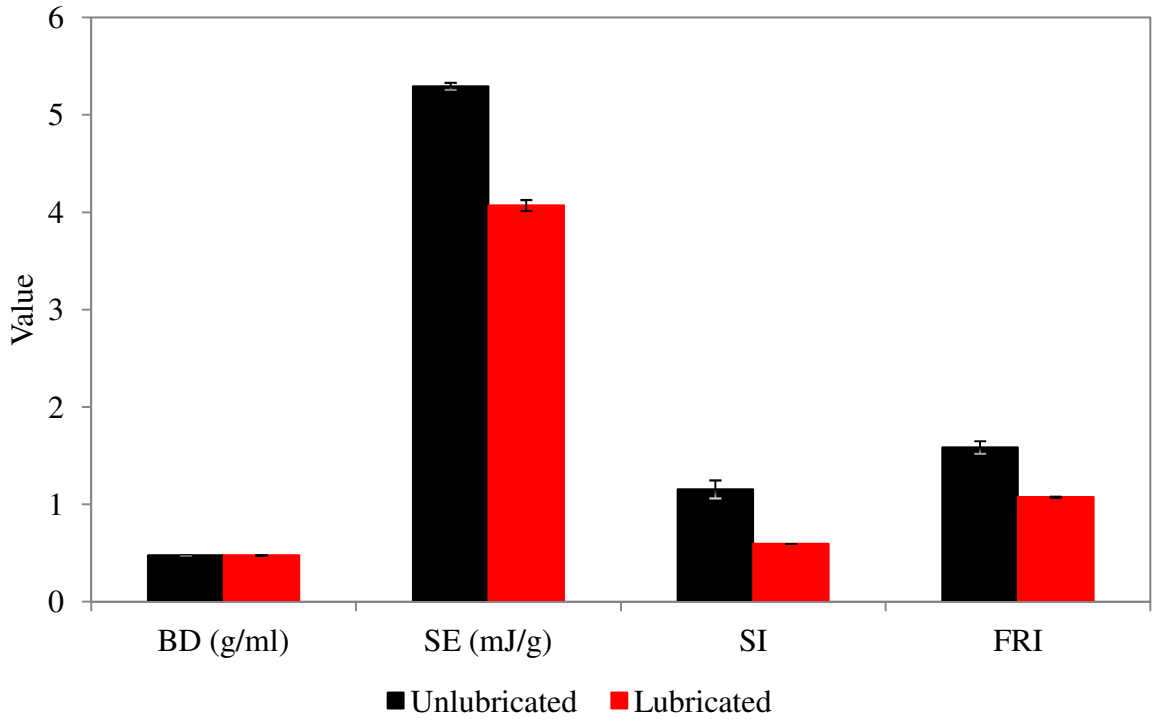


**Figure 4-4 – Parameters measured using the FT4 powder rheometer (BD – bulk density, SE – specific energy, SI – stability index and FRI – flow rate index). Error bars show standard deviation.**

#### 4.2.1.4 Shear cell

The Schulze shear cell was used to measure both the internal friction angle and the wall friction angle. The measured angle of internal friction for a given pre-shear normal stress is shown in Figure 4-5. Addition of magnesium stearate to the formulation appears to have an insignificant effect on the angle of internal friction. At a pre-shear normal stress of 2 kPa the difference in the measured angle of internal friction between un-lubricated and lubricated formulations is ~0.9°. At a pre-shear normal stress of 15 kPa the measured angle of internal friction is the same regardless of magnesium stearate content. This observation is consistent with previously reported work [Yu *et al.*, 2013]. The flow function can be used as an assessment of flowability; it is calculated as the ratio between the major principal stress ($\sigma_1$) and the unconfined yield stress ($\sigma_c$). Figure 4-6 shows the calculated unconfined yield stress

as a function of the calculated major principal stress, it can be seen that both un-lubricated and lubricated powders are classed as easy flowing, and that the addition of magnesium stearate to the formulation has had no significant effect on the calculated flow function. The shear stress as a function of normal stress as measured during wall friction testing is given in Figure 4-7; the coefficient of friction is equal to the gradient. The angle of friction, calculated as the arctan of the gradient, was found to be 3.60° and 3.86° for the un-lubricated and lubricated (0.5 % w/w magnesium stearate) respectively. As seen previously with the angle of internal friction there was no significant effect of magnesium stearate on the measured angle of wall friction.

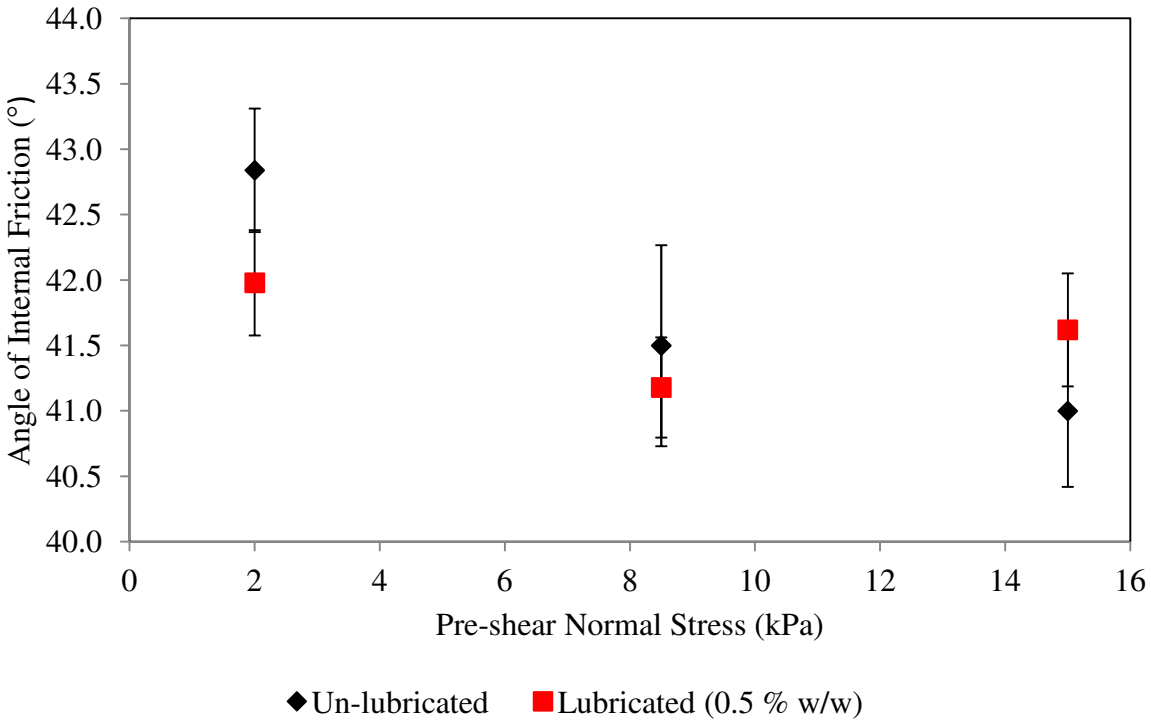


**Figure 4-5 – Calculated angle of internal friction as a function of pre-shear normal stress, error bars show standard deviation n=5.**

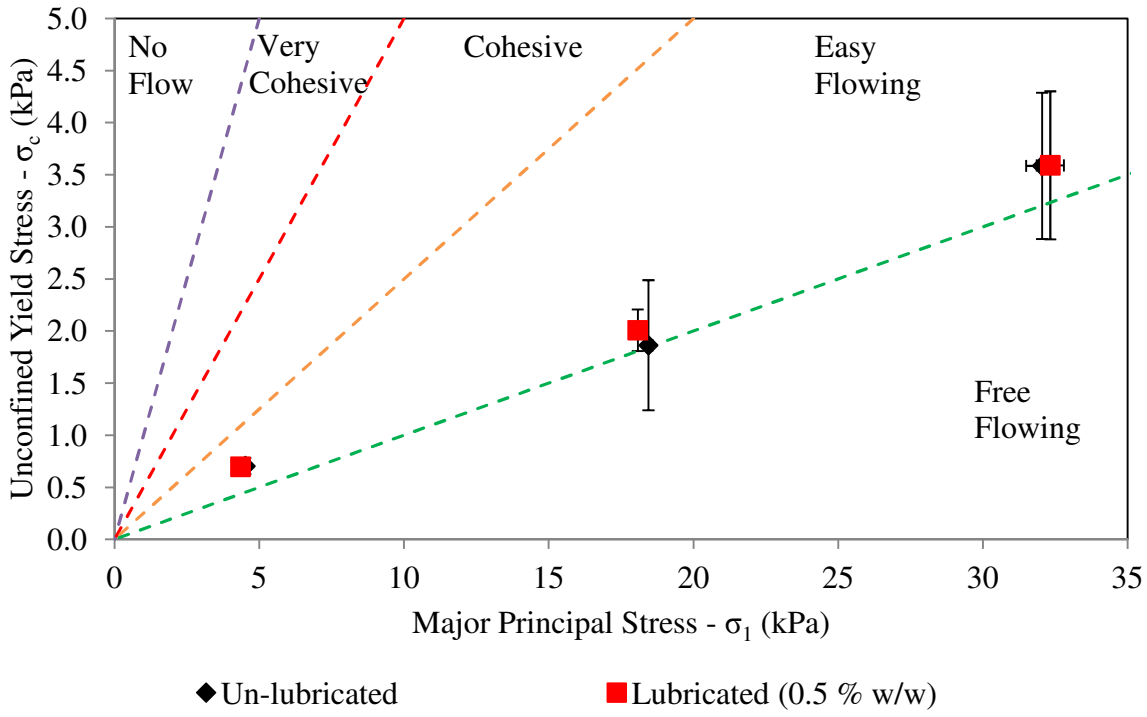


**Figure 4-6 – Measured flow function of un-lubricated and lubricated (0.5 % w/w magnesium stearate) placebo formulations, error bars show standard deviation n=5. Powder flow classifications consistent with traditional shear cell literature definitions [Tomas and Kleinschmidt, 2009].**

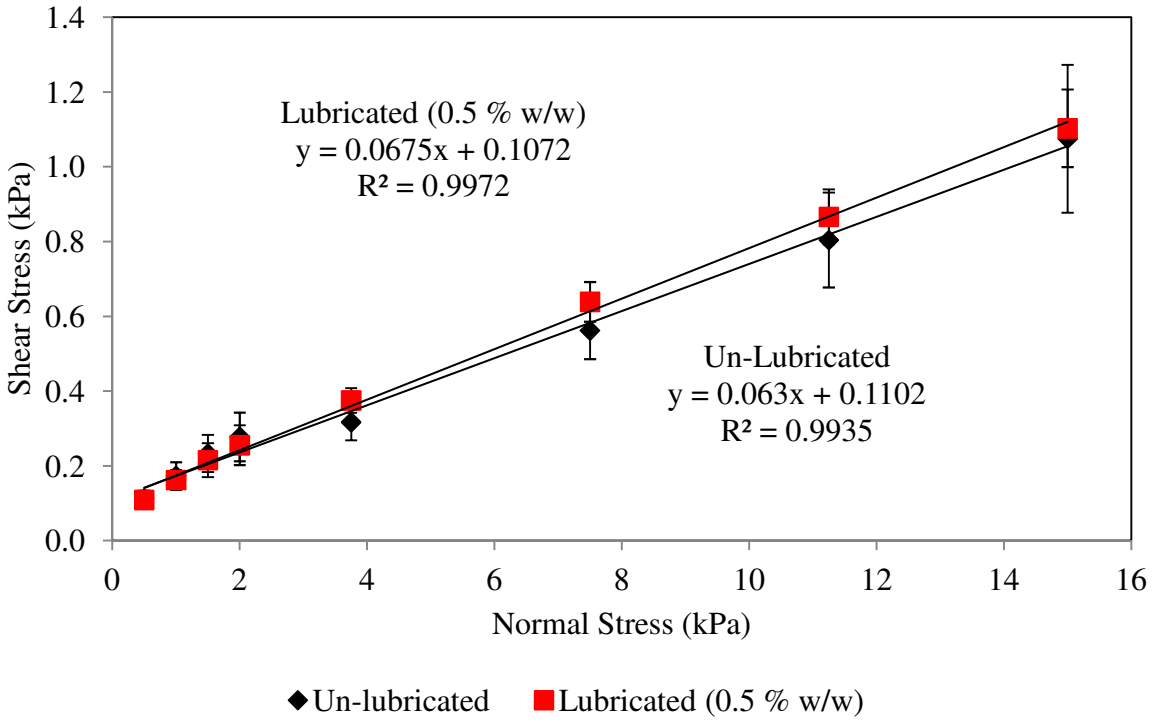


**Figure 4-7 – Shear stress as a function of normal stress for un-lubricated and lubricated (0.5 % w/w magnesium stearate) place formulations measured using the wall friction method. Error bars show standard deviation n=5.**

### 4.2.2 Roller compaction behaviour

#### 4.2.2.1 Mass throughput and roll gap

Roller compacted ribbons, produced with both un-lubricated and lubricated (0.5 % w/w magnesium stearate blended at 15 rpm for 7 minutes) placebo formulations, were manufactured at a range of solid fractions to assess the impact of lubrication on powder transmission through the Alexanderwerk WP120 roller compactor feed system. The roller compactor settings used were described in section 3.3.4.2; in this investigation two 'knurled' roll surfaces were used. A comparison between the mass throughput and corresponding roll gap for the un-lubricated and lubricated formulations is given in Figure 4-8. The mass throughput of roller compacted ribbons was found to be directly related to the rotational speed of the feed auger by an empirical y = mx + c relationship given in Equation 4-1 and Equation 4-2 for the un-lubricated and lubricated (0.5% w/w) conditions respectively:

Un-lubricated $y = 2.83x + 75.84$ ($R^2 = 0.87$) **Equation 4-1**

Lubricated $y = 7.47x + 65.96$ ($R^2 = 0.99$) **Equation 4-2**

where y is the roller compacted ribbon mass throughput (g/min) and x is the feed auger rotational speed (rpm).

Furthermore the results indicated that for a given set of roller compaction parameters (auger speed, hydraulic roll pressure and upper/lower 'knurled' roll surfaces), the addition of magnesium stearate led to an increase in the mass throughput of material, which, since the in-gap ribbon porosity was found to remain constant, as can be observed from Figure 4-9, is directly related to an increase in the roll gap. With the inclusion of 0.5% w/w magnesium stearate the mass throughput was seen to increase by approximately 80–90 % compared to that of the equivalent un-lubricated blend. Correspondingly, whilst the roll gap for the un-

lubricated blend was maintained at a constant 2.2 mm the inclusion of 0.5 % w/w magnesium stearate led to the roll gap increasing to a range between 3.8 – 4.5 mm. The in-gap ribbon porosity as calculated using the method outlined in section 3.2.1.3, remained constant for a given set of conditions (i.e. hydraulic pressure and screw speed), between un-lubricated and lubricated ribbons. As expected, ribbons manufactured using higher pressure and screw speed demonstrated a reduction in the in-gap ribbon porosity as shown in Figure 4-9.

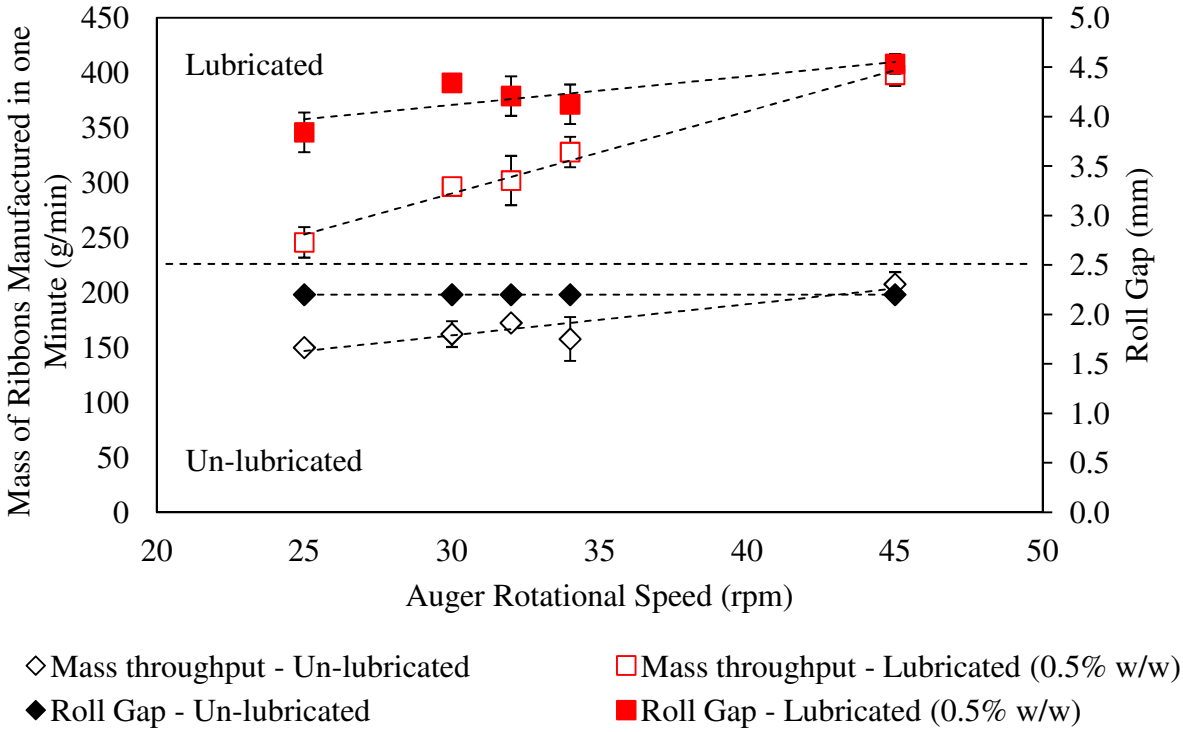


**Figure 4-8 – Comparison of mass throughput; un-lubricated $R^2$ = 0.87, lubricated $R^2$ = 0.99, and roll gap; un-lubricated $R^2$ = 1.00, lubricated $R^2$ = 0.70, for a given set of conditions (auger speed and hydraulic roll pressure). Error bars show standard deviation n=6.**

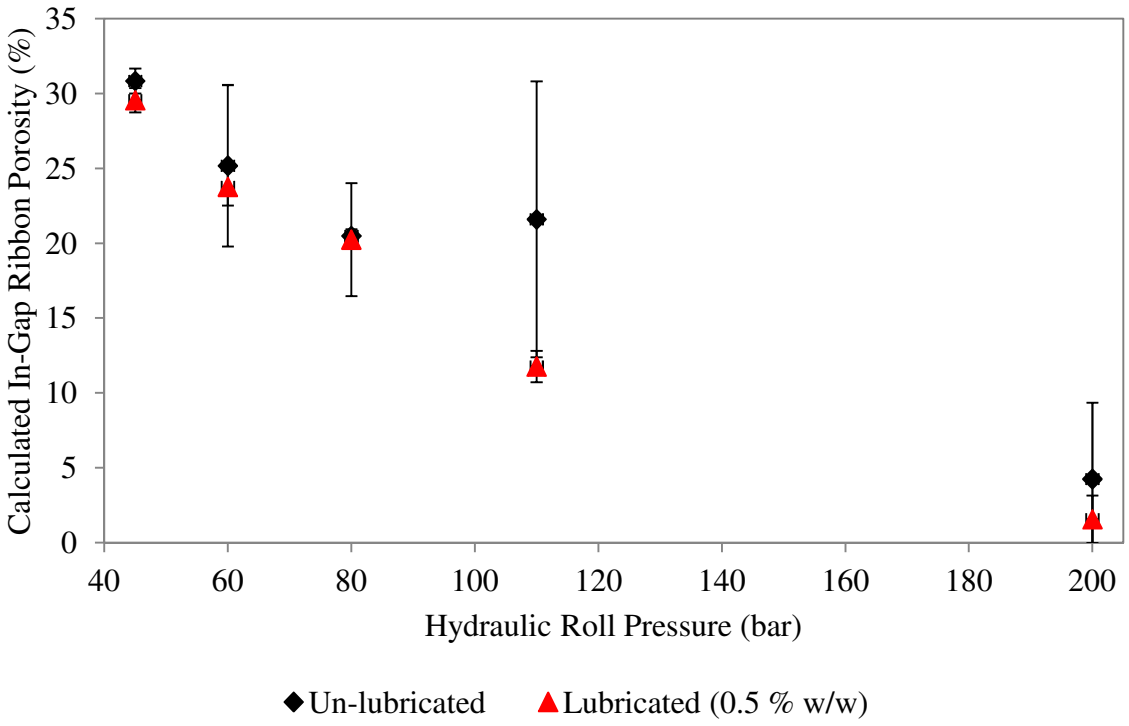


**Figure 4-9 - In-Gap ribbon porosity as a function of hydraulic roll pressure, error bars show standard deviation (n=6).**

Referring back to the physical model outlined in section 2.3.1.1, in this case for a given set of conditions the only difference between the unlubricated run and the lubricated run is the addition of magnesium stearate to the formulation. The three operating parameters (auger speed, roll speed and hydraulic roll pressure) are fixed and as such the significant change in roller compaction performance of the two blends is a direct influence of adding magnesium stearate into the formulation. Since the roller compactor is operating at a steady state (*i.e.* the rollers are not starved of material and there is no build up of material in the pre-nip chamber) the mass of material delivered to the nip region per rotation of the screw feeder is equal to the compacted mass of roller compacted ribbon. Since a higher mass (per unit time) of roller compacted ribbon was produced for the lubricated condition it must be the case that more material is fed through the feeding system per revolution of the screw feeder. To achieve this increase in throughput at least one of the following conditions must be satisfied:

(1) Since the feed chamber has a fixed volume and the auger is rotating with the same velocity in both lubricated and unlubricated conditions the auger chamber should contain a higher mass of material in the lubricated condition, as such the material contained within the flights of the screw is at a higher packing density (i.e. the space between the screw flights is more filled with powder).

(2) The material contained in the feed chamber moves with a faster axial velocity in the x direction travelling towards the rollers.

(3) For condition (2) to be true it implies that the material within the screw flights is less prone to rotating with the movement of the screw feeder without moving forward towards the rollers.

(4) More material is 'gripped' at the roll surface in the lubricated condition.

In the case of the 1$^{st}$ condition the dominating factor will be the compressibility of the material, whereas in the case of the 2$^{nd}$ and 4$^{th}$ condition both the friction acting at the interface between the powder and the equipment surfaces and the friction between particles within the blend becomes the dominant factor. The mechanics of the auger feeder was described by [Metcalf, 1965]. Material fills the space between the auger and tube wall, rotation of the auger causes the material contained within it to rotate; this rotation is opposed by friction acting at the tube wall surface. Rotation of the powder in the auger chamber is avoided if the powder is allowed to move forward axially; again this axial motion is opposed by friction acting on the tube wall but also on the friction acting on the auger face. Material contained within a feed auger will move both rotationally and axially such that the effort against frictional resistance is a minimum. Based on this model, a smooth tube (low wall friction between the powder and tube wall) and a rough screw (high wall friction between the screw face and powder) will favour rotational movement, whereas a rough tube (high wall

friction between the powder and tube wall) and a smooth screw (low wall friction between the powder and screw face) will favour axial motion. The following sections investigate the effect of lubrication in the different regions of the feed system that were identified in Figure 2-5, in order to elucidate the effect of magnesium stearate on the powder flow through the feed system.

#### 4.2.2.2 Roller compactor feed system

An unexpected observation as a result of adding magnesium stearate to a formulation prior to roller compaction was the significant increase in roller compacted ribbon mass throughput. An explanation of how magnesium stearate causes increased throughput requires an understanding of each section of the blend transmission through the roller compactor and the role of friction against the auger face and tube wall surface during powder flow through each section. A schematic overview of the feeding system of the Alexanderwerk roller compactor was provided in Figure 2-5. The blend transmission through the roller compactor feed system is split into the following sections; (a) powder discharge from the hopper into the feed auger chamber and the impact of the hopper stirrer, (b) the effect of frictional forces in the feed auger chamber and the influence of the mixing action on the lubricity of the formulation, (c) the effect of friction at the cheek plate surfaces and the effect of magnesium stearate on the nip angle and pressure profile in the pre nip region; and, (d) the effect of friction at the roll surface and of magnesium stearate on the pressure profile in the nip region. The packing density of the powder blend progressively increases as it transitions through each section increasing the contact points between particles in the blend and at the powder/equipment surface interface.

#### 4.2.2.2.1 Flow through hopper

Flow from hoppers can often lead to variations in throughput, particularly for poor flowing or cohesive powders, due to issues such as bridging or funnel flow [Faqih *et al.*, 2007a]. In order to investigate the effects of flow out of the hopper into the feed auger the roll compactor was operated without the rolls in place. A comparison between the hopper emptying of un-lubricated and lubricated placebo blends is given in Figure 4-10; it can be observed that the presence of magnesium stearate resulted in minimal differences in mass throughput. The throughput was slightly increased for the lubricated blend (roughly a 9 % increase in mass throughput) but not to the same extent as when the rollers were in place (roughly 80-90 % increase in mass throughput). This lack of differentiation could be due to the action of the hopper stirrer which both disrupts bridge formation and helps draw the powder into the auger feed chamber. In both cases the mass throughput was significantly greater without the rollers in place, however, the % reduction in mass throughput caused by having the rollers in place stays relatively constant, increasing from 30.27 to 31.33% at 45 bar/25 rpm and 200 bar/45 rpm (hydraulic roll pressure/feed auger rotational speed) respectively for the lubricated condition; whereas in the un-lubricated condition the decrease in % mass throughput increases with increasing roll pressure from 56.1 to 62 % at 45 bar/25 rpm and 200 bar/45 rpm (hydraulic roll pressure/feed auger rotational speed) respectively.

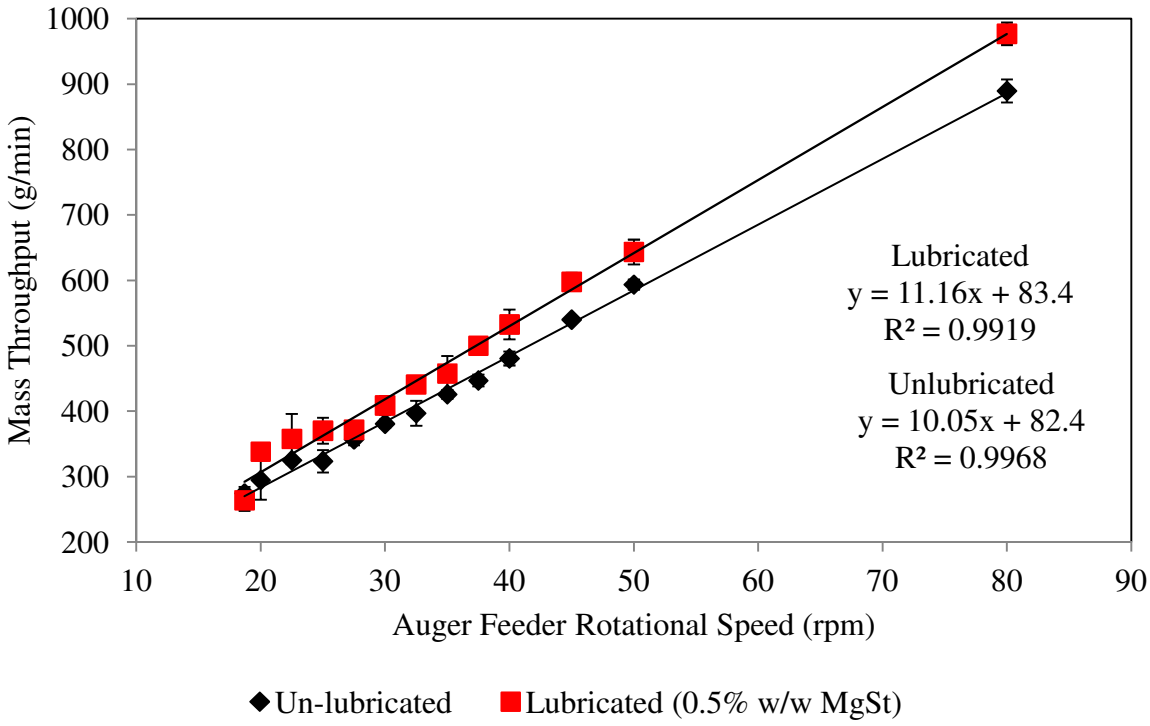


**Figure 4-10 –Mass throughput through the screw feeder without the rollers in place, error bars show standard deviation (n=3).**

The limitation of the aforementioned experiment is that there is no generation of back pressure replicating the restriction to flow of powder into the pre-nip area by the rolls. It may be assumed then, that in this case where the screw feeder is discharging without the influence of the rollers being in place that the density of the material with the feed chamber is lower and as such there is less material contained within the feeding system. Although more material is transported through the feed auger, clearly condition 1 is not satisfied (condition 4 is also not satisfied since there are no roller to influence the throughput) therefore the material must rotate less with the feed chamber and hence move with a faster axial velocity. In the case where the rollers are used the presence of back pressure leads to consolidation of the powder blend within the pre-nip area and hence an increase in the powder bed density. In opposition to this, it is expected to result in an increase in the internal wall friction between both the auger face/powder interface and the tube wall/powder interface within the feed chamber increasing the amount of rotational movement and reducing the axial velocity. Furthermore,

an increase in density immediately before the roller will also impact the forward momentum of the powder bed. There exists a region just before the rollers and immediately after the screw feeder where forward momentum of the powder is only influenced by the force generated by the powder being pushed forward by the leading edge of the screw feeder as shown in Figure 4-11. In this situation we may expect the presence of a lubricant to have an impact on the throughput, i.e. lubricated powder would exhibit lower frictional effects at the cheek plate surface and hence flow would be less restricted at the wall surface as found previously [Miguelez-Moran *et al.*, 2008] leading to increased throughput through the roller compactor. Based on the results observed from this experiment it may be hypothesised that the influence of magnesium stearate on powder feeding during roller compaction is due to wall friction effects occurring at the tube wall surface and screw face, resulting in changes in both material density within the feed chamber and dynamic movement of material through the feed chamber (*i.e.* the influence of rotational movement vs. axial movement).

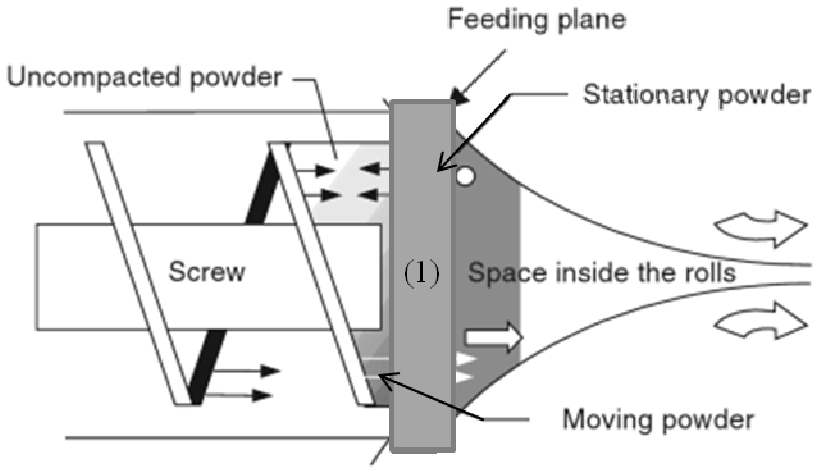


**Figure 4-11 – Diagram of the roller compactor feeding system depicting the region where the forward momentum of the powder is influenced of by the feed pressure generated by the screw feeder.**

#### 4.2.2.2.2 Lubricated roller compactor surfaces

In order to investigate the effects of wall friction within the feeding chamber, roller compaction of an un-lubricated formulation was performed using pre-lubricated equipment

surfaces. To achieve this, a lubricated formulation was first passed through the roller compactor. The system was then emptied of any loose powder, but the equipment surfaces were not thoroughly cleaned in order to ensure that any residual magnesium stearate adhered to the walls remained. Confirmation of the presence of magnesium stearate at the equipment surfaces was obtained using near-infrared spectroscopy. The near infrared spectrum of magnesium stearate has sharp peaks in the 4325 and 4254 $cm^{-1}$ region [Kauffman *et al.*, 2008]. The presence of 0.5 % w/w magnesium stearate within the formulation was identified by the observation of these peaks in the NIR spectrum of the blend. Analysis of the near infrared spectra acquired from the equipment surfaces (*i.e.* roll surface and cheek plate surface), following the lubricated run, showed that the material adhered to the equipment surfaces was consistent with that of the formulation composition including magnesium stearate. As a control 1000 g of un-lubricated and 1000 g of lubricated formulation were roller compacted (in a clean, magnesium stearate free state) using the following process conditions: auger speed 30 rpm, roll speed 3.4 rpm, hydraulic roll pressure 60 bar and knurled-knurled roll surface. The change in roll gap was monitored every 30 seconds, until all the formulation had been used; the results are shown in Figure 4-12. To determine the effect of the presence of lubrication at the equipment surface-powder interface, 1000 g of un-lubricated powder blend was roller compacted using pre-lubricated equipment surfaces. The results, Figure 4-12, indicated that the conveyance of the un-lubricated blend is initially equivalent to that of the lubricated material, both in terms of mass throughput and corresponding roll gap, indicating that the effect of magnesium stearate on powder throughput is dependent upon its presence at the equipment surface. However, the effects were only temporary as the roll gap reduced from 3.4 to 2.5 mm after 180 seconds suggesting that the residual coating of magnesium stearate on the equipment surface was removed as the process continued. The results would, however,

appear to indicate that the level of magnesium stearate required to achieve the more favourable flow behaviour within the roller compaction process could be significantly lower than the 0.5 % used in the formulation, thus providing a potential means to minimise the detrimental impacts of the lubricant whilst retaining the beneficial ones.

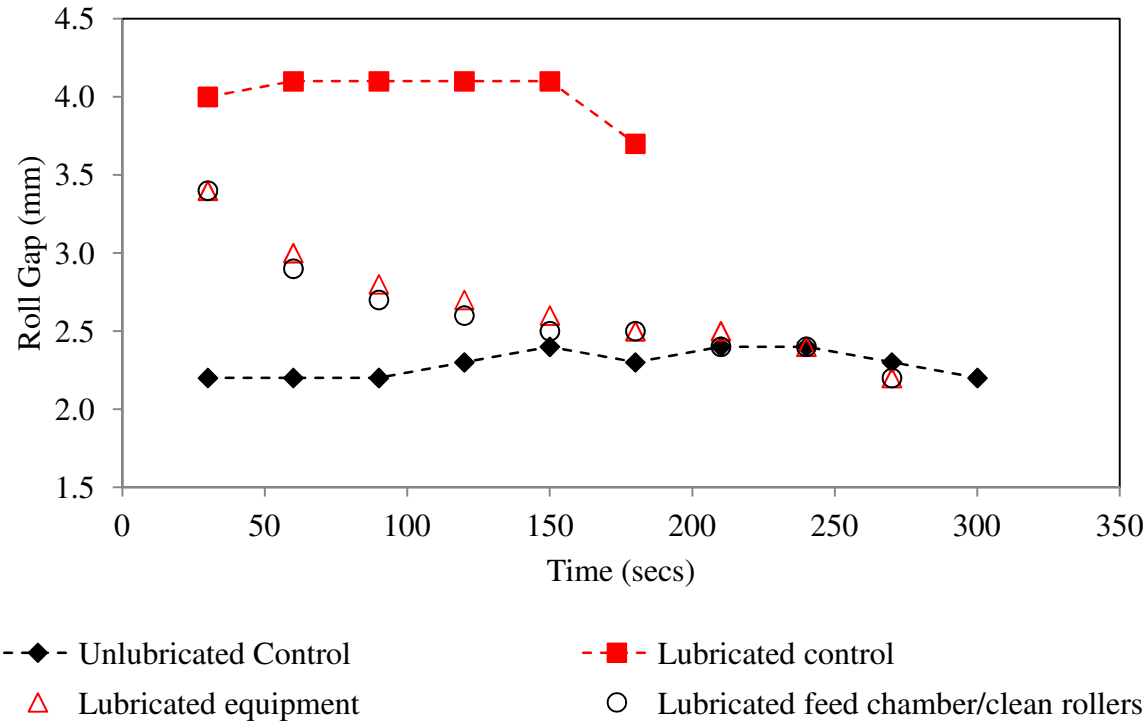


**Figure 4-12 – Change in roll gap over time for an un-lubricated placebo blend using pre-lubricated equipment surfaces; (1) un-lubricated control; (2) lubricated control; (3) un-lubricated placebo blend with fully lubricated equipment surfaces, and; (4) un-lubricated placebo blend with lubricated feeding system but clean rollers. (Process conditions; auger speed = 30 rpm, roll speed = 3.4 rpm and hydraulic roll pressure = 60 bar). Dashed lines are to aid the reader of the upper and lower boundaries of mass throughputs for lubricated and un-lubricated formulations.**

The increase in the powder transmission observed for the lubricated material can be rationalised thus: the powder-wall friction dynamics within feed auger system can be described as two counter-opposing mechanisms. The reduction in friction due to the presence of magnesium stearate can be thought to lead to more efficient axial movement due to reduced friction at the powder-auger interface; alternatively the reduction in friction occurring at the powder/chamber wall interface would lead to less efficient powder transmission due to favouring rotational movement. The balance between these two opposing mechanisms will

control the powder transmission rate through the auger: however, it would be logical to assume that as powder blend within the feed auger becomes more densely packed then the reduction in the friction at the auger face would become the more important factor.

#### 4.2.2.2.3 Effective level of magnesium stearate

In order to investigate if a reduced level of lubricant would still deliver the positive powder flow attributes, the level of magnesium stearate was decreased to investigate lower lubricant levels (0.01, 0.05, 0.1 and 0.25 % w/w) and the blending times with magnesium stearate at 7 minutes and 60 minutes at 15 rpm (105 and 900 revolutions respectively). The longer mixing time was used to achieve a homogeneous distribution of the lubricant throughout the blend. Furthermore, in the formulations with significantly lower magnesium stearate levels the potential surface coverage is limited by the amount of magnesium stearate available to coat the host excipient particles rather than the mixing conditions; as such these formulations should be less sensitive to any additional uncontrolled mixing that occurs within the feeding system of the roller compactor. Additionally, if blending a smaller amount of magnesium stearate to homogeneity is a viable option, it could eliminate the need for a two step blending process, i.e. magnesium stearate can be added during the initial blending stage. This would afford both a reduction in processing time and potentially a more practical approach towards continuous manufacturing. Roller compaction was performed using two knurled rollers, 60 bar roll pressure, 30 rpm auger speed and 3.4 rpm roll speed. The results, Figure 4-13, indicated that even at very low lubricant levels (0.05 % w/w) an increase in mass throughput is still observed, and more importantly, addition of magnesium stearate beyond this level had no further benefit in terms of increasing mass throughput.

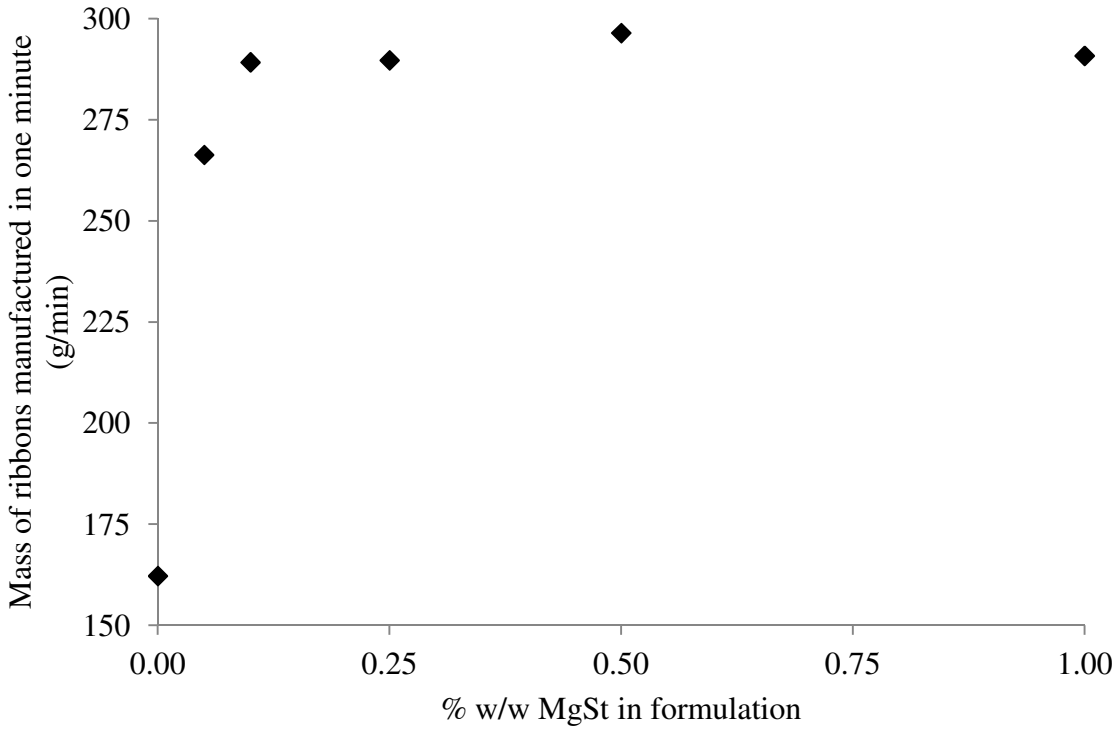


**Figure 4-13 – Effect of magnesium stearate on the mass of ribbons manufactured in one minute (roller compaction conditions: knurled rollers, 60 bar roll pressure, 30 rpm auger speed and 3.4 rpm roll speed). Error bars show standard deviation n=6.**

#### 4.2.2.2.4 Mixing in the feed system

Further complicating the use of magnesium stearate during roller compaction is the potential for further mixing during feeding due to the shear effects imposed of the formulation. The action of the hopper stirrer may change the effect that the magnesium stearate has on the powder blend and hence the final properties of the ribbons and tablets. The effect of mixing time and its potential to cause over-lubrication are well characterised in the literature [Kikuta and Kitamori, 1994, Otsuka *et al.*, 2004, Ragnarsson *et al.*, 1979] and were discussed in section 2.2.2.3. Despite this, further lubrication due to downstream processing is often over-looked. In an attempt to understand the degree of mixing inside the hopper, a 500 g layer of lubricated placebo blend was poured over a 500 g layer of un-lubricated placebo blend within the hopper. The experiment was also done in reverse with lubricated blend transitioning to the un-lubricated blend during the run. In the absence of mixing in the hopper

one would expect a distinct shift in the throughput and roll gap as the two powders transition, *i.e.* for the case of lubricated powder on top of un-lubricated powder one would expect the roll gap to increase from 2.2 mm to around 4 mm as the lubricated blend starts to pass through.

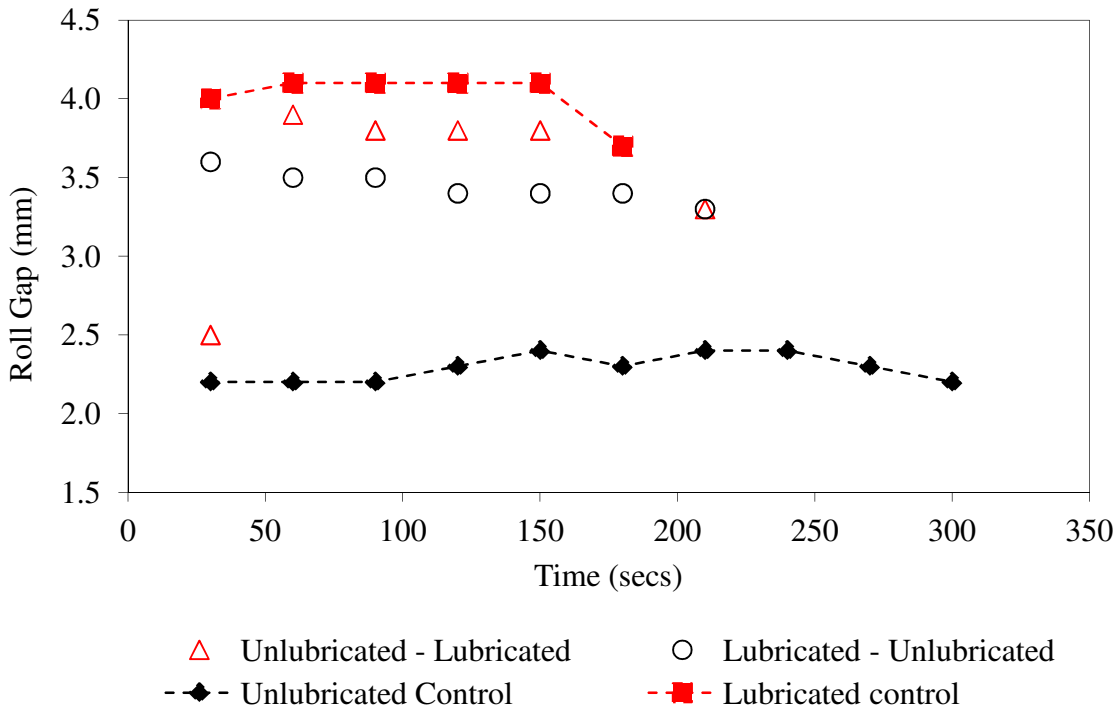


**Figure 4-14 – Change in roll gap over time, (1) un-lubricated control; (2) lubricated control; (3) un-lubricated – lubricated, and; (4) lubricated – un-lubricated. (Process conditions; auger speed = 30 rpm, roll speed = 3.4 rpm and hydraulic roll pressure = 60 bar). Dashed lines are to aid the reader of the upper and lower boundaries of mass throughputs for lubricated and un-lubricated formulations.**

The data, Figure 4-14, shows that the roll gap for the un-lubricated to lubricated formulation starts at 2.5 mm but after 30-60 seconds increases to 3.8 mm and stays constant for the remainder of the experiment; the gap does reduce to approximately 3.4 mm at the end of the run, but this is attributed to the low hopper fill which also leads to less powder being transmitted through the auger feeder. For the lubricated to un-lubricated condition the roll gap begins at 3.6 mm and after 210 seconds had reduced to 3.4 mm. Neither condition led to the same roll gap obtained for the lubricated control, but both had significantly larger roll gaps than the un-lubricated control. This would suggest that mixing is occurring during powder conveyance from the hopper to the rollers, causing a dilution of magnesium stearate

throughout the blend. This mixing, or the presence of magnesium stearate within the feed system, leads to the initially un-lubricated blend behaving more like lubricated material.

In order to investigate the exact location of this mixing, a band of lactose monohydrate was sandwiched between layers of the placebo blend containing lactose anhydrous. Near infra red chemical imaging (NIR), as described in section 3.2.6.1 was used to monitor the presence of the two lactose species, which can be differentiated due to the presence of a water band at around 1900–1940 nm wavelengths in the monohydrate species [Gupta *et al.*, 2005a]. Three conditions were investigated:

Condition 1 - a band of lactose monohydrate in the hopper above the stirrer (to investigate the occurrence of mixing in the hopper).

Condition 2 - a band of lactose monohydrate in the hopper with the stirrer removed (to investigate the occurrence of mixing during the transmission from the hopper into the auger chamber).

Condition 3 - a band of lactose monohydrate in the auger chamber below the stirrer (to investigate the occurrence of mixing within the auger chamber).

Figure 4-15 shows that when the lactose monohydrate is introduced above the hopper stirrer (a) it becomes mixed within the powder blend and there is no distinct transition from purely lactose anhydrous to lactose monohydrate. In condition 2 where the hopper stirrer is removed (b) mixing of the two lactose species occurs but to a lesser degree than observed in condition 1. There is a distinct region of transition from pure anhydrous to a mixed anhydrous/monohydrate and back to pure anhydrous. In condition 3 where the lactose monohydrate plug is located within the auger chamber (c), there is an absence of mixing

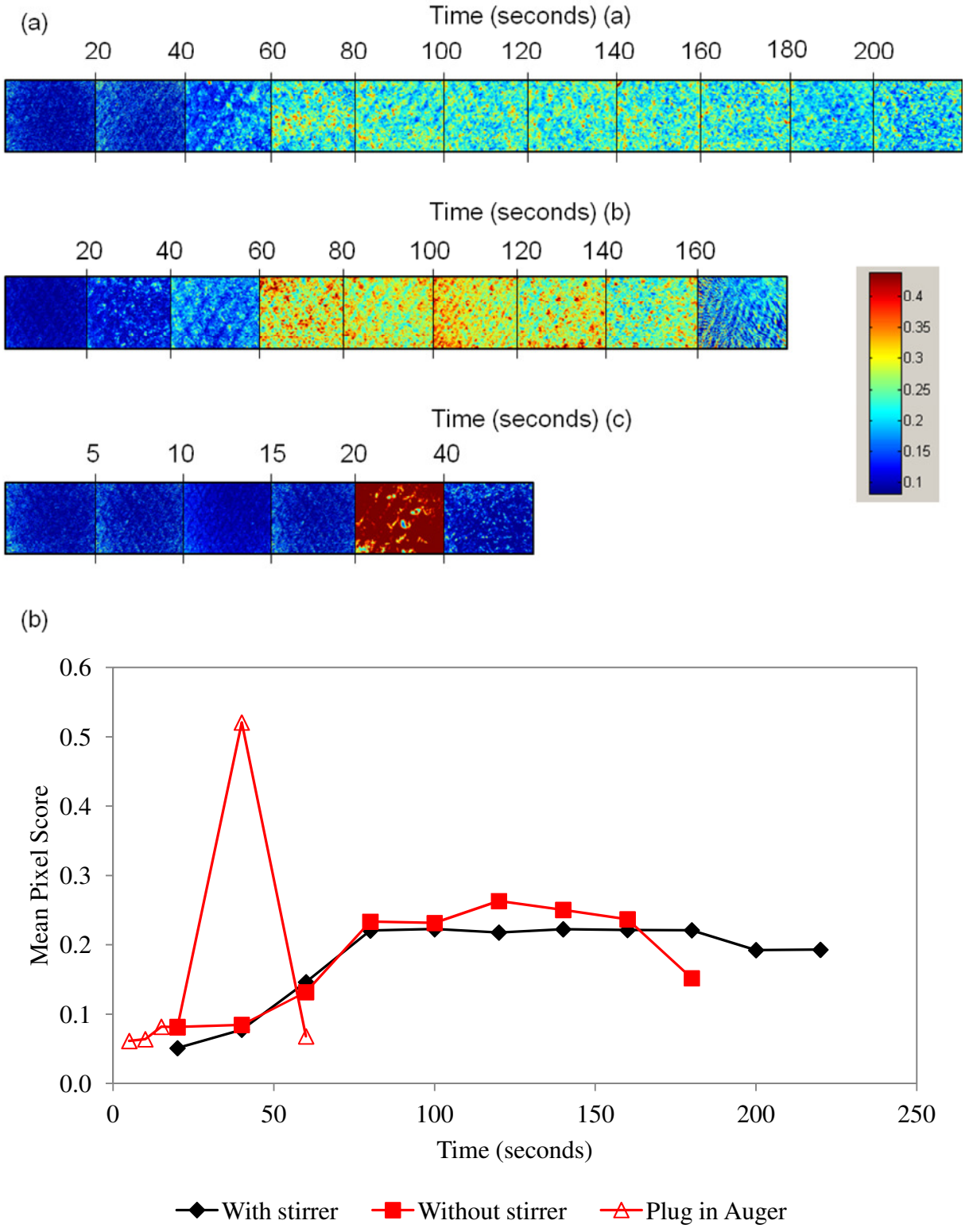


**Figure 4-15 – (4a) NIR images of pieces of ribbon representing the presence of lactose monohydrate for (a) condition 1; (b) condition 2, and; (c) condition 3 (4b) Graphical representation of mean pixel score (higher score represents larger proportion of lactose monohydrate present) from NIR image analysis.**

between the lactose anhydrous and lactose monohydrate; as such the lactose monohydrate is seen to come out as a discrete band. The lack of mixing in the auger feeder would also suggest that the mixing observed in the hopper without the stirrer (b) is likely to occur at the hopper/auger feed interface.

As previously discussed, in section 2.2.2.3 the manufacture of pharmaceutical products is generally conducted in the highly sensitive zone for lubricant mixing. This means that product quality attributes can change significantly due to small changes in processing conditions [Kushner IV and Moore, 2010]. As such the additional mixing that occurs within the feeding system is likely to alter the distribution of magnesium stearate throughout the blend and on the surfaces of the excipient particles. The consequence of this mixing is such that when the blend reaches the nip region it may have different properties to when it was first added to the feed hopper. This effect is likely to be intensified at large scale; whilst residence time may decrease due to increased mass throughput, due to the inclusion of a dual auger feeding system the intensity of mixing will increase, as suggested by Kushner and Moore [Kushner IV and Moore, 2010] magnesium stearate mixing does not only depend upon the time of mixing but other processing conditions as well, i.e. mixing intensity. As such, two ribbons made from identical blends with equivalent solid fractions could theoretically exhibit different ribbon / granule properties (*i.e.* tensile strength, granule tablettability) depending on the degree of additional mixing within the feed system. This mechanism for potential further lubrication within the feeding system has previously been overlooked when modelling roller compaction using a compaction simulator. This method involves comparing the properties, i.e. tensile strength and granule size distribution, of ribbons with equivalent solid fractions produced from roller compaction and compaction simulators [Hein *et al.*, 2008, Zinchuk *et al.*, 2004].

#### 4.2.2.2.5 Instrumented rolls

Roller compaction was performed using the instrumented rolls described in section 3.3.4.3, to measure the pressure profile applied to the powder/ribbon during transition from the nip region to the minimum gap. From the pressure profile important engineering parameters can be measured or derived from the raw data such as the maximum pressure between the rollers and the nip angle. Pressure profiles for the process conditions; auger rotational speed = 45 rpm, hydraulic roll pressure = 200 bar, were not measured due to instrument limitations. In addition it was not possible to measure the pressure profiles for the un-lubricated conditions due to severe adherence of powder to the roll surface during these runs.

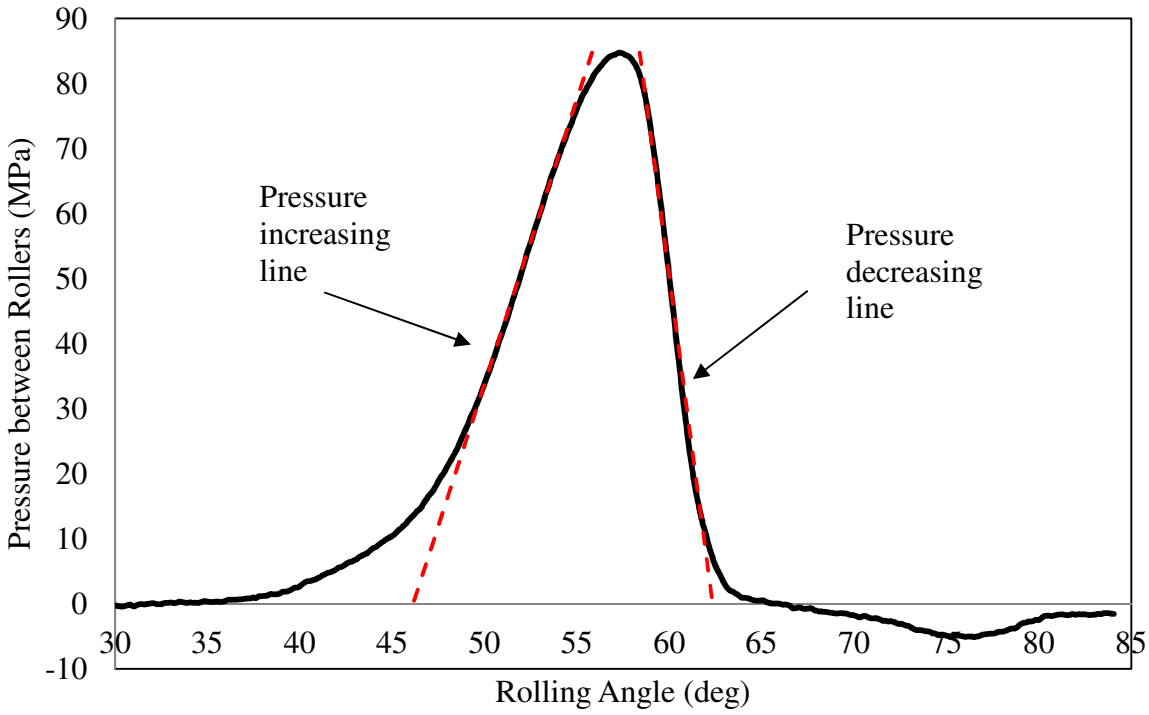


**Figure 4-16 – Typical pressure profile measured during roller compaction of a placebo formulation. (Profile shown here is for magnesium stearate concentration 0.01% w/w, mixed for 7 minutes @ 15 rpm and roller compacted with the following process conditions; auger rotational speed = 32 rpm, hydraulic roll pressure = 80 bar and roll speed = 3.4 rpm.**

A typical pressure profile is given in Figure 4-16, the best fit lines of the linear portion of the pressure increase and pressure decrease regions are displayed; the nip angle is defined

as the difference between the x-intercept of the pressure decreasing line and the x-intercept of the pressure increasing line. The maximum roll pressure between the rolls during compression is simply the maximum value of the pressure profile and is assumed to coincide with the minimum roll gap. It should be noted as discussed in Section 3.3.4.3.1 the angular displacement of the pressure transducer is relative to it starting position rather than an absolute position such as the minimum roll gap. Furthermore, the pressure transducers are not capable of measuring a tensile force. Therefore the negative peak of the graph represents noise from the instrument as the pressure is relieved. In terms of understanding the severity of adhesion to the roll surface it would be useful if the sensors on the instrumented roller were capable of measuring the roller compacted ribbon pull-off force from the surface.

The instrumented roll was used to measure the pressure profiles during roller compaction at all levels of magnesium stearate investigated, and at all the process conditions given previously in Table 3-4 with the knurled-knurled roll surface configuration. At all process conditions the maximum pressure between the two rollers was significantly higher for the formulation containing 0.01 % w/w magnesium stearate than for the formulations containing 0.05 % w/w and above, as shown in Figure 4-17. Interestingly increasing the level of magnesium stearate in the blend beyond 0.05 % w/w had no significant effect on the maximum pressure between the rollers. It was observed that there was a greater difference between the maximum pressures at the centre of the rollers compared to the edges of the rollers for the 0.01 % w/w formulation than any other formulation. The pressure difference between the sensors located on the edges of the roller and sensor located at the centre (δ) is determined using Equation 4-3:

$$\delta = 0.5 \times \frac{(P_1 + P_3)}{P_2} \qquad \textbf{Equation 4-3}$$

where $P_1$ and $P_3$ are the pressure values measured at the transducers at the edge of the roll and $P_2$ is the pressure values measured at the transducer at the centre, ideally δ will be close to unity.

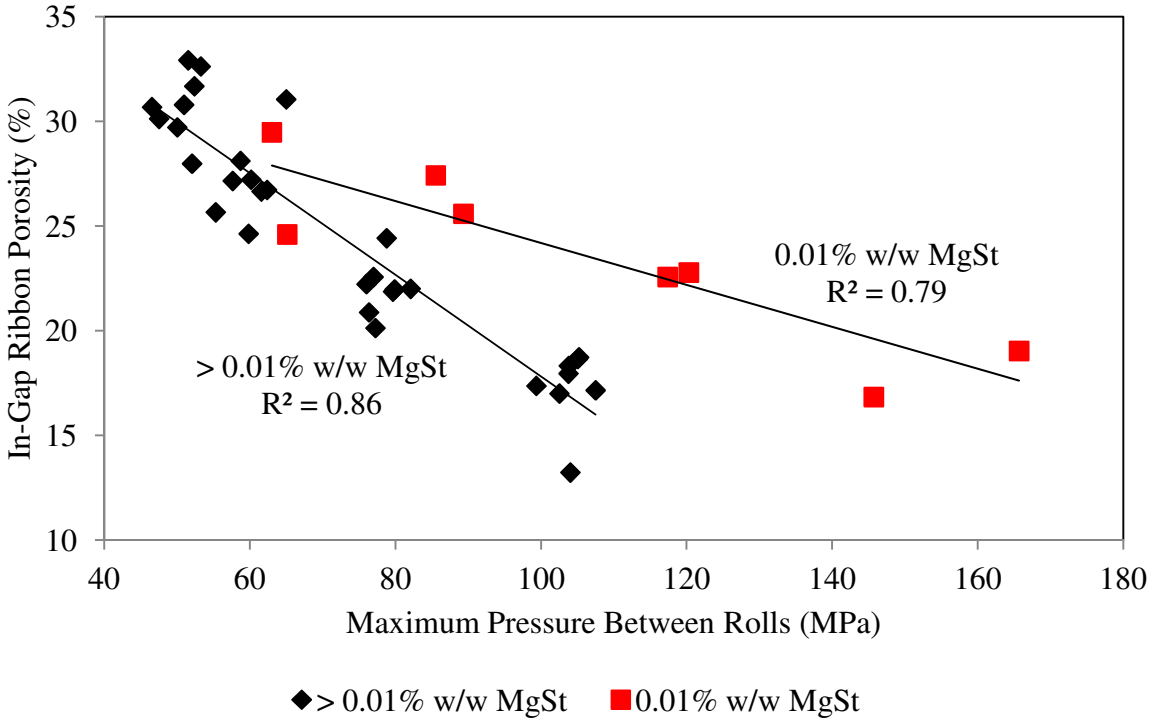


**Figure 4-17 – In-gap ribbon porosity vs. the maximum pressure recorded between the rollers.**

The calculated in-gap ribbon porosity (described by [Gamble *et al.*, 2010]) as a function of maximum pressure between the rollers is given in Figure 4-17, it can be seen that a better correlation between maximum pressure between the rollers and the calculated in-gap ribbon porosity is achieved if the formulation containing 0.01 % w/w magnesium stearate is considered as a separate data set (formulation containing 0.01 % w/w magnesium stearate – $R^2$ = 0.79, formulations containing 0.05 % w/w and above – $R^2$ = 0.86). This observation suggests that the addition of magnesium stearate is having an effect on the densification kinetics in the pre-nip and nip regions of the roller compactor. (Figure 4-18 and Figure 4-19) show the densification kinetics within the nip region of the roller compactor as a function of maximum pressure and as a function of horizontal distance away from the minimum roll gap

respectively. It can be seen that increasing the level of magnesium stearate in the formulation causes densification to occur at a lower pressure and at a distance further away from the minimum roll gap. Figure 4-20 shows how the nip angle changes due to the addition of magnesium stearate to the formulation at a fixed set of roller compaction conditions (knurled rollers, 60 bar hydraulic roll pressure, 30 rpm auger rotational speed and 3.4 rpm roll speed). It can be seen that increasing the amount of magnesium stearate in the formulation from 0.01 % w/w to 0.05 % w/w causes an increase in the calculated nip angle. Further addition of magnesium stearate up to 1.00 % w/w had no significant effect on the nip angle. The calculated nip angles confirm that densification occurs at a further distance away from the minimum roll gap. The results from this study contradicts what has been previous been observed in the literature. Experiments conducted using a custom built roller compactor found that addition of magnesium stearate within a formulation decreased the measured nip angle [Miguelez-Moran *et al.*, 2008]. However, in the aforementioned study the formulation was fed to the roller compactor vertically, using gravity. The Alexanderwerk roller compactor utilized in this study makes use of a force feeding screw auger.

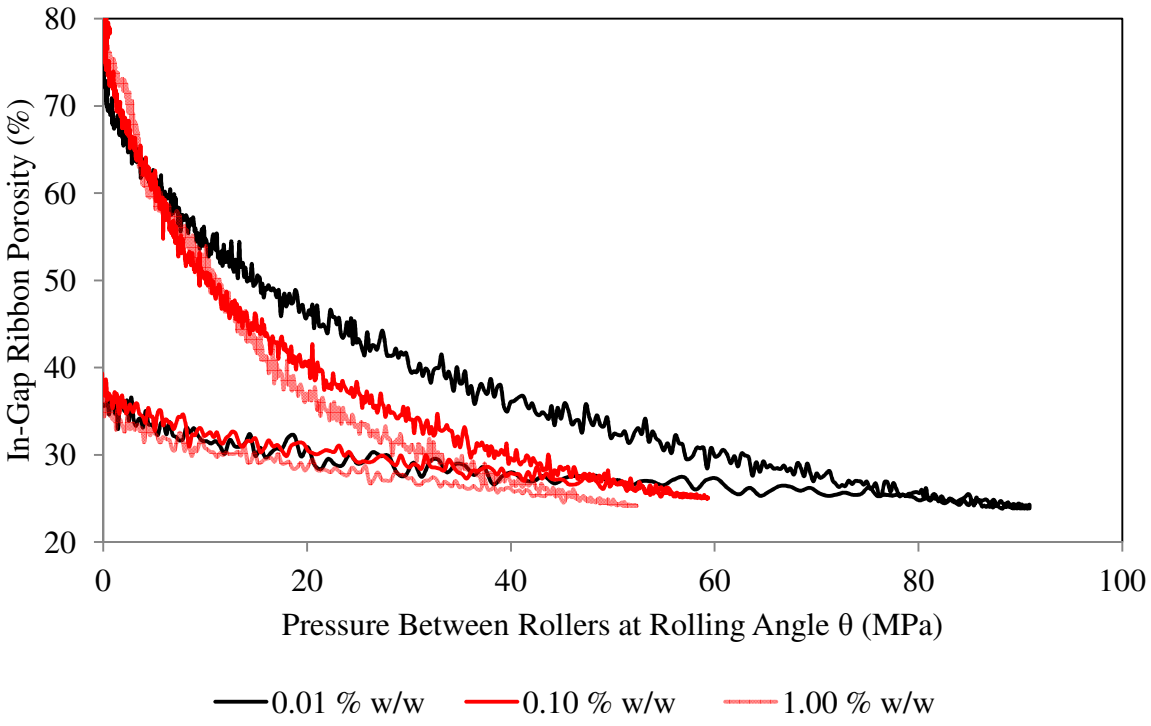


**Figure 4-18 – Densification kinetics of the powder bed as a function pressure applied between the rollers at a given rolling angle.**

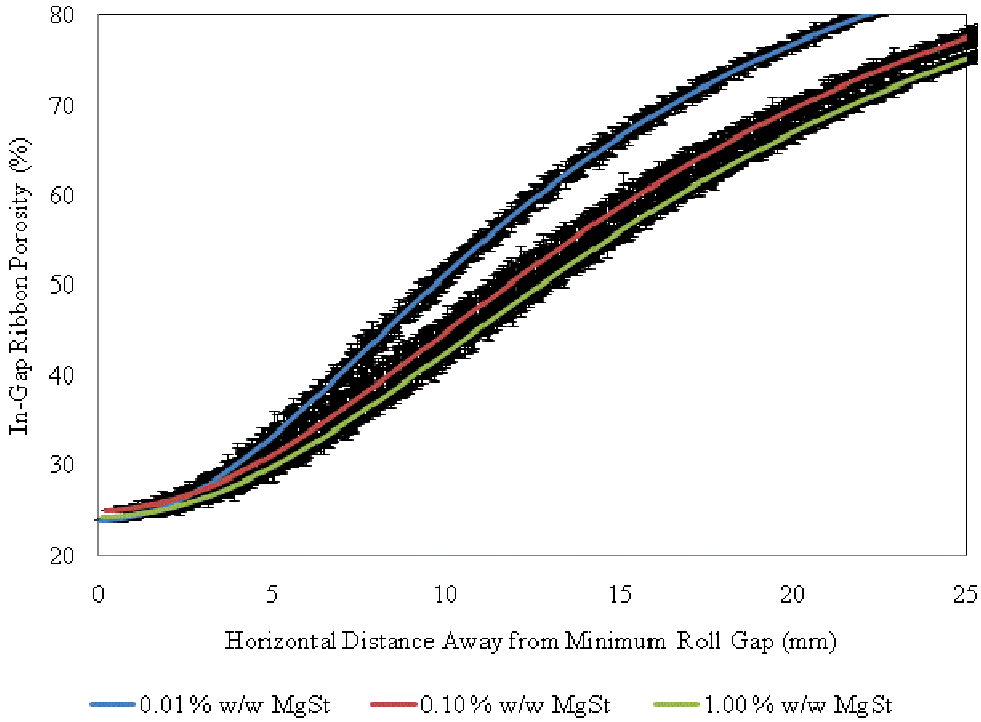


**Figure 4-19 – Densification kinetics of the powder bed as a function of horizontal distance away from the minimum roll gap.**

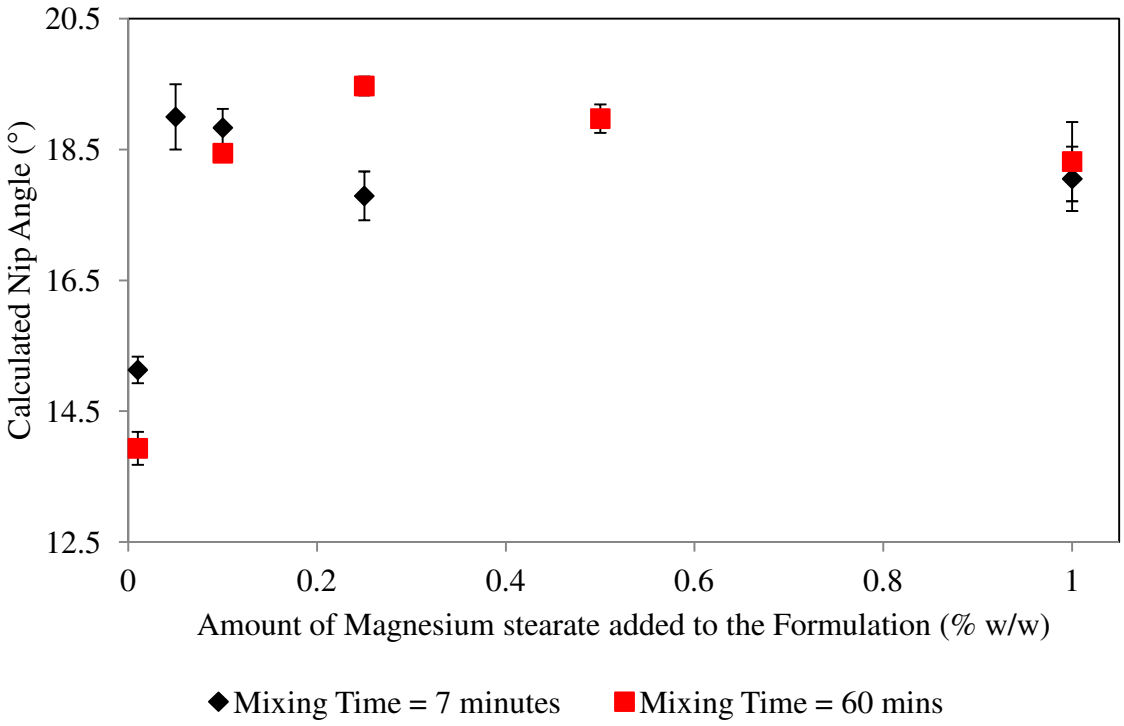


**Figure 4-20 – The effect of increasing magnesium stearate level and mixing time on the calculated nip angle at a fixed roller compaction process condition; hydraulic roll pressure = 60 bar, feed auger rotational speed = 30 rpm, and roll speed = 3.4 rpm. Error bars show standard deviation n=6.**

#### 4.2.2.2.6 Effect of roll surface

As previously discussed, the anti-frictional effects of magnesium stearate was originally hypothesised to be deleterious to the efficiency of roller compaction as it prevents the powder from being 'gripped' at the roll surface and thus could impede the draw of blend into the compaction zone. Knurled roll surfaces are typically used to increase friction at the powder/roll surface interface. Based on the conditions for increased material throughput through the feed system the efficiency of the roll surface to 'grip' the material within the nip region was identified as a potential limiting factor. A comparison of the roller compaction behaviour of un-lubricated and lubricated formulations was performed using varied roll surface configurations, namely; knurled-knurled, knurled (bottom roller) - smooth (top roller) and smooth-smooth. As shown in Figure 4-21, roll surface configuration was found to have no significant impact on the roller compaction of the un-lubricated formulation in terms of mass throughput and roll gap; however, for the lubricated formulation replacing one of the

knurled rollers with a smooth roller led to a reduction in mass throughput and corresponding roll gap, and for one set of conditions (hydraulic roll pressure 200 bar, auger speed 45 rpm and roll speed 3.4 rpm) roller compaction was not possible. Moreover, replacing both knurled rollers with smooth rollers caused powder to build up in the pre-nip region which was not drawn into the rolls resulting in a blockage in the feed system. These results confirm that the presence of magnesium stearate in the formulation leads to a reduction in friction at the roll surface; as the degree of mechanically induced friction is reduced, i.e. by changing knurled rollers for smooth rollers, less powder is 'gripped' at the roll surface when magnesium stearate is present in the formulation. Additionally the bulk powder at the surface of the rolls comes into contact with the powder trapped within the knurling of the roll surface, which even when lubricated has more surface roughness than the smooth roll surfaces, hence providing more friction with which to draw powder. As a result of this reduction in friction between the powder and roll surface it is hypothesised the nip angle will be reduced leading to less material being drawn through the rolls, and when the roll surfaces are entirely smooth the level of friction at the roll surface/powder interface is insufficient to draw the lubricated blend into the roll gap.

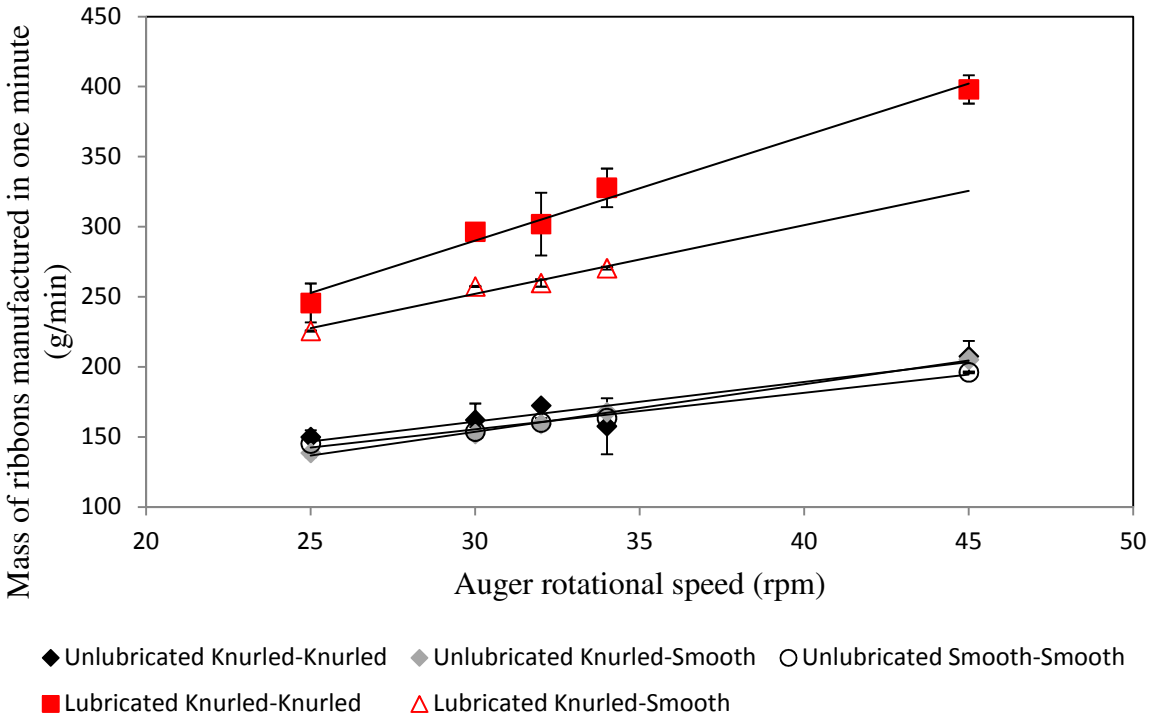


**Figure 4-21 – Roller compacted ribbon mass throughput vs. screw speed for un-lubricated and lubricated placebo formulations roller compacted with different roll surface configurations. Un-lubricated (Knurled-Knurled) $R^2$ = 0.87, un-lubricated (Knurled-Smooth) $R^2$ = 1.00, un-lubricated (Smooth-Smooth) $R^2$ = 0.99, lubricated (Knurled-Knurled) $R^2$ = 0.99 and lubricated (Knurled-Smooth) $R^2$ = 0.97. Error bars show standard deviation n=6.**

#### 4.2.2.2.7 Powder adhesion to the roll and auger surface

In the absence of magnesium stearate from the formulation adherence of the powder on both the roll surface and auger surface is a problem as shown in Figure 4-22 and Figure 4-23. In the event of material adhering to the roll surface the condition of slip is likely to be governed by frictional effect between the adhered powder layer on the roll as opposed to the roll surface. Powder adhered to the roll surface is likely to cause problems when operating the roller compactor in an automated roll gap control mode. Roll gap control uses a set-point for the minimum roll separation; any deviation from this set point will cause an automatic adjustment of the auger feeder rotational speed, such that the roll separation returns to its original set-point. A layer of powder adhered to the surface of the roll will cause the roll gap to open wider, as such the auger rotational speed will automatically reduce to maintain the roll gap at the set-point. The extent of auger rotational speed reduction, and hence mass

throughput, will depend on the thickness of the adhered powder layer. Additionally powder adhered to the roll surface will undergo multiple compaction cycles which could in turn affect the properties of the final granule [Bultmann, 2002]. In the un-lubricated roller compaction experiments, powder adhesion occurred shortly after the start-up (ca. 30-60 seconds), whilst adhesion was not observed during roller compaction of formulations containing magnesium stearate at 0.05 % w/w and above. When the roll surface was pre-lubricated (see section 4.2.2.2.2), adhesion of the un-lubricated blend was not observed until later in the run (ca. 180 seconds). Clearly, magnesium stearate provides an important role in prevention of powder adherence to the roll surface. The adhesion of powder to the roll surface is investigated in more detail in Chapter 5.

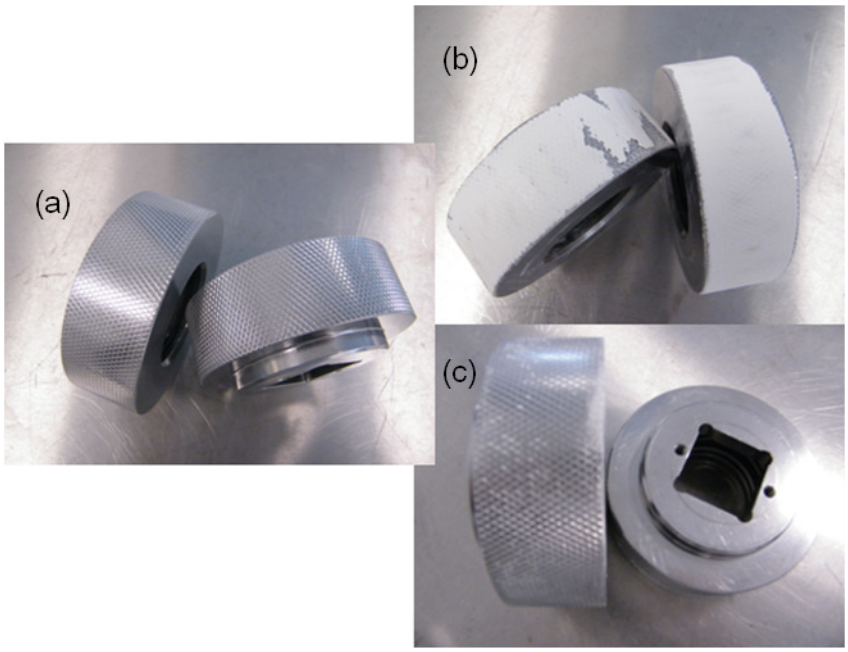


**Figure 4-22 – Effect of addition of magnesium stearate on powder sticking to rollers, (a) clean roller; (b) after roller compaction of a powder blend without magnesium stearate, and; (c) after roller compaction of a powder blend with 0.5% magnesium stearate.**

The effect of powder adhered to the auger face and indeed to the surface of the tube wall will be twofold:

(1) Firstly, due to the adhered layer of material increasing the effective thickness of the auger feeder there is a reduced volume in which the powder can pack into, effectively reducing the mass of material which can be transported per rotation; and,

(2) Adhesion of material on the auger face and tube surfaces will increase the friction experience between the powder and the equipment surfaces.

Based on the results observed using the shear cell, the internal friction was significantly higher than the wall friction. As such in the case where magnesium stearate was absent from the blend and adhesion occurs to the feed chamber surfaces the frictional resistance to movement of powder is likely to favour rotational movement of the powder contained within the feed system as opposed to axial movement. This would further reduce the effective throughput of the screw feeder and hence reduce the mass throughput of roller compacted ribbons. In the case of the lubricated surfaces, adhesion of material to the equipment surfaces is momentarily prevented as such the friction experienced between the auger face and the powder is reduced favouring axial movement of the powder. As the layer of magnesium stearate is removed from the equipment surfaces material adheres to them which both reduces the free volume and increases friction at the auger feeder leading to increased rotational movement and reduce axial velocity.

**Figure 4-23 – Adhesion of material face of the screw feeder (in the absence of magnesium stearate from the formulation)**

### 4.2.3 Post roll compaction properties

#### 4.2.3.1 Ribbon tensile strength

The tensile strength of the un-lubricated and lubricated (0.5% w/w) roller compacted ribbons was measured using a three-point bending method. As expected it was observed (Figure 4-24) that a decrease in ribbon porosity leads to an increase in ribbon tensile strength; however, for equivalent roller compactor settings the un-lubricated ribbons were observed to have significantly higher tensile strength than the lubricated (0.5 % w/w) ribbons.

It has been observed that the addition of 0.5% w/w magnesium stearate into a formulation containing microcrystalline cellulose, lactose anhydrous (in the ratio 3:2) and croscarmellose sodium (fixed at 5.0% w/w) produces ribbons with lower tensile strength. However, whether this observation is due to the presence of magnesium stearate or due to less efficient transmission of forces through the thickness of the ribbon is not yet elucidated. It has been proposed by Gamble *et al.*, that the density distribution through the thickness of the ribbon is not constant, with the outer edges of the ribbon being at a higher density than the

centre [Gamble *et al.*, 2010]. As a result of this difference in density the ribbon compact would be weaker at the centre resulting in a lower overall tensile strength and a greater production of fines due to the centre of the ribbon breaking up in the mill more easily than the outer edges of the ribbon. To ensure that the observation of the differences in ribbon properties are due to the presence of magnesium stearate and not due to differences in the ribbon thickness a further experiment was investigated whereby the un-lubricated formulation was roller compacted to produce ribbon with equivalent thickness as the lubricated condition. The hydraulic roll pressure and roll speed was the same as used previously, see Table 3-4, whilst the feed auger rotational speed was increased to achieve a calculated mass throughput equivalent to the lubricated condition using the empirical relationship giving mass throughput as a function of auger rotational speed shown in Equation 4-1. The roller compaction conditions used are given in Table 4-1; the calculated feed auger rotational speed required to match the lubricated ribbon throughput for the conditions with a hydraulic pressure of 110 bar and 200 bar was outside the operating range of the Alexanderwerk roller compactor. The measured tensile strength of the roller compacted ribbons is given in Figure 4-25, it can be seen that the thickness of the ribbon does not have a significant effect on the ribbon tensile strength; therefore, the reduction in tensile strength observed for the roller compacted condition containing 0.5% w/w magnesium stearate is in fact due to the presence of magnesium stearate rather than due to inefficient transmission of pressure through the ribbon thickness.

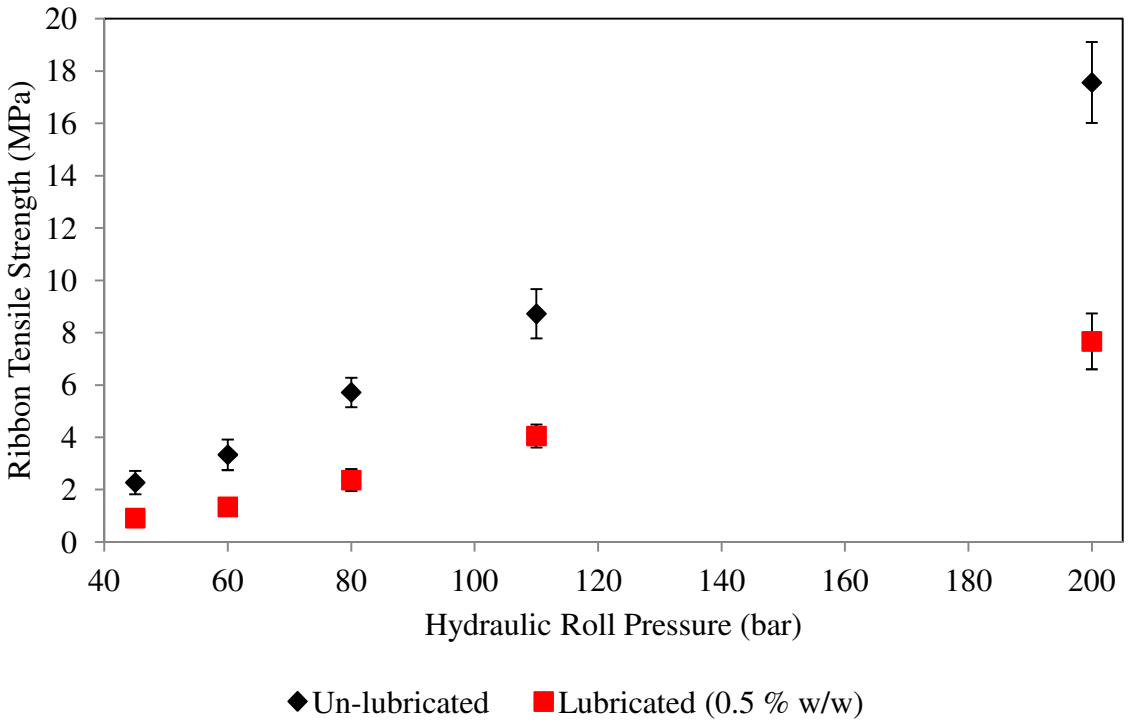


**Figure 4-24 – Comparison of ribbon tensile strength for roller compacted ribbons manufactured with (1) un-lubricated formulation; (2) lubricated (0.5% w/w magnesium stearate) formulation. Error bars show standard deviation n=6.**

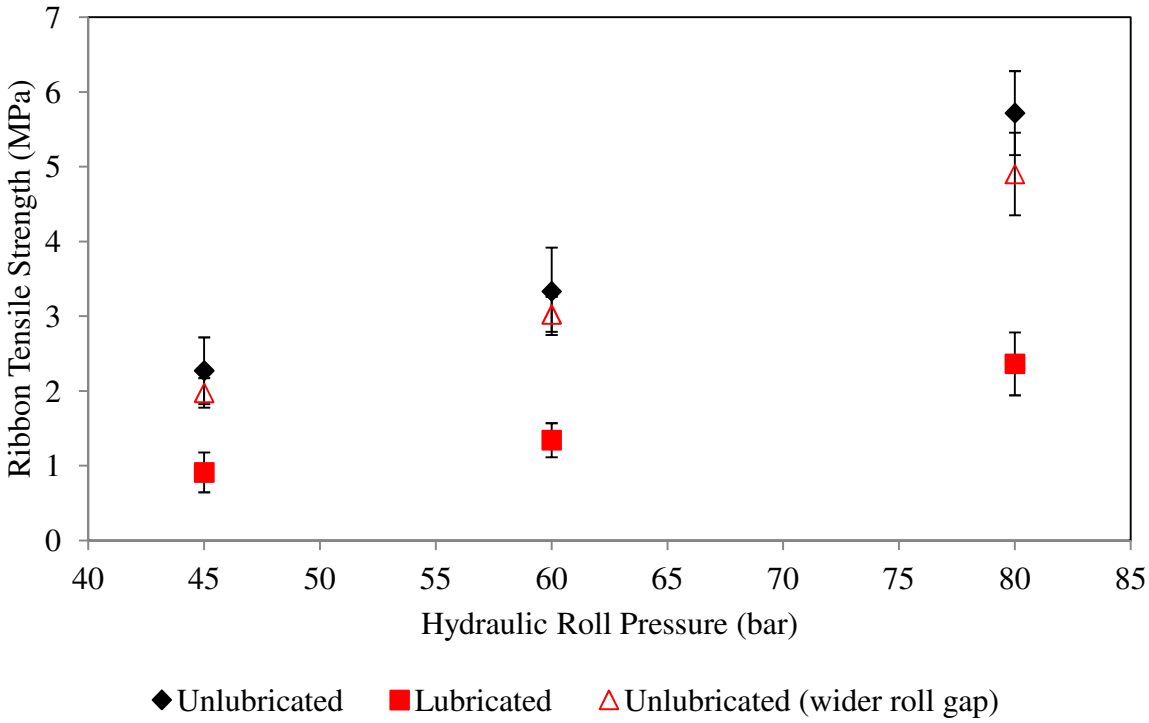


**Figure 4-25 – Comparison of ribbon tensile strength for roller compacted ribbons manufactured with (1) un-lubricated formulation; (2) lubricated (0.5% w/w magnesium stearate) formulation; and, (3) un-lubricated formulation with wider roll gap. Error bars show standard deviation, n=6.**

**Table 4-1 - Feed auger rotational speed required to achieve equivalent mass throughput to lubricated formulation**

| Screw Speed (rpm) | Roll Gap (mm) | Calculated Mass throughput (g/min) | Actual Mass throughput (g/min) |
|---|---|---|---|
| 58.0 | 4.15 | 240.21 | 248.47 |
| 75.6 | 4.50 | 290.06 | 297.07 |
| 77.5 | 4.35 | 295.45 | 295.50 |

#### 4.2.3.2 Mixing sensitivity

Roller compaction was performed on formulations with varying levels of magnesium stearate, which had been mixed for either 7 or 60 minutes. In-gap ribbon porosity and ribbon tensile strength, measurements were recorded for each condition. A mixing sensitivity ratio was defined, Equation 4-4, as a parameter to measure the relative influence that mixing has on the roller compaction behaviour and ribbon compact properties.

$$\frac{\sigma_{@\ 7mins} - \sigma_{@\ 60\ mins}}{\sigma_{@\ 7\ mins}} \qquad \textbf{Equation 4-4}$$

where σ is the ribbon tensile strength (MPa).

Increasing the amount of magnesium stearate contained in the formulation resulted in a decrease in ribbon tensile strength as shown in Figure 4-26. The sensitivity to mixing of the formulations was assessed in terms of mixing sensitivity ratio. Interestingly, at low levels of magnesium stearate addition (< 0.1% w/w) the ribbon tensile strength actually increased with increased mixing duration. The reason for this increase in tensile strength with increased mixing time is possibly due to an incomplete magnesium stearate film developed on the surface of the host excipients allowing the strong excipient-excipient bonds to form during compaction; however the incomplete film developed is enough to reduce interparticulate friction allowing increased densification during compaction. This increased densification during compaction effect has been observed by other authors [Vromans and Lerk, 1988]. As

the level of magnesium stearate in the formulation is increased beyond this point the ribbon tensile strength is significantly (using one-way ANOVA) reduced as a result of increased mixing time, attributed to the development of a more complete film of magnesium stearate on the host excipient surface.

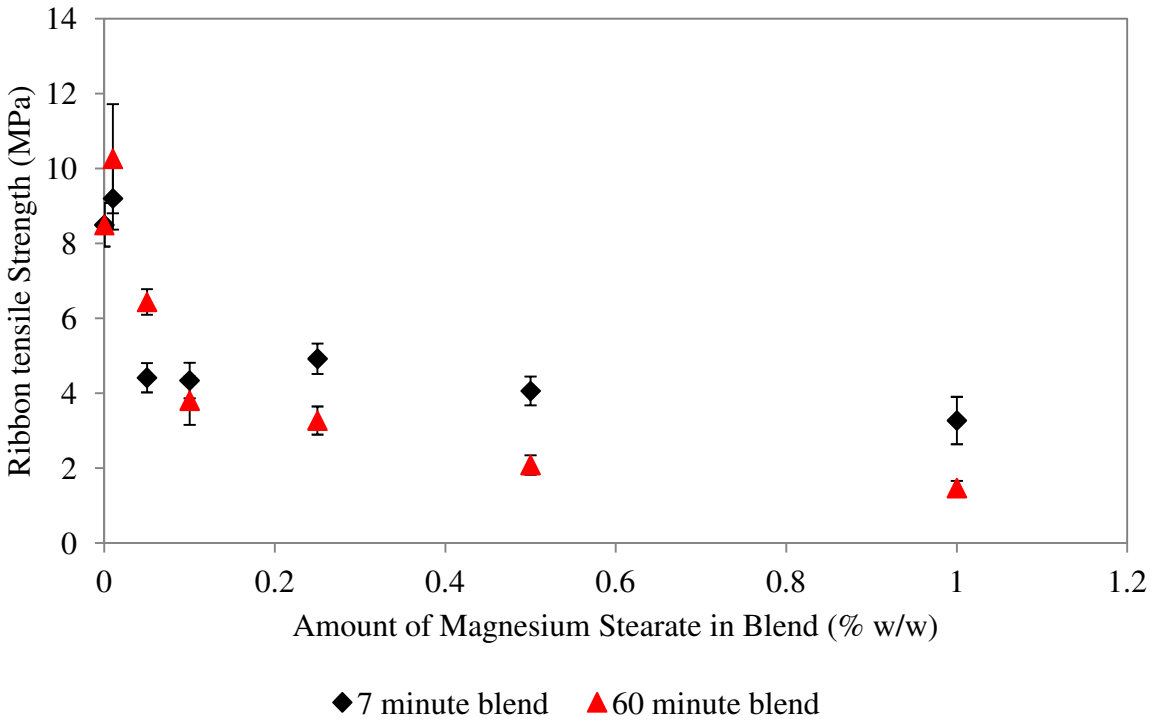


**Figure 4-26 – Ribbon tensile strength (MPa) as a function of lubricant concentration and lubricant blending time (minutes) (data is shown for the following roller compaction conditions; auger speed = 34 rpm, roll speed = 3.4 rpm and hydraulic roll pressure = 110 bar). Error bars show standard deviation n=6.**

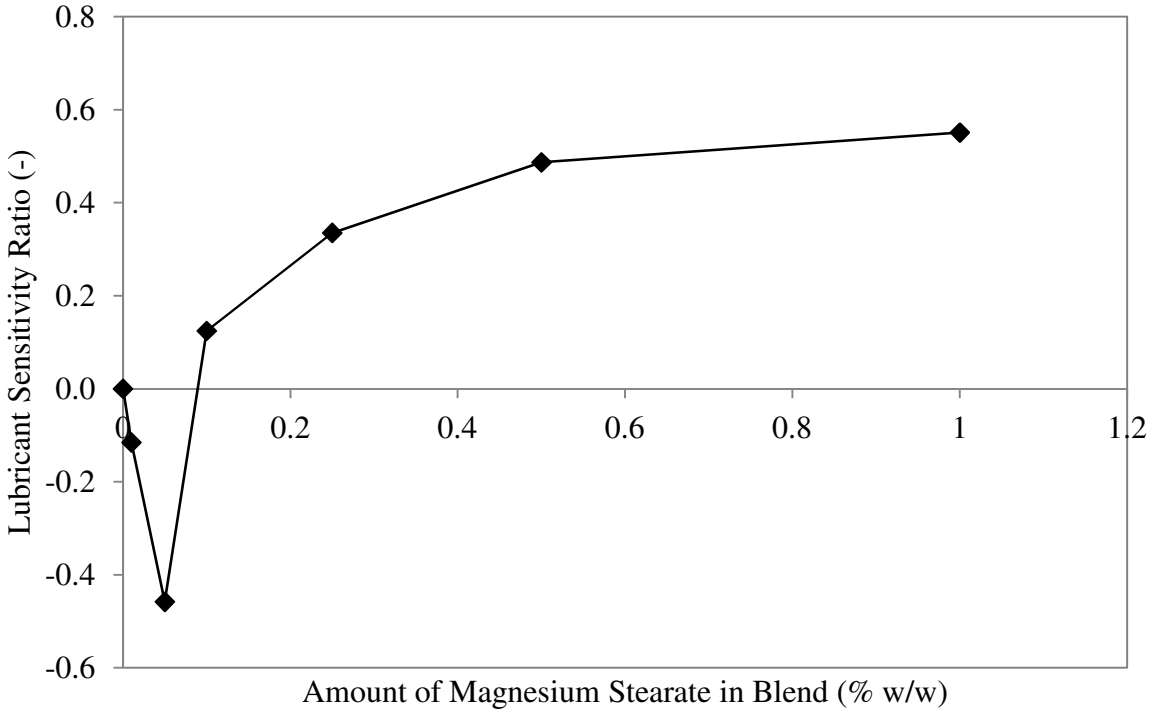


**Figure 4-27 – Lubricant sensitivity ratio as a function of magnesium stearate concentration (data is shown for the following roller compaction conditions; auger speed = 34 rpm, roll speed = 3.4 rpm and hydraulic roll pressure = 110 bar)**

#### 4.2.3.3 Granule size distributions

A typical plot comparing the granule particle size distributions obtained from milling of the un-lubricated and lubricated (0.5% w/w) roller compacted ribbons is given in Figure 4-29 and Figure 4-30 the cumulative distribution and the density distribution respectively. It was observed that ribbons with a higher porosity exhibited an increasingly more bi-modal distribution, with a fines mode (200-400 µm) corresponding to the initial blend particle size distribution and a coarse mode (1000-1200 µm) corresponding to the granular material. As the porosity of the roller compacted ribbons decreased the prevalence of the fines peak reduces. The reduction in fines of the lower porosity ribbons was expected and is attributed to the increased mechanical strength and thus resistance to size reduction during milling. Granules milled from the lubricated ribbons roller compacted at 25 rpm screw speed, 45 bar hydraulic roll pressure and 30 rpm screw speed, 60 bar hydraulic roll pressure bar exhibited higher fines content and a reduced coarse content compared to the milled granules obtained from the un-

lubricated ribbon roller compacted at equivalent conditions. However, at all other roller compaction conditions investigated the fine content of the milled granule was not influenced by the presence of magnesium stearate within the formulation.

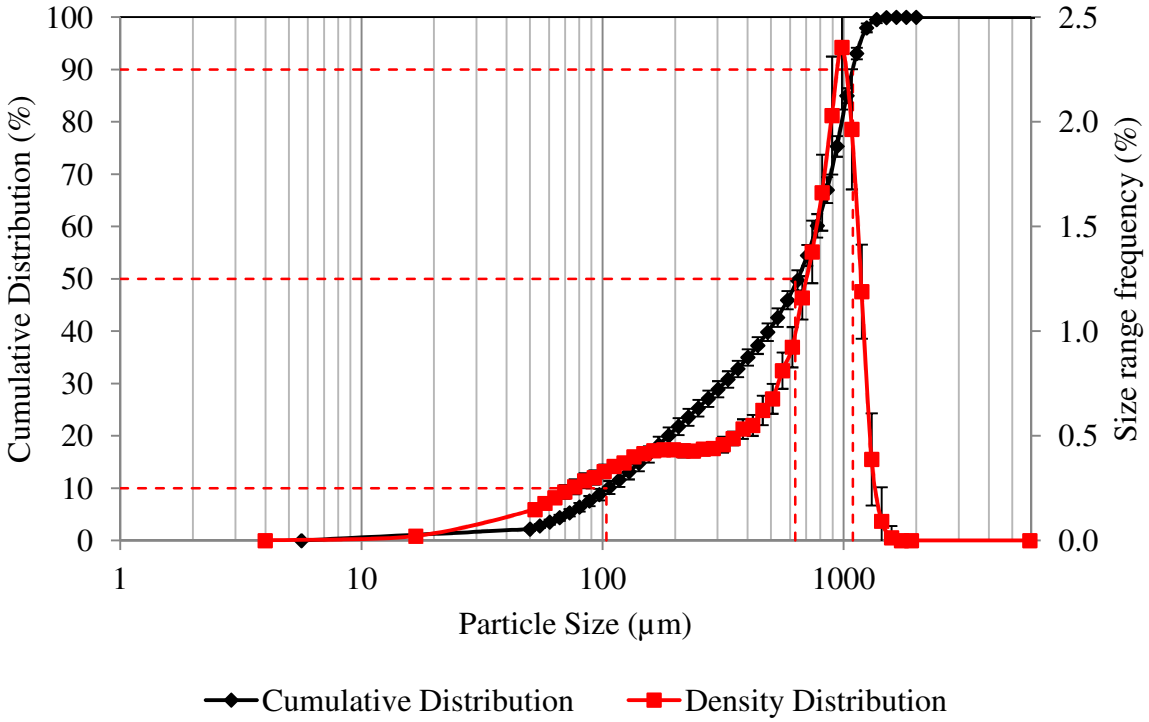


**Figure 4-28 – Typical granule particle size plot showing density distribution and cumulative distribution (with $D_{10}$, $D_{50}$ and $D_{90}$ lines). Roller compaction conditions: roll surface = Knurled/knurled, auger rotational speed = 30 rpm, Roll speed = 3.4 rpm and hydraulic roll pressure = 60 bar, un-lubricated formulation. Error bars show standard deviation n=6.**

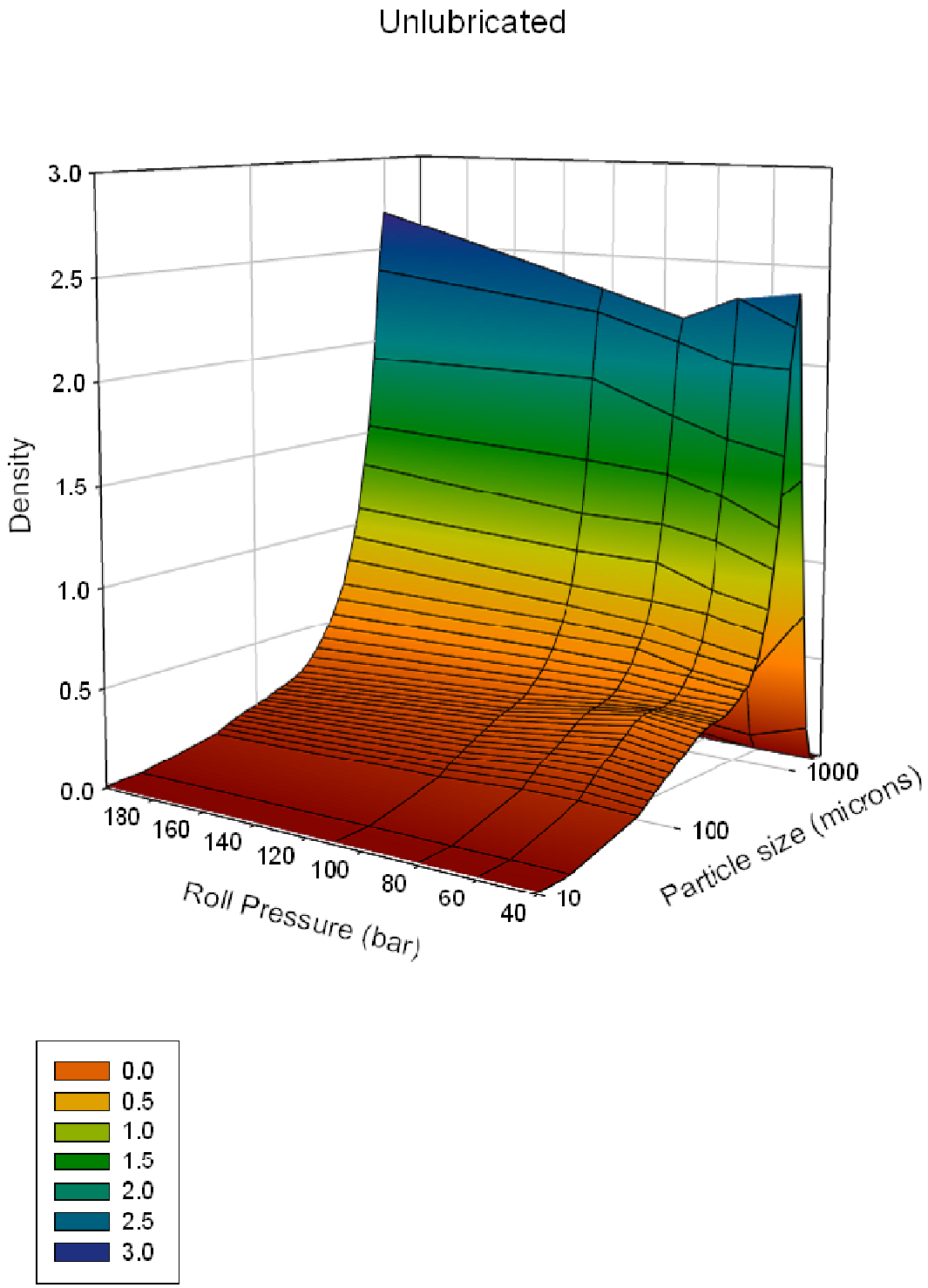


**Figure 4-29 - Particle size density distribution as a function of roll pressure (granules from un-lubricated roller compacted ribbon).**

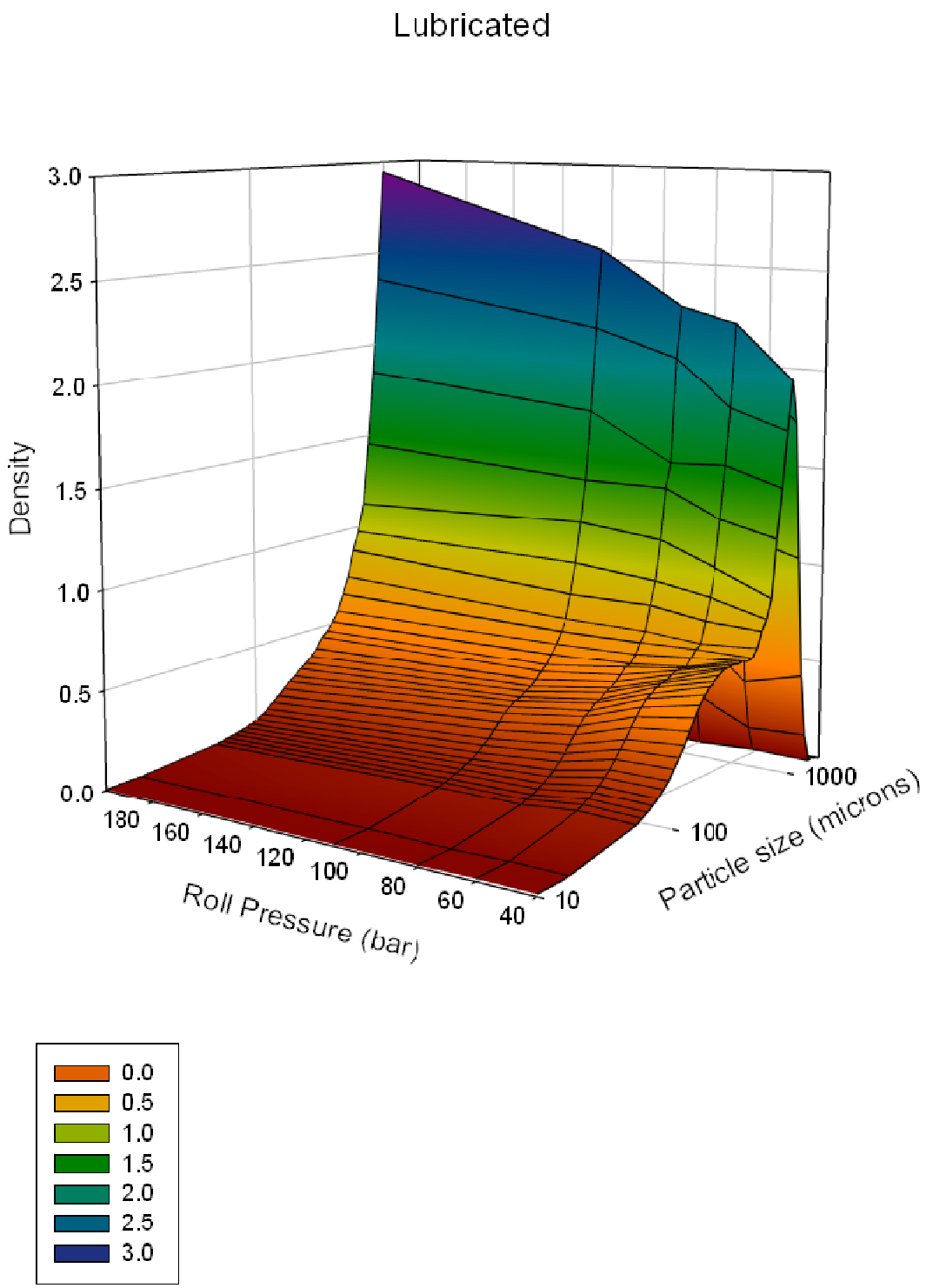


**Figure 4-30 - Particle size density distribution as a function of roll pressure (granules from lubricated roller compacted ribbon).**

#### 4.2.3.4 Granule flow properties

The flow properties of the un-lubricated and lubricated (0.5 % w/w magnesium stearate) placebo granules were measured using the Erweka flow tester instrument; the results are given in Figure 4-31. The granule flow properties were observed to correspond with the measured particle size ($D_{50}$). Increasing the granule $D_{50}$ above approximately 675 µm resulted in improved flow properties. Granules containing 0.5 % w/w magnesium stearate manufactured at equivalent roller compaction process conditions (feed auger rotation speed/hydraulic pressure and roll gap) to the un-lubricated granules had slightly increased flow properties compared to un-lubricated granules; however, the increase was found to be insignificant (ANOVA).

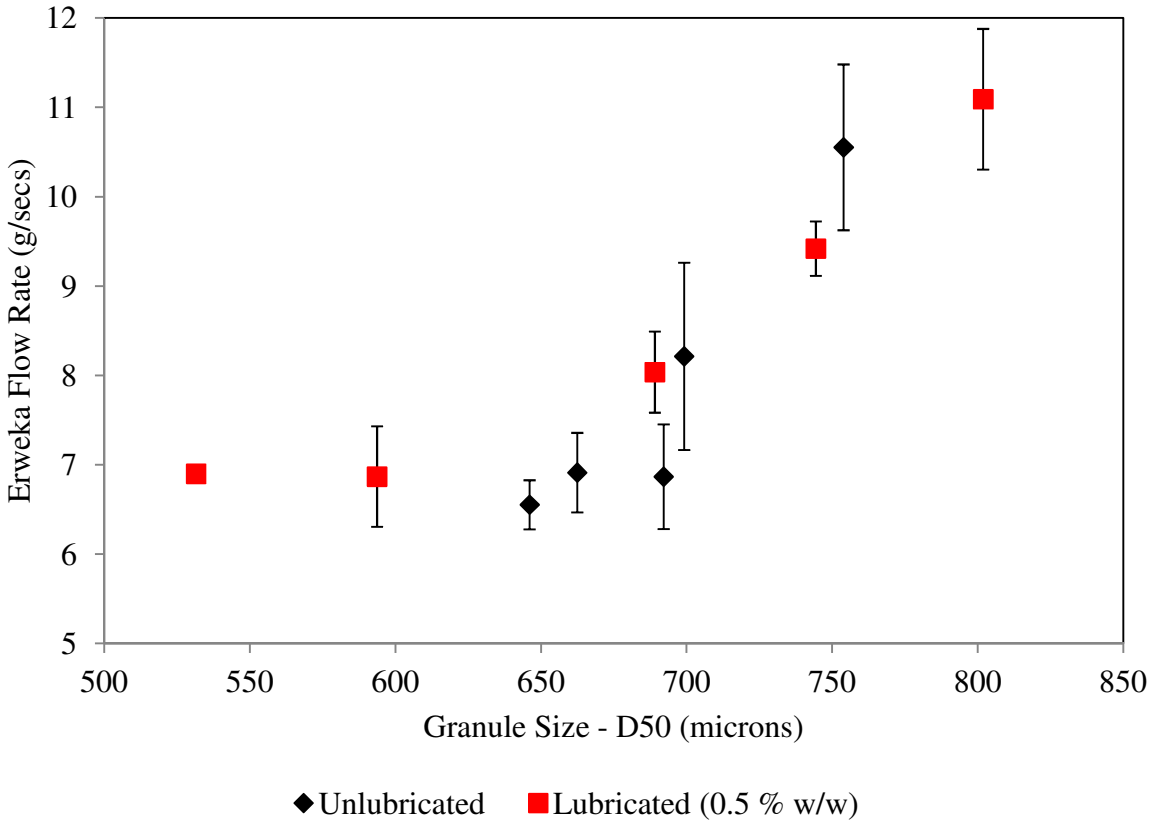


**Figure 4-31 – Measured granule flow rate (Erweka) as a function of particle size D50. Error bars show standard deviation n=6.**

## 4.3 Conclusion

The addition of magnesium stearate as a lubricant to a placebo formulation was observed to increase the throughput of material through the roller compactor, which leads to a subsequent increase in roll gap when knurled roll surfaces were used. Conversely, if two smooth rollers were used then the condition of friction at the roll/powder interface was insufficient to allow the powder to be gripped at the roll surface and hence be drawn through the rollers, causing powder to build up in the pre-nip region, and ultimately, a blockage within the feeding system. The impact of the magnesium stearate on powder conveyance was reproduced using un-lubricated powder when the equipment surfaces were pre-lubricated. This demonstrates that the mechanism of this increase in powder transmission was due to the presence of the lubricant on equipment surfaces within the feed system, even at very low levels, which led to a reduction in frictional forces. This finding would appear to suggest that the level of magnesium stearate within a blend could be significantly reduced, reducing the detrimental impacts of magnesium stearate on granule compactability, whilst maintaining the beneficial impact on the blend conveyance. This was indeed found to be the case; the impact of the amount of magnesium stearate and the mixing time was investigated. It was observed that increasing the level and amount of mixing of magnesium stearate reduces the tensile strength of the roller compacted ribbons. If the level of magnesium stearate was below 0.1% w/w then improvements in mass throughput were still apparent, whilst the effect on tensile ribbon tensile strength was limited. Furthermore increasing the amount of mixing with magnesium stearate at these low levels actually increased the tensile strength of the roller compacted ribbon.

It was also found that mixing occurs within the feed system of the roller compactor, leading to the possibility of further, uncontrolled lubrication of the blend. This potential to

cause over-lubrication of a powder blend could provide a challenge when attempting to scale up the process.

The observations from this study imply that presence of magnesium stearate can be beneficial during roller compaction; however, the feeding mechanism is likely to alter the distribution of magnesium stearate throughout the blend and upon the surfaces of the excipient particles.

# CHAPTER 5

# APPLICATION OF EXTERNAL LUBRICATION DURING THE ROLLER COMPACTION OF ADHESIVE PHARMACEUTICAL FORMULATIONS

# CHAPTER 5

# APPLICATION OF EXTERNAL LUBRICATION DURING THE ROLLER COMPACTION OF ADHESIVE PHARMACEUTICAL FORMULATIONS

## 5.1 Introduction

In Chapter 4 it was observed that one of the roles of magnesium stearate during roller compaction was to prevent the adhesion of formulation to the roll surfaces. It was discussed in section 2.4.2 that the anti-adhesive ability of magnesium stearate depends on it being present at the interface between the equipment surface and powder compact. Indeed, this was observed to be the case when magnesium stearate was initially coated on the roll surface [see section 4.2.2.2.2]. However, the anti-adhesive property of this initial coating was only temporary and adhesion occurred after a slightly extended manufacturing run. Referring to Figure 1-1, this chapter attempts to investigate the lowest level of research questions, namely: how much magnesium stearate is needed and exactly where is it needed to provide its functional role? The novel use of a system capable of continuously applying magnesium stearate directly to the roll surface was investigated as an alternative engineering strategy to

prevent adhesion of pharmaceutical formulations to the roll surface during roller compaction. A further objective is to experimentally determine the amount of magnesium stearate that transfers from the roll surface onto the roller compacted ribbon surface.

From the previous work outlined in Chapter 4, using a roller compactor with a horizontal force fed screw feeder and vertically aligned rollers with a knurled surface, it was found that internal lubrication provides a number of other advantages such as significantly increasing the roller compacted ribbon mass throughput. As a consequence, the roller compaction performance of un-lubricated formulations with the application of external lubrication will be compared to that of the un-lubricated and internally lubricated formulations. The external lubrication system is challenged further by the processing of different API containing formulations which are known to adhere to roll surfaces when insufficient levels of inter-granular magnesium stearate are present.

## 5.2 Results and discussion

### 5.2.1 Qualification of the external lubrication system

An initial range finding study using an un-lubricated placebo formulation was performed as shown in Figure 5-1 to find the effective limits of the external lubrication system. The concentration of the magnesium stearate/IPA suspension was 8% w/w magnesium stearate, the roll distance travelled per shot was initially set at 3 cm and the valve opening time was set at 2 ms. In order to find the minimum effective level of external lubrication needed to prevent adhesion of powder to the roll surface the distance per shot was sequentially reduced until a setting was found to prevent adhesion. To further ensure the minimum settings were found the valve opening time was then reduced until adhesion was no longer prevented. The roller compactor was operated using the following process parameter

settings; 30 rpm screw speed, 3.4 rpm roll speed and 60 bar hydraulic roll pressure. Observations from the initial studies showed that visually, 4 scenarios of sticking severity (ranging from (a) best case to (d) worst case) could be observed as shown in Figure 5-2. The results were consistent with previous experimental results, presented in section 4.2.2.2.7 which demonstrated that roller compaction of the un-lubricated formulation leads to the worst case scenario, (see Figure 4-22 in Chapter 4) where the formulation adheres to the roll surface and forms a complete surface coverage on the rollers. The application of external lubrication during roller compaction was able to prevent the un-lubricated formulation from adhering to the roll surface when operated using suitable settings; it was found that when operated with the shot frequency equal to a travelling roll distance of 3 cm per shot the severity of the roll adherence could be reduced such that an incomplete intermittent roll surface coverage was achieved equivalent to that described by scenario (c). The mechanism causing the intermittent pattern is due to the magnesium stearate spraying zones not overlapping; as such two distinct regions exist on the roll surface (*i.e.* regions with a high magnesium stearate concentration and regions where the roll surface is free of magnesium stearate). The roller compacted ribbon adheres to the magnesium stearate free surface; however since there is less adhesive force acting between the ribbon and the roll surface where there is a high concentration of magnesium stearate at the roll surface the action of the roll scraper removes these ribbon sections from the roll surface. The ribbon adhered to the magnesium stearate free region remains on the roll surface. Subsequent reduction of the travelling roll distance to 2 cm and 1 cm was observed to further reduce the roll adherence severity to a roll adhesion equivalent to that shown in scenario (b) and (a) respectively. At a travelling roll distance of 2 cm the compacted ribbon appeared to be adhered to the roll surface; however, the ribbon was entirely removed from the roll surface by the action of the scraper and the roll surface remained clear

of adhered formulation. At travelling roll distance of 1 cm the ribbon was observed to be free of the roll surface immediately after release from the minimum gap. The minimum shot frequency required to achieve a sticking severity equivalent to that described as scenario (a) was found to be at a travelling roll distance per shot of 1.5 cm and a valve opening time of 2 ms, this shot frequency was taken forward for further experiments.

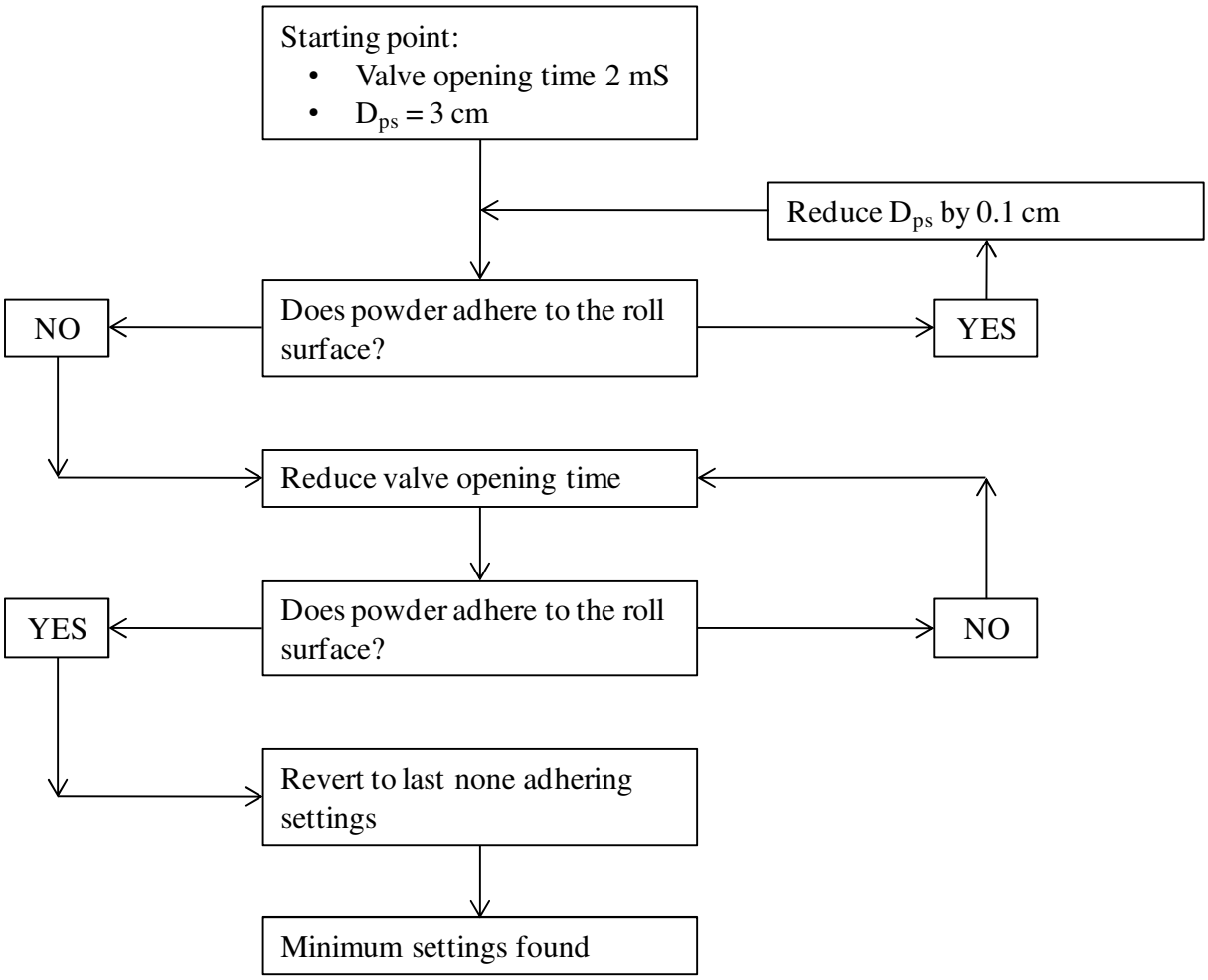


**Figure 5-1 – Decision diagram for determining the minimum distance per shot required to prevent powder adhesion to the roll surface. In previous work (Chapter 4) adhesion was observed within one minute, therefore if no adhesion was observed after one minute then application of external lubrication at each setting was determined to be adequate.**

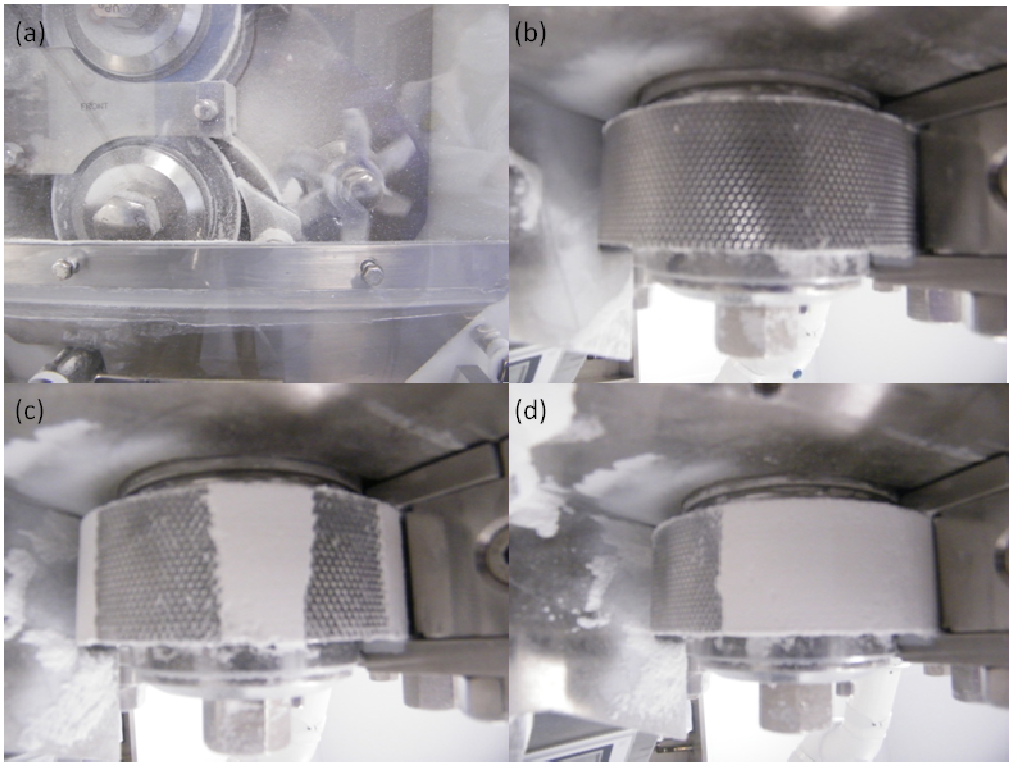


**Figure 5-2 – Scenarios of sticking in order of severity (a) ideal scenario – compacted ribbon is visibly separated from the roll surfaces after release from the minimum gap, both roll surfaces remain clean; (b) compacted ribbon appears to be adhered to the roll surface but is entirely removed by the scrapers and the roll surface remains clean; (c) compacted ribbon is adhered to the roll surface and only partially removed by the action of the scrapers leading to an incomplete 'patchy' pattern on the roll surface; (d) Worst case scenario – compacted ribbon is adhered to the roll surface and is not removed at all by the action of the scraper, roll surface has a complete coating of adhered formulation.**

### 5.2.2 Extended manufacturing campaign

The roller compactor was operated for an extended compaction campaign of 20 minutes using the same roller compaction settings as those described for the range finding study, and the AccuSpray$^{TM}$ was operated with a travelling roll distance per shot of 1.5 cm, magnesium stearate valve opening time of 2 ms and a magnesium stearate suspension concentration of 8% w/w. Whilst 20 minutes is relatively short compared to a full scale manufacturing campaign, adherence to the roll surface of this formulation without any lubrication has previously been demonstrated to occur within significantly less time, ca. 1-2 complete roll rotations after start-up. The process was paused at time intervals of 1, 2, 3, 4, 5, 7.5, 10, 15 and 20 minutes. Inspection of the roll surface, at each time interval during the 20

minute campaign, demonstrated no visual build up of adhered formulation occurring as shown in Figure 5-3(a). Furthermore during operation it could be seen that the compacted ribbon separated from the roll surface immediately after release from the minimum roll gap and this observation did not change for the duration of the campaign. After initially operating the roller compactor for 20 minutes with the application of external lubrication, the AccuSpray™ was turned off to observe how long it would take for the formulation to start to adhere to the roll surface. As seen in Figure 5-3(b), initially the roll surface remains free of adhered formulation. After 1 minute of cessation of external lubrication the formulation is observed to adhere to the roll surface, consistent with roll adhesion equivalent to that shown in scenario (c) in Figure 5-2. Additionally, the roller compacted ribbon was observed to be adhered to the roll surface upon release from the minimum roll gap. As previously reported in section 4.2.2.2.7, when the roll surface is initially coated with a film of magnesium stearate, roll adherence of the formulation on the roll surface can be prevented. The effects are only temporary as the initial film of magnesium stearate is removed from the roll surface and roll adherence subsequently occurs. The application of external lubrication provides a method of continuously reapplying the film of magnesium stearate to the roll surface and hence roll adherence can be prevented long term. It is intuitive that as this film is applied to the surface it is removed by the compacted ribbon as it passes between the rollers. This would lead to the surface of the ribbon being enriched with magnesium stearate and thus some amount of magnesium stearate must be taken through to subsequent milling and tabletting processes.

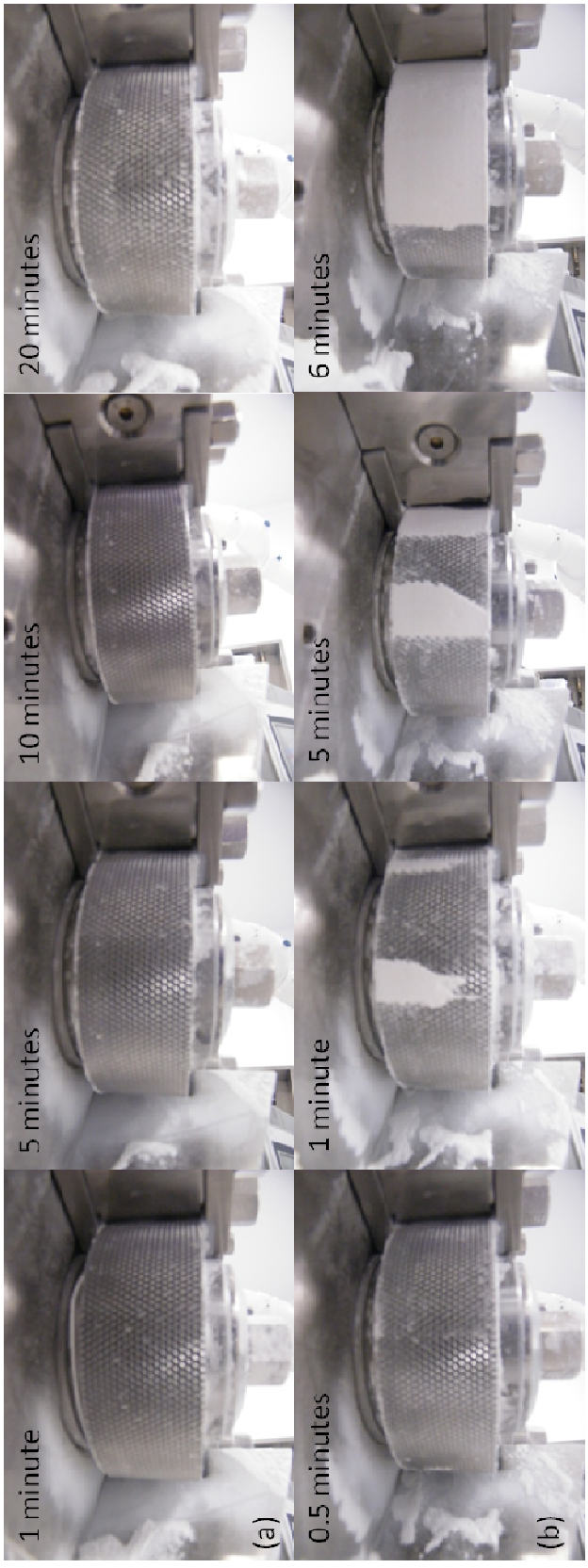


**Figure 5-3 – (a) Images of the roll surface during roller compaction with the application of external lubrication at 1, 5, 10 and 20 minutes, roll surface is consider to be clean and free of adhered formulation; (b) Images of the roll surface after cessation of the external lubrication (after the initial 20 minutes), at 1, 5 and 6 minutes, formulation can be seen adhered to the roll surface after just 1 minute, severity of sticking increasing over time.**

In addition to the visual evidence of the benefits of the external lubrication approach, the variability of the roll gap over time, before and after the system was turned off, was monitored (see Figure 5-4). In the initial period, during which the external lubrication is applied to the roll surface, the roll gap is observed to remain relatively stable, fluctuating between 1.3 and 1.4 mm; slight fluctuation in roll gap is a common phenomenon encountered during roller compaction and is attributed to inconsistent feed rate provided by the screw feeder [Guigon and Simon, 2003]. Immediately after cessation of external lubrication the roll gap remains constant, however, after 35 seconds the roll gap can be seen to increase significantly to 2.2 mm. From this time point onwards the roll gap begins to fluctuate between 1.6 and 2.2 mm. A hypothesis for these observations can be put forward: immediately after cessation of the external lubrication a film of residual magnesium stearate exists on the roll surface which is sufficient to prevent the formulation from adhering to the roll surface. However, as the compacted ribbon passes in-between the rollers this residual film of magnesium stearate is removed and the formulation starts to adhere to the roll surface. The fluctuating roll gap is due to the incomplete roll surface coverage as shown at 1 and 5 minutes in Figure 5-3(b). The larger roll gap corresponds to a patch of adhered formulation passing through the minimum roll gap, whilst the smaller roller gap corresponds to a clean section of the roll surface passing through the minimum roll gap. The implication of a fluctuating roll gap has been investigated previously by Hamden *et al.*, using the exceptional events management framework [Hamdan *et al.*, 2010]. They found that roll gap deviation is automatically compensated for by adjustment of the screw feeder; however, this mitigation strategy does not address the underlying cause of the roll gap fluctuation. Remediation of powder adhered to the roll surface would require a process shutdown, and hence reduction in manufacturing productivity.

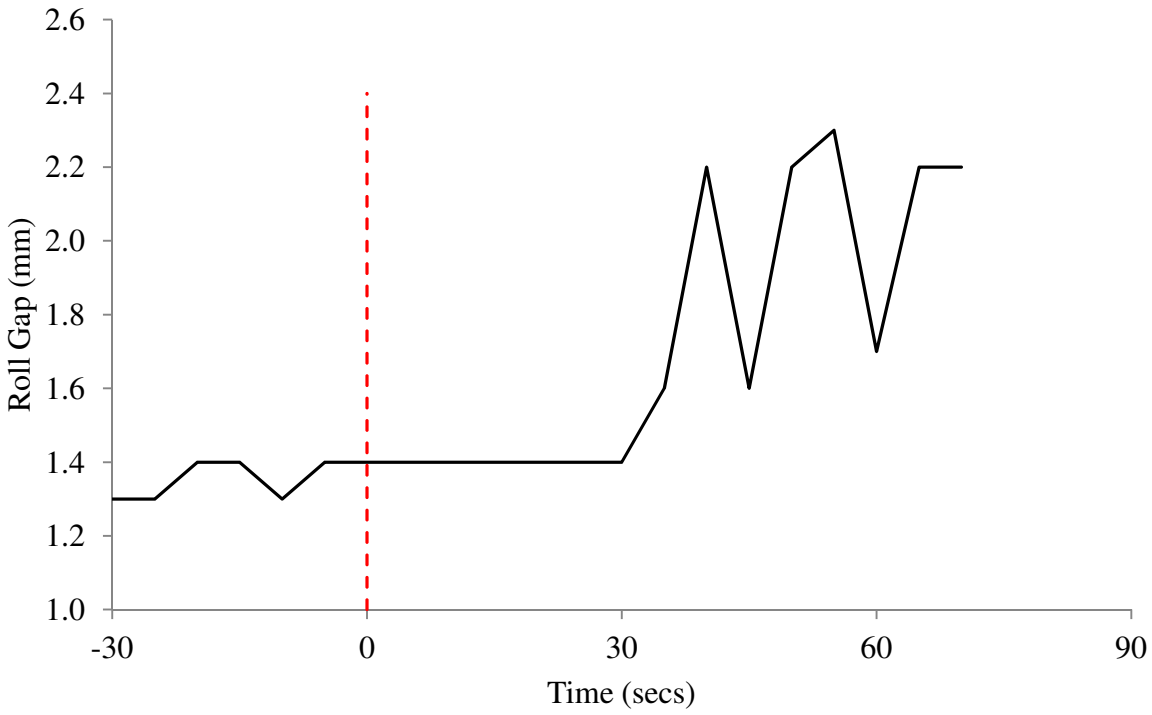


**Figure 5-4 – Change in roll gap over time; initially with the application of external lubrication the roll gap remains relatively stable, after cessation of the external lubrication (denoted by dashed line) the roll gap remains steady for 30 seconds, however, once the residual magnesium stearate is removed from the roll surface the roll gap increases significantly and begins to fluctuate between 2.4 and 1.6.**

### 5.2.3 Determining magnesium stearate content in roller compacted ribbons

The theoretical amount of magnesium stearate that could be transferred from the surface of the rolls to the surface of the roller compacted ribbon can be calculated using the assumption that all the magnesium stearate contained within one shot from the AccuSpray™ is deposited on the roll surface and that all the magnesium stearate on the roll surface is transferred onto the surface of the ribbon. The amount of magnesium stearate used as a percentage of the total formulation is therefore related to the consumption of IPA/magnesium stearate suspension per unit of time (assuming homogenous distribution of magnesium stearate within the suspension) and the mass of ribbon produced per unit of time. Using the AccuSpray™ and roller compaction settings presented in section 5.2.2 the consumption of IPA/magnesium stearate suspension was approximately 0.5 ml/min, whilst the mass of ribbons manufactured was ~ 155 g/min. Therefore the theoretical amount of magnesium

stearate transferred to the roller compacted ribbon surface was approximately 0.03 g/min or 0.59 g during the 20 minute run (at a magnesium concentration of 8 % w/w), equivalent 0.02 % w/w of the total formulation.

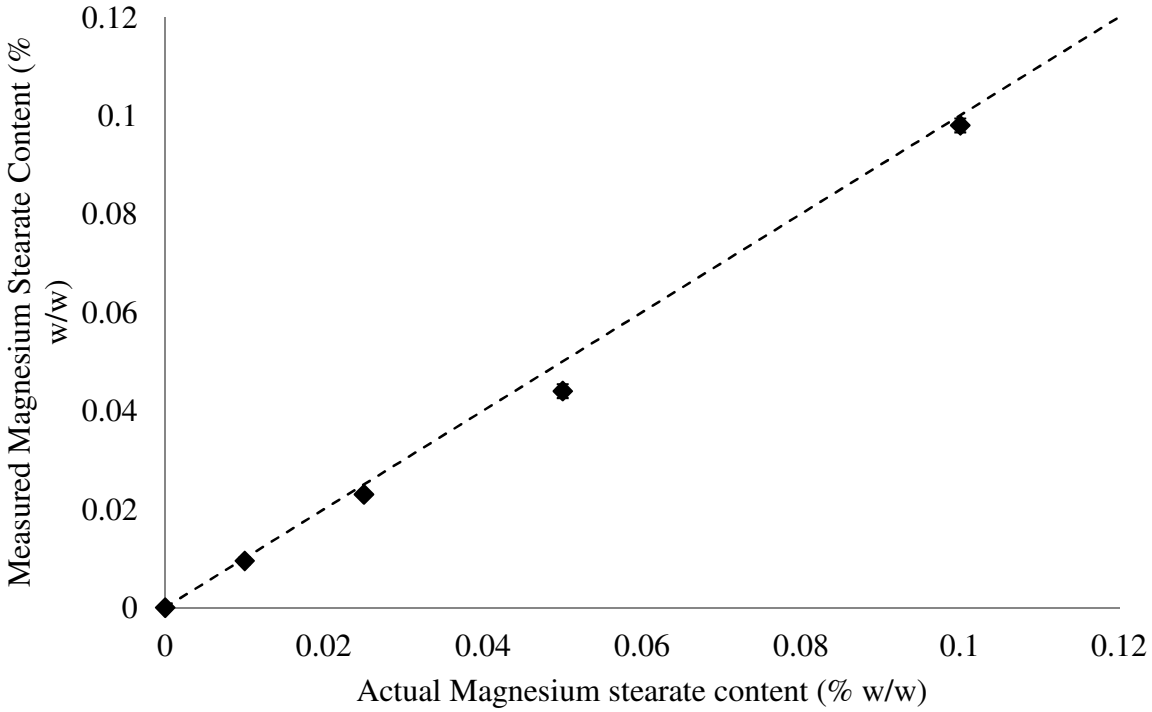


**Figure 5-5 – Measured magnesium stearate content (% w/w) in calibration samples of known magnesium stearate content (% w/w) with error bars, dashed line shows unity line.**

In order to investigate the actual level of magnesium stearate that is transferred from the surface of the roll to the surface of the roller compacted ribbon inductively coupled plasma optical emission spectroscopy (ICP-OES) was utilized as described in section 3.2.6.3. The sensitivity of the test was first established using a calibration set of placebo formulations containing a magnesium stearate content of 0.00, 0.01, 0.025, 0.05 and 0.10 % w/w. The results from the ICP-OES Figure 5-5 demonstrated that the calibration sample set was reproducible and that magnesium stearate content in the 0.25 g sample taken from the blend was representative of the composition of the total blend, more importantly the technique was capable of accurately determining the magnesium stearate contents as low as 0.01 % w/w.

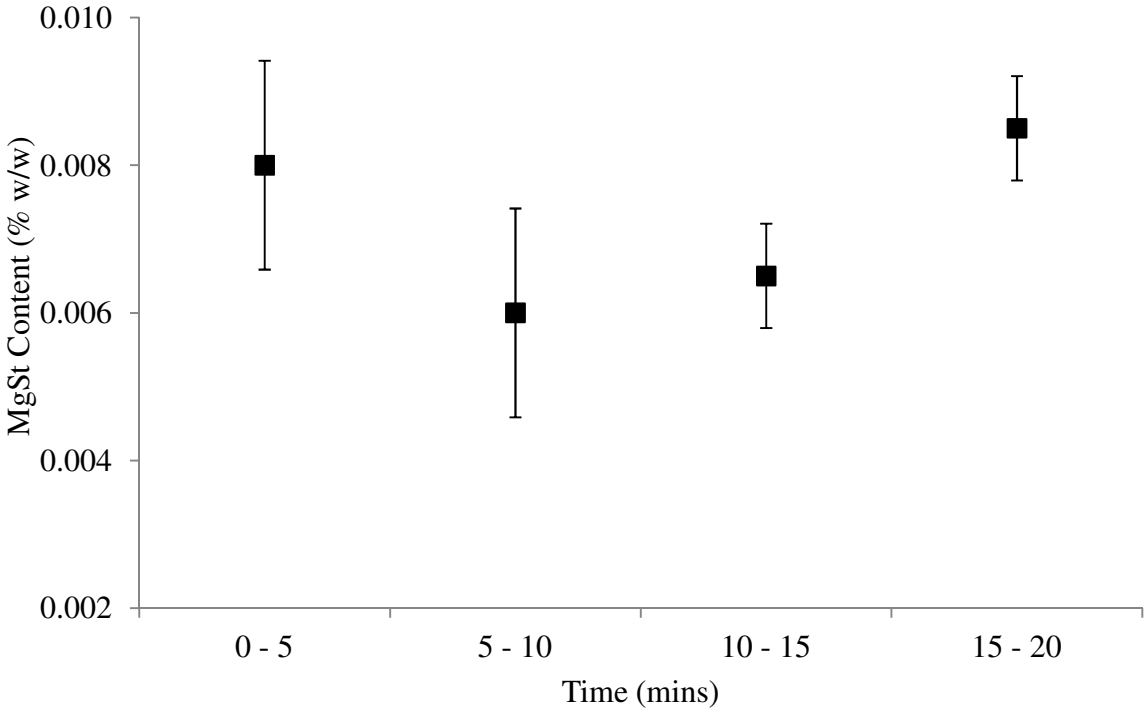


**Figure 5-6 – Amount of magnesium stearate transferred from the roll surface to the ribbon expressed as weight percent (typical amount added ~ 0.25-2.00 % w/w).**

A sub sample of the granules collected during the extended manufacturing campaign at 4 time intervals (0-5 minutes, 5-10 minutes, 10-15 minutes and 15-20 minutes) was then analysed to determine the magnesium stearate content (see Figure 5-6). The measured magnesium stearate content of the roller compacted granule was within the range of the calibration standards and was found to be significantly less than what would be expected when blending magnesium stearate within the formulation. Samples of the milled roller compacted ribbon were taken at 0-5, 5-10, 10-15 and 15-20 minutes. At each condition the level of magnesium stearate in the granule was found to be less than 0.01 % w/w, and there appeared to be no evidence of sequential build up in the amount of magnesium stearate transferred from the roll surface to the ribbon surface during the processing time as shown in Figure 5-6. This indicates that the process was operating at a steady state with no accumulation over time.

### 5.2.4 Effect of external lubrication vs. internal lubrication on roller compacted ribbon throughput

Roller compacted ribbons were manufactured using an un-lubricated formulation, with the application of external lubrication, using the roller compaction settings described in Table 3-4. As shown in Figure 5-7, the use of external lubrication had no impact on the ribbon mass throughput; however, there was a slight reduction in roll gap with the results being similar to un-lubricated material Figure 5-8. This is attributed to the absence of an adhered layer of formulation on the roll surface when lubrication is applied externally to the roll surface. The reported roll gap on the Alexanderwerk software cannot account for an adhered powder layer and as such the actual roll gap could be smaller (if the thin layer of compacted powder which adhered to the roll surface from the previous revolution was not there). As discussed previously in section 4.2.2.1, one of the advantages of adding magnesium stearate to the formulation, for horizontally fed roller compaction systems, is the significant increase in mass throughput (80-90 % increase, compared to the un-lubricated formulation), which ultimately would lead to a considerable reduction in production times. Although application of external magnesium stearate was successful in preventing the formulation from adhering to the roll surface it had no effect on increasing mass throughput. Additionally the calculated in-gap ribbon porosity obtained at each of the manufacturing conditions with the application of external lubrication was equivalent to that of the respective ribbons manufactured without lubrication and ribbons manufactured with lubrication blended within the formulation.

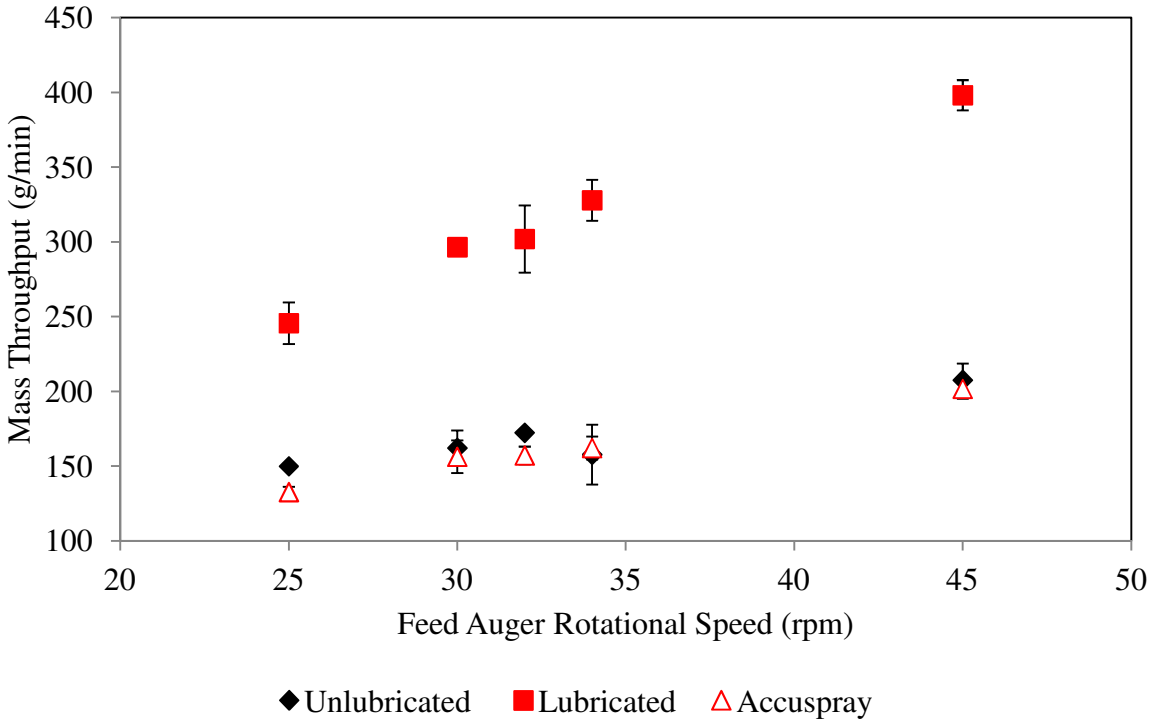


**Figure 5-7 – Comparison of the roller compaction performance of a placebo formulation with internal magnesium stearate (0.5 % w/w) and without magnesium stearate under normal conditions and with the application of external lubrication in terms of mass throughput (g/min) as a function of screw auger rotational speed.**

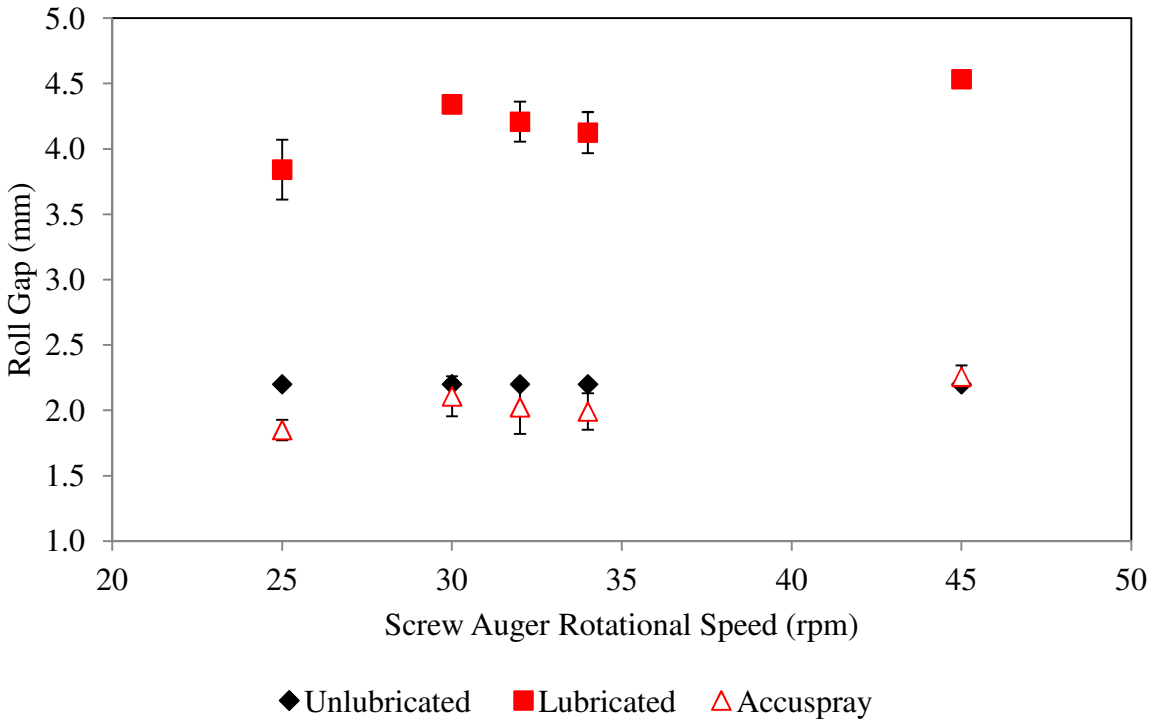


**Figure 5-8 – Comparison of the roller compaction performance of a placebo formulation with internal magnesium stearate (0.5 % w/w) and without magnesium stearate under normal conditions and with the application of external lubrication in terms of roll gap (mm) as a function of screw auger rotational speed.**

### 5.2.5 Effect of roll speed

The previous section demonstrated the potential use of external lubrication as a method to prevent roller compacted ribbons from adhering to the roll surfaces during roller compaction. However the conditions studied did not investigate the effect of roll speed. For a specific lubrication spray rate increasing the roll speed would result in less external lubrication being applied to the roll surface, which could in turn lead to the formulation adhering to the roll surface. From the initial range finding study it was found that for a roll speed of 3.4 rpm a minimum spray rate of 1 shot per 1.5 cm travelling roll distance or 25 shots per revolution was required to prevent roll adhesion. As such the spray rate of the external lubrication system was increased such that the shot frequency was kept constant at increasing roll speeds. It was found that regardless of roll speed as long as shot frequency in terms of roll distance travelled per shot was kept constant then the roller compacted ribbon could be prevented from adhering to the roll surface across all screw speeds and pressures.

### 5.2.6 API containing formulations

Roller compaction of a number of formulations containing drug products manufactured by BMS was performed to verify that the AccuSpray$^{TM}$ system could prevent roll adherence for more industrially relevant formulations. A scanning electron micrograph (SEM) image of each of the drug products used is provided in Figure 5-9. It can be observed that the morphology and size of each of the drug products are different, a summary of the properties are provided in Table 5-1.

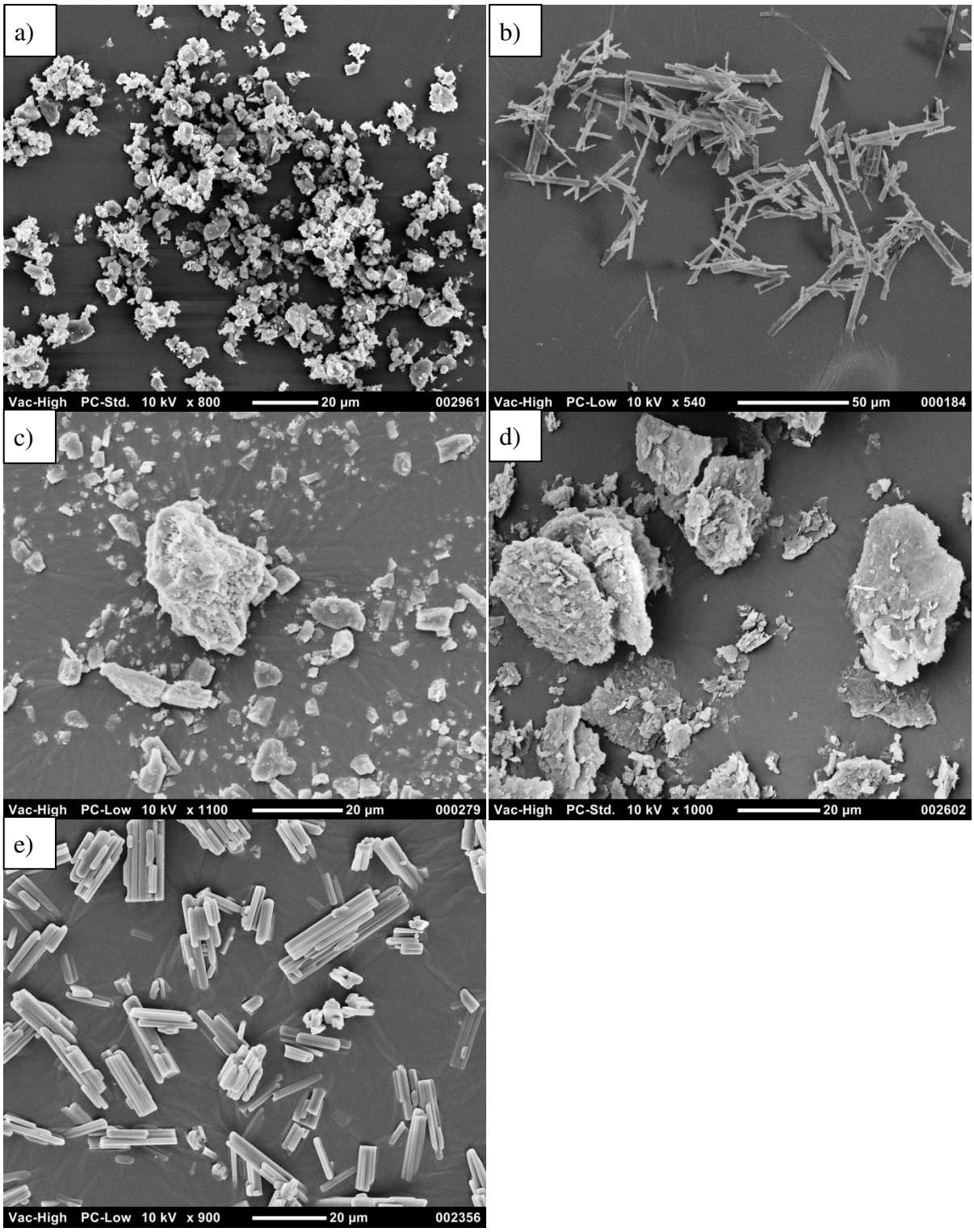


**Figure 5-9 – Scanning electron micrograph images of a) Ibipinabant, b) BMS-663068, c) BMS-791325, d) BMS-754807 and e) Pravastatin.**

**Table 5-1 – Summary of the particle morphology and size for each of the drug substances roller compacted with the use of the AccuSpray™ system. * Morphological descriptions consistent with those presented in [Rawle, 2008]**

| Drug product | Morphology* | Particle size distribution | | |
|---|---|---|---|---|
| | | D10 | D50 | D90 |
| Ibipinabant | Reticular aggregation of plate like particles | 5.3 | 9.0 | 12.9 |
| BMS-663068 | Aggregation of needle like particles | 5.6 | 12.4 | 21.6 |
| BMS-791325 | Plate like particles, with some aggregation into larger reticulated structure | 3.3 | 6.7 | 15.2 |
| BMS-754807 | Regular packing of needle like particles in a foliated structure | 30.7 | 63.9 | 118.6 |
| Pravastatin | Plate like particle with some coating of smaller particles | 9.9 | 15.6 | 22.8 |

Each of the formulations were known to have issues with powder adhesion to the roll surface during roller compaction (particularly some lots of BMS-663068 and BMS-791325) even with the presence of magnesium stearate within the formulation. In this approach unlubricated formulations were used in order to challenge the external lubrication technique. The roller compactor settings used were; 50 rpm screw speed, 7 rpm roll speed, 75 bar hydraulic roll pressure and the roll surface configuration was knurled-knurled.

It was found that using the same travelling roll distance per shot used for the placebo formulation (*i.e.* 1.5 cm) was insufficient to prevent the Pravastatin formulation from adhering to the roll surface. Observation of the roll surface showed an incomplete roll surface coverage with a sticking severity consistent with the description for scenario (c) in Figure 5-3(c). Reducing the distance per shot to 1.0 cm reduced the sticking severity from a situation equivalent to scenario (c) to scenario (b) in Figure 5-3(b), i.e. the compacted ribbon was still adhered to the roll surface after release from the minimum roll gap but the action of the scraper removed the adhered formulation entirely. A further reduction in distance per shot to 0.75 cm was required to ensure that the compacted ribbon was entirely free of the roll surface after release from the minimum gap. Compared to the placebo formulation the formulation containing Pravastatin required a shot frequency twice as fast in order to prevent sticking to

the roll surface. This observation confirms that the formulation containing Pravastatin was notably more adhesive in nature than the placebo formulation. Alternatively, it may be the case that the Pravastatin formulation has a higher affinity for the magnesium stearate and hence is more effective at removing the magnesium stearate from the rollers.

The required spray rate of the external lubrication would depend on the fundamental properties of the formulations. The relative adhesive properties of pharmaceutical formulations can be assessed by measuring ejection forces and scrape-off forces during tabletting [Miller and York, 1988, Wang *et al.*, 2010]. However no such technique exists for measuring the relative adhesive properties of pharmaceutical formulations during roller compaction. The required distance per shot value to prevent adhesion to the roll surface can be used as a parameter to assess the relative adhesiveness of pharmaceutical formulations during roller compaction. Table 5-2, lists the minimum required distance per shot value to prevent adhesion to the roll surface during roller compaction. A wide range (0.25 – 1.50 cm/shot) of values is observed allowing a relative rank order of adhesiveness of different formulations.

**Table 5-2 – Minimum distance per shot required to prevent roll adhesion for a number of different Bristol-Myers Squibb API molecules**

| Drug Product | Drug Load (% w/w) | Minimum $D_{ps}$ (cm) |
|---|---|---|
| Placebo | (-) | 1.50 |
| BMS-754807 | 3 | 0.85 |
| Pravastatin | 20 | 0.75 |
| Ibipinabant | 20 | 0.75 |
| BMS-663068 | 65 | 0.50 |
| BMS-791325 | 40 | 0.25 |

The APIs which had previously been observed to be most problematic during roller compaction (BMS-663068 and BMS-791325) required the highest amount of external lubrication to prevent adhesion to the roll surface. It is interesting to note that even at the low

addition levels of 3% w/w the amount of magnesium stearate required to prevent adhesion for BMS-754807 was still significantly higher than that required for the placebo formulation. Further work would be needed to gain a greater understanding of the link between the fundamental properties of the API/formulation and the required distance per shot to prevent adhesion.

## 5.3 Limitations of external lubrication and potential strategies

Removal of the magnesium stearate from the formulation resulted in significant decrease in roller compacted ribbon mass throughput. Furthermore, powder was observed to adhere to the equipments surfaces not treated with the external lubrication system, such as the blender vessel walls and flights of the screw feeder, as shown in Figure 5-10.

**Figure 5-10 – (left) Powder adhered to the surfaces of the auger feeder after roller compaction of an unlubricated formulation, (right) Powder adhered to the walls of the blender vessel**

During powder blending due to particle-particle collisions and sliding friction on the surface of blending equipment charge builds up of the surfaces of the particles. This process is often referred to as tribo-electric charging [Bailey, 1984, Engers *et al.*, 2006, Supuk *et al.*, 2012]. If the charge is sufficiently high enough powder adhesion to equipment surfaces occurs. The adhesive build up in the blender may result in content uniformity issues of the blended formulation [Pu *et al.*, 2009]. Stresses acting on the blender vessel walls during

mixing would be orders of magnitude lower than those which occur during compaction. It is therefore likely that the mechanism for adhesion to the blended vessel walls is electrostatic in nature. The electrostatic charge is a surface dependent parameter [Thomas *et al.*, 2009]; as such a number of researchers have investigated the use of coating materials such as silicon dioxide as a method to reduce tribo-electric charging. Admixing of binary mixture of API and colloidal silica at a concentration of 0.1% w/w reduces the electrostatic charge built up due to blending compared to the pure drug substance [Engers *et al.*, 2006, Jonat *et al.*, 2004]. The potential to use coating additives, such as colloidal silica, as a method to prevent adhesion of pharmaceutical formulation to the blender walls during mixing, would be interesting for further study.

Adhesion to the flights of the screw feeder during powder feeding was also observed for the unlubricated formulations. The flights on the screw feeder used on the Alexanderwerk have a grooved surface which is likely to increase the friction between the screw flight and the powder. Conversely to this, in powder conveyor through an auger feeder it is actually beneficial to have a smooth auger chamber with a rough or ribbed tube since this favours axial movement of the powder [Metcalf, 1965]. As observed in section 4.2.2.2.6 there was no powder adhesion to the smooth roll surface during roller compaction; whilst significant powder adhesion was observed during roller compaction with knurled (or rough) roll surfaces. It may therefore be possible to reduce the level of powder adhesion to the auger feeder by the use of alternative materials of construction, such as highly polished stainless steel. Alternatively, it was observed in section 4.2.2.2.3 that significantly reduced levels of magnesium stearate which have been homogenously distributed throughout the formulation were sufficient to prevent adhesion to the auger feeder whilst at the same time increasing the

roller compacted ribbon throughput. The compression forces within the feeding chamber will be significantly lower than the compression forces experienced during roller compaction [Michrafy *et al.*, 2011b] as such, the degree of particle fragmentation and deformation that occurs within the feed system will be lower. The adhesive forces between the equipment surfaces and the powder will therefore be smaller in the feed chamber and are overcome by the presence of small amounts of lubricant in the blend.

## 5.4 Conclusions

The application of externally applied lubrication was found to be adequate to prevent both placebo and API containing formulations from adhering to the roll surface during roll compaction in the absence of intra-granular magnesium stearate. This feasibility study has demonstrated the potential benefit of using externally applied magnesium stearate during roller compaction. A scalable parameter, the travelling roll distance per shot, can be defined to control magnesium stearate coverage. If the lubrication spray rate is controlled such that this parameter is kept constant, then sticking to the roll surface can be prevented independent of roll speed. It is further hypothesised that this parameter would be scalable across different roller compactor designs and alternative external lubrication systems. Furthermore, the amount of magnesium stearate that is transferred from the roll surface to the ribbon surface was measured to be less than 0.01 % w/w. This significant reduction in magnesium stearate, compared to internal lubrication, could ultimately lead to tablets with superior mechanical strength and faster dissolution times (based on their magnesium stearate content).

Alternatively dry lubrication systems are also commercially available such as the K-Tron KCLMT-12 which could also be applied in a similar manner for roller compaction. The main difference is that the dry systems provide a constant spray with nearby vacuum to

remove excess material; as such the overall magnesium stearate usage would increase. A spray rate/travelling roll distance could likewise be determined and used for changes in roll speed and scale-up. This would alleviate the use of solvents which are typically avoided in pharmaceutical manufacturing because they can be detrimental to API stability and present safety and environmental issues.

Although the application of external lubrication solves one industrially relevant problem the disadvantage of removing magnesium stearate from the formulation entirely is the significant reduction in ribbon mass throughput compared to inter-granular magnesium stearate. This would have a significant impact on process times especially in the manufacturing environment if the same processing speeds are applied. The secondary advantage of the application of external lubrication is the removal of the lubrication blending stages and hence a reduction in unit operations, manufacturing time and process stoppages due to the occurrence of roll adherence. Other advantages of the external lubrication system include the reduction in variability that is inherent with the lubrication blending strategy, which would be beneficial both from a regulatory and a Quality by Design perspective.

Furthermore, adhesion to other surfaces in the roller compactor feed system and pre-roller compaction blending vessel is likely to occur in the absence of magnesium stearate from the formulation. Other strategies that could be investigated to overcome these issues include control of electrostatic charge build up during blending such as using surface coating powders such as colloidal silica. For the screw feeder where forces are particularly low there is potential that alternative abrasive resistant materials could be used to help prevent adhesion to the surface of the flights. Alternatively addition of small amounts of lubricants homogenously distributed throughout the blend may provided a trade-off between mass

throughput increase and anti-adhesion to the auger feeder walls, whilst limiting the impact of blending sensitivity and the deleterious effect of magnesium stearate on tablet tensile strength and dissolution.

If coupled with an externally lubricated tablet press this method could provide a complete dry granulation manufacturing route with the near absence or significantly reduced levels of magnesium stearate blended within the formulation.

# CHAPTER 6

# POTENTIAL ALTERNATIVE FORMULATION STRATEGIES TO ACHIEVE LUBRICATION DURING ROLLER COMPACTION

# CHAPTER 6

# POTENTIAL ALTERNATIVE FORMULATION STRATEGIES TO ACHIEVE LUBRICATION DURING ROLLER COMPACTION

## 6.1 Introduction

In the previous chapters the impact of magnesium stearate on roller compaction was investigated. The inclusion of magnesium stearate in the pre-roller compaction formulation has been observed to provide two distinct advantages namely; (i) prevention of adhesion to the roll surface and (ii) significantly increases potential ribbon mass throughput (at equivalent roller compaction process parameter settings). Both these advantages can be achieved at significantly smaller quantities than that which is typically used in an industrially relevant formulation. Small amounts internally included within the formulation can sufficiently lubricate the feed system surfaces to provide increased mass throughput whilst very small quantities added directly to the roll surface external to the formulation can replicate the anti-adhesive properties. It is the aim of this chapter to investigate the final part of the primary

strand of research questions originally shown in Figure 1-1 that is; what alternative formulations strategies can be used to achieve lubrication during roller compaction.

By necessity, any potential alternative formulation strategy used to replicate the lubricating ability of magnesium stearate must provide equivalent lubricating properties at low concentrations. Furthermore in light of the findings of the previous chapters in this thesis, the modified formulation must produce a similar effect during roller compaction. However, to comply with the business need any modified formulation must have a reduced impact on the quality attributes of the tablet product.

In this chapter a number of alternative lubricants, namely; sodium stearyl fumarate (Alubra™), glyceryl monostearate, talc and colloidal silica were investigated for their impact on the roller compaction of the platform placebo formulation used in previous chapters. In addition an alternative formulation strategy which utilises compendial excipients co-processed with glyceryl monostearate (LubriTose AN and LubriTose MCC) was compared to the traditional method of adding pure lubricated material to the powder blend.

To further explore the use of alternative lubricants/formulation strategies to overcome the processing and tablet quality issues associated with the use of magnesium stearate an active formulation containing Atenolol was subjected to both roller compaction and a subsequent tablet compaction process. The investigated parameters included the roller compaction performance (roll gap, mass throughput and pressure profile), ribbon tensile strength, granule size distribution, tabletting performance (ejection force and maximum compaction force), tablet tensile strength and dissolution time. Atenolol is one of the most widely used beta blocker drugs in the treatment of cardiovascular diseases such as hypertension, coronary heart disease, arrhythmias, and treatment of myocardial infarction

after the acute event. Conventional Atenolol tablets available in market are not suitable where quick onset of action is required; patients with sudden increase in blood pressure and acute angina attack, have markedly reduced functional ability and are extremely restless, in such cases rapid onset of drug action is of prime importance [Khirwadkar and Dashora, 2013]. It is therefore of interest to study the effect of different lubricant types on the disintegration/dissolution time of Atenolol formulations

## 6.2 Materials and methods

### 6.2.1 Specific formulation details

#### 6.2.1.1 Placebo formulations

**Table 6-1 – LubriTose formulation compositions (125 g of croscarmellose in all formulations)**

| Formulation | MCC (normal) (g) | LubriTose™ MCC (g) | Lactose (normal) (g) | LubriTose™ AN (g) |
|---|---|---|---|---|
| Base | 1425 | - | 950 | - |
| 25 % LubriTose™ MCC | 1068.75 | 356.25 | 950 | - |
| 50 % LubriTose™ MCC | 712.5 | 712.5 | 950 | - |
| 100 % LubriTose™ MCC | - | 1425 | 950 | - |
| 25 % LubriTose™ AN | 1425 | - | 712.5 | 237.5 |
| 50 % LubriTose™ AN | 1425 | - | 475 | 475 |
| 100 % LubriTose™ AN | 1425 | - | - | 950 |

The formulation under investigation was the same as that used in previous chapters (see Table 3-3). To accommodate the addition of additives (lubricants or flow aids) into the formulation the amount of microcrystalline cellulose and lactose was reduced such that the ratio remained at 3:2 whilst the amount of croscarmellose was fixed at 5% w/w. In this chapter the unlubricated formulation described above (and in Table 3-3) is denoted as the 'base' formulation. LubriTose AN and LubriTose MCC was used to replace either the entire amount or some portion of the lactose and microcrystalline cellulose in the 'base' formulation as detailed in Table 6-1.

#### 6.2.1.2 Atenolol formulations

The Atenolol formulations contained a drug loading of 10, 20 or 40% which was added to the 'base' formulation outlined in the previous section. The addition of Atenolol into the formulation was at the expense of the microcrystalline cellulose and lactose (the remaining microcrystalline cellulose and lactose in the formulation remained fixed at a ratio of 3:2). Both magnesium stearate and sodium stearyl fumarate was added at 1.0% w/w whilst in the LubriTose formulations both lactose and microcrystalline cellulose were completely replaced with LubriTose AN and LubriTose MCC.

#### 6.2.1.3 Blending

##### 6.2.1.3.1 Placebo formulations

Blending was performed as outlined in section 3.3.3, for the formulations containing LubriTose™ AN or LubriTose™ MCC, all excipients were added to the initial blend and the total blend time was either 10 minutes or 60 minutes at 15 rpm.

##### 6.2.1.3.2 Mixing sensitivity study

For the mixing sensitivity study samples were taken from the blender at the following time intervals; 0, 1, 2, 3, 4, 5, 7.5, 10, 15, 20, 30, 45, and 60 minutes.

##### 6.2.1.3.3 Atenolol formulations

Formulations containing either sodium stearyl fumarate or magnesium stearate as the lubricant were initially blended as outlined in section 3.3.3; with the exception that atenolol was added to the blending vessel after the microcrystalline cellulose and prior to the addition of lactose. Following the initial blending stage the lubricant was added to the formulation and blended for either 7 or 60 minutes. Formulations containing LubriTose™ AN/MCC were

blended with the immediate addition of all formulation ingredients in the same order as above for either 10 or 60 minutes.

#### 6.2.1.4 Specific roller compaction settings

Roller compaction was performed using the Alexanderwerk WP120 roller compactor (Alexanderwerk, Remscheid, Germany). Placebo formulations were roller compacted as outlined in Table 3-4. The roller compaction conditions for the Atenolol formulations are given in Table 6-2.

**Table 6-2 - Roller compaction manufacturing parameters used for LubriTose™ and Atenolol formulations**

| Parameter | Set point |
|---|---|
| Screw Speed (rpm) | 30 |
| Roll Speed (rpm) | 3.4 |
| Hydraulic Pressure (bar) | 60 |
| Roll Surface | Knurled-Knurled |
| Mill Speed (rpm) | 60 |
| Primary Screen (mm) | 3.2 |
| Secondary Screen (mm) | 1.0 |

## 6.3 Results and discussion

### 6.3.1 Placebo formulations

#### 6.3.1.1 Flow additives

The increase in mass throughput as a result of the inclusion of 0.5% w/w magnesium stearate into the formulation was unexpected. Magnesium stearate has been previously observed to reduce the efficiency of powder draw during roller compaction as shown by a reduction in nip angle. Roller compaction of the un-lubricated formulation with the addition of a well known flow aid, silicon dioxide, was performed. Two grades of silica were investigated; colloidal and micronized. Despite the fact that silicon dioxide is commonly used during processing to improve the flow properties of pharmaceutical formulations, it was

observed, as shown in Figure 6-1, that neither the addition of colloidal nor micronized silicon dioxide had a significant effect on the mass throughput of roller compacted ribbons compared to an un-lubricated formulation. This observation would suggest that the improvement in roller compacted ribbon mass throughput is inherent in the intrinsic anti-friction and anti-adhesive properties of magnesium stearate. Furthermore, despite the fact colloidal silica reduces adhesion forces between particles [Jonat *et al.*, 2004, Meyer and Zimmermann, 2004] by acting as surface roughness and increasing the distance of separation, it had no beneficial effect on preventing adhesion to the roll surfaces of the roller compactor.

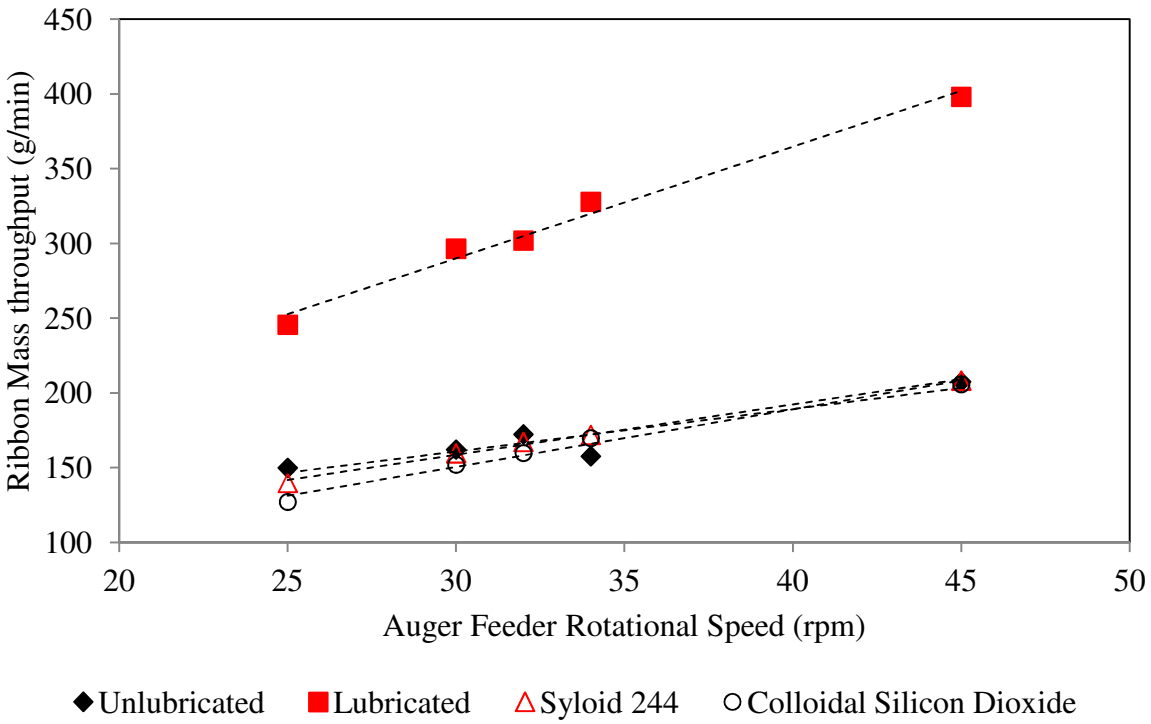


**Figure 6-1 – Comparison of mass throughput; syloid 244 $R^2$ = 1.00 and colloidal silica $R^2$ = 0.97, un-lubricated and lubricated mass throughput included for reference purposes.**

### 6.3.1.2 Anti-adhesive

As a model anti-adhesive, talc was added to the placebo formulation at a concentration of 2 % w/w and 5 % w/w. As one would expect with an anti-adhesive, the adherence of the formulation to the roll surface during roller compaction was not observed. Furthermore, as

shown in Figure 6-2 the addition of talc to the placebo formulation elicits a similar increase in roller compacted ribbon mass throughput. However, even at these high levels the increase in mass throughput is less than that of magnesium stearate.

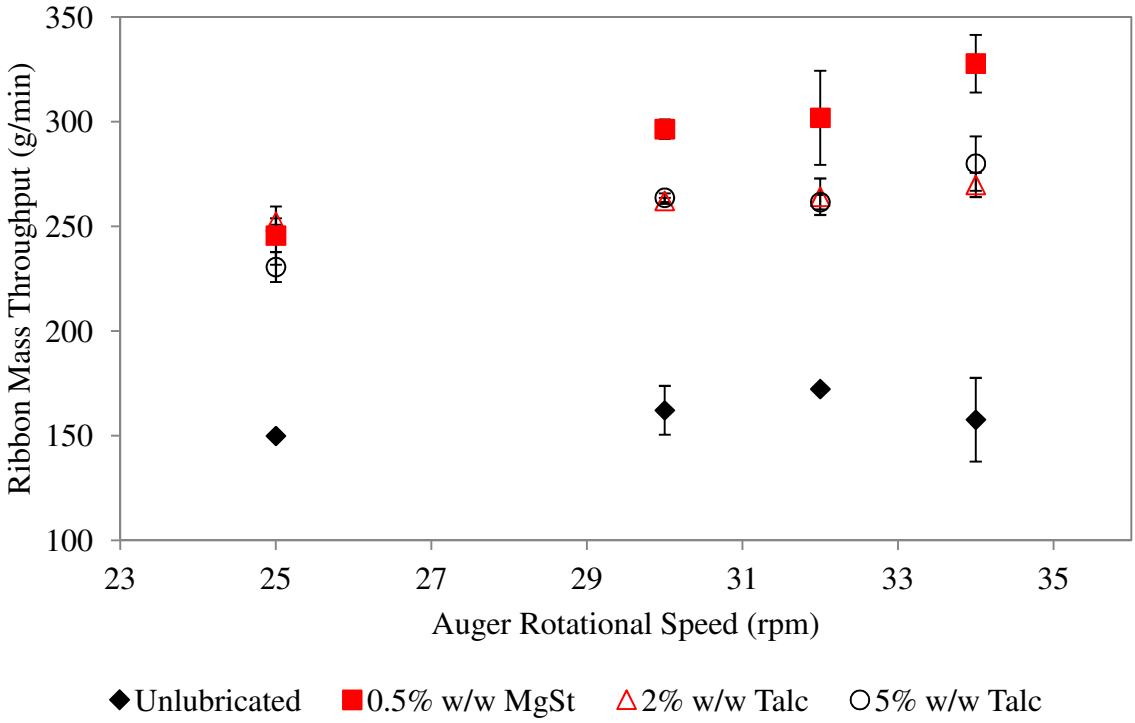


**Figure 6-2 - Roller compacted ribbon mass throughput (g/min) as a function of feed auger rotational speed (rpm) for ribbons manufactured using 2 and 5% w/w Talc (0.5% w/w magnesium stearate and unlubricated ribbons included for reference). Error bars show standard deviation n=6.**

Despite this it can be observed in Figure 6-3 that the addition of 2% w/w talc into the formulation elicited a greater lubricating effect defined in terms of the pressure distribution efficiency ratio. Due to frictional effects at the equipment surfaces the flow of powder into nip region of the roller compactor is impeded. As a result of this restriction to powder flow, the velocity of powder located at the centre of the rollers is faster than that at the equipment edges [Miguelez-Moran *et al.*, 2009, Miguelez-Moran *et al.*, 2008]. This in turn leads to differences in the pressure measured by the pressure transducer located at the centre of the roll compared to the pressure transducers located at the edges. The use of lubricants reduces the effect of friction at the equipment surfaces which negates the difference in pressure between the centre

and edges of the roll surface. It can be observed (Figure 6-3) that a greater difference between the edges of the roll vs. the centre of the roll exists for the unlubricated formulations. The addition of either magnesium stearate or talc is sufficient to reduce this difference with talc at a level of 2% w/w providing the smallest difference. This observation suggests that an optimum level of talc addition exists to provide the maximum lubrication efficacy.

As with magnesium stearate the addition of talc has a significant effect of reducing the tensile strength of roller compacted ribbons, as shown in Figure 6-4. Furthermore, as shown in Figure 6-5 the granule size (D50) of the milled granules is shown to be strongly correlated with the tensile strength of the roller compacted ribbon.

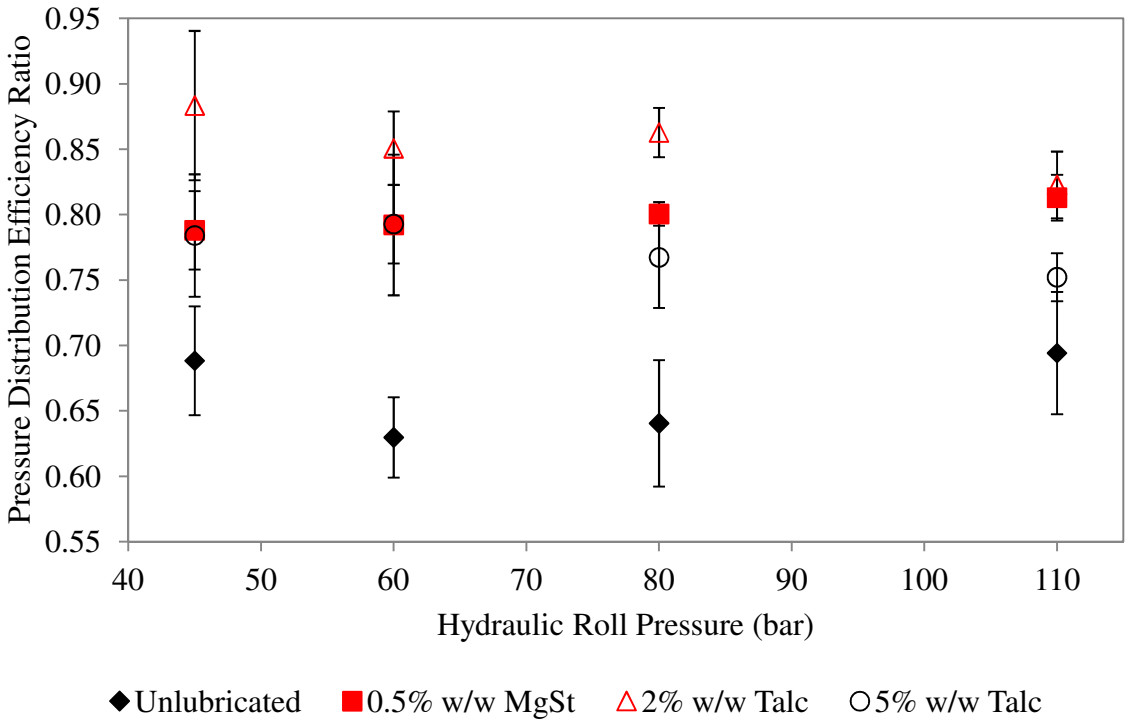


**Figure 6-3 – Pressure distribution efficiency ratio as a function of hydraulic roll pressure. Error bars show standard deviation, n=6.**

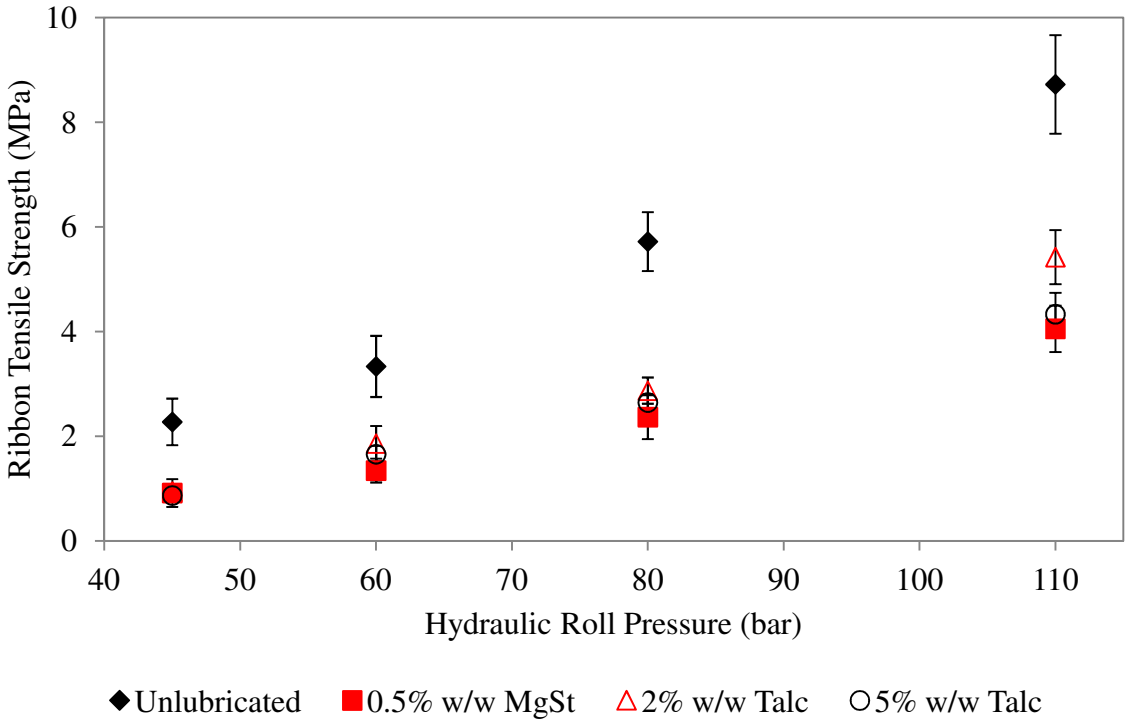


**Figure 6-4 – Ribbon tensile strength (MPa) as a function of hydraulic roll pressure (bar) for ribbons manufactured using 2 and 5% w/w Talc (0.5% w/w magnesium stearate and unlubricated ribbons included for reference)**

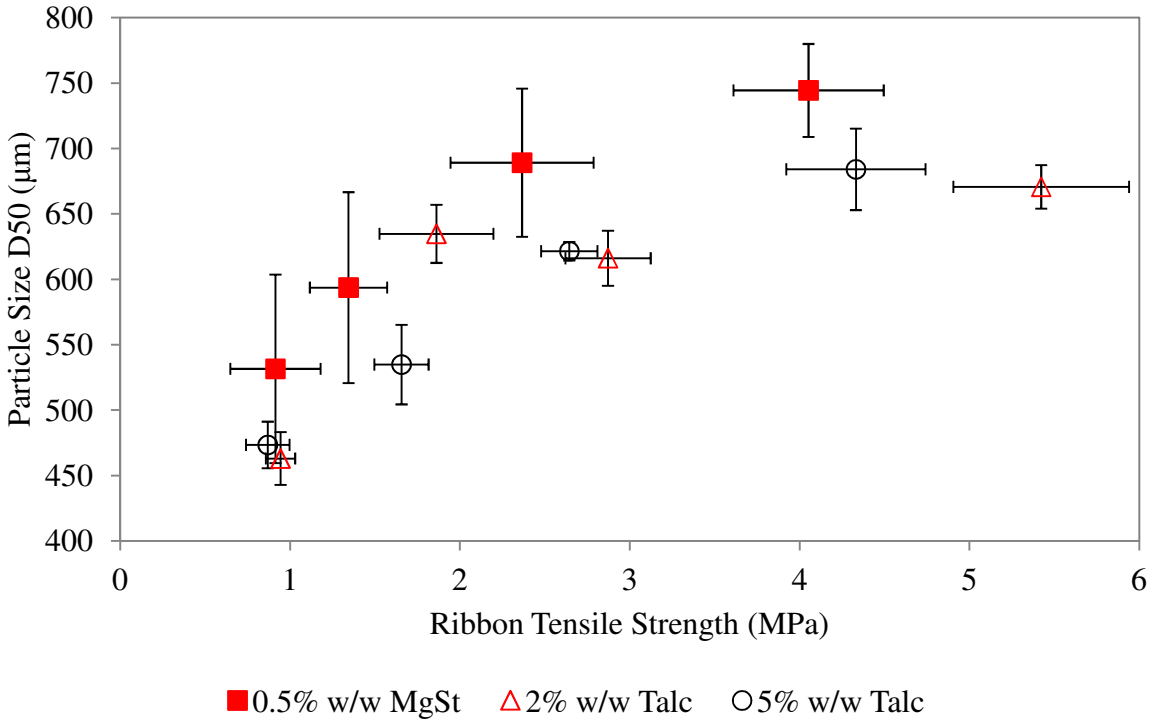


**Figure 6-5 – Particle size D50 as a function of ribbon tensile strength for formulations containing 2 and 5% w/w Talc.**

#### 6.3.1.3 Lubricants

##### 6.3.1.3.1 Sodium stearyl fumarate

As seen previously with the addition of talc to the formulation, sodium stearyl fumarate was observed to provide a similar effect on increasing the roller compacted ribbon mass throughput as magnesium stearate. However, the increase in mass throughput was actually slightly greater for the sodium stearyl fumarate formulations, as shown in Figure 6-6. In addition the use of sodium stearyl fumarate was sufficient to prevent the adhesion of the placebo formulation to the roll surface.

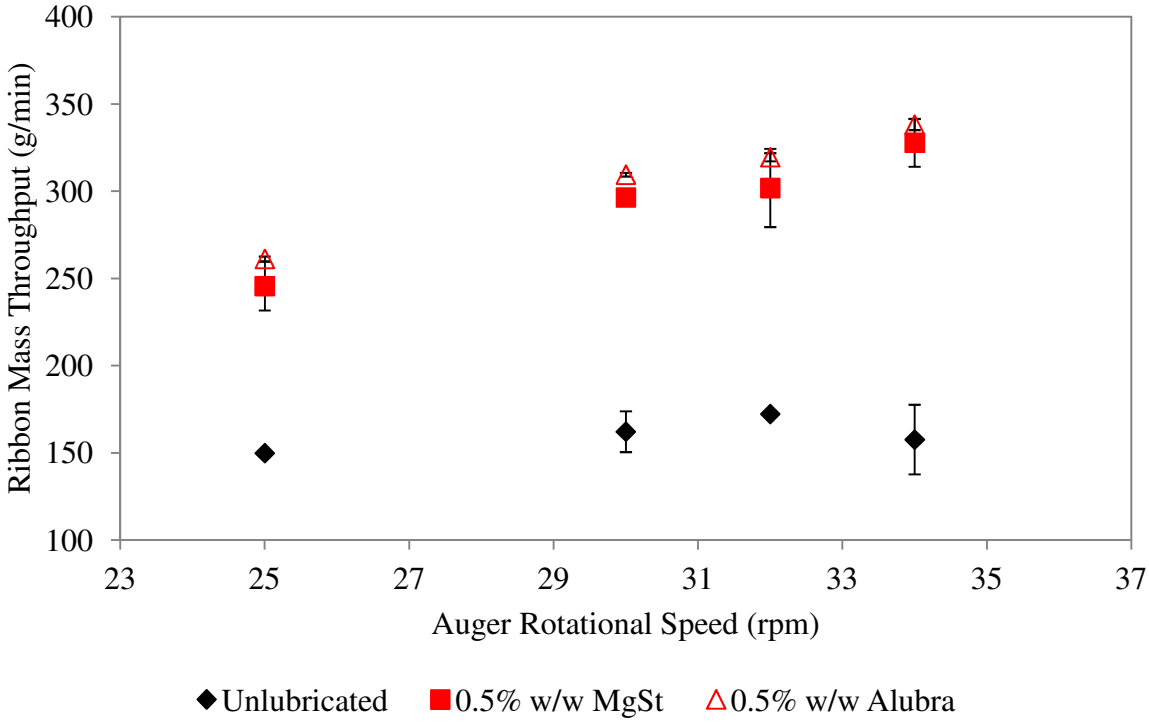


**Figure 6-6 – Roller compacted ribbon mass throughput (g/min) as a function of feed auger rotational speed (rpm) for ribbons manufactured using 0.5% w/w sodium stearyl fumarate (0.5% w/w magnesium stearate and unlubricated ribbons included for reference).**

As can be seen in Figure 6-7, the addition of sodium stearyl fumarate to the placebo formulation elicited a deleterious effect on the tensile strength of the roller compacted ribbons. Despite the reduction in ribbon tensile strength elicited by the inclusion of sodium

stearyl fumarate into the formulation the advantage is that it has previously been observed to have less impact on the dissolution rate of drug products from the solid dosage form product [Shah *et al.*, 1986].

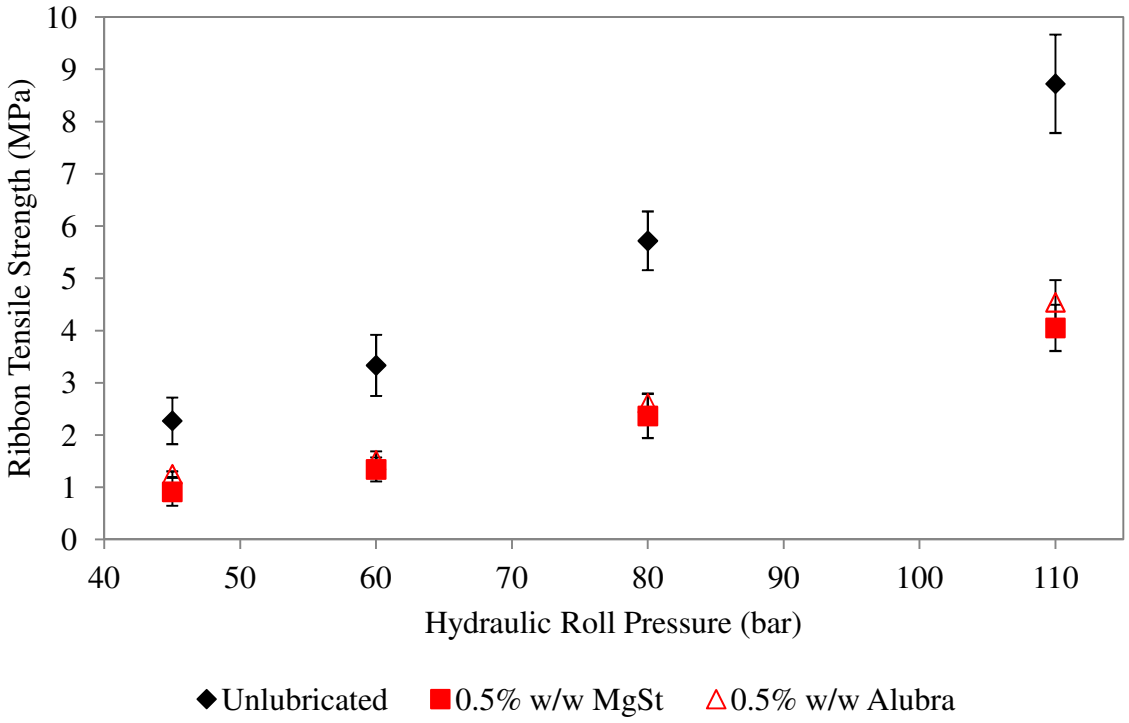


**Figure 6-7 – Ribbon tensile strength (MPa) as a function of hydraulic roll pressure (bar) for ribbons manufactured using 0.5% w/w sodium stearyl fumarate (0.5% w/w magnesium stearate and unlubricated ribbons included for reference).**

#### 6.3.1.3.2 Glyceryl monostearate

Roller compaction of the 'base' formulation using the roller compaction parameters detailed in Table 6-2 resulted in a ribbon mass throughput of 160 g/min and a roll gap of 2.2 mm with the formulation observed to adhere to the roll surface within one minute of start-up. Addition of 0.5 % w/w magnesium stearate to the formulation increases mass throughput to almost 300 g/min, the roll gap to 4.3 mm and prevents the formulation from adhering to the roll surface. A potential alternative lubricant; LubriTose™ MCC (Avicel 102 + 2 % w/w glyceryl monostearate) and LubriTose™ AN (lactose anhydrous + 4 % w/w glyceryl monostearate) has been investigated as an alternative formulation strategy to magnesium

stearate during roller compaction. To determine the effective limits, or the amount of LubriTose™ required in the 'base' formulation to increase mass throughput and prevent adhesion to the roll surface, the level was adjusted so that some portion of the normal Avicel 102 and lactose component was replaced with LubriTose™ MCC or LubriTose™ AN, the formulation compositions were detailed in Table 6-1. For the purposes of this initial study the suitability of LubriTose™ as a potential replacement for magnesium stearate during roller compaction was assessed on its ability to increase roller compacted ribbon mass throughput and to prevent the formulation from adhering to the roll surface as well as the properties of the final ribbon product.

As shown in Figure 6-8 and Figure 6-9, the sole addition of either LubriTose™ MCC or LubriTose™ AN results in an increase of roller compacted ribbon mass throughput and corresponding roll gap. Replacing 25 % of the Avicel 102 content with LubriTose™ MCC only resulted in a slight increase in mass throughput and corresponding roll gap. Further increasing the LubriTose™ MCC content of the formulation to 50 % caused a significant increase in ribbon mass throughput and corresponding roll gap, any subsequent addition of LubriTose™ MCC beyond this level caused no further increase. Adherence of the formulation to the roll surface was observed to occur when there was only 25 % of the Avicel 102 component replaced with LubriTose™ MCC. When replacing the lactose content of the formulation with LubriTose™ AN it was observed that the biggest increase in mass throughput and corresponding roll gap occurred between 0 and 25 %. Further addition of LubriTose™ AN above 25 % of the lactose content had relatively little influence on the mass throughput. Adherence to the roll surface did not occur at any of the levels investigated. The maximum mass throughput and corresponding roll gap was similar in both cases, however

replacing the Avicel 102 with MCC resulted in a slightly higher mass throughput than replacing the lactose with LubriTose™ AN.

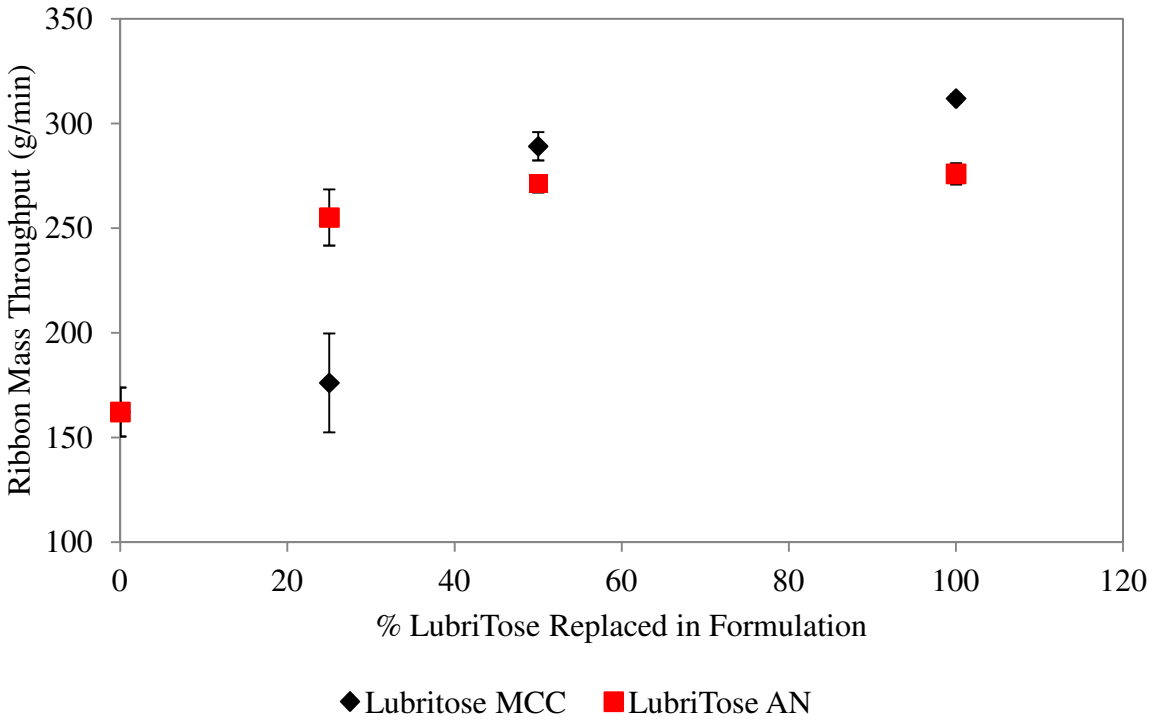


**Figure 6-8 - Roller compactor granule mass throughput with increasing level of LubriTose™ in the formulation.**

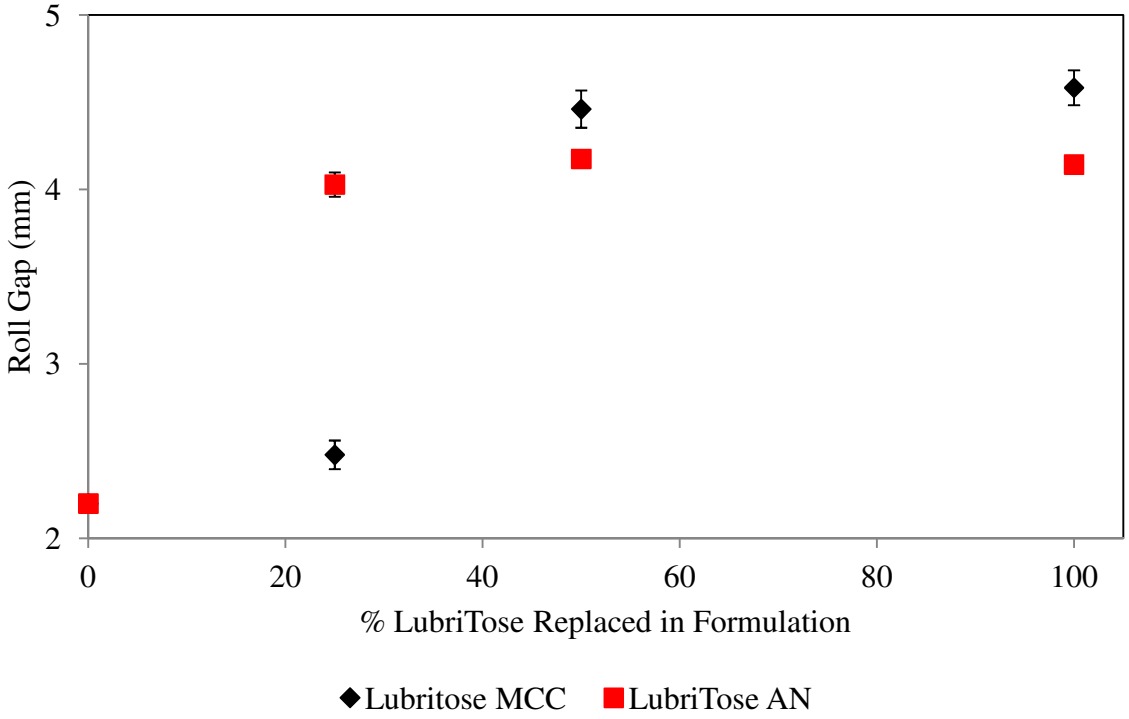


**Figure 6-9 – Roll gap as a function of percent of LubriTose™ replaced in the formulation.**

The greater increase in mass throughput for the LubriTose™ AN at 25 % compared to LubriTose™ MCC at 25 % was unexpected since there was a greater relative content of Avicel 102 in the formulation than lactose. However, LubriTose™ AN contains a 4 % w/w glyceryl monostearate whereas LubriTose™ MCC contains 2 % w/w glyceryl monostearate. The content of LubriTose™ AN/MCC in the formulation was converted to amount of glyceryl monostearate in the formulation using Equation 6-1.

$$M_{GMS} = xM_{LubriTose} \qquad \textbf{Equation 6-1}$$

where $M_{GMS}$ and $M_{LubriTose}$ are the mass of glyceryl monostearate and LubriTose™ (AN/MCC) in the formulation and x is the mass fraction of glyceryl monostearate in the LubriTose™ (x=0.02 and 0.04 for LubriTose™ MCC and LubriTose™ AN respectively).

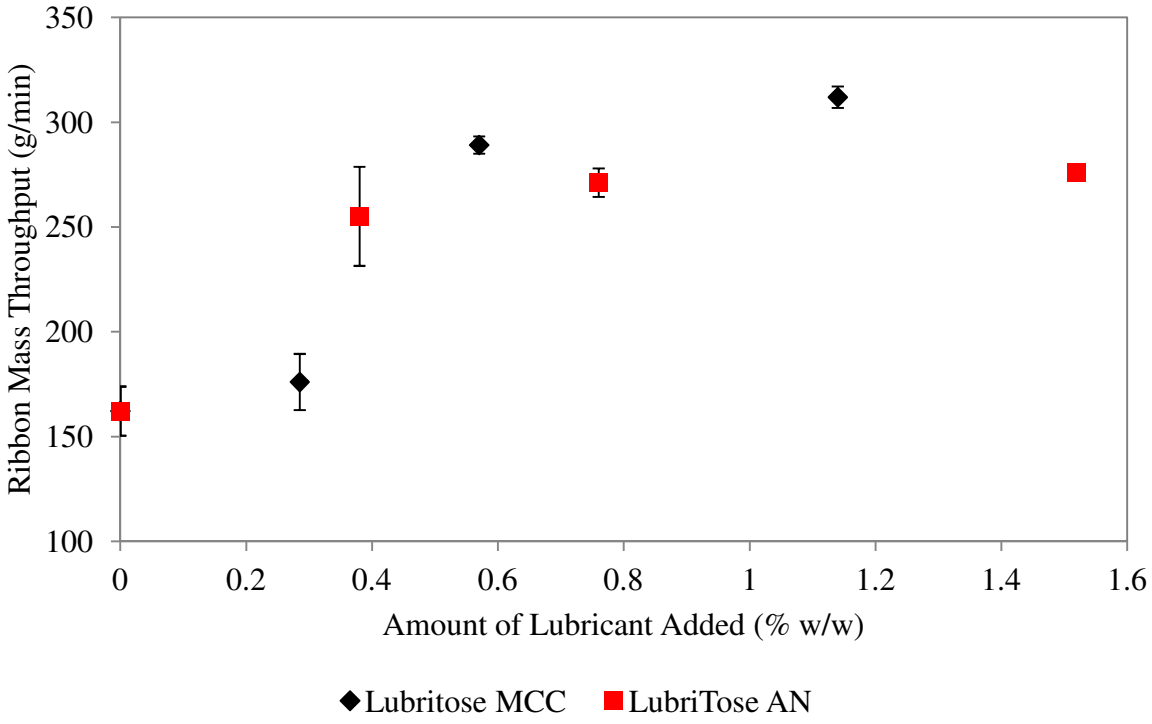


**Figure 6-10 - Increase in mass throughput as a function of total amount of lubricant in the blend.**

The plot of mass throughput vs. lubricant concentration in the formulation is shown in Figure 6-10; the data indicates that the improvement in mass throughput is dependent on the

amount of glyceryl monostearate in the formulation rather than the source (i.e. LubriTose™ AN or LubriTose™ MCC). The optimum level of lubricant appears to be around 0.5 % w/w. This is higher than the optimum level of magnesium stearate which is around 0.1 % w/w as shown previously in section 4.2.2.2.3.

Figure 6-11 shows the tensile strength of the roller compacted ribbons containing LubriTose™ AN and LubriTose™ MCC. The tensile strength of the roller compacted ribbons decreased with increasing levels of LubriTose™ MCC. At addition levels of 25 % LubriTose™ MCC the tensile strength is significantly higher than the corresponding tensile strength of roller compacted ribbons containing magnesium stearate. However, subsequent addition of LubriTose™ MCC resulted in a further decrease in ribbon tensile strength, below that of the corresponding ribbon manufactured using magnesium stearate. Addition of 25% LubriTose™ AN to the formulation resulted in a significant reduction in tensile strength (equivalent to corresponding ribbons manufactured using 0.5% w/w magnesium stearate); however, no further reduction in tensile strength was observed beyond this level of addition.

Overall, the LubriTose™ MCC had the greatest impact on the roller compacted ribbon tensile strength. As a predominately plastically deforming material, microcrystalline cellulose provides more compact strength than the brittle fracturing lactose portion of the formulation. However, it is well known that plastically deforming materials are more sensitive to the deleterious effects of lubricants due to the development of a layer of lubricant on the excipient surface which stays intact during compaction and subsequent deformation. The lubricant coating that exists on the surface of a brittle material such as lactose is disrupted when the excipient particles fracture during compaction resulting in the generation of lubricant free surfaces where stronger excipient-excipient bonds can form. Considering this mechanism it

can be hypothesized that as the portion of LubriTose™ MCC increases in the formulation, the primary inter-particle bonding which takes place would be lubricant coated microcrystalline cellulose-lactose as well as lactose-lactose, whereas when the LubriTose™ AN is increased in the formulation the lubricant film coating the lactose is disrupted allowing both the stronger microcrystalline cellulose-microcrystalline cellulose bonds as well as the microcrystalline cellulose-lactose bonds to dominate. As such the tensile strength of roller compacted ribbons containing LubriTose™ AN is less sensitive to the effects of the lubricant than roller compacted ribbons containing LubriTose™ MCC.

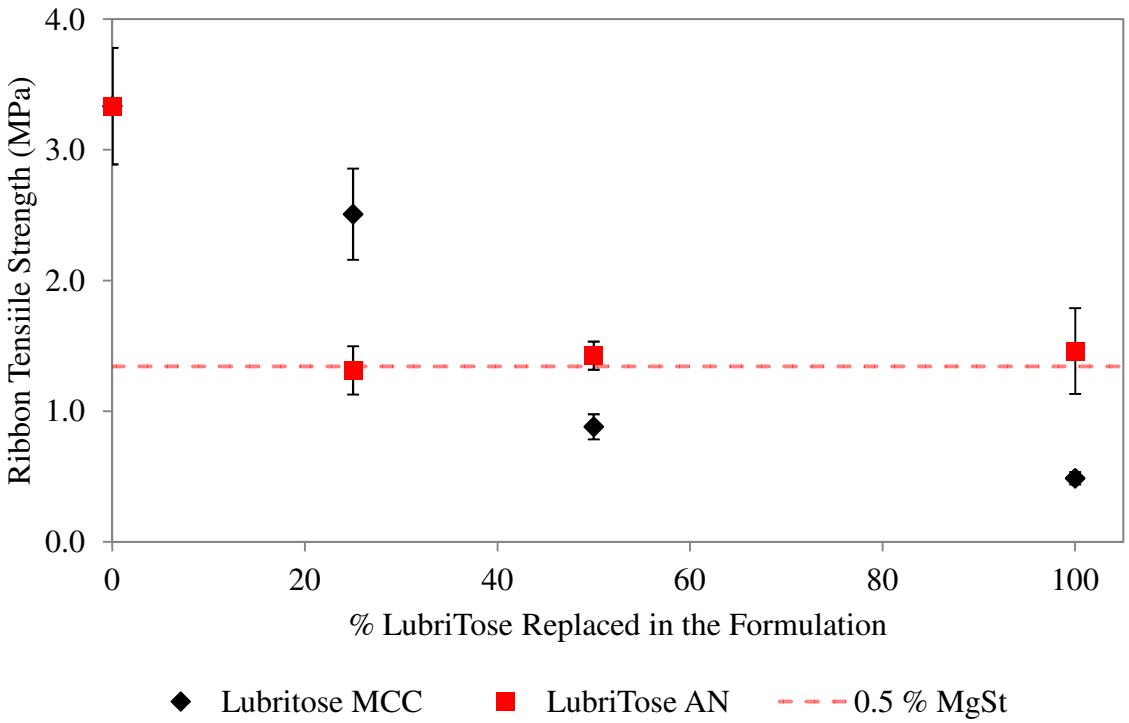


**Figure 6-11 – Ribbon tensile strength as a function of the percent of LubriTose AN or MCC replaced within the formulation (the dashed line shows the tensile strength of ribbons lubricated with 0.5% w/w magnesium stearate roller compacted at equivalent conditions).**

As seen previously, it can be observed (Figure 6-12) that the particle size distribution (D50) of the milled granules is correlated with the tensile strength of the ribbon compacts, where an increase in ribbon tensile strength elicits and increase in particle size. The particle

size reaches a plateau at a ribbon tensile strength of 2-2.5 MPa showing that an optimum tensile strength for roller compacted ribbons with respect to particle size exists. This observation is consistent with the data presented in Figure 6-5 which shows a similar trend whereby the granule size obtained from milling the roller compacted ribbons increases with ribbon tensile strength before reaching a plateau at around a ribbon tensile strength of 2.5 MPa.

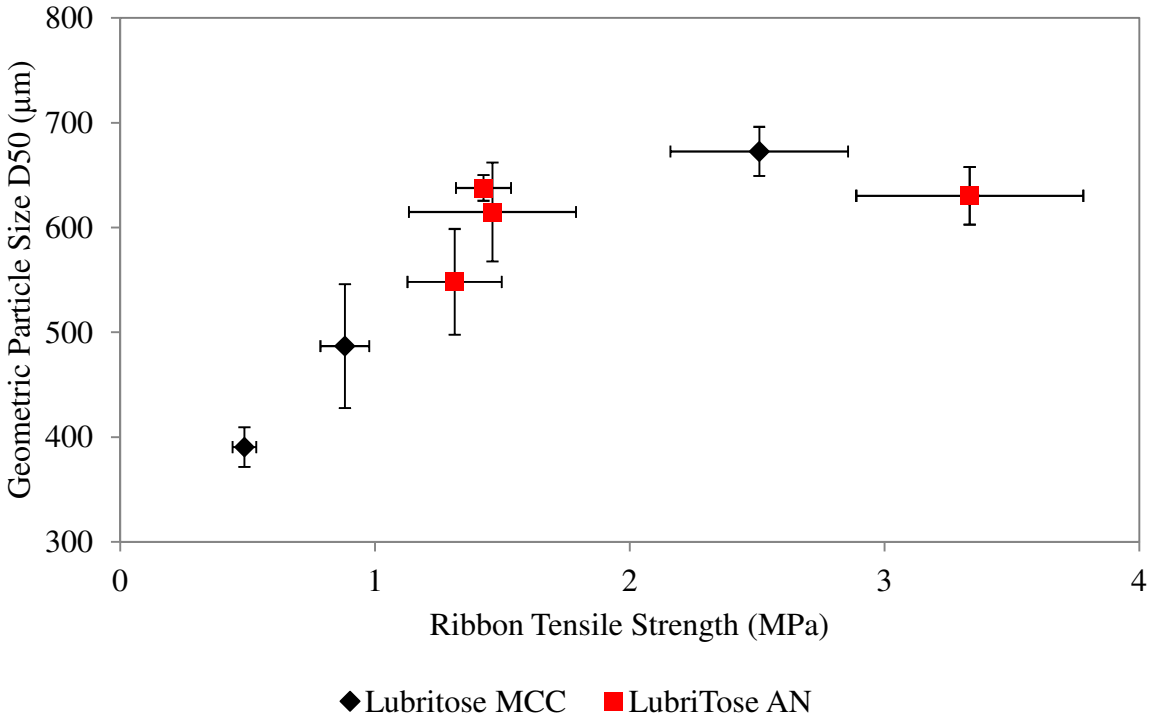


**Figure 6-12 – Particle size (D50) as a function of the roller compacted ribbon tensile strength.**

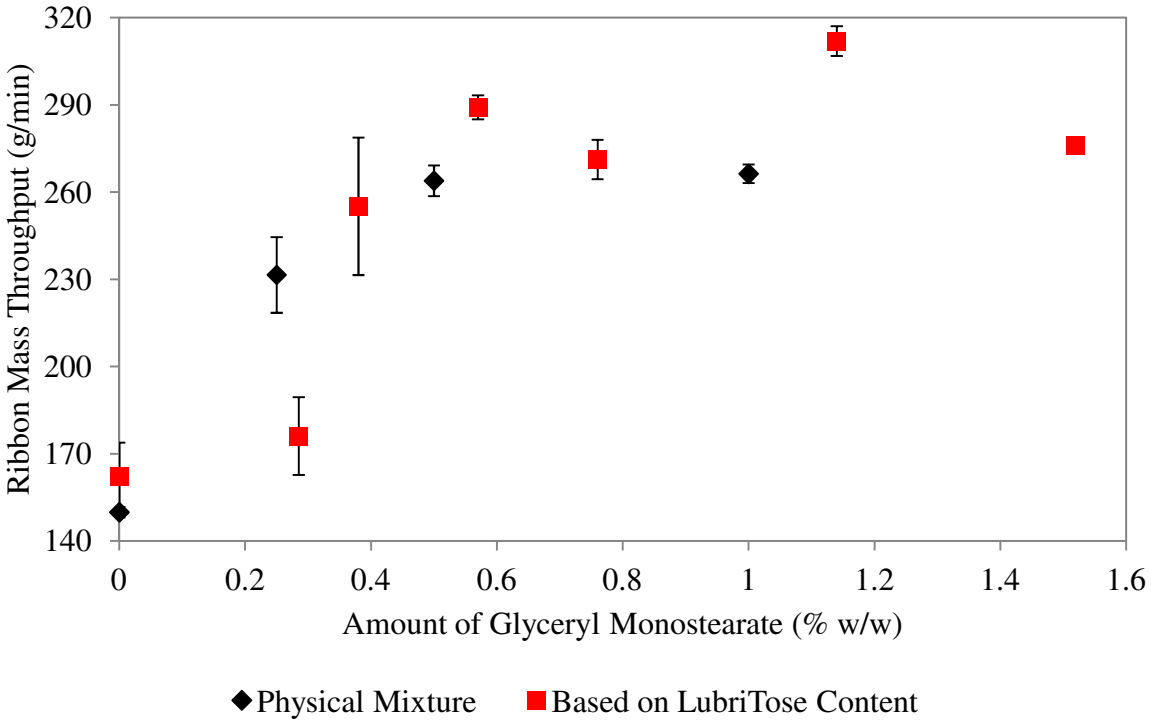


**Figure 6-13 – Comparison of the roller compactor ribbon throughput as a function of amount of glyceryl monostearate (% w/w) added to the formulation.**

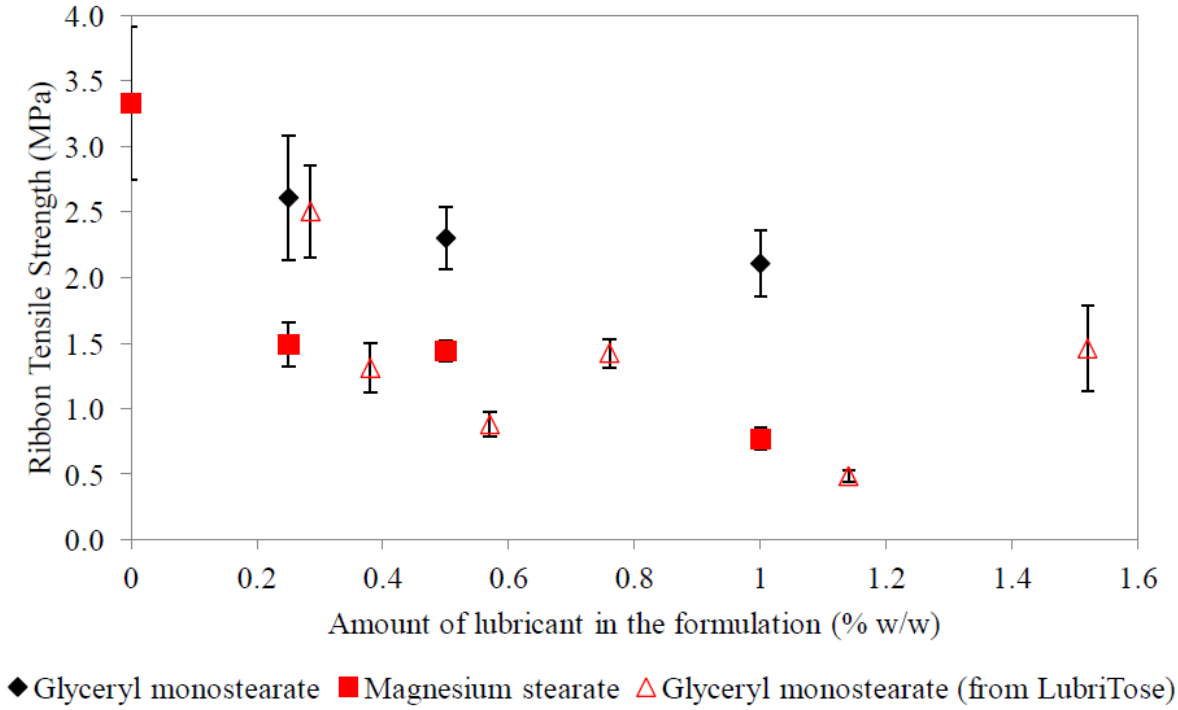


**Figure 6-14 – Ribbon tensile strength of roller compacted ribbons lubricated with either magnesium stearate, a physical mixture with glyceryl monostearate and LubriTose™ (amount of glyceryl monostearate in blend calculated based on LubriTose content.**

In order to compare the lubrication efficacy of the co-processed LubriTose™ material to that of a physical mixture of glyceryl monostearate, roller compaction was performed using the base formulation described in Table 6-1 with the addition of glyceryl monostearate at a concentration of 0.25, 0.5 and 1.0% w/w. It was observed (Figure 6-13) that at a low level of addition the physical mixture of the glyceryl monostearate had more of a beneficial effect on increasing the mass throughput of roller compacted ribbons, however, at higher levels of addition using the co-processed LubriTose™ led to the biggest increase in roller compaction mass throughput.

### 6.3.2 Mixing sensitivity

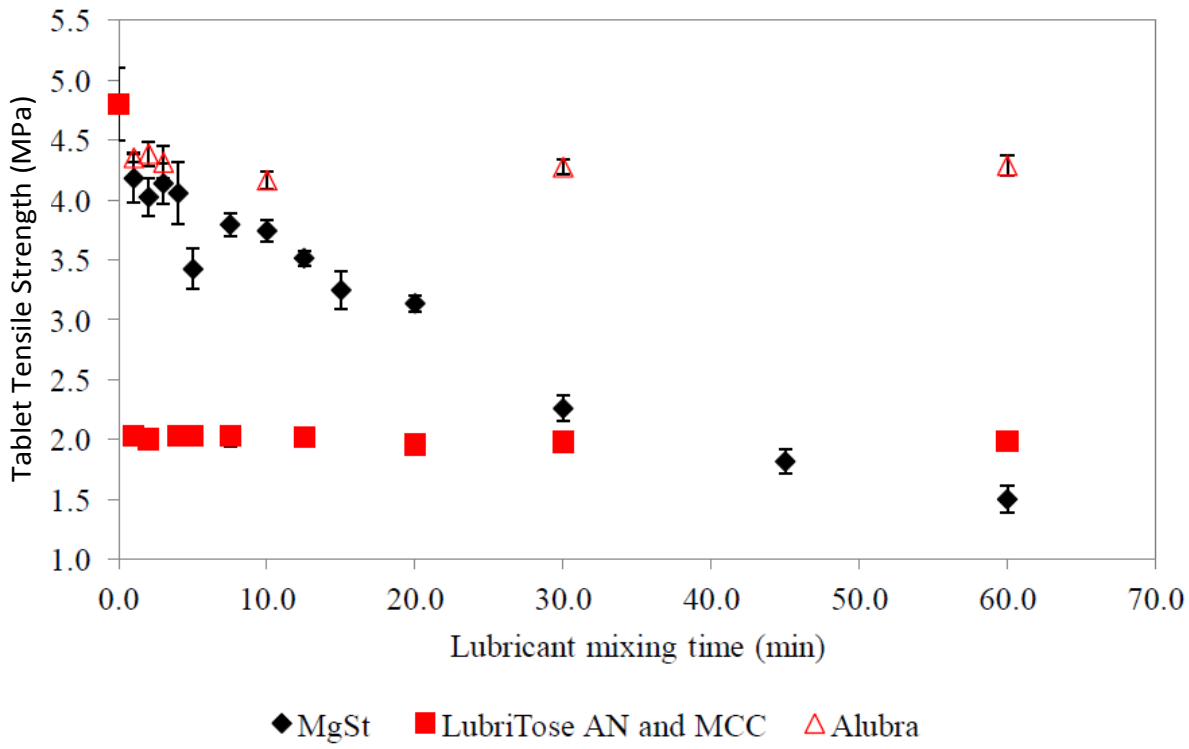


**Figure 6-15 – Mixing sensitivity of placebo formulation lubricated using different lubricants and formulation strategies.**

As discussed in section 2.2.3, a disadvantage of using magnesium stearate as a lubricant during pharmaceutical manufacturing is that its effect on tablet properties such as

tensile strength and disintegration/dissolution is dependent on the duration and intensity of mixing [Kushner IV and Moore, 2010]. The effect of mixing time on the tensile strength of the placebo formulation used in this study is shown in Figure 6-15; as expected it can be observed that the measured tablet tensile decreases with increasing mixing time with magnesium stearate. However, the use of sodium stearyl fumarate as a lubricant appears to have less of an effect on the tablet tensile strength, furthermore there is no mixing sensitivity observed for the sodium stearyl fumarate lubricant. The same is observed when using the LubriTose formulation, however, the tablet tensile strength is significantly lower even after very short blending times.

### 6.3.3 Atenolol formulations

#### 6.3.3.1 Roller compaction

Roller compaction of the Atenolol formulations was carried out at the following process conditions; screw speed = 30 rpm, roll speed = 3.4 rpm, hydraulic roll pressure = 60 bar and roll surface = knurled-knurled. The roller compaction performance of the formulations was assessed by mass throughput (g/min), roll gap (mm), pressure distribution efficiency ratio and observations on sticking to the roll surface. Ribbon tensile strength testing was not possible for the formulations containing above 10% w/w drug loading due to the ribbon splitting along its width.

##### 6.3.3.1.1 Mass throughput

The roller compacted ribbon mass throughput is shown in Figure 6-16, it was observed that sodium stearyl fumarate and magnesium stearate elicited an equivalent effect on the flow properties of the formulation through the auger feeder of the roller compactor at all drug

loads. However, the use of LubriTose™ AN and MCC as lubricants has less of an effect on the improvement of flow properties through the feed auger.

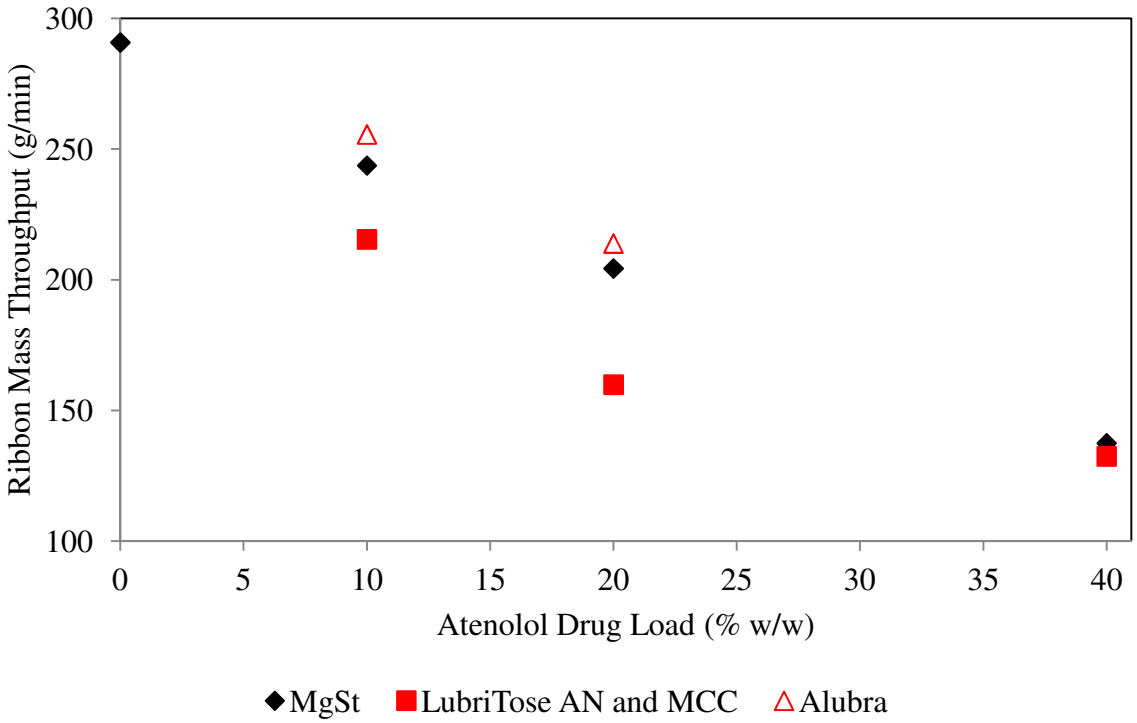


**Figure 6-16 – Roller compacted ribbon mass throughput as a function of Atenolol drug load (% w/w).**

#### 6.3.3.1.2 Pressure distribution efficiency ratio

The pressure distribution efficiency ratios during roller compaction of the Atenolol formulations are shown in Figure 6-17 and Figure 6-18. It can be seen that the lubricating ability of LubriTose™ AN and MCC is comparable to magnesium stearate in terms of its ability to reduce the pressure differential across the width of the ribbon; however at the 10% drug loading level sodium stearyl fumarate was observed to exhibit more favourable lubricating properties. At the 10 % drug load with a both mixing times of 7 and 60 minutes there was no significant difference between the pressure distribution ratio of the formulations containing magnesium stearate or LubriTose AN and MCC. However, the formulation containing the sodium stearyl fumarate as a lubricant had a significantly higher pressure

distribution ratio demonstrating that sodium stearyl fumarate is more able to accommodate the velocity distribution that exists at the equipment surfaces. Increasing the drug loading to 20% w/w elicited a reduction in pressure distribution for all formulations suggesting that a more incomplete lubricant film was developed around the drug and excipient particles. Conversely, at a drug loading of 40% the pressure distribution was observed to increase.

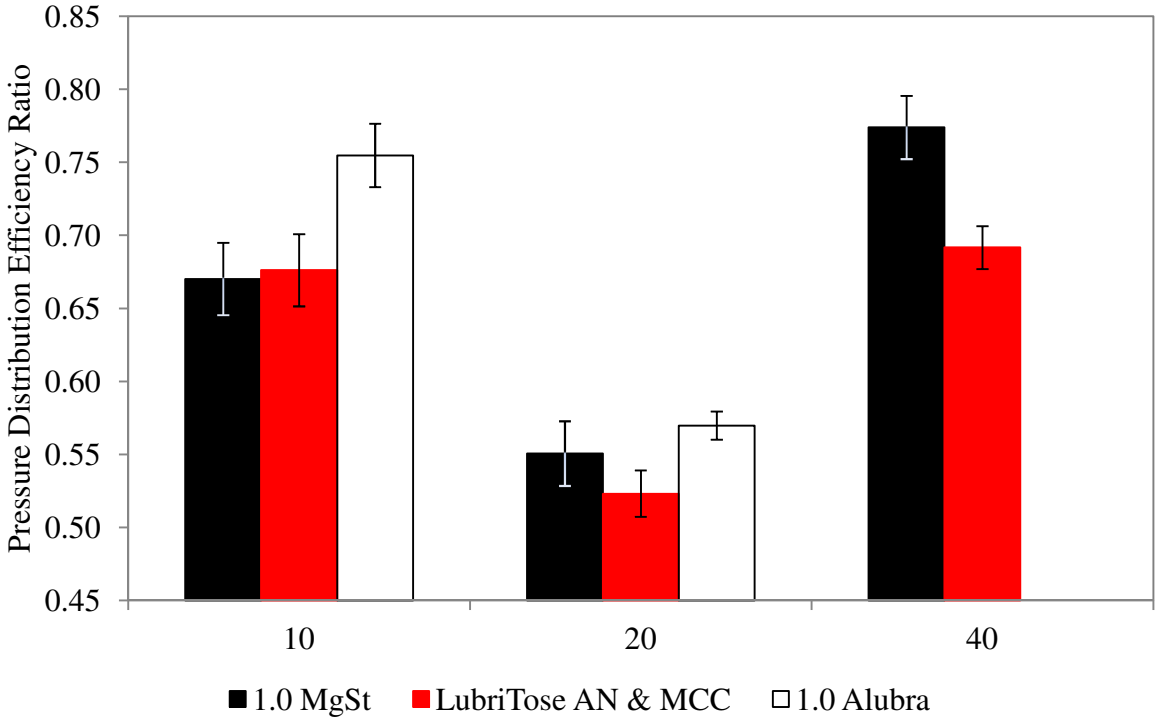


**Figure 6-17 – Pressure distribution efficiency ratio as a function of Atenolol drug load (% w/w) for formulations mixed at 7 minutes (10 minutes for LubriTose™ AN and MCC).**

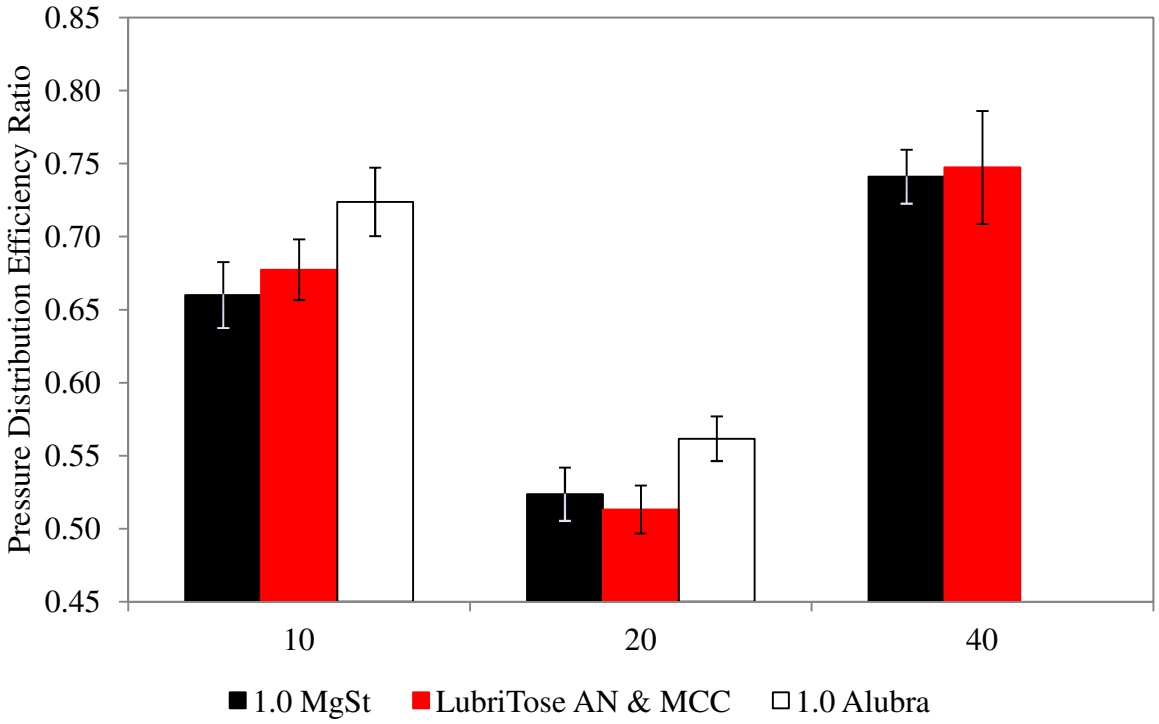


**Figure 6-18 – Pressure distribution efficiency ratio as a function of Atenolol drug load (% w/w) for formulations mixed at 60 minutes.**

#### 6.3.3.1.3 Observations on powder adhesion to the roll surface

Of the formulations used in this study, adhesion to the roll surface was only prevented at the 10% w/w drug load; none of the formulations used in this investigation had sufficient lubricant levels to completely prevent the adhesion of powder to the roll surface at drug levels of 20 and 40% w/w, however, adhesion of powder formulation to the roll surface was observed to be limited to the spaces within the knurled structure of the roll surface as shown in Figure 6-19. The anti-adhesive properties of the formulations containing either LubriTose™ AN and MCC were comparable to those of the formulations containing magnesium stearate or sodium stearyl fumarate. As observed by the decrease in the pressure distribution ratio at a 20% w/w drug loading the amount of lubricant in the formulation is insufficient to develop a complete surface coating on the drug and excipient surfaces due to the high surface area available. The prevention of adhesion at industrially relevant drug

loading would require increasing amounts of lubricant. The need for excessively high levels of lubricants would make Atenolol an ideal candidate for the use of the external lubrication during roller compaction and subsequent tabletting, particularly in light of the fact that rapid drug release is an essential property of Atenolol tablets.

**Figure 6-19 – representative image of the roll surface after roller compaction of the 40% w/w Atenolol drug load formulations with either 1.0% w/w magnesium stearate or LubriTose AN and MCC.**

### 6.3.3.2 Tablet manufacturing

Tablets were manufactured to a solid fraction of 0.85 with a press weight of 400 mg on a single station hand filled tablet press. Compression force, punch displacement and ejection forces were automatically recorded during tablet compression by the tablet press software. No statistically significant differences were recorded for the compression forces of the different lubricants, however, less force was required to achieve equivalent solid fractions at higher drug loads, suggesting that increasing the drug load in the formulation changes the compressibility/compactability of the formulation.

As a general rule for tablet manufacture the force required ejecting the tablet from the tablet die (ejection force) should be no greater than 10-15% of the main compression force. For example if the main compression force of a tablet is 6000 N then the ejection force should

be no more than 600-900 N. Tablets with ejection forces that exceed this value would require further investigate into the formulation (*i.e.* lubricant levels) or into the position of the tablet in the tablet die (ejection force can be influenced by the relative position of the tablet in the die; the closer to the top of the die the lower the overall ejection force). The ejection forces for the 20% Atenolol drug load tablets compressed using the roller compacted granules (without the addition of external lubrication) are shown in Figure 6-20 and Figure 6-21 for the (pre-roller compacted blend) lubricant mixing times of 7 minutes and 60 minutes respectively. It can be observed that the ejection forces of the tablets lubricated with magnesium stearate are notably higher than the tablets containing sodium stearyl fumarate, which are in turn notably higher than the ejection forces of the tablets containing LubriTose™ AN and MCC.

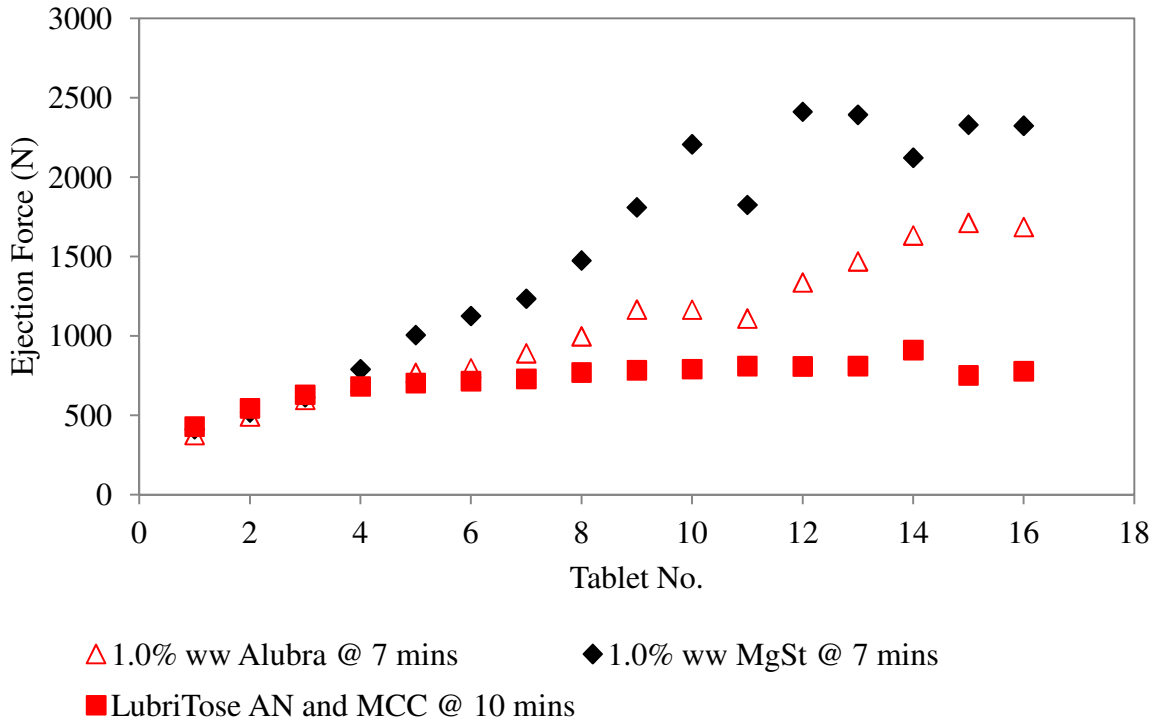


**Figure 6-20 – Ejection force (daN) of tablets compressed to 0.85 solid fraction as a function of tablet number, data is shown for the 20 % drug load at 7 minutes mixing (10 minutes for the LubriTose™ An and MCC formulations).**

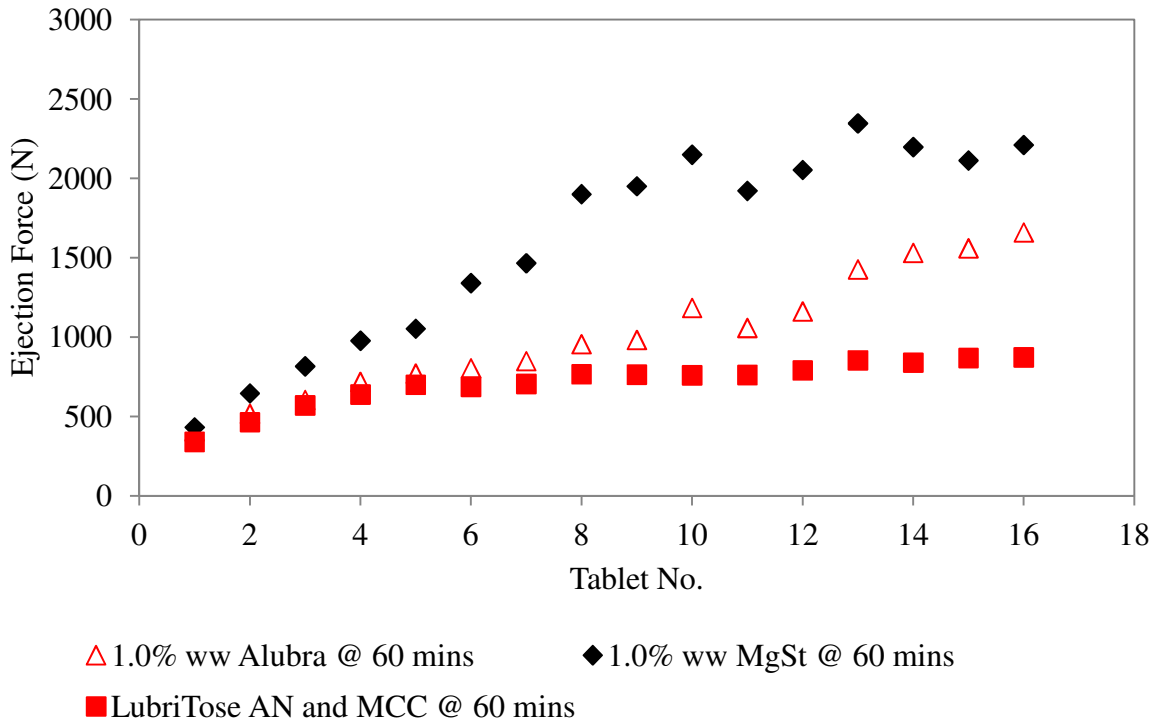


**Figure 6-21 – Ejection force (daN) of tablets compressed to 0.85 solid fraction as a function of tablet number, data is shown for the 20 % drug load at 60 minutes mixing.**

The increase in ejection force for the as-is collected roller compacted granule (granule with no additional extra-granular excipients) compared to that of the initial lubricated pre-blend powder was calculated using Equation 6-2:

$$\frac{E_{f(granule)} - E_{f(Pre-blend)}}{E_{f(Pre-blend)}} \times 100\% \qquad \textbf{Equation 6-2}$$

The % increase in ejection force for the formulations at a drug load of 20% w/w Atenolol at 7 and 60 minutes are shown in Figure 6-22 and Figure 6-23 respectively. It can be observed that granules containing inter-granular magnesium stearate exhibit significantly increased tablet ejection forces compared to the initial lubricated pre-blend powder. In contrast the granule containing LubriTose™ AN and MCC show much smaller increase in ejection forces compared to the initial pre-blend powder. Furthermore it was observed that the tablets manufactured from the granules containing magnesium stearate showed signs of

capping and tablet fracture upon ejection. The percent increase in ejection force for the formulations lubricated using sodium stearyl fumarate is less than that for the magnesium stearate formulations but higher than those of the LubriTose™ formulations. Typical dry granulation process routes require three separate blending stages – (1) initial API blending stage; (2) inter-granular lubrication blending stage, and; (3) extra-granular lubrication blending stage. The ejection forces of the tablets compressed from the roller compacted (as-is) granules containing LubriTose™ AN and MCC do not show the same increase in ejection force exhibited by the tablets compressed from roller compacted granule containing magnesium stearate and sodium stearyl fumarate. As such, there is an indication that roller compacted granule containing LubriTose™ AN and MCC may not need extra-granular lubrication. A potential hypothesis for this observation is based on the location of the lubricant. In the formulations containing magnesium stearate or sodium stearyl fumarate, due to the high surface area of the drug product, there is an incomplete film coating on both the excipient and drug particle surfaces, as such the stronger interaction bonds between lubricant free surfaces are developed during roller compaction. As a consequence the granule surface will have some proportion of unlubricated surface due to some of the lubricant being located within the granule itself. In the case of LubriTose™ AN and MCC the lubricant layer coating the excipient particles is more complete, since the lubricant is fixed at the surface of the excipient particles less lubricant is available for coating the high surface area of the drug particles. As such, the compacted ribbon will have relatively fewer of the strong interaction bonds between lubricant free excipient surfaces. Upon milling the ribbon will break at the interface between the lubricated excipients particles whilst the relatively unlubricated drug product is contained within the granule. As such the surface of the granule will be relatively

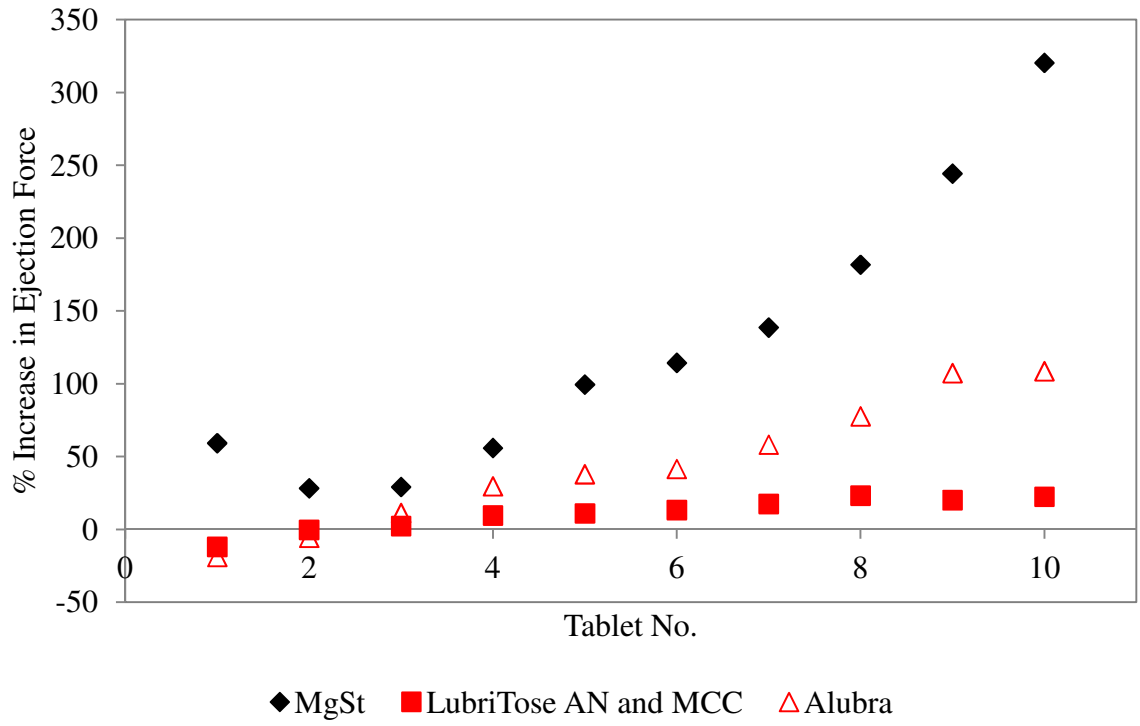


**Figure 6-22 – Percent increase in ejection force of tablets compressed to 0.85 solid fraction as a function of tablet number, data is shown for the 20 % drug load at 7 minutes mixing (10 minutes for the LubriTose™ An and MCC formulations).**

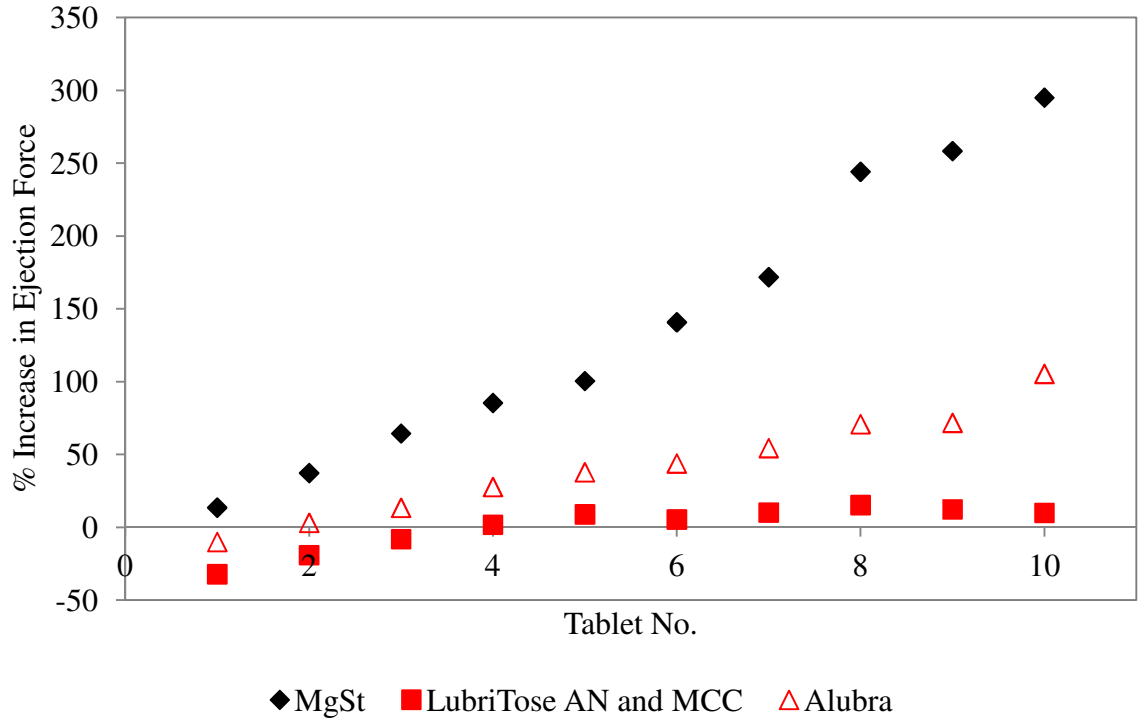


**Figure 6-23 – Percent increase in ejection force of tablets compressed to 0.85 solid fraction as a function of tablet number, data is shown for the 20 % drug load at 60 minutes mixing.**

more lubricated than that of the granules lubricated with magnesium stearate or sodium stearyl fumarate.

#### 6.3.3.3 Tablet properties

##### 6.3.3.3.1 Tablet hardness

Tablet hardness is usually expressed as tensile strength with units of MPa; when developing a tablet for a commercial product it is important that the tablet possess sufficient strength such that it can withstand further processes such as coating and packaging, as well as any handling conditions imposed by the patient. On the other hand, manufacturing a tablet product with exceptionally high strength can be detrimental to the disintegrating properties. As a general rule a formulated tablet should have a tensile strength greater than 2 MPa.

The tablet hardness of tablets compressed using the initial raw powder (at both mixing times) was measured in terms of tensile strength. The lubricant mixing sensitivity ratio was calculated using Equation 6-3;

$$\frac{\sigma_{@\ 7\ mins} - \sigma_{@\ 60\ mins}}{\sigma_{@\ 7\ mins}} \qquad \textbf{Equation 6-3}$$

Where $\sigma_{@\ 7\ \mathrm{mins}}$ and $\sigma_{@\ 60\ \mathrm{mins}}$ are the tablet tensile strength at 7 and 60 minutes respectively.

Tablet tensile strength is shown in Figure 6-24 and Figure 6-25 for the pre-blend formulation mixed at 7 and 60 minutes respectively. It can be observed that tablets lubricated with LubriTose™ AN and MCC have a significantly lower tablet tensile strength than tablets lubricated with magnesium stearate or sodium stearyl fumarate at low mixing times. However as the mixing time is increased the tablet tensile strength of the tablets lubricated with

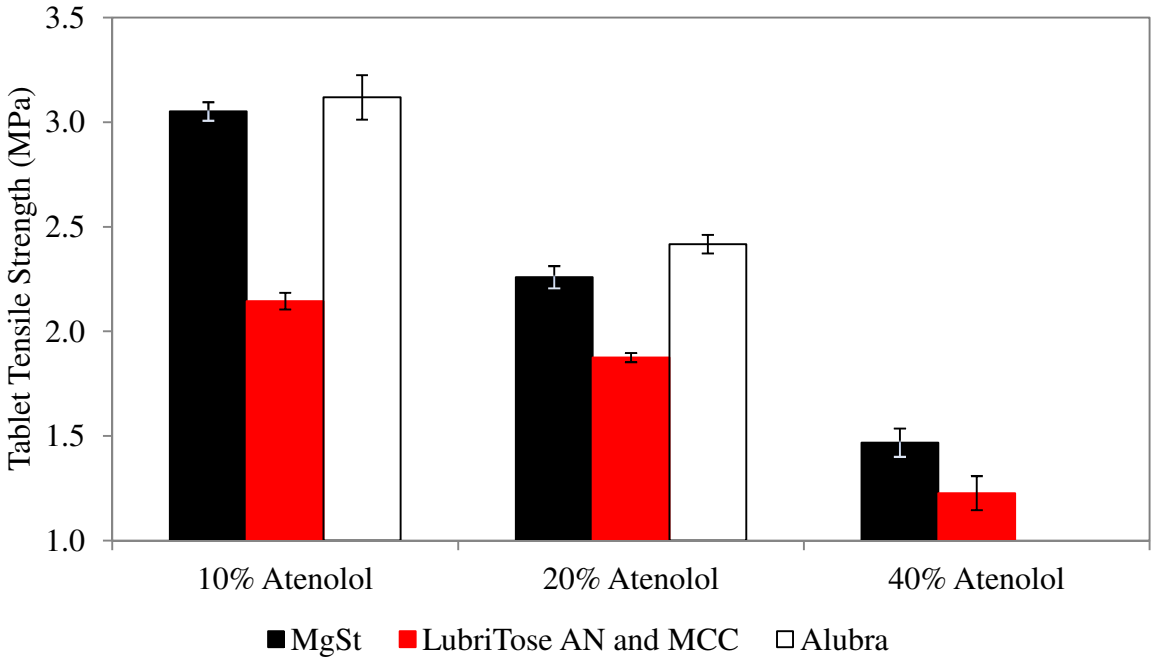


**Figure 6-24 – Tablet tensile strength (MPa) as a function of drug loading (% w/w) and lubricant type at a mixing time of 7 minutes (10 minutes for LubriTose™ AN and MCC formulations).**

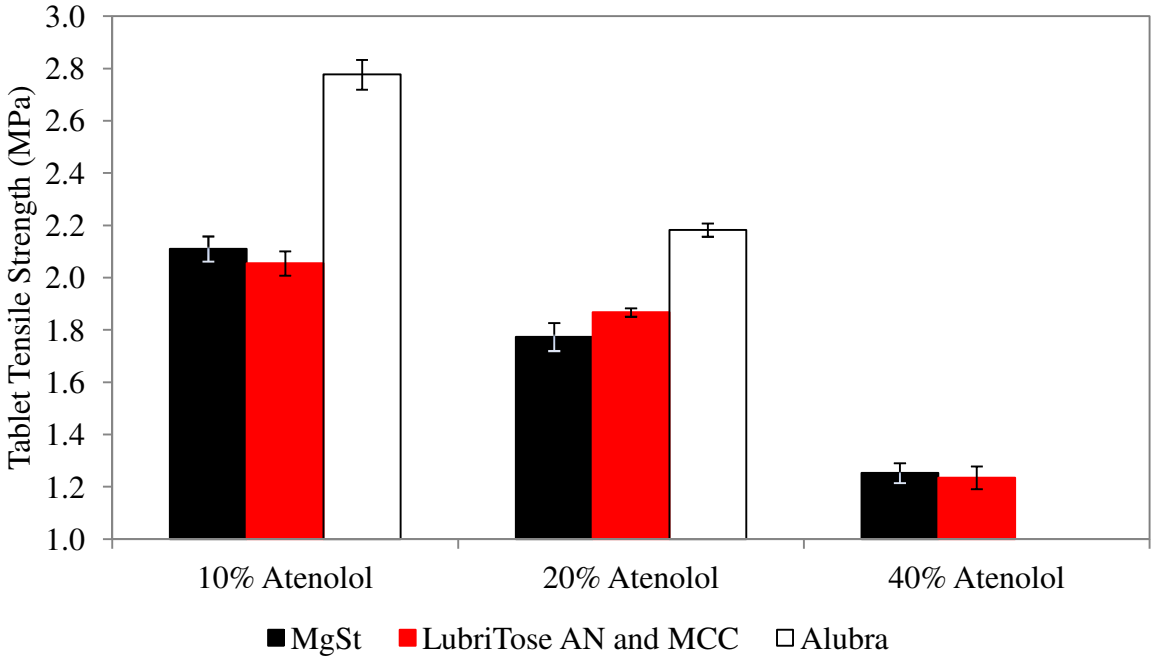


**Figure 6-25 – Tablet tensile strength (MPa) as a function of drug loading (% w/w) and lubricant type at a mixing time of 60 minutes.**

magnesium stearate is equivalent to the LubriTose AN and MCC tablets. At a mixing time of 60 minutes the tablets lubricated with sodium stearyl fumarate have the highest tablet tensile strength.

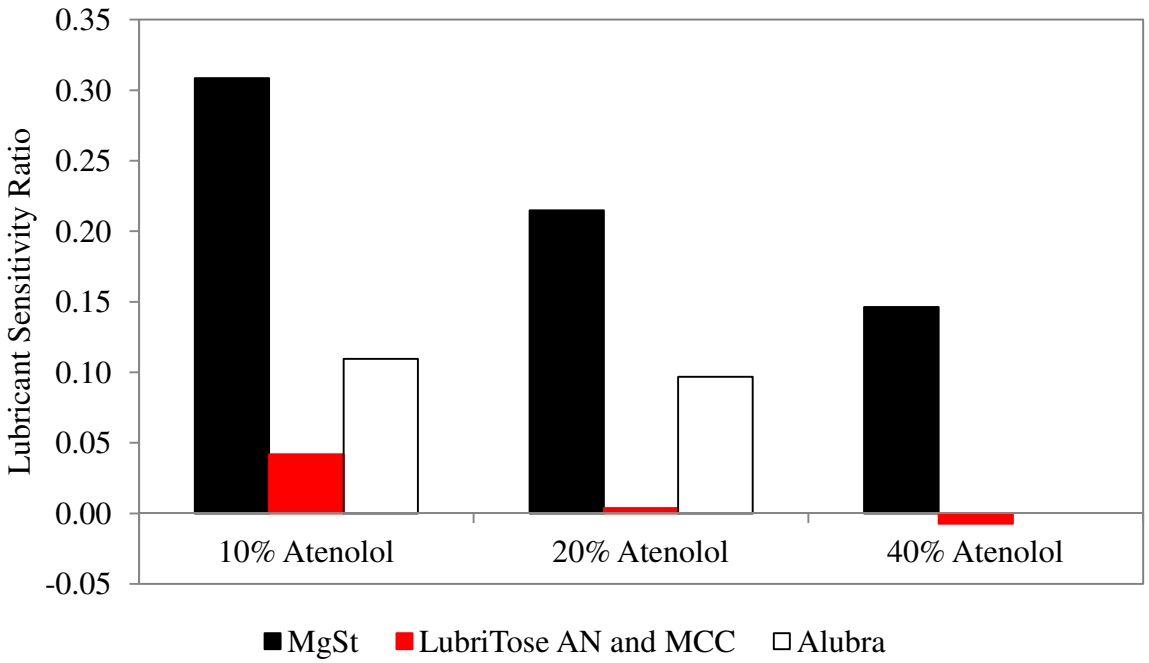


**Figure 6-26 – Lubricant sensitivity ratio as a function of drug loading (% w/w) and lubricant type.**

The lubricant mixing sensitivity ratio is shown in Figure 6-26; it can be observed that magnesium stearate tablets are most sensitive to changes in mixing time followed by sodium stearyl fumarate. However, the tablets lubricated with LubriTose™ AN and MCC are insensitive to the lubricant mixing time. These observations are consistent with the hypothesis presented in section 6.3.3.2. In the co-processed LubriTose™ product, the lubricant is fixed at the surface of the excipient particles and so increasing the mixing time has a negligible effect on the distribution of the lubricant throughout the formulation. However, because a relatively uniform and complete surface coverage of lubricant at the excipient surfaces exists the development of the stronger excipient-excipient bonds are prevented. As such a tablet with lower tablet tensile strength is produced. In the case of lubrication with magnesium stearate, a more incomplete surface coverage is achieved due to the high surface area of atenolol, as such the stronger excipient-excipient bonds can prevail. However, upon prolonged mixing the magnesium stearate agglomerates are broken up allowing the lubricant to spread further

through the blend achieving a more complete surface coverage. The same is true for the tablets containing sodium stearyl fumarate, however, the tablet tensile strength is less affected by the presence of sodium stearyl fumarate.

#### 6.3.3.3.2 Dissolution performance

Tablet dissolution is shown in Figure 6-27 and Figure 6-28 for the tablets compacted from the roller compacted (as-is) granule blended for 7 minutes and 60 minutes respectively. It can be observed that the hydrophilic lubricant sodium stearyl fumarate has the least effect on the drug dissolution profile, followed by magnesium stearate whilst the LubriTose™ AN and MCC formulation had the biggest deleterious effect on the dissolution profile. Furthermore, it was also observed that the formulations containing the magnesium stearate as a lubricant showed a sensitivity to the mixing time.

In this study the granules were used as-is, as such there was no extra-granular lubricant added to the formulation. This was to determine the effect of pre-roller compaction lubrication on the final properties of the tablets. One would expect that the addition of extra-granular lubricants would have a significant effect on the dissolution profiles of the tablets. Considering the hypothesis presented above it is expected that granules containing LubriTose™ AN and MCC will have a more complete lubricant coating than granule lubricated from magnesium stearate and sodium stearyl fumarate. As such the ingress of water in the tablets containing LubriTose™ AN and MCC will be inhibited to a greater degree than those lubricated with magnesium stearate and sodium stearyl fumarate.

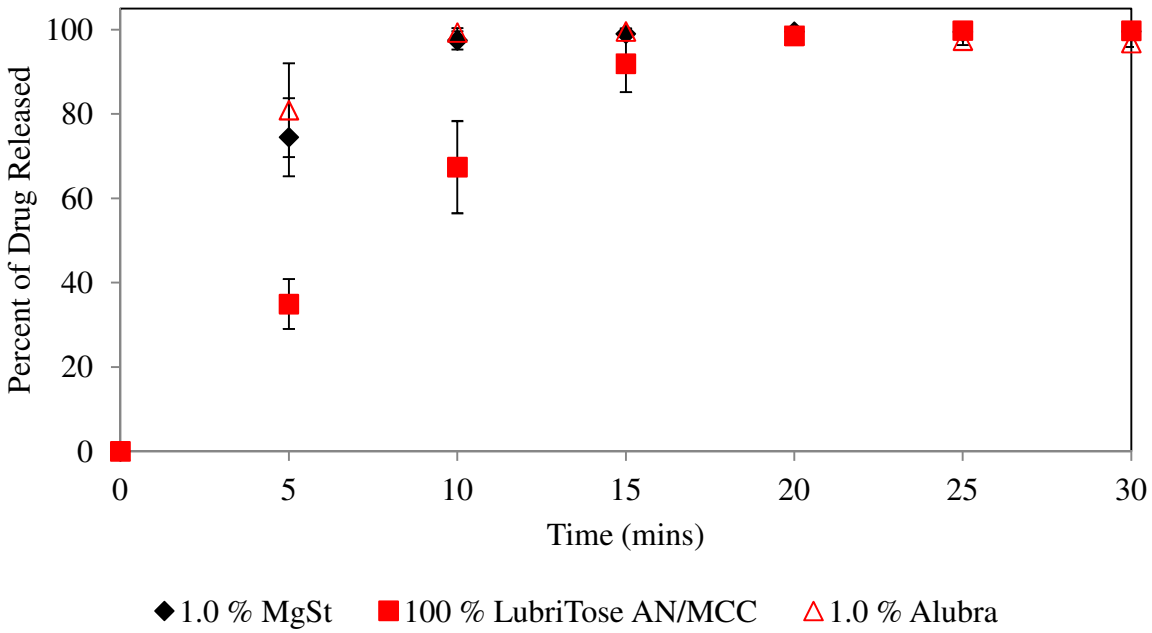


**Figure 6-27 – Percent of drug released as a function of time (minutes), data shown is for the 10% w/w drug load mixed for 7 minutes (10 minutes for the LubriTose™ AN/MCC formulation).**

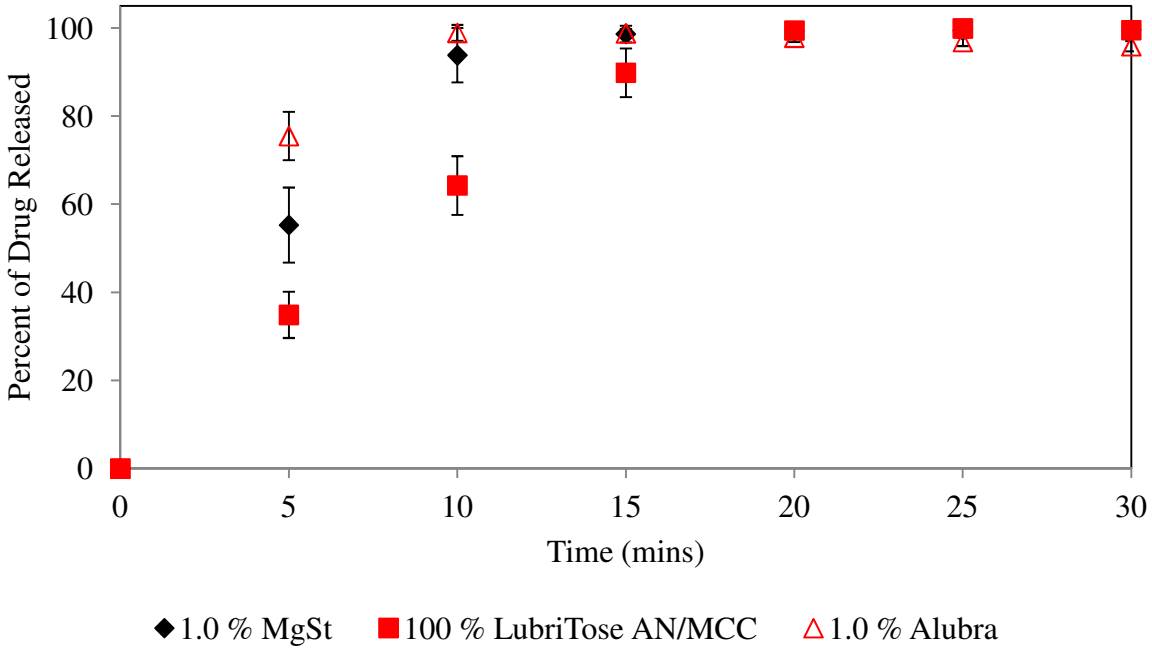


**Figure 6-28 – Percent of drug released as a function of time (minutes), data shown is for the 10% w/w drug load mixed for 7 minutes (10 minutes for the LubriTose™ AN/MCC formulation).**

## 6.4 Conclusion

### 6.4.1 Placebo formulations

The roller compaction performance of a placebo formulation containing microcrystalline cellulose, lactose anhydrous and croscarmellose sodium lubricated with various excipients has been investigated. The results from previous chapters have shown that the inclusion of magnesium stearate into the formulation has a beneficial effect on the flow properties of the formulation through the roller compactor feed auger. This beneficial effect is not observed when a flow aid, colloidal silica, is used within the formulation suggesting that the improvement in flow properties is inherent to the properties of the lubricant. The increase in roller compacted ribbon mass throughput was achieved with the other lubricants used in this investigation. An essential function of a lubricant is its ability to accommodate the velocity distributions at the equipment surfaces, in roller compaction this can be assessed by using the pressure distribution efficiency ratio, defined as the difference between the pressures recorded at the edges of the roll surface versus the pressure at the centre of the roll. The alternative lubricants used in this study were found to be equivalent to magnesium stearate with respect to their ability to reduce the pressure differential that exists across the roll surface.

It has been observed that all lubricants used in this investigation had a similar effect on the ribbon tensile strength to magnesium stearate, which in turn had an effect on the particle size distribution of the final granule. The granule particle size was observed to increase with increase in the ribbon tensile strength; however, to achieve this ribbon with higher solid fraction was required. To produce a ribbon with higher solid fraction requires higher pressure

at the roller compaction stage which may be detrimental to the recompressibility of the granule product.

### 6.4.2 Atenolol formulations

The roller compaction and tabletting performance of an active formulation containing 10, 20 and 40 % w/w Atenolol lubricated with either magnesium stearate, sodium stearyl fumarate or a co-processed excipient known commercially as LubriTose™ MCC and LubriTose™ AN has been investigated. At the 10% w/w Atenolol drug loading no adhesion to the roll surface was observed, however at levels above 10% w/w it was observed that none of the formulations had sufficient anti-adhesive properties to completely prevent the adhesion of powder to the roll surface. The powder adhesion was, however, limited to the spaces between the knurls on the roll surface; furthermore the anti-adhesive performance of the LubriTose™ AN/MCC was comparable to magnesium stearate and sodium stearyl fumarate. However, the disadvantage of using LubriTose™ AN and MCC as a lubricant in this formulation, and indeed co-processed materials in general, is that the level of lubricant is fixed and cannot be increased further, as such the prevention of adhesion of the formulation to the roll surface would require the addition of other lubricants to the formulation.

The anti-friction performance of the three lubricants was assessed by their ability to reduce the pressure differential that exists across the roll width. It was observed that there was no significant difference in the pressure differential across the roll surface for formulations containing LubriTose™ AN/MCC or 1.0 % w/w magnesium stearate, however, sodium stearyl fumarate was observed to show more favourable lubricating properties. An advantage of the LubriTose™ AN/MCC over the sodium stearyl fumarate and magnesium stearate formulations was its ability to retain its lubricating properties post roller compaction. Ejection

forces of tablets compacted from the roller compacted granule containing magnesium stearate were significantly higher than the measured ejection forces of the initial pre-blend powder (> 40 % increase). However, the granules containing LubriTose™ AN/MCC showed a much smaller increase in ejection force (< 4 %). A typical dry granulation process route, which utilizes magnesium stearate as a lubricant, requires three distinct blending stages – an initial API blending step followed by a lubrication blending step prior to roller compaction and a finally an extra-granular lubrication blending step prior to tabletting. Due to the insensitivity to mixing and retention of lubricating properties post roller compaction exhibited by formulations utilizing LubriTose™ AN/MCC as a lubricant the number of blending stages could be reduced to one, whereby all formulation excipients are added simultaneously; this would need to be the subject of further work.

The Atenolol dissolution profiles showed that sodium stearyl fumarate had the least effect on reducing drug release rate followed by magnesium stearate then LubriTose™ AN and MCC. However, in this investigation no extra-granular lubricants were used in the tablets; as such further increasing the levels of lubricant in the tablet product is likely to have an effect on the drug release rate. Furthermore, due to the adhesive properties of Atenolol, even at the high levels of lubricant used in this study the adhesion of the formulation to the roll surface was not prevented. As such more lubricant would be required for the roller compaction stage, which would have a further effect on the drug release profiles.

Due to its highly adhesive nature the successful manufacture of Atenolol requires high lubricant loading which is likely to have a detrimental effect on the rate of drug release. Since an essential property of Atenolol is rapid drug release rate, it would provide an interesting

drug product to study the effect of the external lubrication during both roller compaction and tabletting.

# CHAPTER 7

# PROCESS DEVELOPMENT AND OPTIMISATION USING SURROGATE ACTIVE PHARMACEUTICAL INGREDIENTS

# CHAPTER 7

# PROCESS DEVELOPMENT AND OPTIMISATION USING SURROGATE ACTIVE PHARMACEUTICAL INGREDIENTS

## 7.1 Preface

The work in this chapter is part of a BMS initiative on "surrogate" API's. This concept is being developed within BMS as a means of substituting API's in a process (e.g. when a material is scarce) but still learning about potential process conditions and outcomes for the scarce material.

The concept is being developed as part of an initiative within BMS, led by Dr Admassu Abebe.

The work in this chapter has been carried out as follows:

1) The selection of API's by "similarity scoring" was carried out by the project team, using metrics developed by Dr. Ana Ferreira and other supporting information;

2) The selection of process route to investigate, drug levels and formulation to be tested was developed by the project team;

3) The DoE plan was developed by Dr Jim Bergum and the project team;

4) Piramal (India) did the formulation work, gathered process data and collected in process and end of process data. Additional testing was carried out by the project team;

5) The data was collated by the project team.

The work in this chapter consists of data analysis of the raw data provided by the team, with context provided after discussion with the team.

The interpretation of the data, which has been shared with the team, is based on evaluation of the data provided for this work package. The team is also working on other work packages (including "dissimilar" API's, and alternative loading levels) to get a fuller picture of the value of the surrogate API context so final conclusions may be different from what is included here.

## 7.2 Introduction

The work investigated in this chapter deviates from the main body of work, but falls within the remit of formulation challenges encountered during the development of a tablet product. The work picks up on the secondary strand of research questions presented in Figure 1-1

As discussed in section 2.5 roller compaction formulation design and optimisation is a material and time intensive process driven mostly by design of experiment and trial and error based approaches. A significant challenge, therefore, is presented when developing a process and formulation for a newly developed API which is likely to be both in short supply/high demand and costly to manufacture. Mechanistic and computational modelling has previously been used to overcome these issues with limited success. A relatively unexplored area of

research is the initiative investigated here whereby a different API which is sufficiently similar in its material properties can be used as a surrogate for the investigational API. As introduced in section 2.5.4, assessment for surrogacy is based on similarity scoring of physical/chemical parameters considered to be critical to material performance. The surrogate API should ideally be a material which is held in large amounts and from a project which is no longer under development. The potential advantages of the surrogate API initiative are as follows;

(1) If the proof-of-concept is successful, the use of surrogate material will be a viable strategy to support accelerated drug product development by removing constraints related to the shortage of drug substance.

(2) Reduction in the required amount of investigation API during development and in addition makes use of an otherwise un-needed material from a project no longer in development.

(3) Successful application of a surrogate material can provide a like for like comparison of the actual process; as such post development the formulation design and roller compaction process parameters optimised for the surrogate material can be substituted directly for processing of the investigational API. This is a particular advantage over the mechanistic and computional modelling techniques where a significant amount of roller compaction process parameter setting work would be required post development

(4) Furthermore if successful the surrogate API project could be used to develop a database of optimised roller compaction settings and formulation design for APIs with different material properties. As such any API under development which exhibits similar material properties to those contained within the database can take

advantage of pre-optimised formulation and process parameters potentially reducing the amount of work required during development.

Two API lots (BMS-562247 and BMS-770767, hereafter referred to as API 1 and API 2 were chosen for surrogacy based on their similarities in specific surface area and particle size. Each API lot was subjected to roller compaction using a specified design of experiments (DoE) using roll gap and roll pressure as the factors. A third API (BMS-663068-03, hereafter referred to as API 3) was subjected to roller compaction using the same DoE. The third API was used as a dissimilar API, and as such the chosen properties (specific surface area and particle size) were significantly different to that of API 1 (and hence API 2). The hypothesis to be tested for each section was;

Section (1) – Similar APIs

- Null hypothesis ($H_0$): the roller compaction performance of the two formulations (API 1 and API 2) is different
- Alternative hypothesis ($H_1$): the roller compaction performance of the two formulations (API 1 and API 2) is the same

Section (2) – dissimilar APIs

- Null hypothesis ($H_0$): the roller compaction behaviour of the two formulations (API 1 and API 3) is the same
- Alternative hypothesis ($H_1$): the roller compaction behaviour of the two formulations (API 1 and API 3) is different

The importance of testing the hypothesis for the dissimilar API is to confirm the validity of the alternative hypothesis ($H_1$) stated for the similar API. Each formulation has a

drug loading of 10 % w/w, rejecting the null hypothesis ($H_0$) from both section (1) and (2) would help validate the applicability of surrogate APIs since it would confirm that the roller compaction performance observed for each formulation is not due to formulation excipients having the greatest impact on roller compaction performance.

## 7.3 Method

### 7.3.1 Manufacturing process

**Table 7-1 – Formulations (10 % w/w drug loading)**

| Ingredients | Grade Used | Category | % w/w |
|---|---|---|---|
| Intra-Granular Materials | | | |
| API | N/A | Active | 10.00 |
| Microcrystalline Cellulose | Avicel PH 102 | Diluent | 37.25 |
| Anhydrous Lactose | NF DT | Diluent | 46.50 |
| Croscarmellose Sodium | Ac-Di-Sol | Disintegrant | 2.00 |
| Silicon Dioxide | Syloid 244 | Glidant | 1.00 |
| Magnesium Stearate | USP NF | Lubricant | 0.75 |
| Extra-Granular Materials | | | |
| Croscarmellose Sodium | Ac-Di-Sol | Disintegrant | 2.00 |
| Magnesium Stearate | USP NF | Lubricant | 0.50 |
| Total | | | 100.0 |

The manufacturing and post manufacturing testing was undertaken by Piramal Healthcare (Piramal Pharmaceutical Development Services Pvt. Ltd., Ahmedabad, India). This section describes the background information required to understand the manufacturing process. Each formulation contained identical excipients and quantities as shown in Table 7-1, each formulation was 750 g. The manufacturing process route was as follows.

#### 7.3.1.1 Pre-blend

The API and all inter-granular excipients (except magnesium stearate) were added to a 3 L bin blender and tumble blended for 20 minutes at 20 rpm. The blended material was then passed through a Quadro Comil using a flat impeller blade rotating at a speed of 3,250 rpm

and a 0.6 mm screen. The formulation was then re-blended in the 3 L bin blender with the inclusion of magnesium stearate at a rotational speed of 20 rpm for 5 minutes.

#### 7.3.1.2 Roller compaction

Each API formulation was roller compacted using an Alexanderwerk WP 120 roller compactor (Alexanderwerk, Remscheid, Germany). The roller compaction conditions; roll pressure and roll gap were used in this investigation as the DoE factors. For clarity the experimental design is shown in Figure 7-1 and Table 7-2, and the complete list of experiments performed is given in Table 7-3. The roll surface used was a combination of a smooth upper roll and a knurled lower roll. The roll speed was fixed at a rotational speed of 8 rpm, whilst the screw speed was automatically adjusted to accommodate the specified roll gap by operating the Alexanderwerk WP120 in roll gap control mode. As such unlike in previous chapters the screw speed used in this study was a dependent variable. The roller compacted ribbon was broken up in the mill chamber using an upper screen of 3.15 mm and a lower screen of 1.0 mm at a rotary speed of 80 rpm.

**Table 7-2 - DoE factors**

| | **Actual (uncoded) Units** | | **Experimental (coded) units** | |
|---|---|---|---|---|
| **API** | **Hydraulic Roll Pressure (Bar)** | **Roll Gap (mm)** | **Hydraulic Roll Pressure** | **Roll Gap** |
| API 1 | 40 (L) | 2.0 (L) | -1.0 | -1.0 |
| API 2 | 55 (C) | 2.3 (C) | 0.2 | 0.0 |
| API 3 | 65 (H) | 2.6 (H) | 1.0 | 1.0 |

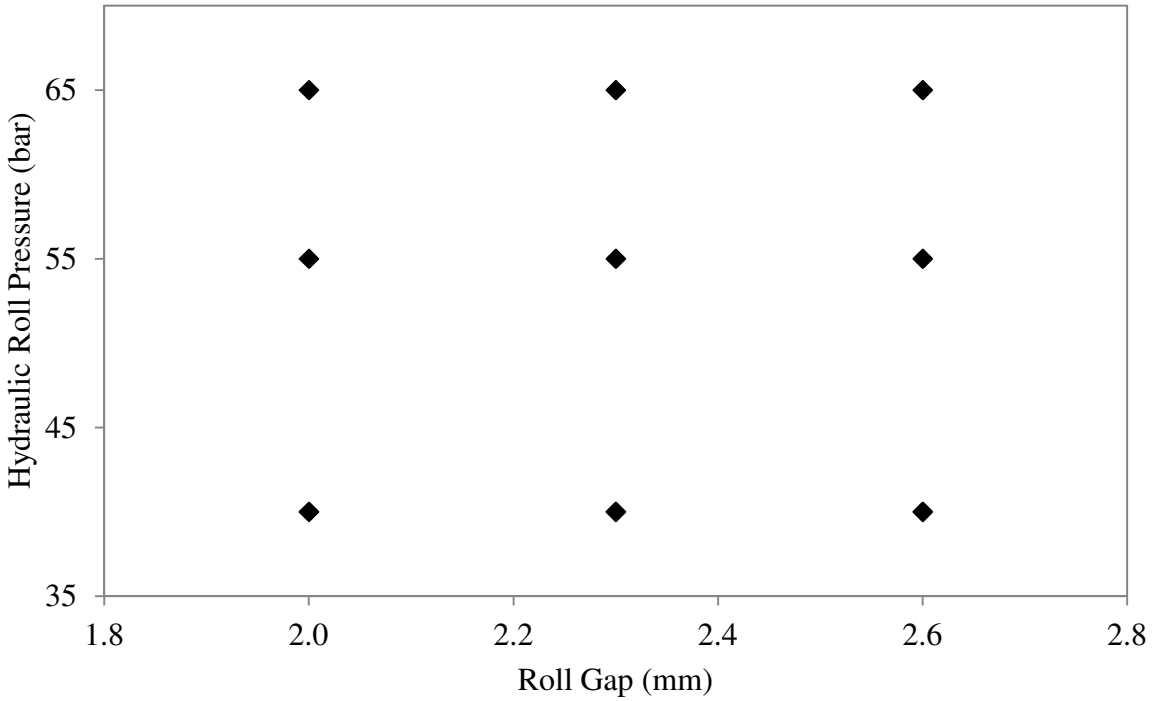


**Figure 7-1 – Roller compact DoE.**

**Table 7-3 – Roller compaction conditions studied arranged in standard order, actual experiments were completed in random order (centre points at standard order 5 were done in triplicate)**

| Standard Order | Roll Pressure (bar) | Roll Gap (mm) |
|---|---|---|
| 1 | 40 | 2.0 |
| 2 | 55 | 2.0 |
| 3 | 65 | 2.0 |
| 4 | 40 | 2.3 |
| 5 | 55 | 2.3 |
| 6 | 65 | 2.3 |
| 7 | 40 | 2.6 |
| 8 | 55 | 2.6 |
| 9 | 65 | 2.6 |

#### 7.3.1.3 Final blend

The granules collected from the roller compactor were blended with the extra-granular excipients using another two step blending processes where the croscarmellose sodium was first blended using a Contra-blender bin for 20 minutes at 20 rpm. The granules were then blended for a further 5 minutes at 20 rpm following the addition of magnesium stearate.

#### 7.3.1.4 Tablet compression

Tablet compression was performed on a Korsch XL100, using flat faced round punches 5.55 mm in diameter. The turret was operated at a rotational speed of either 30 or 40 rpm to control the tablet weight at 95-105 mg. The aim of the tablet press operation was to produce tablets of approximately 11 SCU (approximately 77 N) for each of the formulations containing API 1, API 2 and API 3.

#### 7.3.1.5 Testing plan

The responses measured during this investigation are shown in Table 7-4.

### 7.3.2 Statistical analysis

#### 7.3.2.1 Analysis of variance and response surface analysis

Assessment for surrogacy was based on API 1; as such the hypothesis for section 1 was assessed between API 1 and API 2, whilst the hypothesis for section 2 was assessed between API 1 and API 3. Two statistical methods were used to test the surrogacy hypothesis;

(1) Analysis of Variance (ANOVA) to determine if there are any statistical differences between the roller compaction performance of the two API lots based on the response data
(2) Response surface and regression analysis to determine if the DoE factors impact the key quality attributes in a statistically similar/dissimilar manner

The statistical techniques used in Chapter 7 are routine techniques and further information can be obtained from most statistical text books for example: [Armstrong and James, 1996].

The statistical analysis was interpreted using a combination of MiniTab statistical software and Microsoft Excel.

**Table 7-4 - Measured response variables**

| Stage of Process | Response Variable |
|---|---|
| Powder properties (Initial Blend) | Discharge from blender |
| | Bulk Density |
| | Mass flow rate |
| | Cohesivity / Shear |
| | Absolute Density |
| Roller Compaction | Screw Speed (rpm) |
| | Vacuum |
| | Average Mass Throughput (g/min) |
| | Ribbon Envelope Density |
| | Ribbon Dimensions |
| | Ribbon Tensile strength |
| | Ribbon Quality |
| Granule Properties (final blend) | Particle Size Distribution / %fines* |
| | Particle Size Distribution / %fines* |
| | Bulk Density |
| | Tap Density |
| | Mass flow rate & Angle of Repose |
| Compression Characteristics | Main Compression Force (kN) |
| | Pre-compression Force (kN) |
| | Ejection Force (N) |
| | Disk Speed |
| | Fill Depth |
| Tablet Properties | Tablet Thickness (mm) |
| | Tablet Weight (mg) |
| | Tablet Hardness (SCU) |
| | Disintegration Time (mins) |
| | Friability (%) |
| | Moisture (% w/w) |
| | Content Uniformity |

***** Fine material is considered to be any particles less than 100 μm size

#### 7.3.2.2 Sensitivity analysis

It can be seen from Table 7-2 that the conditions used for roll pressure, *i.e.* 40 bar, 55 bar, and 65 bar, is not strictly an orthogonal experimental design since the centre point is slightly off centre (the true centre would be 52.5 bar). The implication of this deviation in the experimental design was investigated by using a sensitivity analysis. The sensitivity analysis was conducted using two methods;

1) The confidence intervals of the model coefficients obtained from the regression model using the actual centre points (55 bar) were compared with the confidence intervals of the model coefficients obtained from the regression model using the true centre points (52.5 bar) (using the same set of response data)
2) Random noise (between ± 10%) was added to the predicted response data generated from the regression model using the actual centre points; a regression model was derived from the new data points and the model coefficients of the noise data was compared to the model coefficients of the actual data. 200 regression models were derived using this method. The random noise was generated using the following excel function, Equation 7-1:

$$x_n \times \left(1 + \left(\frac{RANDBETWEEN(-10,10)}{100}\right)\right) \qquad \textbf{Equation 7-1}$$

Where $x_n$ is a predicted data point calculated using a regression model, and the excel function RANDBETWEEN(-10,10) generates a random number between -10 and 10.

## 7.4 Results

### 7.4.1 Similar APIs (API 1 vs. API 2 at 10 % drug load)

#### 7.4.1.1 Analysis of variance (ANOVA)

The ANOVA calculated F-values for the output parameters comparing the mean response of API 1 with API 2 (black bars) and API 1 with API 3 (red bars) are given in Figure 7-2. It can be observed from the calculated F-values that there are no significant differences between the mean response of API 1 compared to the mean response of API 2 for the majority of parameters measured (*i.e.* most of the F-value are below the significance line).

In contrast, the calculated F-value comparing the dissimilar APIs show that for a number of the measured parameters the mean response for API 1 was calculated to be significantly different to the mean response for API 3.

The calculated F-values which show significant differences between the mean response of API 1 vs. API 2 and API 1 vs. API 3 are summarised in Table 7-5. The parameters with statistical differences between the mean responses are investigated further in the following sections.

**Table 7-5 - Output parameters with statistically significant differences (From ANOVA calculated F ratio), (-) indicates that there were no significant differences between the response for the two API lots.**

| | Confidence level | | Mean Value | | |
|---|---|---|---|---|---|
| Parameter | API 1 vs. API 2 | API 1 vs. API 3 | API 1 | API 2 | API 3 |
| Screw Speed | - | 95 % | 50.7 | 51.4 | 56.5 |
| Vacuum | - | 99 % | -0.76 | -0.77 | -0.67 |
| Envelope Density (g/ml) | 90 % | - | 1.16 | 1.21 | 1.20 |
| Ribbon Tensile Strength (MPa) | 90 % | - | 1.67 | 1.29 | 2.13 |
| Tap Density (g/ml) | 95 % | - | 0.817 | 0.833 | 0.827 |
| Carr's Index (-) | 95 % | 95 % | 19.6 | 22.8 | 22.3 |
| Angle of Repose (°) | - | 99 % | 37.7 | 37.2 | 39.9 |
| Percent Retained Sieve 40 | - | 99 % | 32.3 | 32.0 | 35.1 |
| Percent Retained Sieve 80 | - | 99 % | 7.7 | 8.0 | 6.5 |
| Percent Retained Sieve 140 | - | 99 % | 11.1 | 11.3 | 9.6 |
| Percent Retained Sieve 200 | - | 99 % | 4.5 | 5.3 | 5.1 |
| Main Compression Force (kN) | 99 % | 99 % | 5.68 | 6.69 | 2.55 |
| Pre-Compression Force (kN) | 95 % | 99 % | 1.35 | 1.45 | 0.1 |
| Ejection Force (N) | 90 % | 99 % | 157.7 | 166.6 | 5.3 |
| Fill Depth (mm) | 95 % | 99 % | 7.16 | 7.05 | 6.97 |
| Average Tablet Thickness (mm) | 99 % | 99 % | 3.14 | 3.09 | 3.63 |
| Disintegration Time (min) | - | 99 % | 6.7 | 6.8 | 9.7 |
| Moisture Content (% w/w) | 95 % | 99 % | 2.1 | 2.0 | 2.4 |
| Average Content Uniformity | - | 99 % | 98.9 | 98.6 | 100.0 |

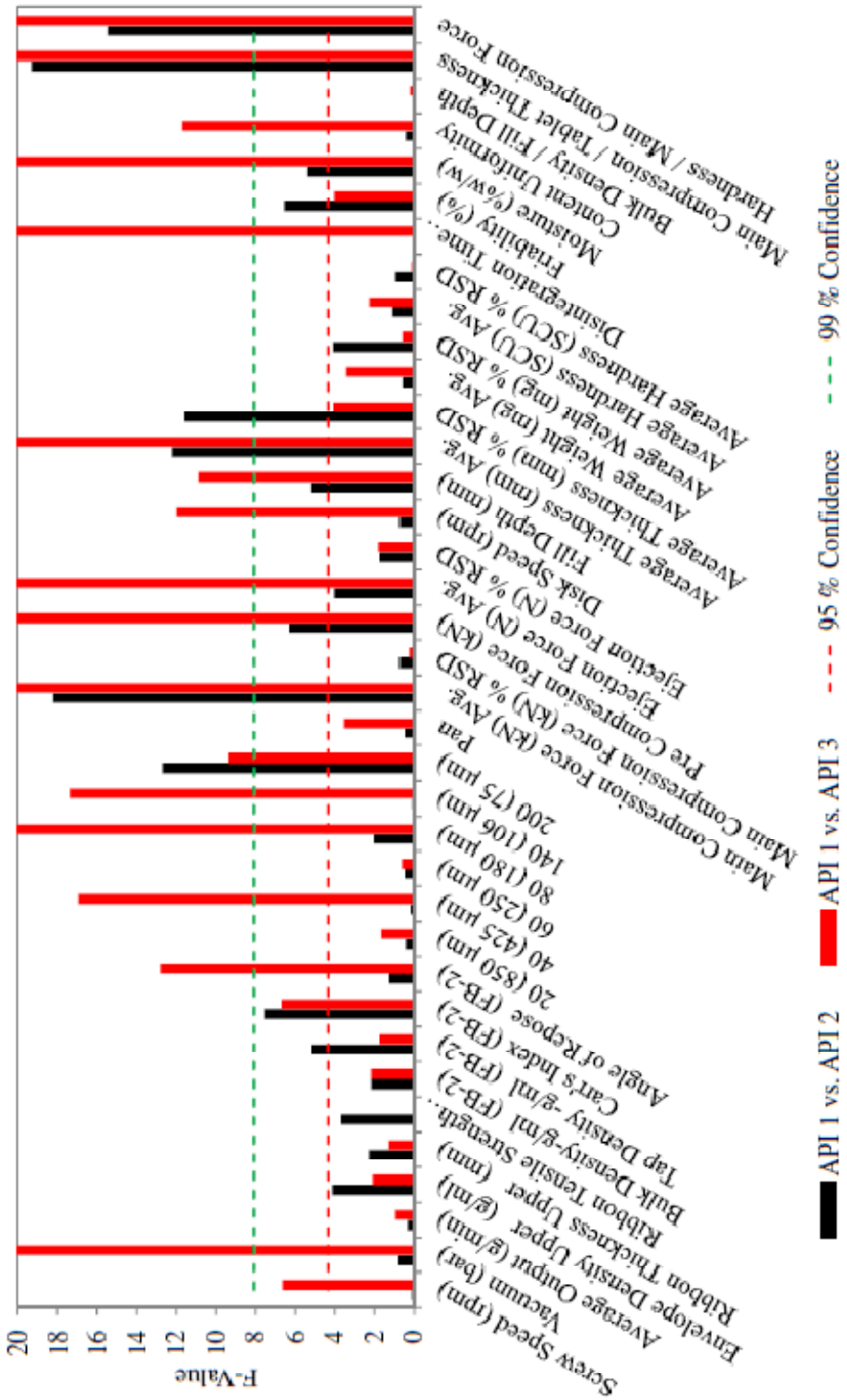


**Figure 7-2 - F-Values calculated from ANOVA test - above dashed green line significant differences at the 99 % confidence level, above red dashed line significant difference at the 95 % confidence level (upper limit of the F-value set at 20 for clarity, some of the F-values exceed this level) .**

#### 7.4.1.1.1 Roller compaction performance

##### 7.4.1.1.1.1 Screw speed

The mean response for the screw speed required to maintain the roller compactor at the set DoE factor level was observed to be significantly different between API 1 and API 3. As discussed in section 3.3.4.1, the lower roll of the Alexanderwerk roller compactor is fixed in place, whilst the upper roll (also known as the slave roll) is floating and as such can move along the vertical plane. In this study, each DoE experiment was operated using roll gap control; as such the roll pressure and roll gap were fixed as per the DoE experimental conditions whilst the screw speed was automatically adjusted to achieve the target roll gap (at a set roll pressure and roll speed). Any differences in screw speed between the two API formulations would indicate differences in the flow characteristics of the blend through the roller compactor feed chamber (as described in section 4.2.2.1 when investigating the flow of lubricated and unlubricated formulations). The screw speed required to maintain a set roll gap is shown in Figure 7-3, it can be seen that a higher screw speed is required to supply the same mass of powder to the rollers when roller compacting the formulation containing API 3, indicating that the formulation containing API 1 has improved flow properties compared to the formulation containing API 3. In contrast the screw speed for API 2 is very similar to the screw speed required for API 1 (see Figure 7-3).

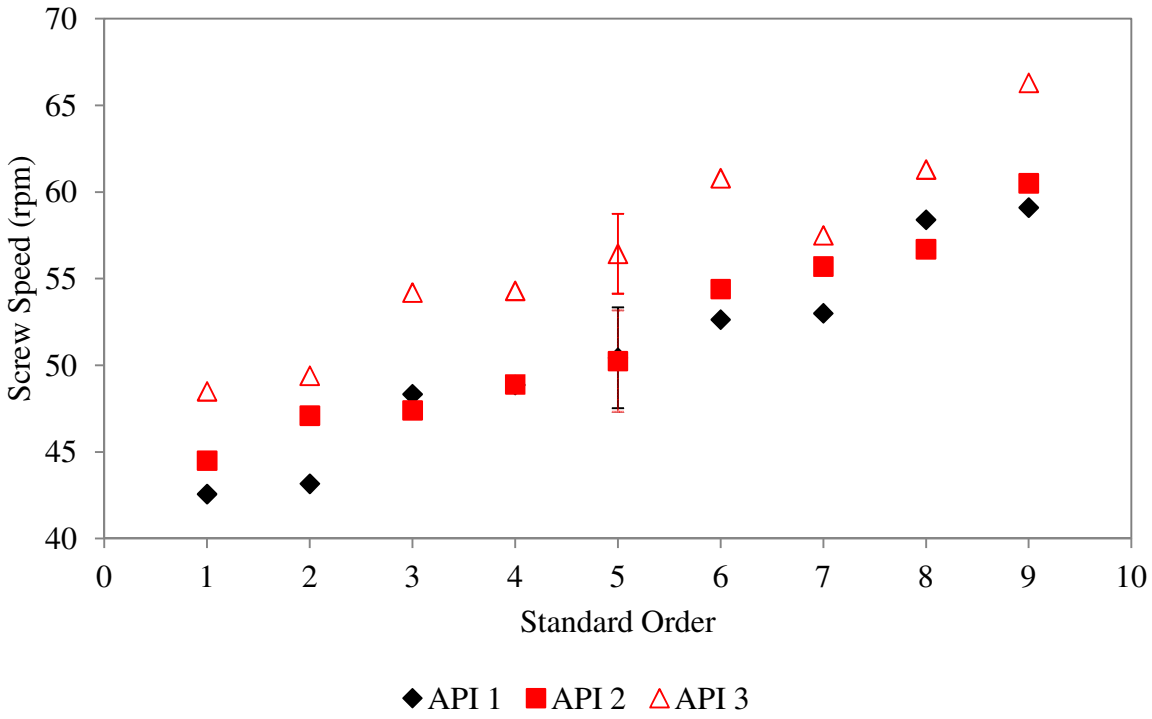


**Figure 7-3 – Measured screw speed against standard order, the centre points (standard order 5) are an average of the screw speed at roll pressure = 55 bar and roll gap = 2.3. The error bars show the standard deviation of the 3 centre point repeats.**

#### 7.4.1.1.1.2 Envelope density

Ribbon envelope density was calculated to be significantly different at the 90 % confidence level for API1 vs. API 2; the ANOVA calculated P-value was 0.07. Lamination of the roller compacted ribbons manufactured using API 1 was observed at the following experimental parameters; RP = 40 bar, RG = 2.3 mm (run 4) and RP = 55 bar, RG = 2.3 mm (run 5). The measured response data for envelope density is shown in Figure 7-4. It can be observed that the response data for API 2 and API 3 follows the increase in pressure whereby an increase in pressure elicits an increase in envelope density. The same observation was made for the placebo formulation roller compacted at different pressure discussed in chapter 4. However, the response data for API 1 shows more variability and does not follow the same trend as API 2 and API 3.

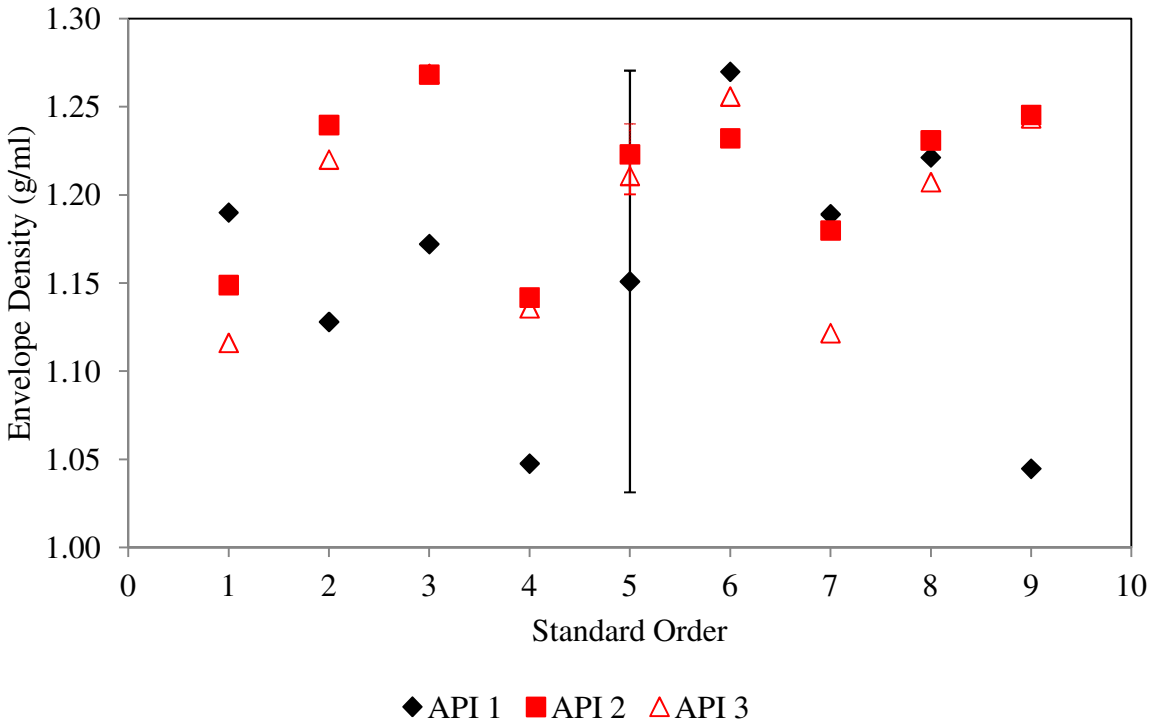


**Figure 7-4 – Measured envelope density against standard order, the centre points (standard order 5) are an average of the envelope density at roll pressure = 55 bar and roll gap = 2.3. The error bars show the standard deviation of the 3 centre point repeats.**

#### 7.4.1.1.1.3 Ribbon tensile strength

The calculated P-value for ribbon tensile strength of API 1 vs. API 2 and API 2 vs. API 3 was 0.055 and 0.077 respectively; the cut off value for significance at the 95 % confidence interval is 0.05. The tensile strength data is shown in Figure 7-5; it can be observed that ribbons compacted from API 3 have the highest tensile strength followed by those compacted from API 1 whilst ribbons of API 2 exhibited the weakest ribbon tensile strength. The tensile strength of all three APIs follows a similar pattern whereby the tensile strength increases with increased compaction load. However, ribbons compressed with a wider roll gap demonstrate a slight reduction in ribbon tensile strength. Furthermore, there is a degree of overlap of the error bars shown for the repeated centre points. Figure 7-6 shows the ribbon tensile strength as a function of envelope density, as one might expect following the discussion in chapter 4, the envelope density shows some correlation with the ribbon tensile

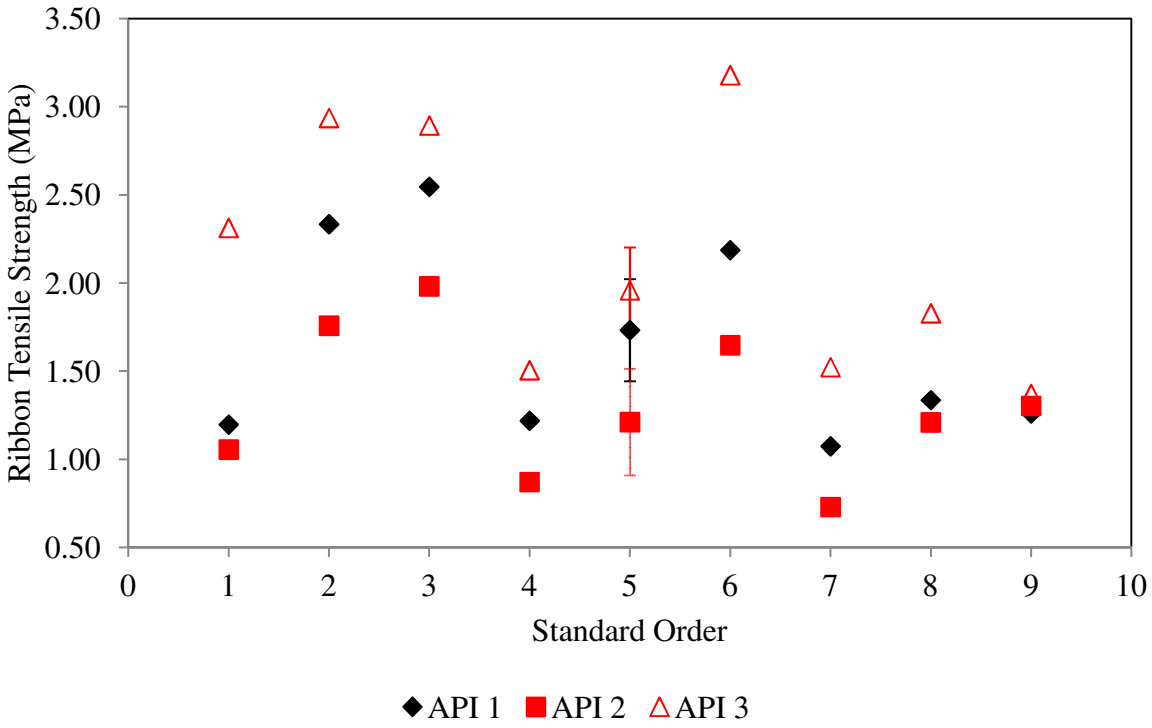


**Figure 7-5 – Measured ribbon tensile strength against standard order, the centre points (standard run order 5) are an average of the ribbon tensile strength at roll pressure = 55 bar and roll gap = 2.3. The error bars shows the standard deviation of the three centre point repeats.**

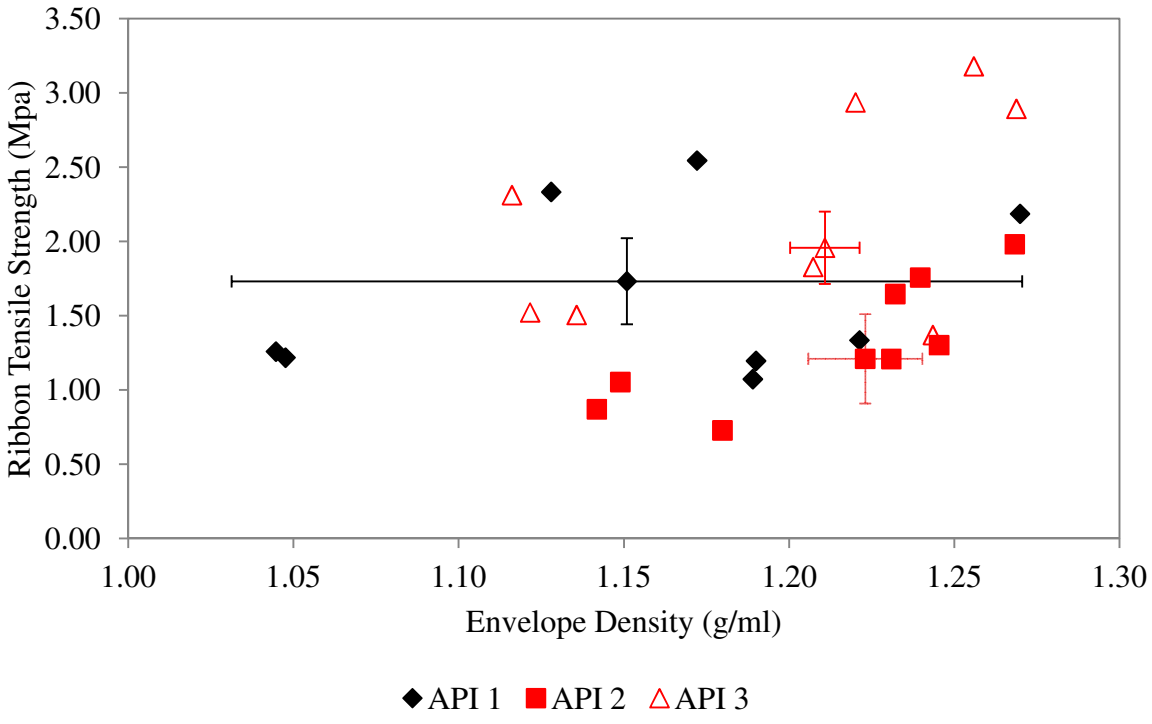


**Figure 7-6 – Ribbon tensile strength as a function of ribbon compact density, the centre points are an average of the ribbon tensile strength and ribbon compact density at roll pressure = 55 bar and roll gap = 2.3. The error bars shows the standard deviation of the three centre point repeats.**

strength particularly for API 2 ($r^2$ = 0.762); however, the tensile strength response is also dependent on the roll gap during compaction

#### 7.4.1.1.2 Granule properties

##### 7.4.1.1.2.1 Density and flow properties

The result from the ANOVA test showed that there were significant differences between the mean response for the tap density, Carr's Index and tablet die fill depth between API 1 and API 2 (calculated P-values were 0.034, 0.013 and 0.034 respectively), and significant differences between the mean response for the Carr's index and angle of repose between API 1 and API 3 (calculated P-values were 0.017 and 0.002 respectively). As shown in Figure 7-7 API 1 generally had a lower tap density than API 2 and API 3, although there is some degree of overlap. Whilst the data does indicate that there is some degree of difference between the tap density of the granule from API 1 and API 2 it should be considered that the standard deviation error bars shown in Figure 7-7 extend the full range of data indicating that the significant difference calculated from the ANOVA may be due to either sampling error or batch-to-batch variability rather than a physical difference between the tapped density of the granule manufactured from the two APIs.

Carr's index is a parameter derived from the bulk and tapped density as described in section 3.2.1. From the calculated F-values, there was no significant difference between the bulk density for either the similar APIs or the dissimilar APIs and there were no significant differences between the tapped density of the dissimilar APIs. As such, it is considered that the differences calculated from the Carr's index are as a result of the mathematical treatment of the data (*i.e.* the small and statistically insignificant differences in bulk and tapped density

will be exacerbated when combined to calculate the Carr's index) rather than a physical meaning.

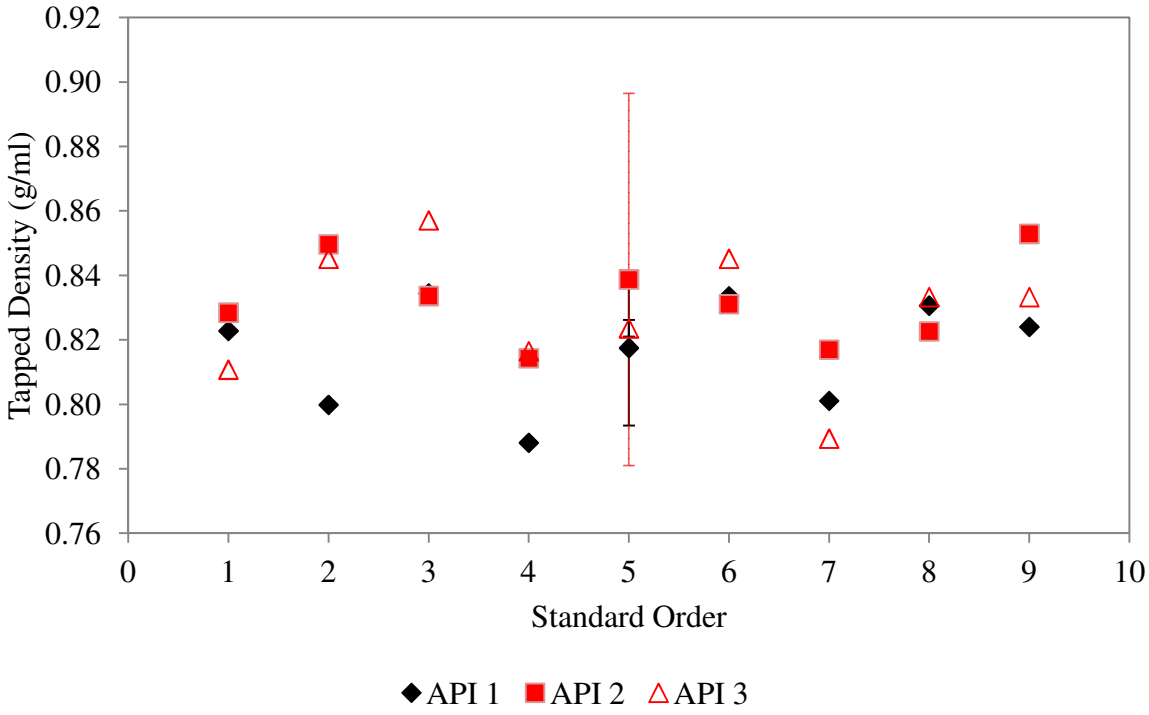


**Figure 7-7 - Granule tap density arranged in standard order.**

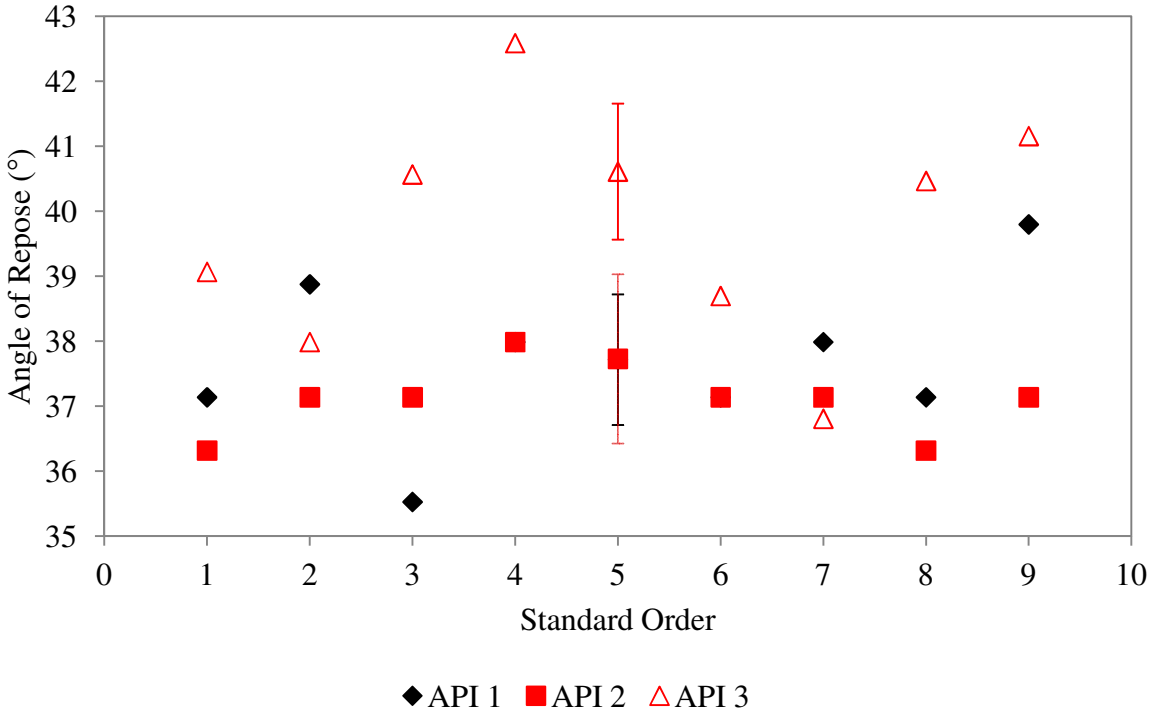


**Figure 7-8 - Granule angle of repose arranged in standard order.**

The response data for angle of repose is shown in Figure 7-8; it can be observed that the measured angle of repose is higher at nearly all experimental conditions for the granule containing API 3 indicating that API 3 granule has reduced flow properties compared to API 1. In contrast the angle of repose for API 2 is closely matched to that of API 1 for the majority of the DoE runs.

#### 7.4.1.1.2.2 Particle size

The F-value calculated using ANOVA suggests that there were significant differences in the particle size distributions of API 1 and API 3 granules (at the 99% confidence level). Figure 7-9 shows the percentage of granule retained on the sieve size 140 (size range 106 – 180 μm) as a function of the percentage of granule retained on the sieve size 40 (size range 425 – 850 μm). It can be observed that a larger percentage of granule were retained on the sieve size 40 for the granule containing API 3, whilst the reverse is observed for the percentage of granule retained on the sieve size 140. This observation suggests that there exists a greater proportion of coarse material in the granule obtained from the ribbon containing API 3. The particle size data shown here is based on a sieve cut; that is, the granules retained on sieve 40 are anything between 425-850 μm. In section 4.2.3.3 particle size distribution was measured using the QicPic image analysis system, which allows for greater accuracy and discrimination between particle sizes. Figure 7-10 shows the particle size data obtained from the sieve technique using the same format as the QicPic system, i.e. cumulative percentage as a function of particle size. It can be observed that the granules from API 1 have a larger percentage of smaller sized granules, however, in comparison to the images shown in Figure 4-28 the particle size resolution is much lower; furthermore the actual granular material is contained within the first sieve cut, i.e. > 850 μm, and with the data available no further breakdown of particle size within this sub sample of material is possible.

A greater degree of particle size distribution data accuracy would be afforded by the use of the QicPic particle sizing system.

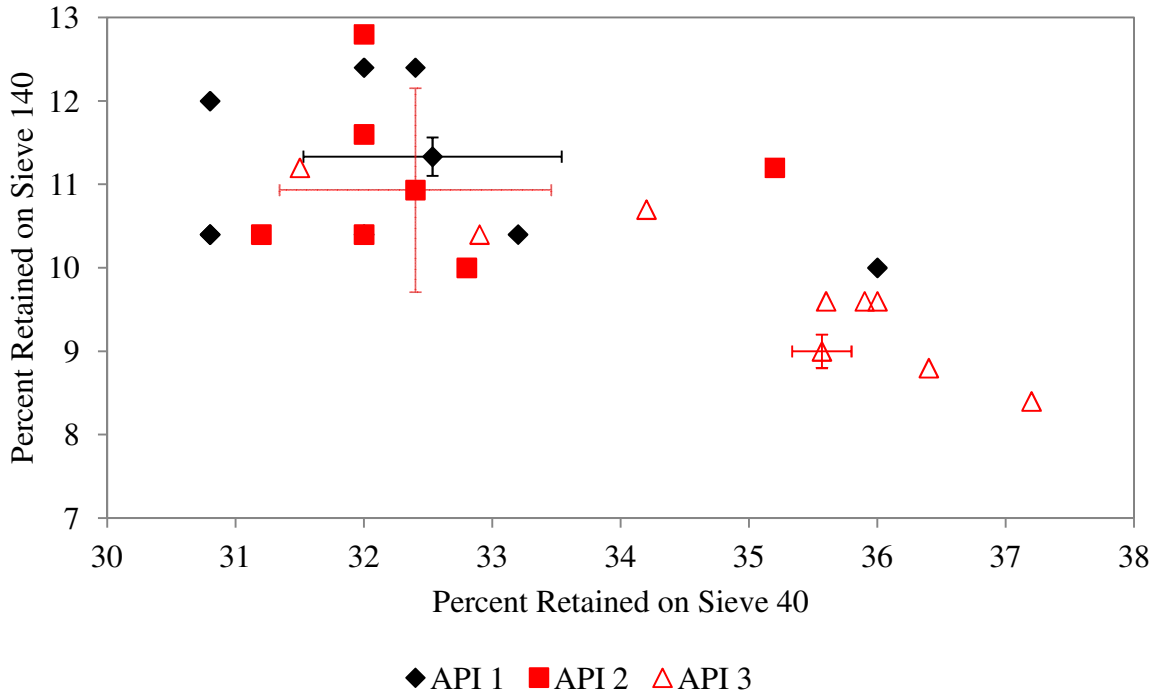


**Figure 7-9 – Mass percent of granules retained on sieve size 140 as a function of Mass percent of granules retained on sieve size 40 for API 1 and API 3, error bars show the standard deviation of the centre point repeats.**

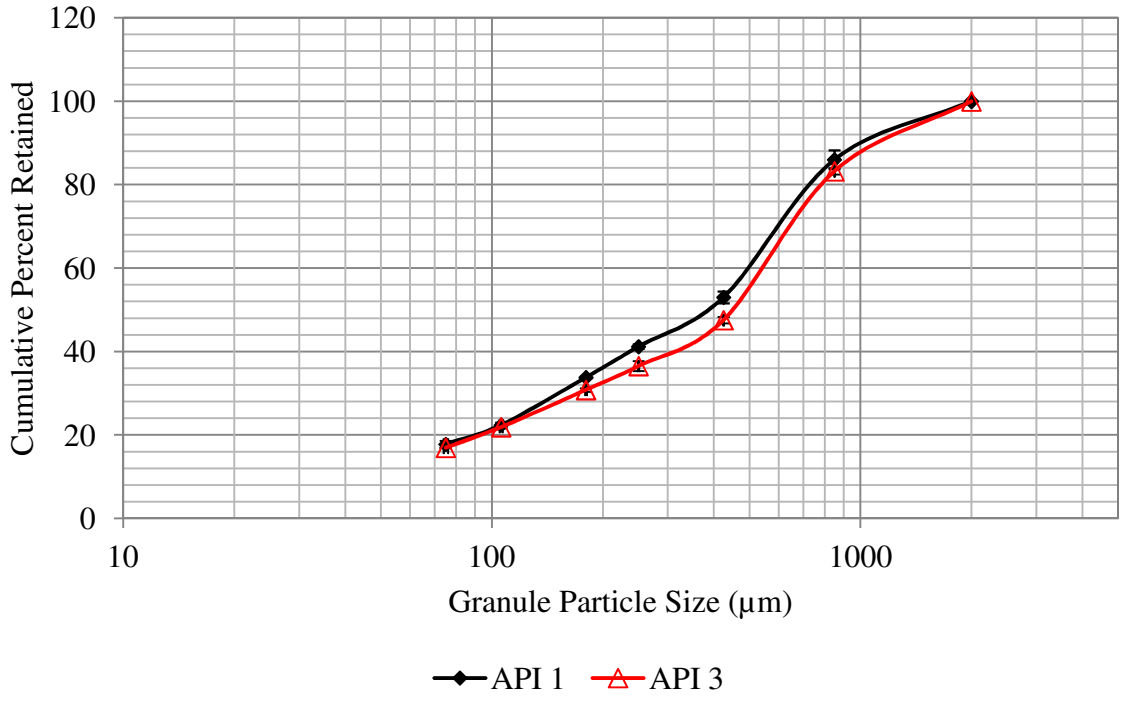


**Figure 7-10 – Cumulative percent retained on each sieve size, data shown is for the centre point conditions, i.e. roll pressure = 55 bar, roll speed = 2.3 bar. Error bars show standard deviation of the 3 repeated centre points.**

#### 7.4.1.1.3 Tablet compaction

##### 7.4.1.1.3.1 Compression characteristics

From the ANOVA table (Table 7-5) the responses for main compression force and tablet thickness of both the similar and dissimilar APIs were observed to be significantly different. The tablet compaction process was controlled to a tablet hardness of 10-11 SCU. The tablet manufacturing process is designed around three tablet properties: (1) tablet weight; (2) tablet thickness; and, (3) tablet hardness. The three tablet properties are inter-linked such that changing one of them will elicit a change in the other two. Of the three parameters tablet weight is always the most important parameter because it directly controls drug potency (amount of API present within the tablet). The second most important parameter is often the tablet hardness because the tablet product must be strong enough to endure the mechanical stresses and forces applied during coating, packaging, transportation and handling. As such the response of the third parameter; tablet thickness, is often a response of setting the other two parameters at the same pre-determined level.

For all formulations the tablet weight was fixed at 100 mg (10 % drug loading) whilst the tablet hardness was controlled to between 10-11 SCU. The resulting tablet thickness, and hence solid fraction, is therefore a measure of the compactability of the formulation, whilst the required main compression pressure to achieve that thickness is a measure of the compressibility of the formulation. Here, the blend compressibility is defined as the ability to reduce in volume due to an applied pressure (*i.e.* volume vs. compaction pressure); whilst the blend compactability is defined as the increase in tablet strength due to the application of pressure (*i.e.* tablet hardness vs. compaction force). Figure 7-11, shows the average tablet thickness of the API containing formulations as a function of main compression force. It can be observed that there are slight differences in the compression force of API 1 and API 2,

whilst at the same time the tablets from API 1 tend to have a slight increase in thickness compared to the tablets of API 2. However, in contrast the differences in compression force and tablet thickness of API 1 vs. API 3 are much more apparent and there is a clear distinction between API 1/API 2 and API 3.

Furthermore it can be observed in Figure 7-12, that even though there was no significant difference in the tablet hardness between the two APIs (which was indeed the case from the results from the ANOVA, P-value = 0.311), however, a slightly higher compression pressure was required for API 2 to achieve the same tablet hardness for API 1 (at a lower compression pressure). Again the force required to compact API 3 to the same tablet hardness as API 1 and API 2 was distinctively lower. This observation suggests that the API 3 formulation is more compactable than the API 1 formulation which is in turn more compactable than API 2, which is a consistent order to that observed previously on the differences in the tensile strength of the ribbons manufactured from the three APIs (see section 7.4.1.1.1). However, caution should be applied to the ANOVA result; although statistical differences were observed between the compaction pressure response of API 1 and API 2 it is likely that from a practical perspective the differences in compaction pressure may be physically irrelevant. The average compaction pressure applied was 5.68 kN and 6.69 kN for API 1 and API 2 respectively, whist the average compaction for API 3 was 2.55 kN.

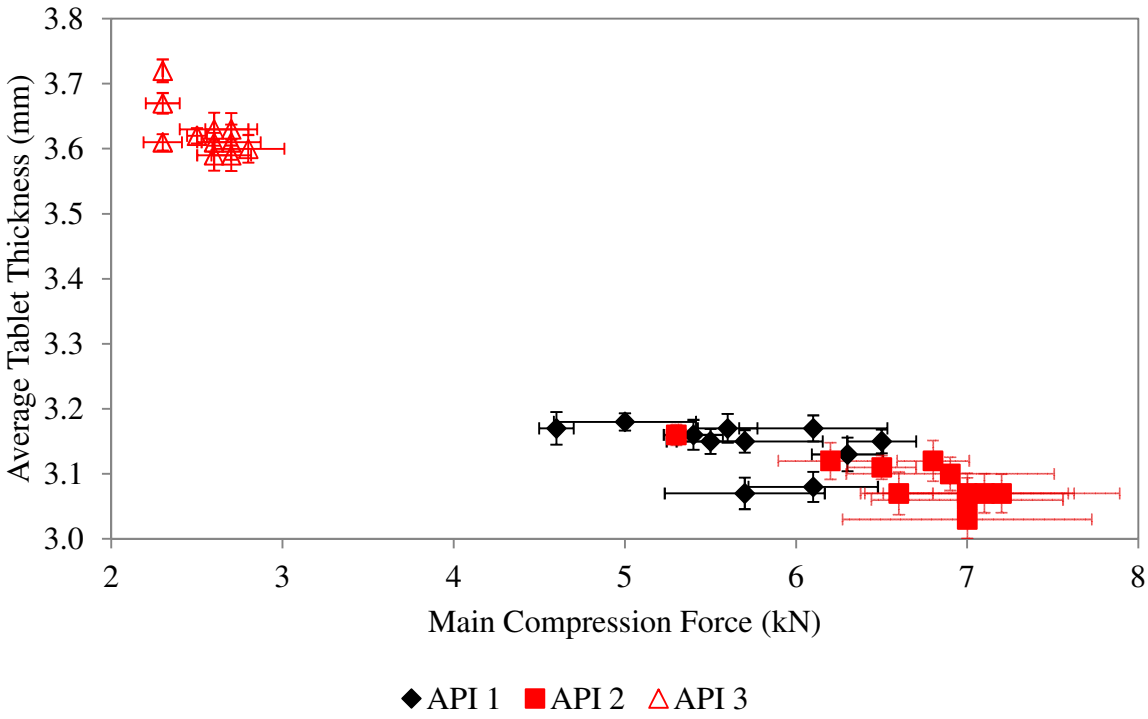


**Figure 7-11 – Tablet thickness as a function of main compression force for API 1, API 2 and API 3, error bars show the standard deviation of the actual data points.**

Unlike with previous responses there is no overlap between the standard deviation error bars from the repeated centre points between API 1 and API 2. The difference observed warrants further exploration of drug levels to ensure that any differences in compaction pressure are not exacerbated at reduced excipient levels / increased drug levels. Should difference in compactability and compressibility of the drug product exist they are more likely to be observed at higher drug loads were the properties of the drug product will dominate the compaction process.

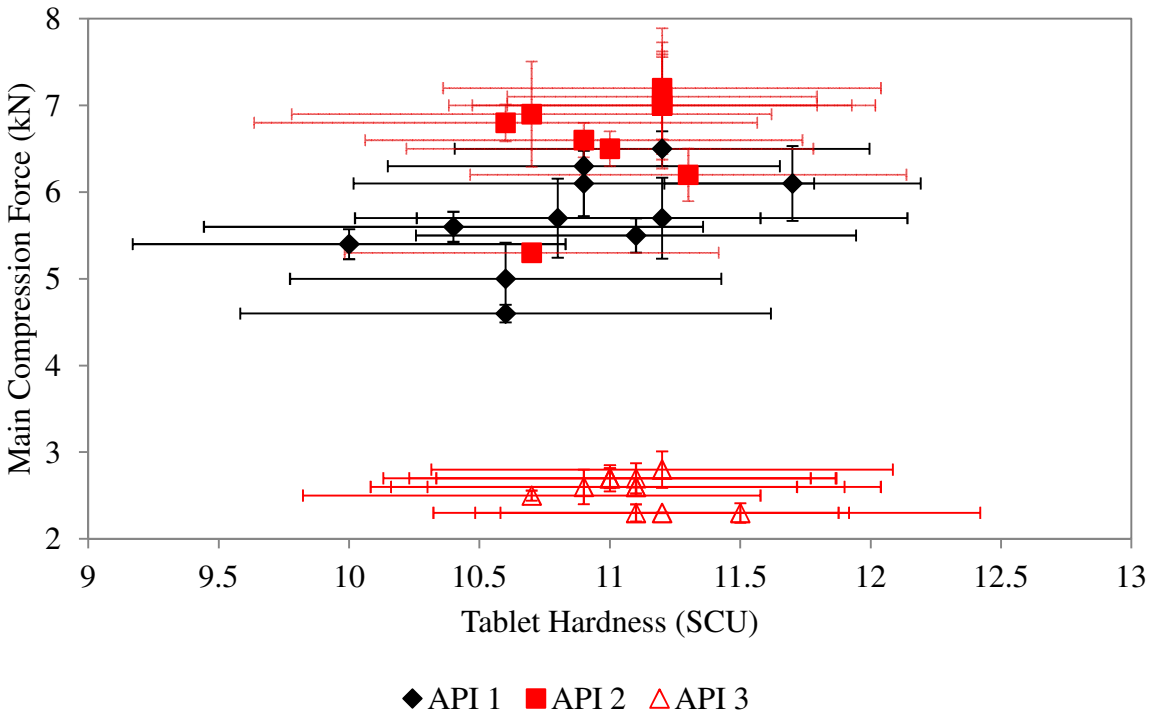


**Figure 7-12 – Main compression force as a function of tablet hardness for API 1 and API 3, error bars show the standard deviation of the actual data points.**

#### 7.4.1.1.3.2 Tablet disintegration

Tablet disintegration is a critical quality attribute of all pharmaceutical formulations; the accuracy of prediction for disintegration data is of paramount importance for the surrogate API project. In the comparison between API 1 and API 2 no significant differences existed between the disintegration of the two APIs deemed to be similar. The F-value calculated for the disintegration time response of API 1 vs. API 3 indicates that there is significant difference in the disintegration characteristics of the two dissimilar APIs. Figure 7-13 shows the disintegration time of API 1, API 2 and API 3 against the standard order for experimental condition. It can be observed that in all instances the time required for complete disintegration was significantly longer for API 3 than for API 1. In contrast the disintegration times of the API 2 tablets are generally consistent with those of API 1. Conversely to some observations in the literature [Rambali *et al.*, 2001] there was no systematic increase in the disintegration times with increasing roller compaction pressure; as such the effect on disintegration time is

more likely due to the formulation composition rather than the compaction process parameters.

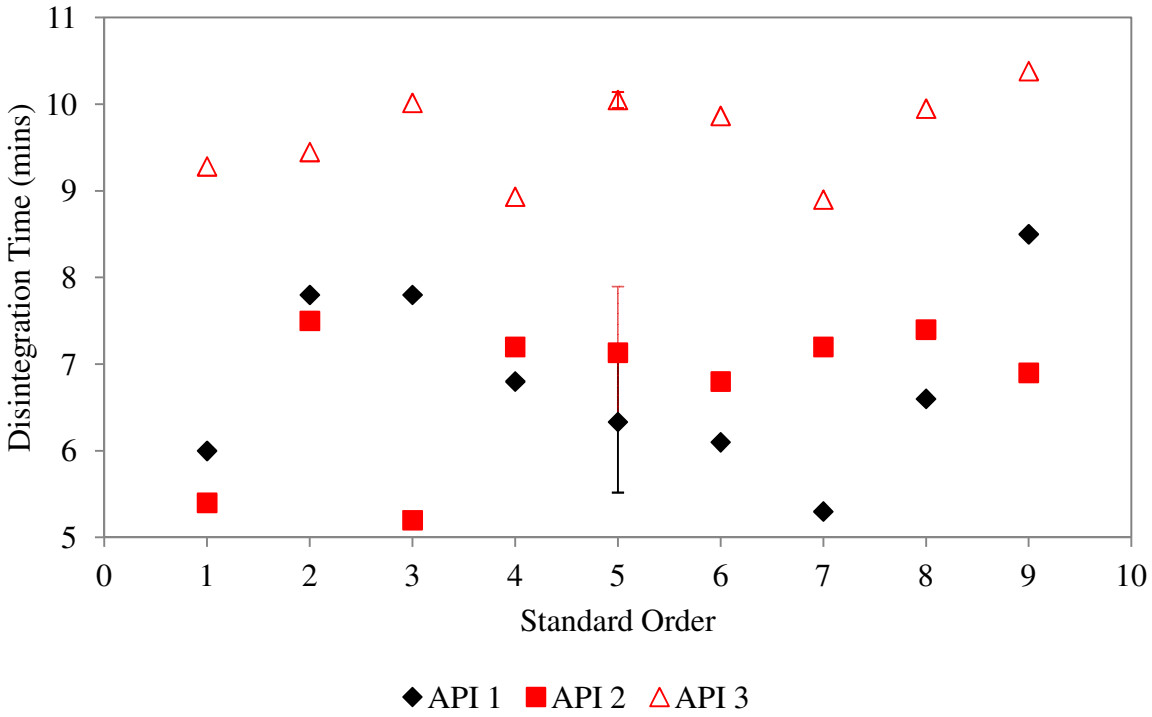


**Figure 7-13 – Measured disintegration time against standard order, the centre points (standard order 5) are an average of the disintegration time at roll pressure = 55 bar and roll gap = 2.3. The error bars show the standard deviation of the 3 centre point repeats.**

### 7.4.1.2 Response surface and regression analysis

The limitation of ANOVA is that it is only capable of detecting significant differences in the actual values of the data sets, it cannot imply whether the differences are large enough to have a physical meaning. Another set of useful statistical tools is response surface and regression analysis. These techniques can be used to determine if (1) a factor from the DoE has a significant impact on an output parameter; and, (2) if the two API lots being studied are impacted by the significant factors in a statistically similar way.

**Table 7-6 - Output parameters significantly impacted by the DoE factors (RP – linear roll pressure, RG – linear roll gap, $RP^2$ – quadratic roll pressure, $RG^2$ – quadratic roll gap and RP*RG – interaction term**

| Response | Significant Factors | | |
|---|---|---|---|
| | API 1 | API 2 | API 3 |
| Screw Speed | RP<br>RG | RP<br>RG | RP<br>RG |
| Envelope Density | None | RP<br>$RP^2$ | RP |
| Ribbon Tensile Strength | RP<br>RG<br>RP*RG | RP<br>RG | RP*<br>RG |
| Percent Retained on Sieve 40 | RP<br>RG | RP<br>$RG^2$<br>RP*RG | RP |
| Main Compression Force | RP | RP | RP<br>$RG^2$ |
| Fill Depth | None | None | RP<br>$RP^2$ |
| Disintegration | None | None | Roll Pressure |

The response surface analysis was performed using the Minitab statistical software; it was found that several output parameters were not significantly impacted by either of the DoE factors. As such it is not possible to determine if these parameters are affected by the DoE factors in a similar way. The output parameters which were significantly impacted by the DoE factors are summarized in Table 7-6. Roller compaction performance

#### 7.4.1.2.1.1 Screw speed

Both roll pressure and roll gap had a significant impact on the response for the screw speed. The regression models for API 1, API 2 and API 3 are given in Equation 7-2 - Equation 7-4 respectively;

$$SS_{API\ 1} = 50.44 + 2.54(RP) + 6.07(RG) \quad \textbf{Equation 7-2}$$

$$SS_{API\ 2} = 51.26 + 2.07(RP) + 5.65(RG) \quad \textbf{Equation 7-3}$$

$$SS_{API\ 3} = 56.2 + 3.35(RP) + 5.50(RG) \quad \textbf{Equation 7-4}$$

where $SS_{API\ 1}$, $SS_{API\ 2}$ and $SS_{API\ 3}$ are the predicted screw speed response for API 1, API 2 and API 3 respectively.

The coefficients given in the above regression models are both positive showing that an increase of either DoE factor elicits an increase in screw speed for all three compounds. This is expected and is in agreement with the results presented in chapter 4 where it was observed that to maintain a constant roll gap at increasing levels of hydraulic roll pressure an increase in screw speed was required. Furthermore as demonstrated by Equation 4-1 an increase in screw speed was required to increase the roll gap from 2.2 mm to 4.4 mm. The response surface plot for API 1 and API 3 is given in Figure 7-14(a) – (c). In both cases the regression model adequately explains the variation in the data with a regression coefficient of 0.905 and 0.914 for API 1 and API 3 respectively. The confidence intervals for the regression coefficients are shown in Figure 7-15, it can be observed that the confidence intervals of coefficients for both roll pressure and roll gap overlap suggesting that there is no evidence of a significant difference in the way the DoE factors affect screw speed for API 1 and API 3. However, there is an offset in the confidence intervals for the constant coefficient. The offset of the confidence intervals for the constant coefficients indicates that the value of the screw speed for API 1 and API 3 at the centre point of the DoE is significantly different. As such, from the screw speed regression analysis it can concluded that the screw speed variable responds in a similar manner to changes in the DoE factors, however, the actual response of the screw speed at a given level for each DoE factor is a significantly different for API 1 and API 3 (as shown in section 7.4.1.1.1.1).

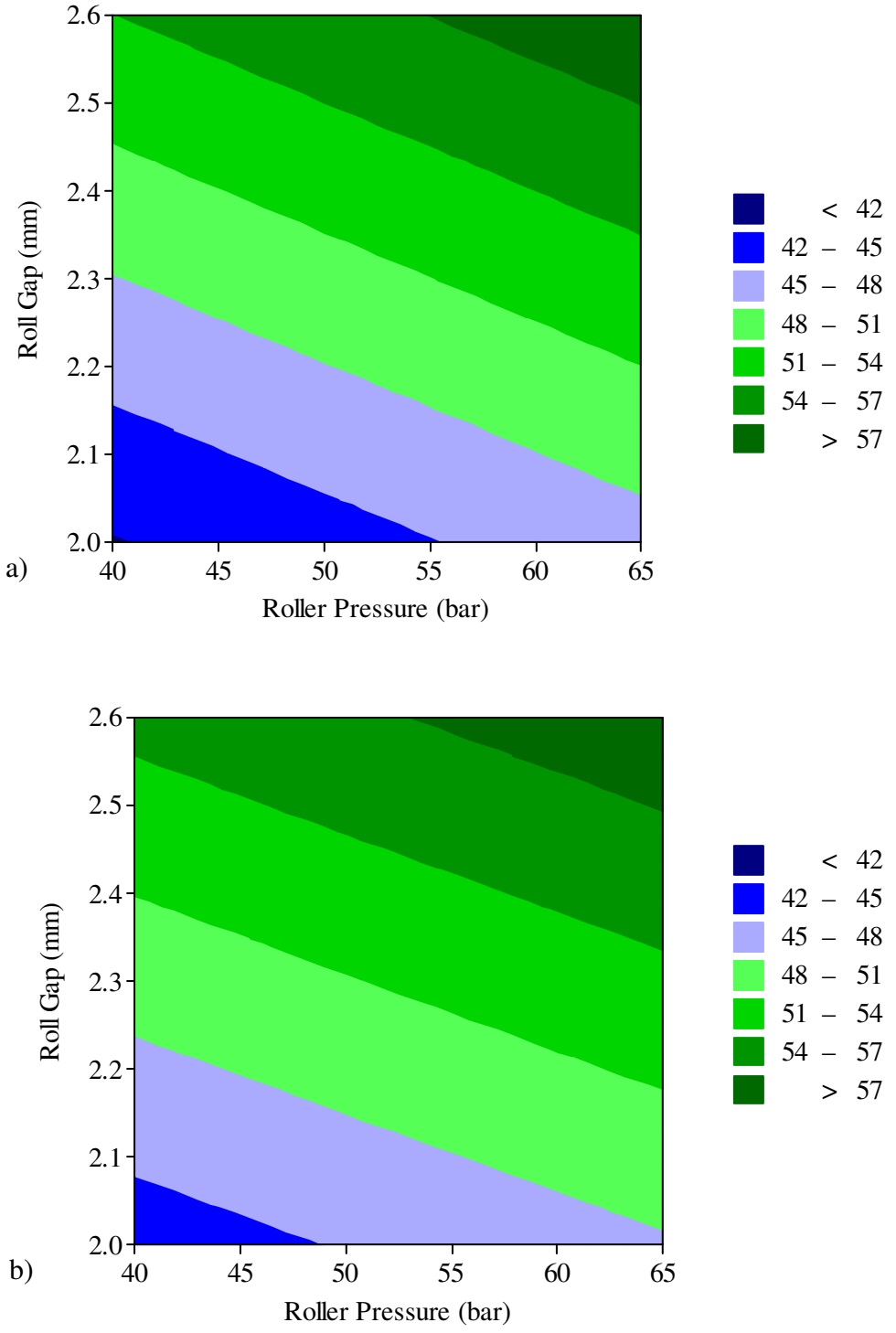


**Figure 7-14 - Surface plot for screw speed during roller compaction of (a) API 1; (b) API 2 and, (c) API 3.**

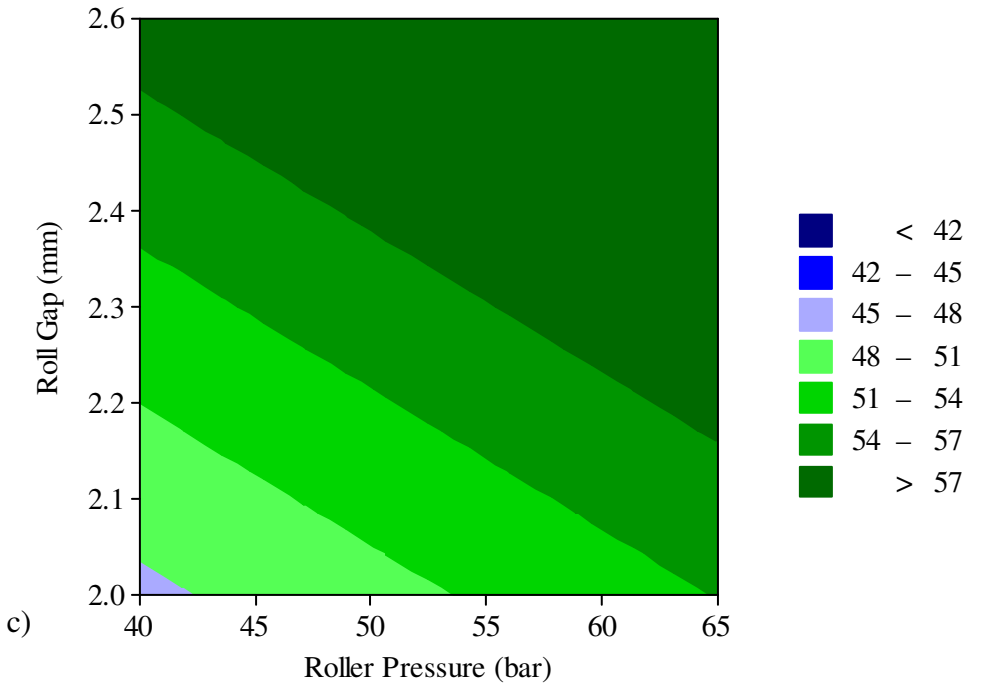


**Figure 14 continued - Surface plot for screw speed during roller compaction of (a) API 1; (b) API 2 and, (c) API 3**

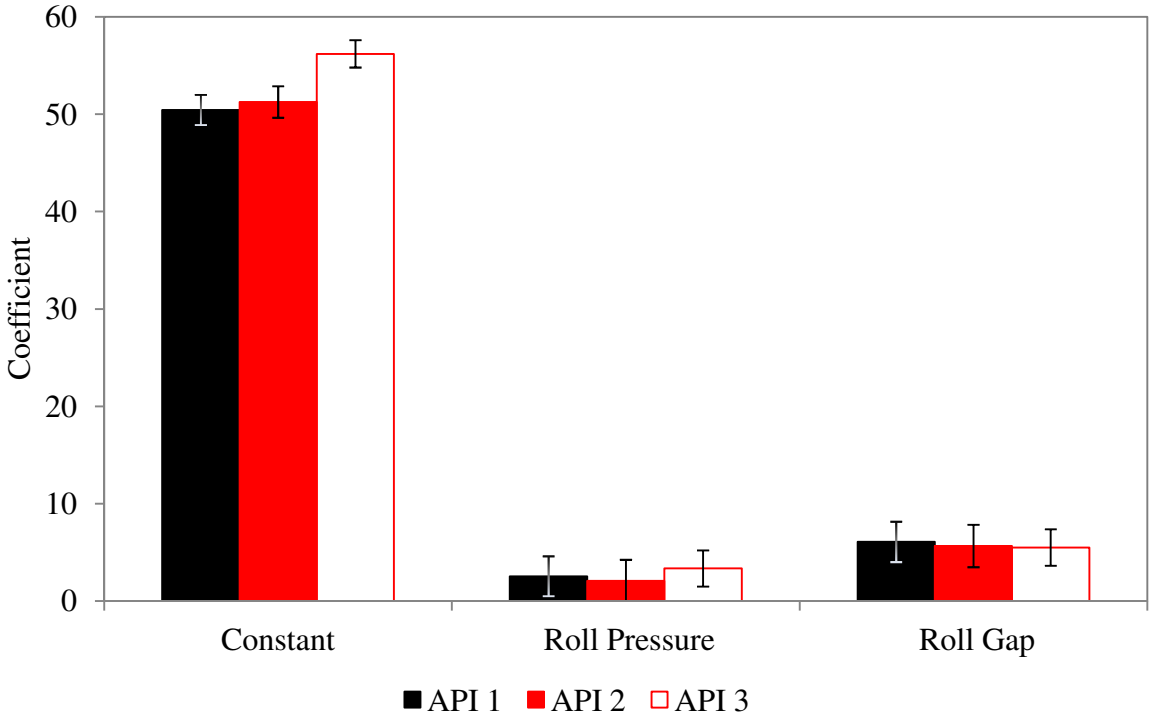


**Figure 7-15 – Regression coefficients for the screw speed model for API 1 and API 3 with confidence intervals.**

#### 7.4.1.2.1.2 Envelope density

The regression model for envelope density response for API 1 inadequately explained the variation in the response data (correlation coefficient = 0.052). The low predictability of the regression model was due to the lack of significant dependence on the DoE factors. The main effects plot for the measured envelope density response for API 1 as a function of roll pressure and roll gap is given in Figure 7-16, it can be observed that there is no systematic change in envelope density with a change in the DoE factors. Variability in the envelope density of roller compacted ribbons is a common observation [Guigon and Simon, 2003], and may be the reason why the results shown here show no systematic changes in response to DoE factors. In contrast to API 1, it was calculated from the regression model for API 2 and API 3 that envelope density was significantly impacted by roll pressure. The regression model for the envelope density of API 2 and 3 is given in Equation 7-6.

$$\rho_{API\ 2} = 1.22 + 0.05(RP) - 0.02(RP^2) \quad \textbf{Equation 7-5}$$

$$\rho_{API\ 3} = 1.19 + 0.7(RP) \quad \textbf{Equation 7-6}$$

The regression model for the envelope density quite accurately predicts the response data for API 2 and API 3 ($r^2$ = 0.963 and $r^2$ = 0.986 respectively), and the positive coefficient for the roll pressure shows that an increase in roll pressure leads to an increase in ribbon envelope density, this observation is consistent with that presented in chapter 4 for the placebo formulation.

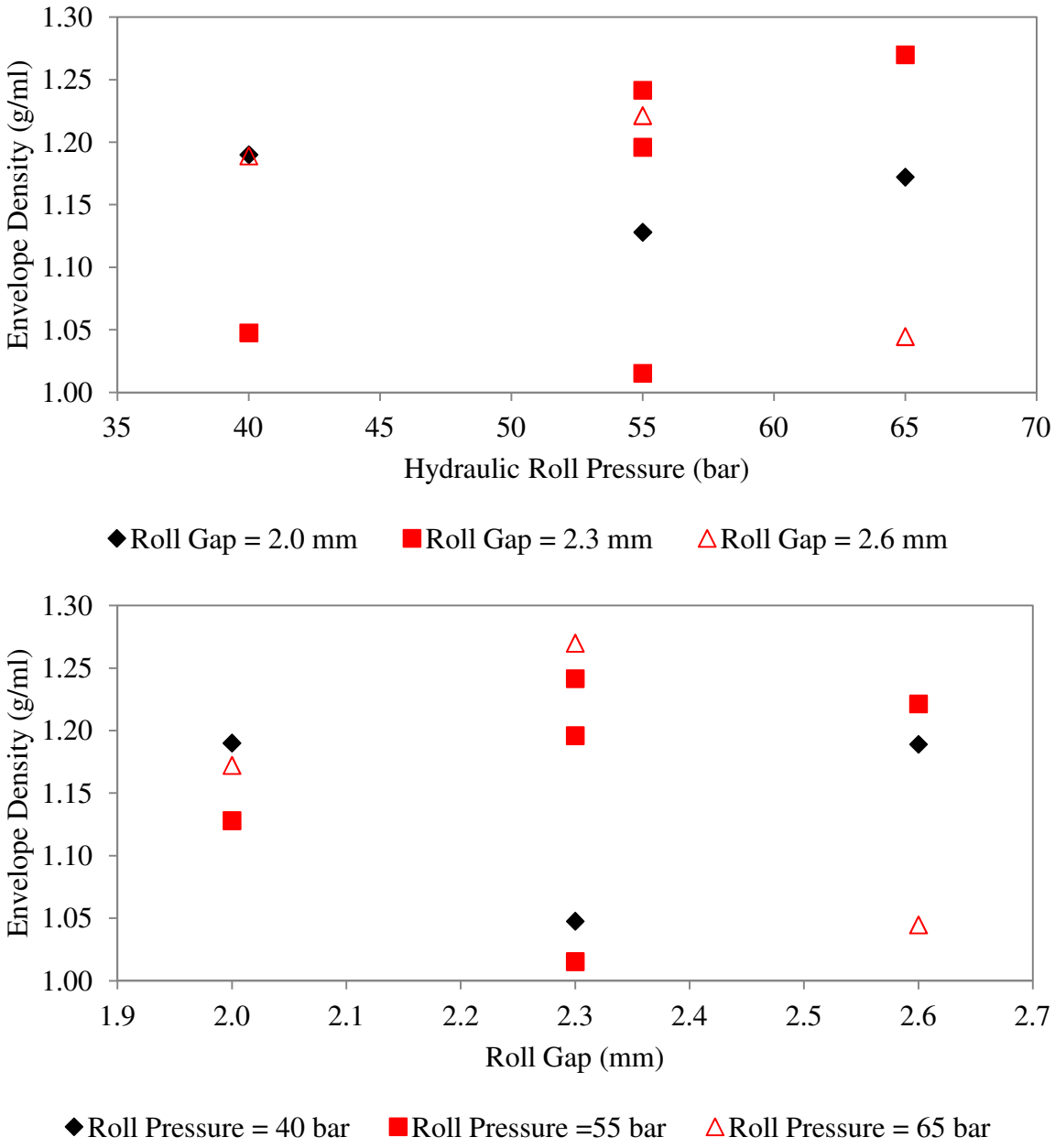


**Figure 7-16 – Main effects plot for the envelope density for API 1 (top) as a function of hydraulic roll pressure; and, (bottom) as a function of roll gap.**

The regression model coefficients with the respective confidence intervals are given in Figure 7-17, it can be observed that the envelope density responds to changes in the roll pressure in a statistically similar way, however, there is a very slight offset in the constant coefficient.

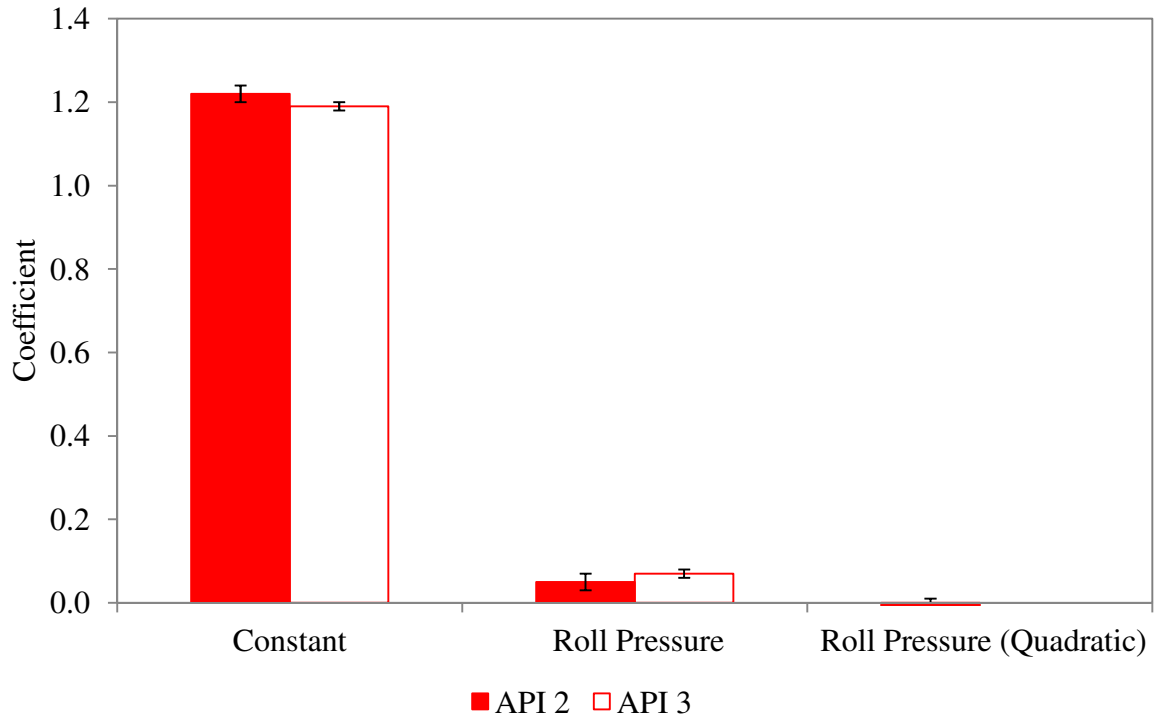


**Figure 7-17 – Regression coefficients for the envelope density model for API 2 and API 3 with confidence intervals, *Envelope density model for API 1 did not have any significant terms and as such is excluded.**

#### 7.4.1.2.1.3 Ribbon tensile strength

Both the roll pressure and roll gap had a significant impact on the ribbon tensile strength of all three API lots, in addition the interaction between roll pressure and roll gap was also significant for API 1. A surface plot showing the effect of the DoE factors on the ribbon tensile strength for each API lot is given in Figure 7-18; firstly it can be seen that the general shape of the curves for API 1 differ to those from API 2 and API 3, this is due to the inclusion of the interaction term in the tensile strength model for API 1. However, it can be seen that generally the tensile strength responds to the DoE factors in a similar way, such that an increase in roll pressure or a decrease in roll gap elicits an increase in ribbon tensile strength.

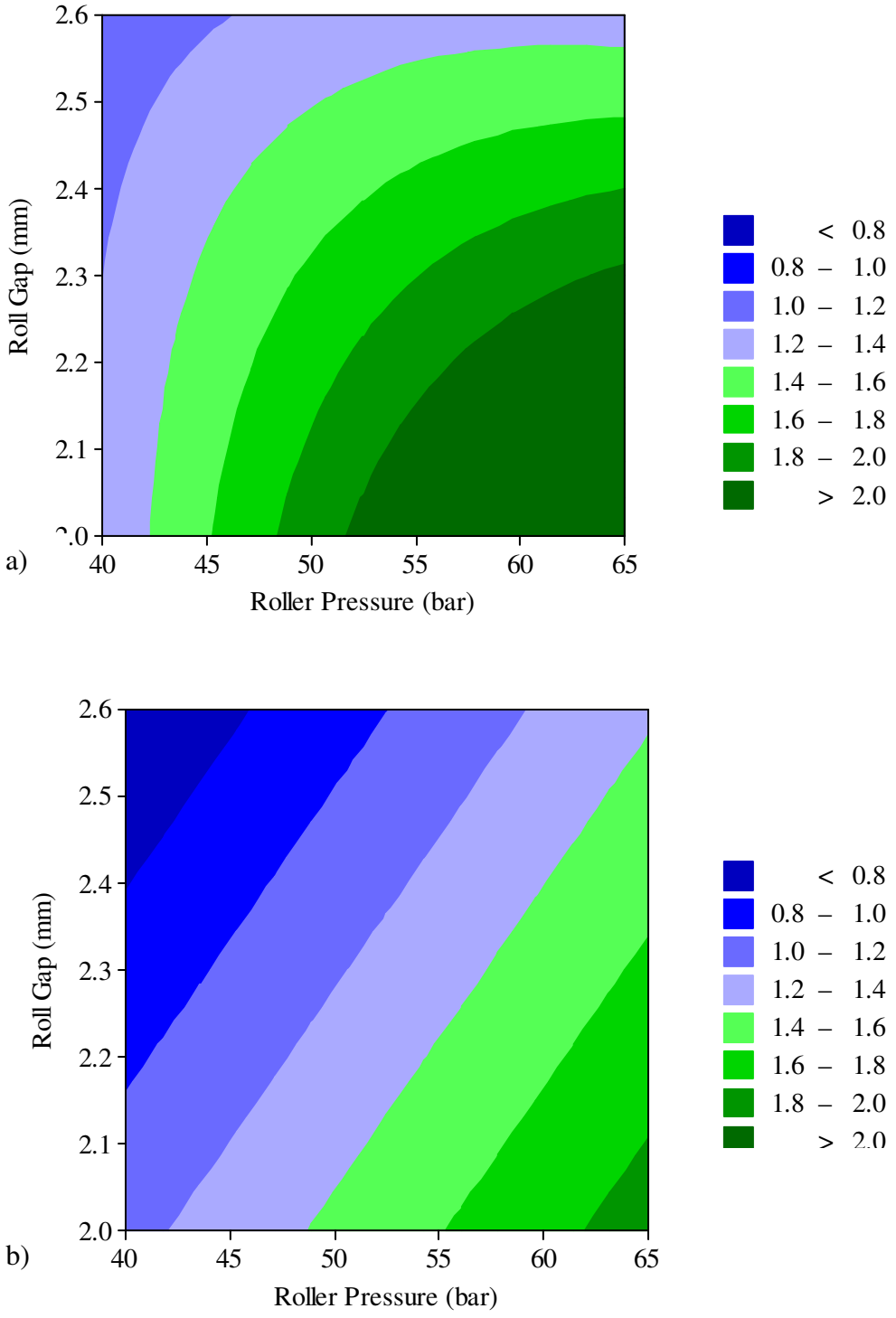


**Figure 7-18 – Surface plot for ribbon tensile strength (a) API 1, (b) API 2 and (c) API 3.**

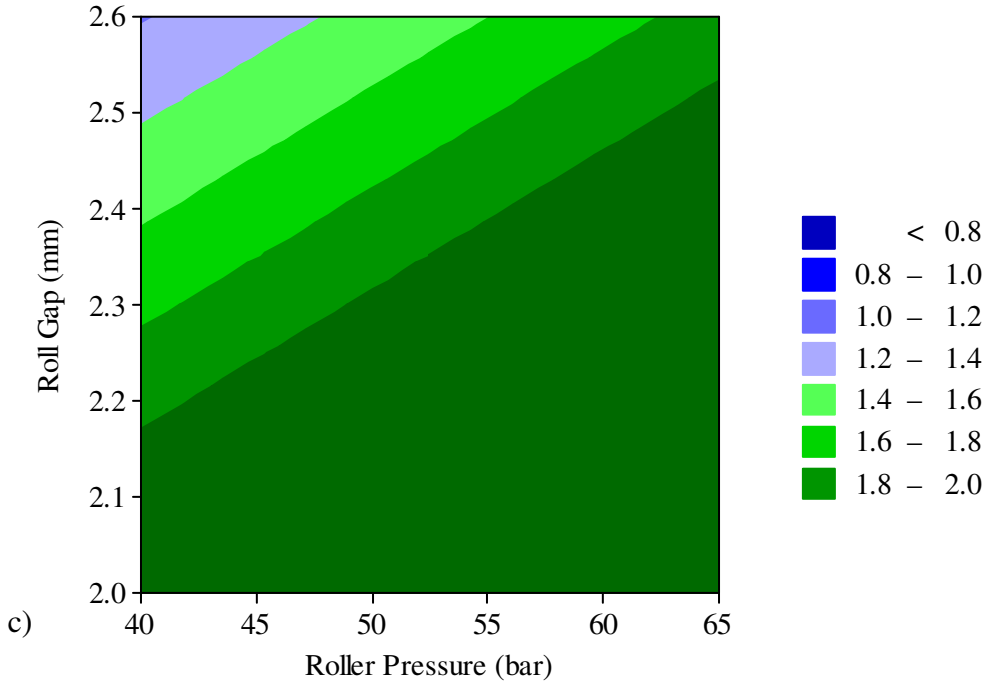


**Figure 7-18 continued – Surface plot for ribbon tensile strength (a) API 1, (b) API 2 and (c) API 3.**

The regression models for API 1, API 2 and API 3are given in Equation 7-7 to Equation 7-8 respectively.

$$\sigma_{API\,1} = 1.630 + 0.427(RP) - 0.381(RG) - 0.297(RP)(RG) \quad \textbf{Equation 7-7}$$

$$\sigma_{API\,2} = 1.256 + 0.378(RP) - 0.259(RG) \quad \textbf{Equation 7-8}$$

$$\sigma_{API\,3} = 2.099 + 0.343(RP) - 0.570(RG) \quad \textbf{Equation 7-9}$$

The model accurately predicts the measured ribbon tensile strength for API lots as indicated by the $R^2$ values (API 1 = 0.90, API 2 = 0.81 and API 3 = 66.8).

To determine whether the impact of roll pressure and roll gap on the ribbon tensile strength of the three API lots is statistically different the confidence intervals of the coefficients are shown in Figure 7-19. It can be seen that the confidence intervals for the regression coefficients of API 1 and API 2 lots overlap indicating that there is no evidence of a statistically significant difference in the impact of the DoE factors on the ribbon tensile

strength of the two API lots (API 1 and API 2). However the constant coefficient for the ribbon tensile strength of API 3 appears to be significantly higher than API 1 and API 2.

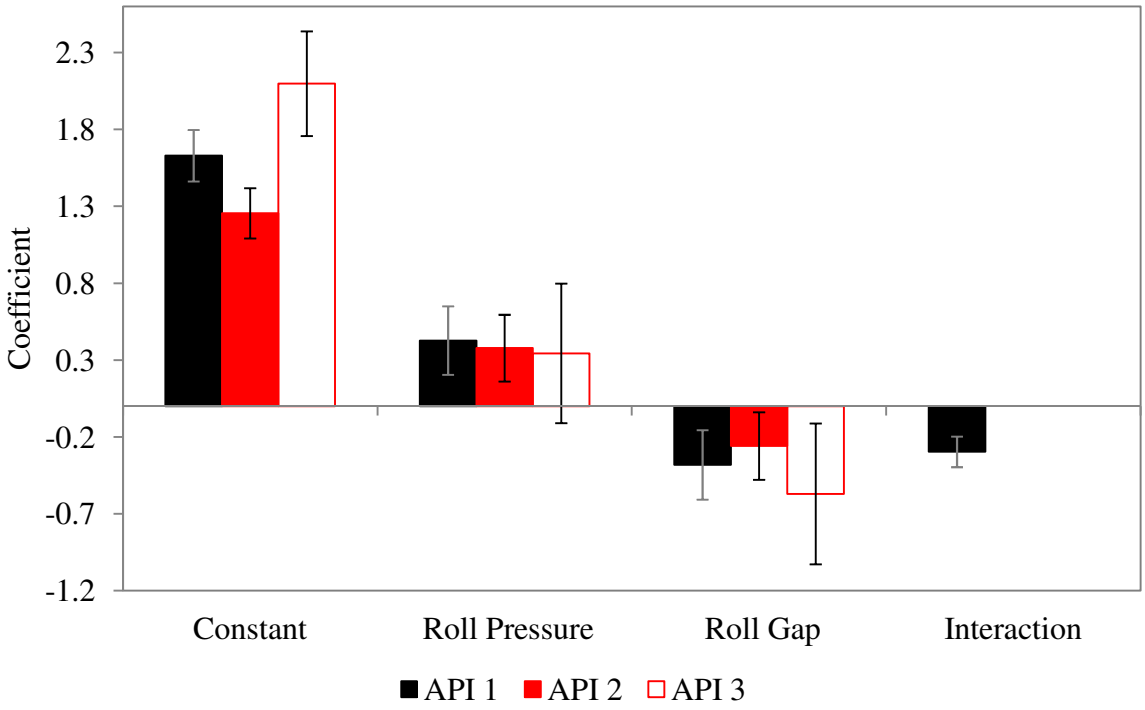


**Figure 7-19 – Regression coefficients for the ribbon tensile strength model for API 1 and API 2 with confidence intervals.**

#### 7.4.1.2.2 Granule properties

From the response surface analysis it was calculated that the only granule property response which significantly impacted by the DoE factors was the granule size defined by the mass percent retained on sieve size 40 (granule sized between 425-850 µm). In all three cases it was calculated from the derived regression model that the roll pressure had a significant impact on the response. In the case of API 1 and API 2 the roll gap also had a significant impact. The regression models for API 1, API 2 and API 3 are given in Equation 7-10 to Equation 7-12 respectively.

$$\%\text{retained}(\text{S40})_{API\ 1} = 32.21 + 1.27(RP) + 1.00(\text{RG}) \quad \textbf{Equation 7-10}$$

$$\%\text{retained}(\text{S40})_{API\ 1} = 32.73 + 1.28(\text{RP}) - 0.75(\text{RG}) - 1.48(\text{RG}^2) + 1.21(RP * RG) \quad \textbf{Equation 7-11}$$

$$\%\text{retained}(\text{S40})_{API\ 3} = 34.96 + 1.88(RP) \quad \textbf{Equation 7-12}$$

The regression coefficient for roll pressure is positive for both API 1 and API 3 indicating that an increase in roll pressure leads to an increase in the mass percent of granule retained on the sieve size 40. As expected this observation is in agreement with the results presented in chapter 4. Increasing the compaction pressure during roller compaction increases the solid fraction and the ribbon tensile strength. Ribbons with a higher tensile strength are more resistant to size reduction during milling and hence the resulting granule has an increased particle size distribution. The confidence intervals of the coefficients are shown in Figure 7-20, it can be observed that the confidence intervals for roll pressure overlap suggesting that the percent of granule retained on sieve size 40 responds similarly to an change in roll pressure, however there is a significant difference in the constant coefficient indicating that the measure response at the centre of the design is significantly different. In addition the roll gap was observed to have a significant impact on the percent of granule retained on sieve size 40 for API 1 but not for API 3. It is therefore concluded that there are significant differences in the percent of granules retained on the sieve size 40, as a function of the applied roll pressure during roller compaction of API 1 and API 3.

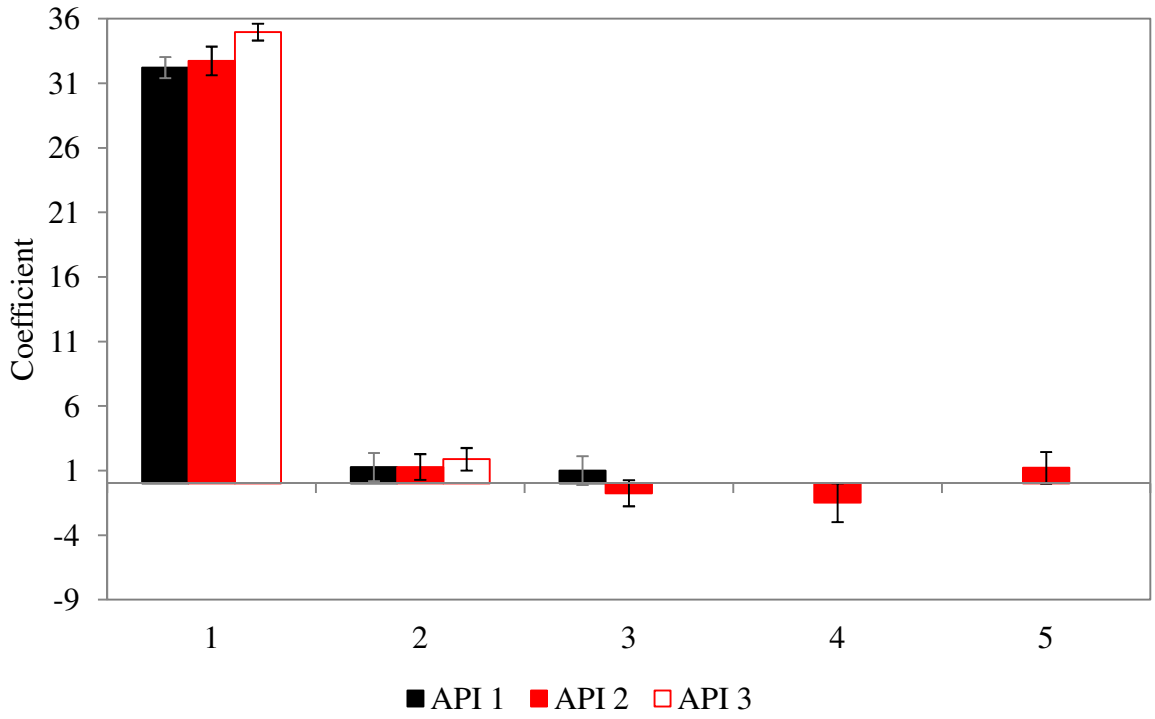


**Figure 7-20 – Regression coefficients for the mass percent of granule retained on sieve size 40 model for API 1 and API 3 with confidence intervals.**

#### 7.4.1.2.3 Tablet compaction and performance

##### 7.4.1.2.3.1 Main compression force

As discussed previously, the strategy applied during tabletting was to manufacture tablets with hardness in the range of 10-11 SCU, as such the main compression force applied was the minimum required to obtain a tablet with the specified hardness. Regression analysis for main compression force during tabletting indicates that roll pressure was the only DoE factor which has a significant impact for API 1 and 2 whilst roll pressure, and the quadratic roll gap term was calculated to have a significant impact on the main compression force response of API 3.

The regression model for the main compression force of API 1, API 2 and API 3 are given in Equation 7-13 to Equation 7-15 respectively.

$$F_{API\ 1} = 5.635 + 0.520(RP) \quad \textbf{Equation 7-13}$$

$$F_{API\ 2} = 6.647 + 0.483(RP) \quad \textbf{Equation 7-14}$$

$$\mathrm{F}_{API\ 3} = 2.64 + 0.15(RP) + 0.07(\mathrm{RG}) - 0.19(\mathrm{RG}^2) \quad \textbf{Equation 7-15}$$

The model for the main compression force is not as accurate for API 1 and API 2, however the experimental data is well modelled for API 3, as demonstrated by the $R^2$ values (API 1 = 0.52, API 2 = 0.48, API 3 = 0.84).

As one might expect the positive coefficient for roll pressure indicates that applying more force at the roller compaction stage necessitates the need for more force to be applied at the tablet compaction stage, this is a common observation in the roller compaction literature. The coefficient for the linear term for roll gap is not significant; however, it must be included since the quadratic term for roll gap is significant. The negative coefficient indicates that an increase in roll gap results in a reduction in main compression force during tabletting. It has been hypothesised that an increase in roll gap leads to less transmission of forces through the roller compacted ribbon, as such the centre of the ribbon is likely to be less compacted that the upper and lower outer edge. The variability in density through the thickness of the ribbon is likely to increase as the thickness of the ribbon is increased and thus the material within the centre of the roller compacted ribbon will have experience less compaction and hence will retain compressibility. The observation of a negative coefficient for the quadratic roll gap term may capture this hypothesis. However, from the main effects plot of the actual data it can be seen that main compression force either increases or stays constant with increasing roll gap (see Figure 7-21).

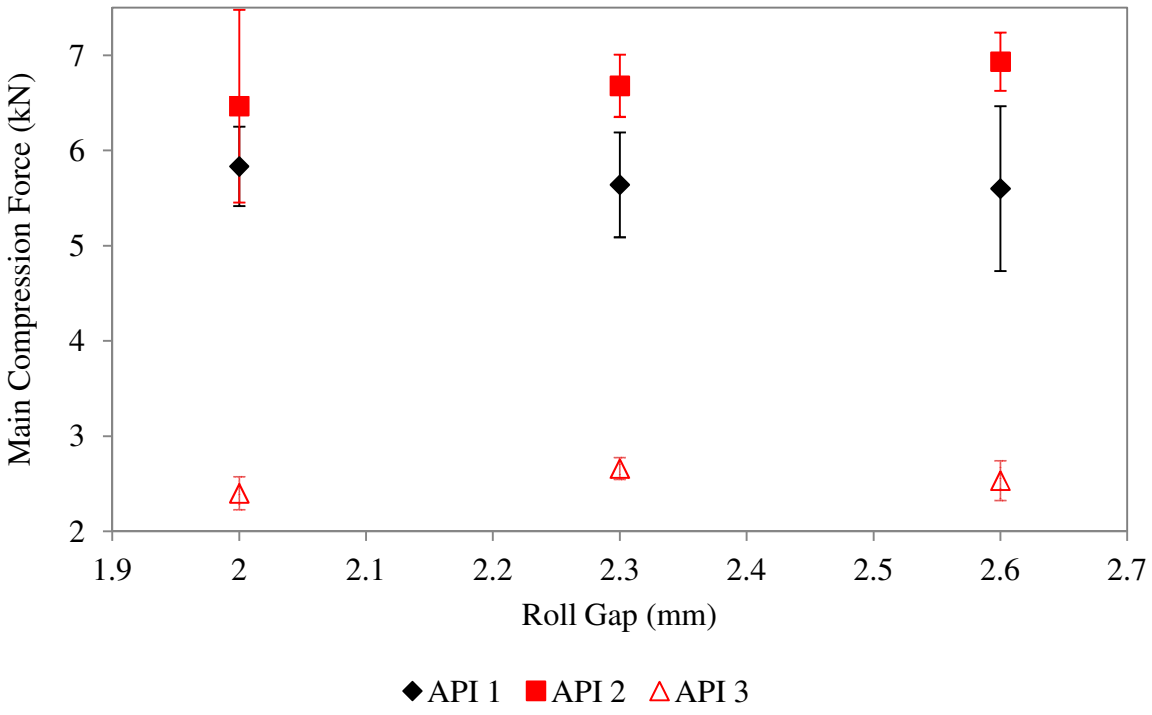


**Figure 7-21 – Main effects plot for the main compression force (kN) as a function of roll gap (mm).**

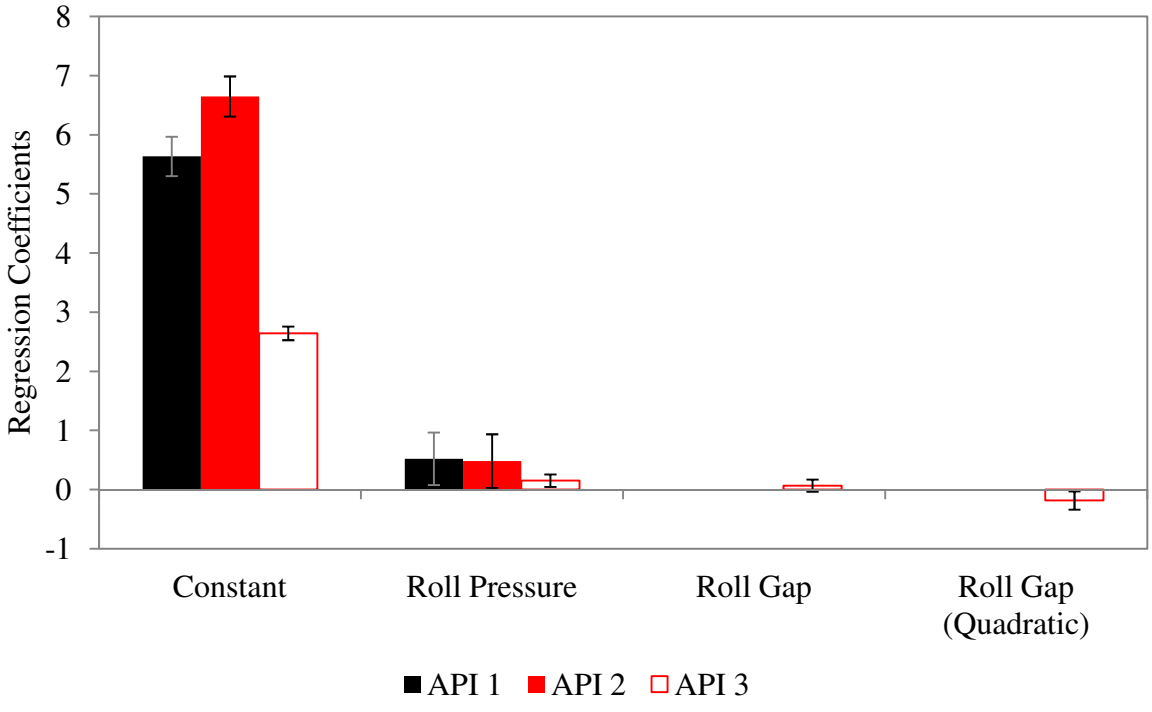


**Figure 7-22 – Regression coefficients for the main compression force model for API 1, API 2 and API 3 with confidence intervals.**

To determine whether the impact of roll pressure on the main compression force of the three API lots is statistically different the confidence intervals of the coefficients are

calculated as shown in Figure 7-22. It can be seen that the confidence intervals for the regression coefficients for roll pressure of the two similar API lots overlap indicating that there is no statistically significant difference of the impact of the DoE factor on the main compression force during tabletting of API 1 and API 2. However, there is no overlap between the confidence intervals for the constant coefficient. However in contrast it can be observed that there is a clear distinction between the constant coefficient for API 1 and API 3. However, there is an overlap in the confidence intervals of the roll pressure coefficients showing that the main compression responds in a similar manner to a change in roll pressure for both API 1 and API 3. Furthermore the confidence intervals for all the DoE terms of each compound almost cross the Y = 0 axis, indicating that the impact on main compression force due changes of the DoE factors is minimal.

#### 7.4.1.2.3.2 Fill depth

From the calculated response surface for fill depth it was observed that none of the DoE factors were significant for API 1 and API 2 whilst both the linear and quadratic roll pressure terms were observed to be significant for API 3. The R squared value for the regression models were 0.529, 0.449 and 0.972 for API 1, API 2 and API 3 respectively. The low R square value for API 1 compared to API 3 is to be expected because there was no significant impact of the DoE factors on the fill depth for API 1, as such the DoE factors don't explain the variability observed. The reduced regression model for API 3, including linear and quadratic roll pressure terms only, is given in Equation 7-16:

$$\text{Fill Depth}_{API\,3} = 7.17 - 0.07(RP) - 0.01(\text{RP}^2) \qquad \textbf{Equation 7-16}$$

The negative coefficients for the linear and quadratic roll pressure terms indicate that an increase in roll pressure elicits a reduction in fill height during tabletting. Since the tablet weight is controlled at 100 mg for all compaction conditions the reduction in die fill depth

indicates an increase in the packing density during die fill. This observation is in agreement with the regression model presented for the tap density of API 3, which indicated that an increase in roll pressure elicits an increase in tap density (and hence increase in packing density). This correlation between tapped density and die fill depth can be confirmed in Figure 7-23 where it is observed that an increase in tapped density results in a decrease in fill depth.

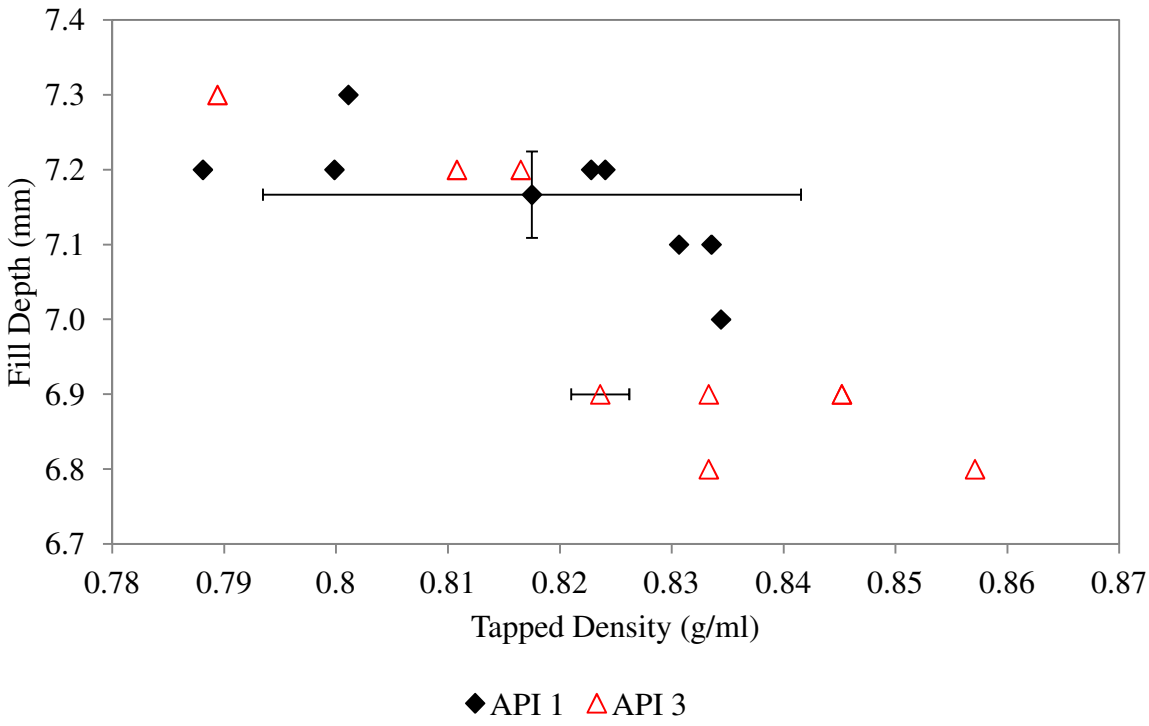


**Figure 7-23 – Tablet die fill depth as a function of granule tapped density for API 1 and API 3, error bars show the standard deviation of the centre point repeats.**

#### 7.4.1.2.3.3 Disintegration time

The response surface analysis for disintegration time indicated that roll pressure had a significant impact on the disintegration of API 3; whilst none of the DoE factors were calculated to have a significant effect on the disintegration time of API 1 and API 2. The regression model for API 3 is given in Equation 7-17:

$$\text{Disintegration Time}_{API\,3} = 9.67 + 0.55(RP) \qquad \textbf{Equation 7-17}$$

The positive coefficient for roll pressure shows that increasing the roll pressure during roller compaction increasing the disintegration time of the tablets. This is potentially due to the increase in granule density, observed as an increase in envelope density for API 3 in section 7.4.1.2.1.2. The increase in granule density will impede the uptake of water during disintegration and hence increase the disintegration time of the tablet. The confidence intervals for the regression coefficients are given in Figure 7-24, it can be observed that there is a significant difference between the constant coefficients of the two APIs, which translates the differences noted in section 7.4.1.1.3.2.

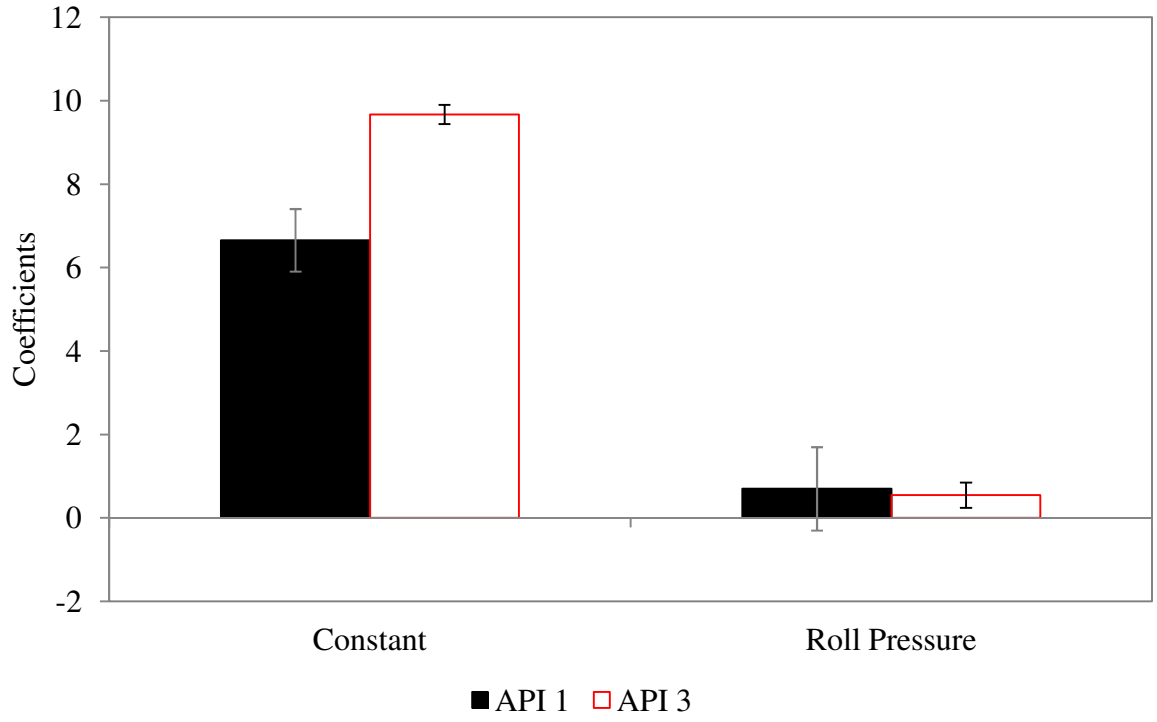


**Figure 7-24 - Regression coefficients for the disintegration time model for API 1 and API 3 with confidence intervals.**

### 7.4.2 Sensitivity analysis results

As discussed previously in section 0, the experimental levels used for the DoE factor roll pressure, were not strictly orthogonal since the centre point was slightly off centre (low = 40 bar, high = 65 bar, actual centre point used = 55 bar, true centre = 52.5 bar). Using the true centre point would give the experimental design rotatability, which would ensure that each of

the experimental conditions contributes equally to the total information, and gives the same precision in all directions from the centre. Furthermore, in an orthogonal design all of the terms are independent. As such since the centre point for roll pressure is closer to the high level for pressure the design is not rotatable, and the interpolation precision of the regression models may be reduced between the centre point and the low level. The influence of the non orthogonal design on the precision of the regression model was investigated. Two regression models were derived from the response data for ribbon tensile strength (API 1 formulation); the first regression model used the actual centre points for roll pressure, whilst the second regression model used the true experimental centre for the roll pressure. The response data for tensile strength was the same for both regression models. The derived model coefficients are shown in Figure 7-25 it can be seen that the derived coefficients are in close agreement; furthermore the coefficient confidence intervals from each model are observed to overlap suggesting that there is no significant difference between the coefficients for each model. Figure 7-26 shows the predicted response from the true centre model versus the predicted response from the actual centre model. The predicted response data sets from the two models were observed to be highly correlated ($R^2$ = 0.998), and there is no significant difference between the two predicted data sets (ANOVA, P-value = 1.000).

To further test the sensitivity of the model, random noise (between ± 10%) was added to the response predicted using the regression model with the actual centre point that was used in the experimental data. 200 ‘new’ response data sets were generated using this method and the regression coefficients were derived for each of the response data sets. The model coefficients derived for each run are given in Figure 7-27, it can be seen that whilst the model coefficients fluctuate above and below the actual centre model coefficients they are well within the confidence limits suggesting that there is no significant difference between the

'noise' generated regression coefficients and the actual centre points model coefficients. Furthermore there were no significant differences between the predicted responses from each of the 'noise' generated models (ANOVA, P = 1.000).

In summary, it was observed that there were no significant differences in the coefficients derived from the ribbon tensile strength data, and hence it is expected that the precision of the regression models is not influenced by the lack of true orthogonal experimental design. The experimental design analysed in this chapter deviated slightly from a true orthogonal because the centre point for the roll pressure was slightly off centre compared to the low and high limits. The potential limitation of such an experimental design is that the precision of any interpolated responses may be reduced. The regression coefficients derived from experimental response data were tested for their sensitivity to both fluctuations in the roll pressure centre point and error in the response data.

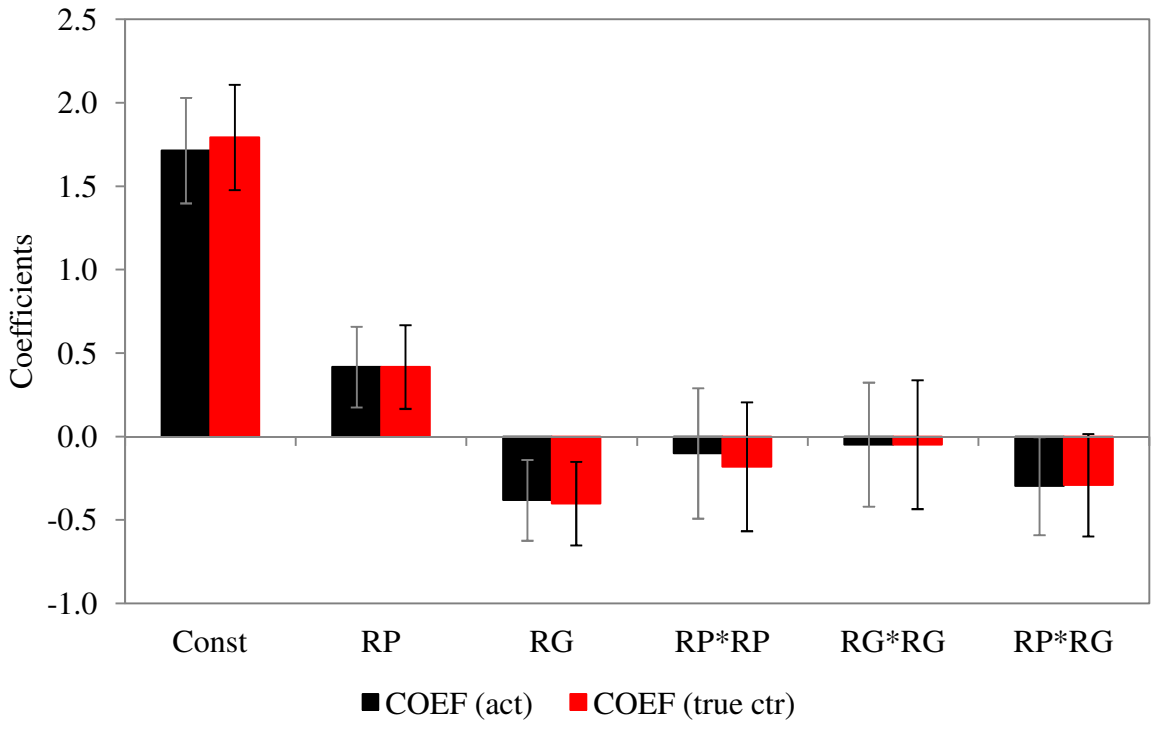


**Figure 7-25 – Regression model coefficients (coded data) for ribbon tensile strength of API 1, for (1) black bars – actual centre roll pressure = 55 bar, and (2) red bars – true centre roll pressure = 52.5 bar. Error bars show confidence intervals. (const = constant, RP = roll pressure and RG = roll gap).**

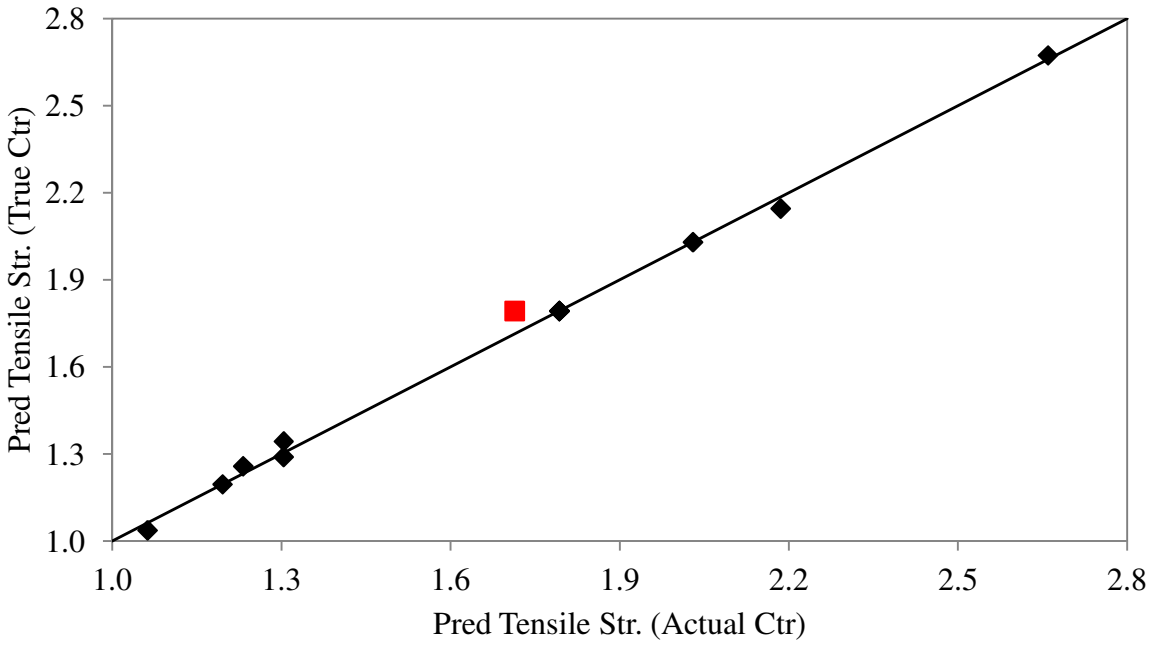


**Figure 7-26 – Predicted ribbon tensile strength response data using the true centre regression model against the predicted ribbon tensile strength response data using the actual centre regression model. The highlighted data point shows the tensile strength predicted using each regression model at the true experimental centre (i.e. roll pressure = 52.5 bar and roll gap = 2.3 mm).**

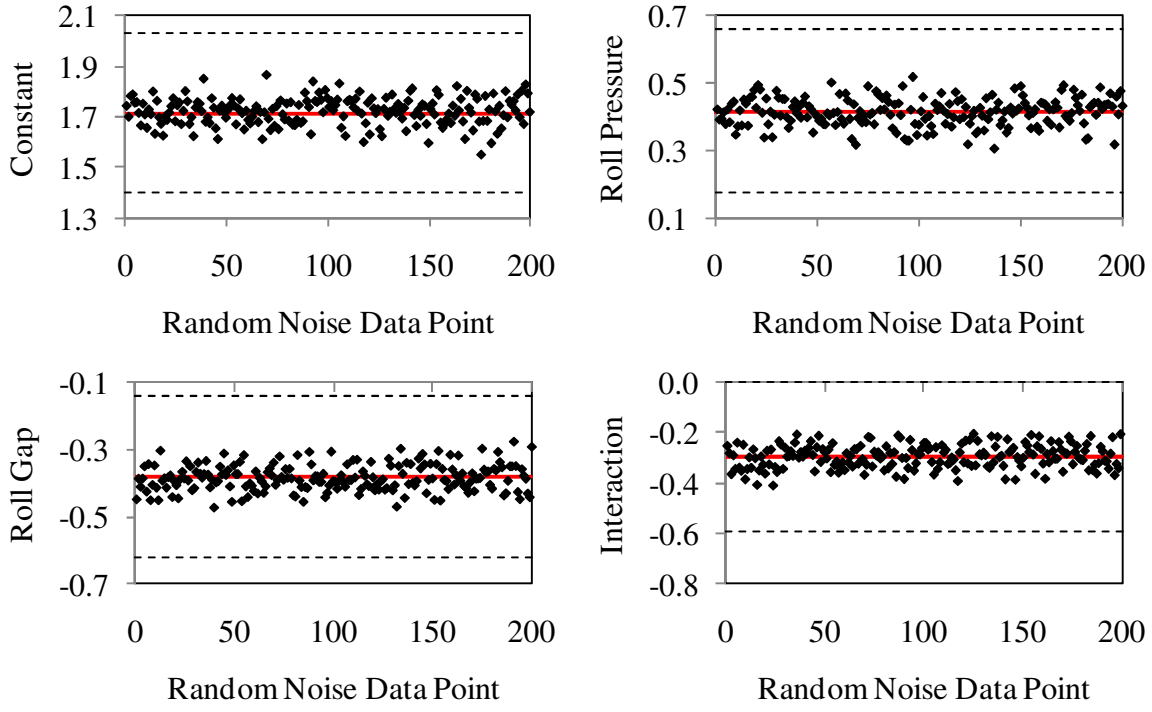


**Figure 7-27 – Regression model coefficients calculated from the regression analysis of the 'noise' contaminated tensile strength response data. The red line represents the actual regression coefficients, whilst the upper and lower black dashed lines represent the confidence interval.**

## 7.5 Conclusion

A statistical analysis has been conducted in order to determine (1) whether a material with similar material properties can be used as surrogate during process development, and (2) if two API lots (API 1 and API 3) with dissimilar material properties deviate in terms of the process parameters required to formulate the product and the properties of the intermediate products. A design of experiments was followed which used roll gap and roll pressure as input variables (factors). The statistical analysis was carried out in two parts; initially analysis of variance was used to determine if the there were any statistically significant differences between the roller compaction performance of the three API lots. For the responses that were indicated as being significantly different regression and response surface analysis was used to determine if the outputs were impacted by the DoE factors in a similar way.

The results from the ANOVA test for the similar APIs showed that there were some statistically significant differences between the responses of API 1 and API 2. Of those factors which indicated significant differences regression analysis was used. It was found that for ribbon tensile strength both roll gap and roll pressure had a significant impact, whereas for main compression force only the roll pressure had a significant impact. The confidence intervals of the regression coefficients were calculated and compared for the two API lots, the overlapping of the confidence intervals for each of the regression coefficients indicate that the two APIs respond in a similar way.

In contrast the results from the ANOVA test for the dissimilar APIs showed that there were significant differences in a number of measured responses of both the process parameters required to manufacture tablets within the required target weight and hardness range and also in the measured responses of the intermediate product properties. Of those responses calculated to have statistically significant differences it was found that the response

to changes in the DoE factors, *i.e.* roll pressure and roll gap, was statistically similar. However the constant coefficient, which determines the level of the response at the centre point of the DoE, was found to significantly different between API 1 and API 3. This offset in the actual values of the response confirms that statistically significant differences exist between the two dissimilar APIs.

Although some of the responses measured for API 1 and API 2 showed that there were some statistically significant differences in the responses measured, put into the context of the differences of responses between API 1 and API 3 it can be concluded that the small differences between the response of API 1 and API 2 are of no practical significance.

The learning that can be taken forward from the surrogate API study is that firstly any investigational API with material properties that fall within the two extremes of API 1 and API 3 (API 1 and API 3 have the most dissimilar properties in the current BMS API inventory) can be successfully roller compacted at a 10 % drug loading. The target tablet weight and hardness could be achieved with all three compounds tested, but for API 1 and API 2 this was achieved at the expense of different process settings. In the case of API 1 and API 3 the process settings to achieve the target weight and hardness were similar. If the API in development is in short supply or costly to make, then another API with suitably similar material properties can be used as a surrogate to identify the required range of processing parameters and intermediate product properties.

# CHAPTER 8

# OVERALL CONCLUSIONS AND SUGGESTIONS FOR FURTHER WORK

# CHAPTER 8

# OVERALL CONCLUSIONS AND SUGGESTIONS FOR FURTHER WORK

## 8.1 Overall conclusions

A systematic study of the impact of lubrication of pharmaceutical formulations during roller compaction has been carried out. The major conclusions that can be drawn from this study are thus:

- Magnesium stearate has a profound effect on the transition of powder through the hopper and feed auger assembly; roller compacted ribbon mass throughput and consequentially roll gap were significantly increased. The increase in ribbon mass throughput was accompanied by an increase in nip angle indicative of increased powder densification in the pre-nip region immediately before the rollers.
- The shear induced mixing that a powder experiences as it transitions through the hopper and auger feeder assembly may further increase the lubricity of the formulation which may have an unpredictable effect on the quality attributes of the final product, particularly on scale up where the shear forces involved will increase.

- The pressure applied across the width of the ribbon is more homogenous when magnesium stearate is added to the formulation. The pressure applied during roller compaction is lower when magnesium stearate is mixed in the formulation.
- Magnesium stearate reduces the tablet tensile strength of the roller compacted ribbons which upon milling produces granules with a smaller particle size distribution.
- The beneficial impact of magnesium stearate on the roller compaction process is apparent at much lower concentrations than the 0.5% w/w which is typically added to the formulation. Furthermore, at these low levels of addition, increasing the mixing time with magnesium stearate (which usually further increases the deleterious effects of magnesium stearate) actually increases ribbon tensile strength.

The novel use of a technique to externally apply magnesium stearate to the roll surface during roller compaction has been investigated in the first instance.

- Magnesium stearate internally blended within a formulation prevents the adhesion of pharmaceutical formulation to the roll surface. The direct application of external lubrication at the roll surface is sufficient to prevent roll adhesion even in the absence of internal lubrication.
- The amount of magnesium stearate which will be transferred from the roll surface to the surface of the roller compacted ribbon (and hence be contained in the final tablet product) is significantly less than the amount that is commonly added to the bulk formulation.
- A scalable parameter; travelling roll distance per shot ($D_{pS}$), has been defined which ensures that an equal amount of magnesium stearate is applied to the roll surface per rotation at any roll speed and roll dimension.

- The minimum required travelling roll distance per shot to prevent adhesion is material dependent, and may be used as a qualitative indication of the relative adhesiveness of pharmaceutical formulations.

A novel alternative range of lubricants (LubriTose™) and sodium stearyl fumarate (Alubra™) have been studied to investigate their effect on the roller compaction process and subsequent tabletting of the granules. It can be concluded that:

- Use of LubriTose™ and sodium stearyl fumarate in the pre-roller compaction formulation provide an equivalent effect to magnesium stearate.
- LubriTose™ granules retain equivalent lubricating properties to the initial powder blend following roller compaction, tablet ejection force of tablets compacted from the LubriTose™ granules were lower than the ejection force of tablets from the initial powder blend. This was not observed with the magnesium stearate and Alubra tablets, where the ejection force of the tablets compacted from the granule were significantly higher than that of the initial powder (without the addition of extra-granular lubrication).
- Atenolol is noted for its highly adhesive properties; roller compaction of formulations containing as high as 1% w/w magnesium stearate/Alubra and following complete substitution of microcrystalline cellulose and lactose for LubriTose™ was inadequate to prevent powder adhesion to the rollers during roller compaction. A drug product exhibiting such high adhesive properties would be a good candidate for the external lubrication technique.
- The hydrophilic lubricant Alubra had least effect on Atenolol tablet dissolution, followed by magnesium stearate. The biggest impact on drug dissolution was observed

for the LubriTose™ tablets. The dissolution testing of tablets was performed on tablets containing intra-granular lubricant only.

With respect to the surrogate active pharmaceutical ingredient project, the major conclusions drawn from the statistical analysis that was carried out are:

- Roller compaction and tablet manufacturing performance of a material that is in short supply or costly to make can be reasonably well characterised by using another product in the R&D inventory that has exhibits similar material properties.
- The similarity in manufacturing performance of two materials with similar material properties was supported by the statistical analysis of the manufacturing of two materials exhibiting differences in material properties. Whilst tablets from the two different materials could be manufactured to the same tablet hardness endpoint, they were so at the expense of different manufacturing settings. Therefore no accurate process settings could be derived from processing materials with different material properties.

## 8.2 Suggestions for further work

- External lubrication has been applied to the roll surface during roller compaction and it has been observed that the roller compacted granule will contain significantly less magnesium stearate than would be used when magnesium stearate is added to the formulation internally. Coupling the external lubrication during roller compaction with a fully externally lubricated tablet press may have significant advantages to the quality properties of the final tablet product.
- A more fundamental study on the surface energy and adhesion properties of different pharmaceutical formulations may elucidate correlations between the minimum

required travelling roll distance per shot to prevent adhesion to the roll surface and the adhesion properties of the formulation, it would also be beneficial to investigate the surface coverage of magnesium stearate on the roll surface to identify (1) the magnesium stearate layer thickness; and (2) to assess what percentage of the roll surface actually contains magnesium stearate particles vs. what percentage of the roll surface is 'clean' and the homogeneity of the surface coating across the width and length (circumference) of the roller.

- The increase in mass throughput is a particular benefit of adding magnesium stearate to the formulation pre-roller compaction. Experimental evidence from this study has shown that the increase in mass throughput is partly due to the effect of friction at the surface of the auger feeder. The effect of alternative materials of construction of the auger feeder on roller compactor throughput should be investigated.

## References

Akseli, I., Iyer, S., Lee, H. P., and Cuitino, A. M., A quantitative correlation of the effect of density distributions in roller-compacted ribbons on the mechanical properties of tablets using ultrasonics and X-ray Tomography. American Association of Pharmaceutical Scientists, 2011; 12(3):834-853.

Alexanderwerk AG, Alexanderwerk WP120 instruction manual. Remscheid/Germany.

Almaya, A. and Aburub, A., Effect of particle size on compaction of materials with different deformation mechanisms with and without lubricants. AAPS PharmSciTech, 2008; 9(2):414-418.

Aoshima, H., Miyagisnima, A., Nozawa, Y., Sadzuka, Y., and Sonobe, T., Glycerin fatty acid esters as a new lubricant of tablets. International Journal of Pharmaceutics, 2005; 293(1-2):25-34.

Arida, A. I. and Al-Tabakha, M. M., Cellactose® a co-processed excipient: A comparison study. Pharmaceutical Development and Technology, 2008; 13(2):165-175.

Armstrong, N. A. and James, K. C., *Pharmaceutical Experimental Design and Interpretation*. Pharmaceutical Sciences, ed. M.H. Rubinstein and C.G. Wilson. 1996, London: Taylor & Francis.

Atkins, P. and de Paula, J., *Physical Chemistry*. 2006: W. H. Freeman.

Bacher, C., Olsen, P. M., Bertelsen, P., Kristensen, J., and Sonnergaard, J. M., Improving the compaction properties of roller compacted calcium carbonate. International Journal of Pharmaceutics, 2007; 342(1-2):115-123.

Bacher, C., Olsen, P. M., Bertelsen, P., and Sonnergaard, J. M., Compressibility and compactibility of granules produced by wet and dry granulation. International Journal of Pharmaceutics, 2008a; 358(1-2):69-74.

Bacher, C., Olsen, P. M., Bertelsen, P., and Sonnergaard, J. M., Granule fraction inhomogeneity of calcium carbonate/sorbitol in roller compacted granules. International Journal of Pharmaceutics, 2008b; 349(1-2):19-23.

Bailey, A. G., Electrostatic phenomena during powder handling. Powder Technology, 1984; 37(1):71-85.

Balicki, M. and Michrafy, A., Numerical methods for predicting roll press powder compaction parameters. 2003.

Barra, J. and Somma, R., Influence of the physicochemical variability of magnesium stearate on its lubricant properties: Possible solutions. Drug Development and Industrial Pharmacy, 1996; 22(11):1105-1120.

Billany, M. R. and Richards, J. H., Batch variation of magnesium stearate and its effect on the dissolution rate of salicylic acid from solid dosage forms. Drug Development and Industrial Pharmacy, 1982; 8(4):497-511.

Bindhumadhavan, G., Seville, J. P. K., Adams, M. J., Greenwood, R. W., and Fitzpatrick, S., Roll compaction of a pharmaceutical excipient: Experimental validation of rolling theory for granular solids. Chemical Engineering Science, 2005; 60(14):3891-3897.

Bozic, D. Z., Dreu, R., and Vrecer, F., Influence of dry granulation on compactibility and capping tendency of macrolide antibiotic formulation. International Journal of Pharmaceutics, 2008; 357(1-2):44-54.

Bracconi, P., Andrès, C., and Ndiaye, A., Structural properties of magnesium stearate pseudopolymorphs: Effect of temperature. International Journal of Pharmaceutics, 2003; 262(1-2):109-124.

Bultmann, J. M., Multiple compaction of microcrystalline cellulose in a roller compactor. *Eur. J. Pharm. Biopharm.*, 2002; 54(1):59-64.

Carr, J. F. and Walker, D. M., An annular shear cell for granular materials. Powder Technology, 1968; 1(6):369-373.

Chang, C. K., Alvarez-Nunez, F. A., Rinella Jr, J. V., Magnusson, L. E., and Sueda, K., Roller compaction, granulation and capsule product dissolution of drug formulations containing a lactose or mannitol filler, starch, and talc. AAPS PharmSciTech, 2008; 9(2):597-604.

Chowhan, Z. T. and Chi, L. H., Drug-excipient interactions resulting from powder mixing IV: Role of lubricants and their effect on in vitro dissolution. Journal of Pharmaceutical Sciences, 1986; 75(6):542-545.

Daugherity, P. D. and Chu, J. H., Investigation of serrated roll surface differences on ribbon thickness during roller compaction. Pharmaceutical Development and Technology, 2007; 12(6):603-608.

Dec, R. T., Zavaliangos, A., and Cunningham, J. C., Comparison of various modeling methods for analysis of powder compaction in roller press. Powder Technology, 2003; 130(1-3):265-271.

Desai, D. S., Rubitski, B. A., Varia, S. A., and Newman, A. W., Physical interactions of magnesium stearate with starch-derived disintegrants and their effects on capsule and tablet dissolution. International Journal of Pharmaceutics, 1993; 91(2-3):217-226.

Dürig, T. and Fassihi, R., Mechanistic evaluation of binary effects of magnesium stearate and talc as dissolution retardants at 85% drug loading in an experimental extended- release formulation. Journal of Pharmaceutical Sciences, 1997; 86(10):1092-1098.

Engers, D. A., Fricke, M. N., Storey, R. P., Newman, A. W., and Morris, K. R., Triboelectrification of pharmaceutically relevant powders during low-shear tumble blending. Journal of Electrostatics, 2006; 64(12):826-835.

Ertel, K. D. and Carstensen, J. T., An examination of the physical properties of pure magnesium stearate. International Journal of Pharmaceutics, 1988; 42(1-3):171-180.

Falzone, A. M., Peck, G. E., and McCabe, G. P., Effects of changes in roller compactor parameters on granulations produced by compaction. Drug Development and Industrial Pharmacy, 1992; 18(4):469-489.

Faqih, A., Alexander, A., Muzzio, F., and Tomassone, M., A method for predicting hopper flow characteristics of pharmaceutical powders. *Chem. Eng. Sci*, 2007a; 62(5):1536-1542.

Faqih, A. M. N., Mehrotra, A., Hammond, S. V., and Muzzio, F. J., Effect of moisture and magnesium stearate concentration on flow properties of cohesive granular materials. International Journal of Pharmaceutics, 2007b; 336(2):338-345.

Feng, T., Wang, F., Pinal, R., Wassgren, C., and Carvajal, M. T., Investigation of the variability of NIR in-line monitoring of roller compaction process by using fast fourier transform (FFT) analysis. AAPS PharmSciTech, 2008; 9(2):419-424.

Freeman, R., New Insights into powder flowability. Innovations in Food Technology, 2001.

Freeman, R., The importance of air content on the rheology of powder: An emperical study. American Laboratory News, 2004.

Freeman, R., Measuring the flow properties of consolidated, conditioned and aerated powders - A comparative study using a powder rheometer and a rotational shear cell. Powder Technology, 2007; 174(1-2):25-33.

Freeman, R. E., Cooke, J. R., and Schneider, L. C. R., Measuring shear properties and normal stresses generated within a rotational shear cell for consolidated and non-consolidated powders. Powder Technology, 2009; 190(1-2):65-69.

Freitag, F. and Kleinebudde, P., How do roll compaction/dry granulation affect the tableting behaviour of inorganic materials? Comparison of four magnesium carbonates. European Journal of Pharmaceutical Sciences, 2003; 19(4):281-289.

Freitag, F., Reincke, K., Runge, J., Grellmann, W., and Kleinebudde, P., How do roll compaction/dry granulation affect the tableting behaviour of inorganic materials?: Microhardness of ribbons and mercury porosimetry measurements of tablets. European Journal of Pharmaceutical Sciences, 2004; 22(4):325-333.

Fukui, E., Miyamura, N., and Kobayashi, M., Effect of magnesium stearate or calcium stearate as additives on dissolution profiles of diltiazem hydrochloride from press-coated tablets with hydroxypropylmethylcellulose acetate succinate in the outer shell. International Journal of Pharmaceutics, 2001; 216(1-2):137-146.

Gamble, J. F., Tobyn, M., Dennis, A. B., and Shah, T., Roller compaction: Application of an in-gap ribbon porosity calculation for the optimization of downstream granule flow and compactability characteristics. Pharmaceutical Development and Technology, 2010; 15(3):223-229.

Gereg, G. W. and Cappola, M. L., Roller compaction feasibility for new drug candidates laboratory to production scale. Pharmaceutical Technology, 2002; Tabletting & Granulation:14-23.

Ghorab, M. K., Chatlapalli, R., Hasan, S., and Nagi, A., Application of thermal effusivity as a process analytical technology tool for monitoring and control of the roller compaction process. AAPS PharmSciTech, 2007; 8(1).

Gruber, P., Glasel, V. I., Klingelholler, W., and Liske, T., Direct lubrication of tablet tools, a contribution to the optimization of tablet manufacture. Drugs Made in Germany, 1991; 34(1):24-30.

Guest, R., *Croscarmellose Sodium Monograph*, in *Handbook of pharmaceutical excipients*, R.C. Rowe, P.J. Sheskey, and M.E. Quinn, Editors. 2009, Pharmaceutical Press: London.

Guigon, P. and Simon, O., Roll press design - Influence of force feed systems on compaction. Powder Technology, 2003; 130(1-3):41-48.

Gupta, A., Peck, G. E., Miller, R. W., and Morris, K. R., Nondestructive Measurements of the Compact Strength and the Particle-Size Distribution after Milling of Roller Compacted Powders by Near-Infrared Spectroscopy. Journal of Pharmaceutical Sciences, 2004; 93(4):1047-1053.

Gupta, A., Peck, G. E., Miller, R. W., and Morris, K. R., Influence of ambient moisture on the compaction behavior of microcrystalline cellulose powder undergoing uni-axial compression and roller-compaction: A comparative study using near-infrared spectroscopy. Journal of Pharmaceutical Sciences, 2005a; 94(10):2301-2313.

Gupta, A., Peck, G. E., Miller, R. W., and Morris, K. R., Real-time near-infrared monitoring of content uniformity, moisture content, compact density/tensile strength, and young's modulus of roller compacted powder blends. Journal of Pharmaceutical Sciences, 2005b; 94(7):1589-1597.

Hamad, M. L., Gupta, A., Shah, R. B., Lyon, R. C., Sayeed, V. A., and Khan, M. A., Functionality of magnesium stearate derived from bovine and vegetable sources: Dry granulated tablets. Journal of Pharmaceutical Sciences, 2008; 97(12):5328-5340.

Hamdan, I. M., Reklaitis, G. V., and Venkatasubramanian, V., Exceptional events management applied to roller compaction of pharmaceutical powders. Journal of Pharmaceutical Innovation, 2010; 5(4):147-160.

Hariharan, M., Wowchuk, C., Nkansah, P., and Gupta, V. K., Effect of formulation composition on the properties of controlled release tablets prepared by roller compaction. Drug Development and Industrial Pharmacy, 2004; 30(6):565-572.

He, X., Secreast, P. J., and Amidon, G. E., Mechanistic study of the effect of roller compaction and lubricant on tablet mechanical strength. Journal of Pharmaceutical Sciences, 2007; 96(5):1342-1355.

Hein, S., Picker-Freyer, K. M., and Langridge, J., Simulation of roller compaction with subsequent tableting and characterization of lactose and microcrystalline cellulose. Pharmaceutical Development and Technology, 2008; 13(6):523-532.

Herting, M. G. and Kleinebudde, P., Roll compaction/dry granulation: Effect of raw material particle size on granule and tablet properties. International Journal of Pharmaceutics, 2007; 338(1-2):110-118.

Herting, M. G. and Kleinebudde, P., Studies on the reduction of tensile strength of tablets after roll compaction/dry granulation. European Journal of Pharmaceutics and Biopharmaceutics, 2008; 70(1):372-379.

Hervieu, P. and Dehont, F., Granulation of pharmaceutical powders by compaction. An experimental study. Drug Development and Industrial Pharmacy, 1994; 20(1):65-74.

Hussain, M. S. H., *Magnesium Stearate Lubrication in Pharmaceutical Processes*, in *Postgraduate School of Studies in Pharmacy*. 1988, University of Bradford: Bradford.

Inghelbrecht, S. and Paul Remon, J., The roller compaction of different types of lactose. International Journal of Pharmaceutics, 1998; 166(2):135-144.

Inghelbrecht, S. and Remon, J. P., Reducing dust and improving granule and tablet quality in the roller compaction process. International Journal of Pharmaceutics, 1998a; 171(2):195-206.

Inghelbrecht, S. and Remon, J. P., Roller compaction and tableting of microcrystalline cellulose/drug mixtures. International Journal of Pharmaceutics, 1998b; 161(2):215-224.

Jahn, T. and Steffens, K. J., Press chamber coating as external lubrication for high speed rotary presses: Lubricant spray rate optimization. Drug Development and Industrial Pharmacy, 2005; 31(10):951-957.

Jenike, A. W. and Shield, R. T., On the plastic flow of coulomb solids beyond original failure. Journal of Applied Mechanics 26, Trans., 1959; ASME(81):599-602.

Johanson, J. R., A Rolling Theory for Granular Solids. Journal of Applied Mechanics, 1965:842-848.

Johnson, K. L., Kendall, K., and Roberts, A. D., Surface energy and the contact of elastic solids. Proceedings of the Royal Society of London. Series A, Mathematical and Physical Sciences, 1971; 324(1558):301-313.

Jonat, S., Hasenzahl, S., Gray, A., and Schmidt, P. C., Mechanism of glidants: Investigation of the effect of different colloidal silicon dioxide types on powder flow by atomic force and scanning electron microscopy. Journal of Pharmaceutical Sciences, 2004; 93(10):2635-2644.

Kauffman, J. F., Tumuluri, V., Guo, C., Spencer, J. A., Doub, W. H., Nichols, G. A., Randle, S. R., and Wu, S., Near infrared spectroscopy of magnesium stearate hydrates and multivariate calibration of pseudopolymorph composition. Journal of Pharmaceutical Sciences, 2008; 97(7):2757-2767.

Khirwadkar, P. and Dashora, K., Formulation and Evaluation of Fast Dissoloving Tablets Atenolol. Journal of Chemical and Pharmaceutical Sciences, 2013; 6(2):113-119.

Kikuta, J.-I. and Kitamori, N., Effect of Mixing Time on the Lubricating Properties of Magnesium Stearate and the Final Characteristics of the Compressed Tablets. Drug Development and Industrial Pharmacy, 1994; 20(3):343-355.

Kleinebudde, P., Roll compaction/dry granulation: Pharmaceutical applications. European Journal of Pharmaceutics and Biopharmaceutics, 2004; 58(2):317-326.

Korachkin, D., Gethin, D. T., Lewis, R. W., and Tweed, J. H., Friction measurement and lubrication in unloading and ejection stages in powder pressing cycle. Powder Metallurgy, 2008; 51(1):14-30.

Kushner IV, J. and Moore, F., Scale-up model describing the impact of lubrication on tablet tensile strength. International Journal of Pharmaceutics, 2010; 399(1-2):19-30.

Lecompte, T., Doremus, P., Thomas, G., Perier-Camby, L., Le Thiesse, J. C., Masteau, J. C., and Debove, L., Dry granulation of organic powders - Dependence of pressure 2D-distribution on different process parameters. Chemical Engineering Science, 2005; 60(14):3933-3940.

Lee, J., Intrinsic adhesion force of lubricants to steel surface. Journal of Pharmaceutical Sciences, 2004; 93(9):2310-2318.

Léonard, G. and Abatzoglou, N., Stress distribution in lubricated vs unlubricated pharmaceutical powder columns and their container walls during translational and torsional shear testing. Powder Technology, 2010; 203(3):534-547.

Léonard, G. and Abatzoglou, N., Lubrication of pharmaceutical powder/wall interfaces and electrostatic effects. Powder Technology, 2011; 208(1):54-62.

Lerk, C. F. and Bolhuis, G. K., Interaction of lubricants and colloidal silica during mixing with excipients. II. Its effect on wettability and dissolution velocity. Pharmaceutica Acta Helvetiae, 1977; 52(3):39-44.

Lerk, C. F., Bolhuis, G. K., and Smedema, S. S., Interaction of lubricants and colloidal silica during mixing with excipients. I. Its effect on tabletting. Pharmaceutica Acta Helvetiae, 1977; 52(3):33-39.

Lim, H., Dave, V. S., Kidder, L., Neil Lewis, E., Fahmy, R., and Hoag, S. W., Assessment of the critical factors affecting the porosity of roller compacted ribbons and the feasibility of using NIR chemical imaging to evaluate the porosity distribution. International Journal of Pharmaceutics, 2011; 410(1-2):1-8.

Liu, L. X., Marziano, I., Bentham, A. C., Litster, J. D., E.T.White, and Howes, T., Effect of particle properties on the flowability of ibuprofen powders. International Journal of Pharmaceutics, 2008; 362(1-2):109-117.

Llusa, M., Levin, M., Snee, R. D., and Muzzio, F. J., Measuring the hydrophobicity of lubricated blends of pharmaceutical excipients. Powder Technology, 2010; 198(1):101-107.

Malkowska, S. and Khan, K. A., Effect of recompression on the properties of tablets prepared by dry granulation. Drug Development and Industrial Technology, 1983; (9):331-347.

Mansa, R. F., Bridson, R. H., Greenwood, R. W., Barker, H., and Seville, J. P. K., Using intelligent software to predict the effects of formulation and processing parameters on roller compaction. Powder Technology, 2008; 181(2):217-225.

Mehrotra, A., Llusa, M., Faqih, A., Levin, M., and Muzzio, F. J., Influence of shear intensity and total shear on properties of blends and tablets of lactose and cellulose lubricated with magnesium stearate. International Journal of Pharmaceutics, 2007; 336(2):284-291.

Metcalf, J. R., The mechanics of the screw feeder. ARCHIVE: Proceedings of the Institution of Mechanical Engineers 1847-1982 (vols 1-196), 1965; 180(1965):131-146.

Meyer, K. and Zimmermann, I., Effect of glidants in binary powder mixtures. Powder Technology, 2004; 139(1):40-54.

Michrafy, A., Diarra, H., Dodds, J. A., and Michrafy, M., Experimental and numerical analyses of homogeneity over strip width in roll compaction. Powder Technology, 2011a; 206(1-2):154-160.

Michrafy, A., Diarra, H., Dodds, J. A., Michrafy, M., and Penazzi, L., Analysis of strain stress state in roller compaction process. Powder Technology, 2011b; 208(2):417-422.

Miguelez-Moran, A. M., Wu, C. Y., Dong, H., and Seville, J. P. K., Characterisation of density distributions in roller-compacted ribbons using micro-indentation and X-ray micro-computed tomography. European Journal of Pharmaceutics and Biopharmaceutics, 2009; 72(1):173-182.

Miguelez-Moran, A. M., Wu, C. Y., and Seville, J. P. K., The effect of lubrication on density distributions of roller compacted ribbons. International Journal of Pharmaceutics, 2008; 362(1-2):52-59.

Miller, R. W., *Roller compaction technology*. Handbook of pharmaceutical granulation technology, ed. D.M. Parikh. 1997, Ney York: Marcel Dekker, Inc. 99-150.

Miller, R. W. and Sheskey, P. J., *Roller compaction technology for the pharmaceutical industry*. Encyclopedia of pharmaceutical technology, ed. J. Swarbrick and J.C. Boylan. 2003, New York: Marcel Dekker. 1-19.

Miller, T. A. and York, P., Frictional assessment of magnesium stearate and palmitate lubricant powders. Powder Technology, 1985a; 44(3):219-226.

Miller, T. A. and York, P., Physical and chemical characteristics of some high purity magnesium stearate and palmitate powders. International Journal of Pharmaceutics, 1985b; 23(1):55-67.

Miller, T. A. and York, P., Pharmaceutical tablet lubrication. International Journal of Pharmaceutics, 1988; 41(1-2):1-19.

Moody, G., Rubinstein, M. H., and FitzSimmons, R. A., Tablet lubricants I. Theory and modes of action. International Journal of Pharmaceutics, 1981; 9(2):75-80.

Moore, F., Okelo, G., Colón, I., and Kushner, J., Improving the hardness of dry granulated tablets containing sodium lauryl sulfate. International Journal of Pharmaceutics, 2010; 400(1-2):37-41.

Muliadi, A. R., Litster, J. D., and Wassgren, C. R., Modeling the powder roll compaction process: Comparison of 2-D finite element method and the rolling theory for granular solids (Johanson's model). Powder Technology, 2012; 221:90-100.

Navaneethan, C. V., Missaghi, S., and Fassihi, R., Application of powder rheometer to determine powder flow properties and lubrication efficiency of pharmaceutical particulate systems. AAPS PharmSciTech, 2005; 6(3).

Nedderman, R. M., *Statics and Kinematics of Granular Materials*. 1992, Cambridge: Cambridge University Press.

Nesarikar, V. V., Patel, C., Early, W., Vatsaraj, N., Sprockel, O., and Jerzweski, R., Roller compaction process development and scale up using Johanson model calibrated with

instrumented roll data. International Journal of Pharmaceutics, 2012a; 436(1-2):486-507.

Nesarikar, V. V., Vatsaraj, N., Patel, C., Early, W., Pandey, P., Sprockel, O., Gao, Z., Jerzewski, R., Miller, R., and Levin, M., Instrumented roll technology for the design space development of roller compaction process. International Journal of Pharmaceutics, 2012b; 426(1-2):116-131.

Ong, J. T. H., Chowhan, Z. T., and Samuels, G. J., Drug-excipient interactions resulting from powder mixing. VI. Role of various surfactants. International Journal of Pharmaceutics, 1993; 96(1-3):231-242.

Otsuka, M., Yamane, I., and Matsuda, Y., Effects of lubricant mixing on compression properties of various kinds of direct compression excipients and physical properties of the tablets. Advanced Powder Technology, 2004; 15(4):477-493.

Papp, M. K., Venkatesh, G., and Harmon, T., Specialised techniques for developing odt dosage forms. ONdrugDelivery, 2010; (3):8-10.

Parrott, E. L., Densification of powders by concavo-convex roller compactor. Journal of Pharmaceutical Sciences, 1981; 70(3):288-291.

Patel, B. A., Adams, M. J., Turnbull, N., Bentham, A. C., and Wu, C. Y., Predicting the pressure distribution during roll compaction from uniaxial compaction measurements. Chemical Engineering Journal, 2010.

Patel, S., Kaushal, A. M., and Bansal, A. K., Effect of particle size and compression force on compaction behavior and derived mathematical parameters of compressibility. Pharmaceutical Research, 2007; 24(1):111-124.

Patel, S., Kaushal, A. M., and Bansal, A. K., Compaction behavior of roller compacted ibuprofen. European Journal of Pharmaceutics and Biopharmaceutics, 2008; 69(2):743-749.

Peter, S., Lammens, R. F., and Steffens, K. J., Roller compaction/Dry granulation: Use of the thin layer model for predicting densities and forces during roller compaction. Powder Technology, 2010; 199(2):165-175.

Phadke, D. S. and Eichorst, J. L., Evaluation of particle size distribution and specific surface area of magnesium stearate. Drug Development and Industrial Pharmacy, 1991; 17(6):901-906.

Pingali, K. C., Saranteas, K., Foroughi, R., and Muzzio, F. J., Practical methods for improving flow properties of active pharmaceutical ingredients. Drug Development and Industrial Pharmacy, 2009; 35(12):1460-1469.

Podczeck, F. and Miah, Y., The influence of particle size and shape on the angle of internal friction and the flow factor of unlubricated and lubricated powders. International Journal of Pharmaceutics, 1996; 144(2):187-194.

Pu, Y., Mazumder, M., and Cooney, C., Effects of electrostatic charging on pharmaceutcial powder blending homogeneity. Journal of Pharmaceutical Sciences, 2009; 98(7):2412-2420.

Ragnarsson, G., Holzer, A. W., and Sjogren, J., The influence of mixing time and colloidal silica on the lubricating properties of magnesium stearate. International Journal of Pharmaceutics, 1979; 3(2-3):127-131.

Rambali, B., Baert, L., Jans, E., and Massart, D. L., Influence of the roll compactor parameter settings and the compression pressure on the buccal bio-adhesive tablet properties. International Journal of Pharmaceutics, 2001; 220(1-2):129-140.

Rao, K. P., Chawla, G., Kaushal, A. M., and Bansal, A. K., Impact of solid-state properties on lubrication efficacy of magnesium stearate. Pharmaceutical Development and Technology, 2005; 10(3):423-437.

Rashid, I., Al-Remawi, M., Leharne, S. A., Chowdhry, B. Z., and Badwan, A., A novel multifunctional pharmaceutical excipient: Modification of the permeability of starch by processing with magnesium silicate. International Journal of Pharmaceutics, 2011; 411(1-2):18-26.

Rashid, I., Daraghmeh, N., Al-Remawi, M., Leharne, S. A., Chowdhry, B. Z., and Badwan, A., Characterization of the impact of magnesium stearate lubrication on the tableting properties of chitin-Mg silicate as a superdisintegrating binder when compared to Avicel® 200. Powder Technology, 2010; 203(3):609-619.

Rawle, A. F., *Particle Morphology and Characterization in Preformulation*. Preformulation in Solid Dosage Form Development, ed. M.C. Adeyeye and H.G. Brittain. 2008: Informa Healthcare. 145-184.

Riepma, K. A., Vromans, H., Zuurman, K., and Lerk, C. F., The effect of dry granulation on the consolidation and compaction of crystalline lactose. International Journal of Pharmaceutics, 1993; 97(1-3):29-38.

Roblot-Treupel, L. and Puisieux, F., Distribution of magnesium stearate on the surface of lubricated particles. International Journal of Pharmaceutics, 1986; 31(1-2):131-136.

Rowe, R. C., Interactions in the ternary powder system microcrystalline cellulose, magneisum sterate and colloidal silica - a solubility parameter approach. International Journal of Pharmaceutics, 1988; 45:259-261.

Salonen, J., Salmi, K., Hakanen, A., Laine, E., and Linsaari, K., Monitoring the acoustic activity of a pharmaceutical powder during roller compaction. International Journal of Pharmaceutics, 1997; 153(2):257-261.

Saw, H. Y., Davies, C. E., Jones, J. R., Brisson, G., and Paterson, A. H. J., Cohesion of lactose powders at low consolidation stresses. Advanced Powder Technology, 2013; 24(4):796-800.

Schmitt, R. and Feise, H., Influence of Tester Geometry, Speed and Procedure on the Results from a Ring Shear Tester. Particle & Particle Systems Characterization, 2004; 21(5):403-410.

Schönert, K. and Sander, U., Shear stresses and material slip in high pressure roller mills. Powder Technology, 2002; 122(2-3):136-144.

Schulze, D., Ring shear tester RST-01.01, RST-01.pc and RST-XS Instruction Manual.

Shah, A. C. and Mlodozeniec, A. R., Mechanism of surface lubrication: Influence of duration of lubricant-excipient mixing on processing characteristics of powders and properties of compressed tablets. Journal of Pharmaceutical Sciences, 1977; 66(10):1377-1382.

Shah, N. H., Stiel, D., Weiss, M., Infield, M., and Malick, W., Evaluation of two new tablet lubricants - sodium stearyl fumarate and glyceryl behenate. Measurement of physical parameters (compaction, ejection and residual forces) in the tableting process and the effect on the dissolution rate. Drug Development and Industrial Pharmacy, 1986; 12(8-9):1329-1346.

Shah, R. B., Tawakkul, M. A., and Khan, M. A., Comparative evaluation of flow for pharmaceutical powders and granules. AAPS PharmSciTech, 2008; 9(1):250-258.

Sheskey, P. J., Robb, R. T., Moore, R. D., and Boyce, B. M., Effects of lubricant level, method of mixing, and duration of mixing on a controlled-release matrix tablet containing hydroxypropyl methylcellulose. Drug Development and Industrial Pharmacy, 1995; 21(19):2151-2165.

Simon, O. and Guigon, P., Correlation between powder-packing properties and roll press compact heterogeneity. Powder Technology, 2003; 130(1-3):257-264.

Skinner, G. W., Harcum, W. W., Barnum, P. E., and Guo, J. H., The evaluation of fine-particle hydroxypropylcellulose as a roller compaction binder in pharmaceutical applications. Drug Development and Industrial Pharmacy, 1999; 25(10):1121-1128.

Sommer, K. and Hauser, G., Flow and compression properties of feed solids for roll-type presses and extrusion presses. Powder Technology, 2003; 130(1-3):272-276.

Sun, C. and Himmelspach, M. W., Reduced tabletability of roller compacted granules as a result of granule size enlargement. Journal of Pharmaceutical Sciences, 2006; 95(1):200-206.

Supuk, E., Zarrebini, A., Reddy, J. P., Hughes, H., Leane, M. M., Tobyn, M. J., Timmins, P., and Ghadiri, M., Tribo-electrification of active pharmaceutical ingredients and excipients. Powder Technology, 2012; 217(0):427-434.

Swaminathan, V. and Kildsig, D. O., An Examination of the Moisture Sorption Characteristics of Commercial Magnesium Stearate. AAPS PharmSciTech, 2001; 2(4):Article 28.

Takeuchi, H., Nagira, S., Aikawa, M., Yamamoto, H., and Kawashima, Y., Effect of lubrication on the compaction properties of pharmaceutical excipients as measured by die wall pressure. Journal of Drug Delivery Science and Technology, 2005; 15(2):177-182.

Thomas, A., Saleh, K., Guigon, P., and Czechowski, C., Characterisation of electrostatic properties of powder coatings in relation with their industrial application. Powder Technology, 2009; 190(1â€“2):230-235.

Tomas, J. and Kleinschmidt, S., Improvement of flowability of fine cohesive powders by flow additives. Chemical Engineering Technology, 2009; 32(10):1470-1483.

Uchimoto, T., Iwao, Y., Ikegami, Y., Murata, T., Sonobe, T., Miyagishima, A., and Itai, S., Lubrication properties of potential alternative lubricants, glycerin fatty acid esters, to magnesium stearate. International Journal of Pharmaceutics, 2010; 386(1-2):91-98.

Uchimoto, T., Iwao, Y., Takahashi, K., Tanaka, S., Agata, Y., Iwamura, T., Miyagishima, A., and Itai, S., A comparative study of glycerin fatty acid ester and magnesium stearate on the dissolution of acetaminophen tablets using the analysis of available surface area. European Journal of Pharmaceutics and Biopharmaceutics, 2011; 78(3):492-498.

Uzunović, A. and Vranić, E., Effect of magnesium stearate concentration on dissolution properties of ranitidine hydrochloride coated tablets. Bosnian journal of basic medical sciences / Udruženje basičnih mediciniskih znanosti = Association of Basic Medical Sciences, 2007; 7(3):279-283.

Van Veen, B., Bolhuis, G. K., Wu, Y. S., Zuurman, K., and Frijlink, H. W., Compaction mechanism and tablet strength of unlubricated and lubricated (silicified) microcrystalline cellulose. European Journal of Pharmaceutics and Biopharmaceutics, 2005; 59(1):133-138.

Vasilenko, A., Glasser, B. J., and Muzzio, F. J., Shear and flow behavior of pharmaceutical blends - Method comparison study. Powder Technology, 2011; 208(3):628-636.

Vromans, H. and Lerk, C. F., Densification properties and compactibility of mixtures of pharmaceutical excipients with and without magnesium stearate. International Journal of Pharmaceutics, 1988; 46(3):183-192.

Wada, Y. and Matsubara, T., Pseudopolymorphism and lubricating properties of magnesium stearate. Powder Technology, 1994; 78(2):109-114.

Wang, J., Wen, H., and Desai, D., Lubrication in tablet formulations. European Journal of Pharamaceutics and Biopharmaceutics, 2010; 75(1):1-15.

Wang, L. H. and Chowhan, Z. T., Drug-excipient interactions resulting from powder mixing. V. Role of sodium lauryl sulfate. International Journal of Pharmaceutics, 1990; 60(1):61-78.

Weyenberg, W., Vermeire, A., Vandervoort, J., Remon, J. P., and Ludwig, A., Effects of roller compaction settings on the preparation of bioadhesive granules and ocular minitablets. European Journal of Pharmaceutics and Biopharmaceutics, 2005; 59(3):527-536.

Wu, C. Y., Hung, W. L., Miguelez-Moran, A. M., Gururajan, B., and Seville, J. P. K., Roller compaction of moist pharmaceutical powders. International Journal of Pharmaceutics, 2010; 391(1-2):90-97.

Wu, S. J. and Sun, C., Insensitivity of compaction properties of brittle granules to size enlargement by roller compaction. Journal of Pharmaceutical Sciences, 2007; 96(5):1445-1450.

Yamamura, T., Ohta, T., Taira, T., Ogawa, Y., Sakai, Y., Moribe, K., and Yamamoto, K., Effects of automated external lubrication on tablet properties and the stability of eprazinone hydrochloride. International Journal of Pharmaceutics, 2009; 370:1-7.

Yu, S., Adams, M., Gururajan, B., Reynolds, G., Roberts, R., and Wu, C. Y., The effects of lubrication on roll compaction, ribbon milling and tabletting. Chemical Engineering Science, 2013; 86:9-18.

Zhou, Q., Armstrong, B., Larson, I., Stewart, P. J., and Morton, D. A. V., Improving powder flow properties of a cohesive lactose monohydrate powder by intensive mechanical dry coating. Journal of Pharmaceutical Sciences, 2010a; 99(2):969-981.

Zhou, Q. T., Armstrong, B., Larson, I., Stewart, P. J., and Morton, D. A. V., Understanding the influence of powder flowability, fluidization and de-agglomeration characteristics on the aerosolization of pharmaceutical model powders. European Journal of Pharmaceutical Sciences, 2010b; 40(5):412-421.

Zinchuk, A. V., Mullarney, M. P., and Hancock, B. C., Simulation of roller compaction using a laboratory scale compaction simulator. International Journal of Pharmaceutics, 2004; 269(2):403-415.

Zuurman, K., Riepma, K. A., Bolhuis, G. K., Vromans, H., and Lerk, C. F., The relationship between bulk density and compactibility of lactose granulations. International Journal of Pharmaceutics, 1994; 102(1-3):1-9.

Zuurman, K., Van Der Voort Maarschalk, K., and Bolhuis, G. K., Effect of magnesium stearate on bonding and porosity expansion of tablets produced from materials with

different consolidation properties. International Journal of Pharmaceutics, 1999; 179(1):107-115.